UNIVERSIDADE DE SÃO PAULO

FACULDADE DE ZOOTECNIA E ENGENHARIA DE ALIMENTOS

PROGRAMA DE PÓS-GRADUAÇÃO EM ENGENHARIA DE ALIMENTOS

MATHEUS ANDRADE CHAVES

ENRICHMENT OF CORNSTARCH WITH CURCUMIN AND VITAMIN D$_3$ COENCAPSULATED IN LYOPHILIZED LIPOSOMES USING HIGH SHEAR WET AGGLOMERATION

Pirassununga

2022

MATHEUS ANDRADE CHAVES

ENRICHMENT OF CORNSTARCH WITH CURCUMIN AND VITAMIN D₃ COENCAPSULATED IN LYOPHILIZED LIPOSOMES USING HIGH SHEAR WET AGGLOMERATION

Versão corrigida

Tese apresentada à Faculdade de Zootecnia e Engenharia de Alimentos da Universidade de São Paulo como parte dos requisitos para a obtenção do Título de Doutor em Ciências.

Área de Concentração: Ciências da Engenharia de Alimentos

Orientadora: Profa. Dra. Samantha Cristina de Pinho

Coorientador: Prof. Dr. Gustavo César Dacanal

Pirassununga

2022

ii

The good thing about Science is that it's true whether or not you believe

in it.

- Neil deGrasse Tyson

To my supervisor Samantha, thank you for being one of the most amazing

people that ever came into my life. Words are not enough to say how grateful I am

and always will be!

BIOGRAPHY

The author, Matheus Andrade Chaves, was born on September 7, 1991 in Mirassol (São Paulo, Brazil) but lived most of his life in Jaú (São Paulo, Brazil), as the eldest of Marilene Martinez Andrade Chaves and Luiz Fernando Costa Chaves. Food Engineer, he graduated from the University of São Paulo (USP) in 2014. During his undergraduate program, he carried out scientific initiations for two years with CNPq and FAPESP scholarships under the supervision of Prof. Cintia Bernardo Gonçalves (*in memoriam*) and Prof. Samantha Cristina de Pinho. At the end of his undergraduate program, he completed an internship year at the Institut National Supérieur des Sciences Agronomiques, de l'Alimentation et de l'Environnement (AgroSup Dijon, Dijon, France) with CAPES scholarship under the Brasil-França-Agricultura (BRAFAGRI) program.

At the beginning of 2015, Matheus joined the Science of Food Engineering Master's degree program at the School of Animal Science and Food Engineering of the University of São Paulo with a CAPES scholarship under the supervision of Prof. Samantha Cristina de Pinho. After six months, he was awarded with a FAPESP scholarship, with whom he remained until the end of 2016. During his Masters, Matheus also joined the Education Improvement Program (PAE) of USP for one year and half, carrying out a volunteer internship in Thermodynamics and two funded internships in Transport Phenomena.

At the beginning of 2017, Matheus joined the Science of Food Engineering Doctorate degree program at the School of Animal Science and Food Engineering of the University of São Paulo with a CAPES scholarship under the supervision of Prof. Samantha Cristina de Pinho. As it happened during his Master's degree, Matheus was awarded with a FAPESP scholarship after the first months of his doctoral research. He also joined the PAE program, this time for two years, carrying out a funded internship in Cold chain/Refrigeration process and three volunteer internships in Unit Operations and Physical-Chemistry. At the end of his Doctoral program, Matheus worked for 14 months at the Department of Industrial Engineering of the University of Salerno (UNISA, Fisciano, Italy), funded by BEPE-FAPESP scholarship, under the supervision of Prof. Ernesto Reverchon.

ACKNOWLEDGMENTS

First of all, I would like to thank my parents Marilene and Luiz Fernando, my sister Mariana, and my grandmother Deize, for their love, support, and patience, especially when I was not in my best mood. I know I can be complicated. Thank you for all that you have done for me and all that you are still doing. I hope to make you proud!

I cannot express enough thanks to my supervisor, mentor, friend, and "second-mom" Samantha for all the commitment, patience, learning, encouragement, concern, and support over the past 8 years. Thank you for believing in me and in my potential, all that I have achieved is because of you! If I love to be a teacher and a researcher, a lot is due to you! You are my truly inspiration and I hope to be half of the person that you are someday! As I always say, our partnership is for life! Thank you so much!

I thank my co-supervisor Prof. Gustavo César Dacanal for all his help, advices, and willingness during the final agglomeration step of this work.

I sincerely thank João Carlos for all the support and encouragement over the last year, especially when I was alone in a different country and afraid of the future. Thank you for always saying that everything will be alright at the end.

I could not have been accomplished this work without my special lab-mates who have always made the laboratory a welcoming place. Thank you, Thais, Letícia, Marluci, Natália, and Nayla, I hope our paths will cross somewhere again!

I am extremely thankful to laboratory technicians Marcelo Thomazini and Rodrigo Vinicius Lourenço for their help, patience, and willingness throughout all these years. I also thank Ana Mônica Quinta Barbosa Bittante, Keila Kazue Aracava, Nilson José Ferreira, and Leonardo Martins Pozzobon for their help and partnership over these years.

I have genuine pleasure to thank Prof. Ernesto Reverchon and Dr. Lucia Baldino for the opportunity to work at the Università degli Studi di Salerno with the SuperLip apparatus. It was a truly honor to work with some of the best.

I would like to thank my supercritical colleagues Mariangela, Paola, Ida, Antonio, and Gianroberto for their help, friendship, and support. Despite the pandemic, it was a great pleasure and a truly honor to work with such amazing people.

I owe a deep sense of gratitude for professors Samantha, Isabel, Alessandra, Milena, and Gustavo for the opportunities to develop my teaching skills during the PAE program.

ABSTRACT

CHAVES, M. A. **Enrichment of cornstarch with curcumin and vitamin D₃ coencapsulated in lyophilized liposomes using high shear wet agglomeration**. 2021. 297p – PhD – Thesis - School of Animal Science and Food Engineering, University of São Paulo, Pirassununga, 2021.

Nowadays, the increasingly search for healthier foods is a recurrent practice by consumers. Therefore, there is a continuous to develop new technologies for the controlled release of bioactives in food formulations. Curcumin is the main compound extracted from turmeric plant with well-known antioxidant, anti-inflammatory and antimicrobial properties that has been used in food industry as a spice, preservative, and natural colorant. Vitamin D₃ (cholecalciferol) is a liposoluble prohormone molecule with a key role in the health of teeth and bones, since its intake promotes an increase in the absorption of calcium by the blood. Despite their benefits, the incorporation of curcumin and vitamin D₃ into aqueous-based food formulations can be hindered by their high hydrophobicity. Such problem can be overcome by encapsulating both bioactives into lipid carriers as liposomes. Liposomes have high biocompatibility with epithelium cells, as well as low toxicity. From an industrial viewpoint, the production of liposomes using the hydration of proliposomes method appears as an easily scalable process and presents several advantages over the other methods discussed in literature such as lower cost and the need for no organic solvents other than ethanol for manufacturing. Alternatively, supercritical methods to produce liposomes are environmentally friendly and result in high encapsulation efficiencies. The main objective of this work was to produce a new enriched cornstarch containing curcumin and vitamin D₃ coencapsulated in lyophilized liposomes using a high shear wet agglomeration method. This technique is widely used for the production of powders with improved flowability properties. Lyophilized vesicles were prepared using two phospholipids, soybean hydrogenated Phospholipon 90H and fat-free unpurified Lipoid S40. To this purpose, the feasibility for the production of proliposomes and liposome dispersions using different phospholipid ratios was first tested. Proliposomes were characterized using methods often used for food powders, whereas methods used for colloidal suspensions were applied to characterize the liposome dispersions. These liquid dispersions were lyophilized and the resulted powders also characterized. At last, the lyophilized vesicles were blended to commercial cornstarch using maltodextrin as liquid binder and high shear wet agglomeration

as the main process. Overall, all systems herein proposed were suitable for the retention of curcumin and vitamin D_3 over the storage time. Phospholipid ratio proved to have the major influence on physicochemical parameters of carriers. Cornstarch samples presented improved technological and handling properties and retained up to 96.7% of curcumin and 98.2% of vitamin D_3 after 30 days of storage. This work provided an innovative and potential purpose for a simple and widespread process as high shear wet agglomeration and allowed to develop a new functional product with high-added value using low-cost ingredients.

RESUMO

CHAVES, M. A. **Enriquecimento de amido de milho com curcumina e vitamina D₃ coencapsuladas em lipossomos liofilizados utilizando aglomeração úmida de alto cisalhamento**. 2021. 297p – Tese de Doutorado – Faculdade de Zootecnia e Engenharia de Alimentos, Universidade de São Paulo, Pirassununga, 2021.

Atualmente, a crescente busca por alimentos mais saudáveis é uma prática recorrente por parte dos consumidores. Sendo assim, torna-se necessário o desenvolvimento de novas tecnologias para a fortificação e posterior liberação controlada de bioativos em alimentos. A curcumina é o principal pigmento extraído da planta de açafrão-da-terra (*Curcuma longa l*) e possui, dentre outros benefícios, conhecidas propriedades antioxidantes e anti-inflamatórias. Na indústria alimentícia, a curcumina é utilizada como condimento, conservante e corante natural devido a sua característica coloração amarela. Por sua vez, a vitamina D_3 (colecalciferol) é uma molécula lipossolúvel com um papel fundamental na saúde dos dentes e ossos, uma vez que sua ingestão promove um aumento na absorção de cálcio pelo sangue. Apesar de todos os seus benefícios, a hidrofobicidade das moléculas de curcumina e vitamina D_3 dificulta a direta incorporação de ambas em formulações alimentícias com base aquosa. Tal problema pode ser contornado ao encapsular esses bioativos em carreadores lipídicos como os lipossomas. Nesse contexto, a matriz lipídica do lipossoma apresenta uma alta biocompatibilidade com as células do epitélio, além de baixa toxicidade. Do ponto de vista industrial, a produção de lipossomas por hidratação de prolipossomas aparece como um processo facilmente escalonável, além de apresentar diversas vantagens sobre os outros métodos discutidos na literatura, tais como menor custo e a redução do uso de solventes orgânicos. Por outro lado, a produção de lipossomas a partir de fluidos supercríticos é ambientalmente correta e resulta em vesículas com altas eficiências de encapsulação. Este trabalho teve por principal objetivo a fortificação de amido de milho com curcumina e vitamina D_3 coencapsuladas em lipossomas liofilizados a partir de aglomeração úmida de alto cisalhamento, técnica amplamente utilizada pela indústria para a produção de pós alimentícios com melhores propriedades de fluidez. As vesículas liofilizadas tiveram por base Phospholipon90H, contendo fosfolipídios purificados e hidrogenados, e LipoidS40, constituído majoritariamente por espécies insaturadas. A viabilidade da produção de prolipossomas e de dispersões de lipossomas utilizando diferentes

proporções destes fosfolipídios foi investigada. Os prolipossomas foram caracterizados utilizando-se técnicas frequentemente aplicadas para pós, enquanto as dispersões foram caracterizadas a partir de técnicas para suspensões coloidais. As dispersões foram então liofilizadas e os pós resultantes também caracterizados. Por fim, os liofilizados foram aglomerados com amido de milho utilizando-se maltodextrina como solução ligante a partir da técnica de alto cisalhamento. Em síntese, todos os sistemas produzidos ao longo deste trabalho se mostraram satisfatórios para a encapsulação de curcumina e vitamina D_3. A proporção de fosfolipídios foi o parâmetro que apresentou uma maior influência nas propriedades físico-químicas de todos os carreadores estudados. As propriedades tecnológicas do amido de milho foram melhoradas após a aglomeração com lipossomas liofilizados, sendo que os mesmos retiveram até 96,7% de curcumina e 98,2% de vitamina D_3 após 30 dias de armazenamento. Este estudo proporcionou a produção de um ingrediente completamente novo, rico em nutrientes e de alto valor agregado, a partir de matérias-primas de baixo custo e de um processo simples e habitual da indústria alimentícia.

Palavras-chave: nanoencapsulação, liofilização, tecnologia supercrítica, aglomeração úmida, fosfolipídios insaturados.

LIST OF FIGURES

LIST OF TABLES

ACRONYMS / ABBREVIATIONS

ABTS = 2,2'-azino-bis(3-ethylbenzothiazoline-6-sulfonic acid

AFM = Atomic force microscopy

AIC = Akaike information criterion

Aw = Water activity

CI = Carr's index

CIE = *Commission Internationale de l'Éclairage*

CUR = Curcumin

DLS = Dynamic light scattering

DMSO = Dimethyl sulfoxide

DPPH = 2,2-diphenyl-1-picrylhydrazyl

DSC = Differential scanning calorimetry

EDTA = Ethylenediamine Tetraacetic acid

EPC = Egg Phosphatidylcholine

FDA = Food & Drug Administration

FE-SEM = Field-Emission Scanning Electron microscopy

FTIR = Fourier-Transform Infrared microscopy

G' = Storage modulus

G'' = Loss modulus

GXL = Gas-expanded liquid

HPLC = High performance liquid chromatography

HR = Hausner ratio

IU = International Unit

LOD = Limit of detection

LOQ = Limit of quantification

LPC = Lysophosphatidylcholine

LS40 = Lipoid S40

MC = Moisture content

MLV = Multilamellar vesicle

MSC = Micronised sucrose coating method

NAS = non -agglomerated starch

P90H = Phospholipon 90H

PBS = Phosphate-buffered saline

PC = Phosphatidylcholine

PCS = Photon Correlation Spectroscopy

PDI = Polydispersity Index

PE = Phosphatidylethanolamine

PI = Phosphatidylinositol

PL = Proliposome

rpm = Rotation per minute

RVA = Rapid Visco Analyzer

SC-CO$_2$ = Supercritical carbon dioxide

SEM = Scanning electron microscopy

SPC = Soy Phosphatidylcholine

SuperLip = Supercritical Assisted Liposome Formation

TG = Triglycerides

Tg = Glass transition temperature

ULV = Unilamellar vesicle

v/v = Volume ratio

VD3 = Vitamina D$_3$

w/v = Mass in volume ratio

w/w = Mass ratio

WHO = World Health Organization

XRD = X-Ray Diffraction

xx

SUMMARY

xxvi

INTRODUCTION

Nowadays, there is a growing interest in the use of liposomes by the food industry in a variety of applications. These systems present several advantages over the other lipid carriers such as low toxicity and high bioavailability, easy scalability and compatibility with bioactives of different natures.

In the literature, several studies discuss the incorporation of bioactives in liposomes, but little is found about the encapsulation of more than one bioactive molecule into their lipid bilayer structure. Coencapsulation is a technique often found in studies applied to medical and pharmaceutical areas and aims to increase the bioactive potential of two or more compounds. In foods, such process can be used with the purpose of developing new nutrient-rich ingredients or formulations.

Among the methods to produce liposomes, the hydration of proliposomes appears as a simple, reproducible, reliable, and easily scalable method. Proliposomes can be produced by coating micronized carriers, such as sucrose, which gives them food grade status. Alternatively, despite of its higher price for equipment acquisition and installation, supercritical technologies have also been used to produce liposomes with higher trapping efficiency without using large amounts of organic solvents.

However, due to the known instability found for liposomes in liquid dispersion form, lyophilization emerged as a promising approach to ensure long-term stability of lipid vesicles. In food, this practice is applied to increase the stability of several products, promoting decreased microbiological contamination and simplifying shipping and storage. Because of the relative fragility of vesicle structure, an important knowledge of the lyophilization process is necessary. To this end, the use of an adequate cryoprotectant is mandatory as it protects the lipid bilayer structure from possible damages related to cold.

Moreover, wet agglomeration is another process extensively found in food industry. It is usually employed to improve the solubility of powdered foods, enabling their reconstitution upon contact of liquids, such as water or milk. Also, it leads to improved handling properties of food powders as higher fluidity and lower cohesiveness.

This Doctoral Thesis aimed to verify the feasibility of producing a new and functional cornstarch fortified with curcumin and vitamin D_3 coencapsulated in lyophilized liposomes using high shear wet agglomeration. Chapter I consists in a presentation of a brief literature

review on interesting issues for the realization of this work as importance of the processes used and the reasons behind the choice of bioactive molecules. The following chapters describe the production and characterization of all the systems produced throughout this PhD Thesis, such as the proliposomes, liposome dispersions, lyophilized liposomes and agglomerated cornstarch particles.

A schematic representation presenting all the steps performed throughout this work is exhibited in Fig. 1. Firstly, the technique of producing proliposomes (micronized sucrose coating) and its subsequent hydration to produce liposome dispersions were investigated to verify their effectiveness for the encapsulation of bioactives separately. Thus, Chapter II shows the results regarding the production and characterization of proliposomes and dispersions encapsulating curcumin alone, whereas Chapter III brings the results obtained for vitamin D_3 encapsulation. After assess that systems promoted the entrapment of bioactives effectively, coencapsulation tests were continued (Chapter IV). From the results obtained, it was observed that dispersions did not remain stable for a long period of time, corroborating the need for lyophilization. In the meantime, the feasibility of using the produced dispersions in yogurt fortification was verified (Chapter V). For comparative purposes, vitamin D_3 (Chapter VI) and curcumin/co-loaded liposomes (Chapter VII) were produced using supercritical technology.

Finally, dispersions were lyophilized and blended with cornstarch using wet agglomeration (Chapter VIII). The enriched-cornstarch particles were then physicochemically characterized over 30 days of storage using typical methods applied to food powders.

Figure. 1. Schematic representation of the steps of this PhD Thesis

Production of proliposomes

- Phospholipon 90H (P90H) and Lipoid S40 (LS40) – P90H:LS40 ratios were tested
- P90H:LS40 - F50 (50:50 w/w), F70 (30:70 w/w) and F100 (0:100 w/w)
- Curcumin alone (**Chapter II**)
- Vitamin D3 alone (**Chapter III**)
- Co-entrapped carriers (**Chapter IV**)

Production of liposome dispersions

- Hydration of proliposomes method
- **Chapter II** – curcumin-loaded liposomes
- **Chapter III** – vitamin D_3-loaded liposomes
- **Chapter IV** – co-loaded liposomes

Production of liposome dispersions

- Supercritical CO_2 assisted technology (SuperLip)
- **Chapter V** – vitamin D_3-loaded liposomes
- **Chapter VI** – curcumin and co-loaded liposomes
- BEPE (*Bolsa de Estágio de Pesquisa no Exterior*)
- Grant number 2019/08345-3
- Università degli Studi di Salerno (Fisciano, Italy)

Production of pineapple enriched-yogurt

- Direct incorporation of co-loaded vesicles into yogurt formulations (**Chapter IV**)
- Physicochemical, rheological and sensorial evaluations were performed
- Scientific Initiation Scholarship (Vinicius Franckin, PUB-USP 2018-2019)

Production of lyophilized liposomes and enriched-cornstarch particles

- **Chapter VIII**
- Dispersions were lyophilized using sucrose as cryoprotectant
- Enriched-cornstarch particles were blended to lyophilized vesicles using wet agglomeration
- Maltodextrin used as binder solution.

Reference: Own source

Chapter 1. LITERATURE REVIEW

Chapter 1. LITERATURE REVIEW OF RELEVANT RESEARCH: A summary approach of the main issues covered by this study.

1.1 CURCUMIN: Definition and applications

Color is an attribute with direct influence on the acceptability and purchase appeal of food products. Along taste, texture and aroma, color is considered one of the characteristics that also help to analyze food quality. Colorants are food additives employed by industry for different purposes, including: (I) restore color lost during processing; (II) enhance an already existing hue; (III) standardize the coloration of different batches and (IV) color foods that lack coloration (Lakshmi, 2014).

Colorants can be classified into four categories: (a) natural; (b) identical to natural; (c) synthetic and (d) inorganic (Lakshmi, 2014). Artificial dyes are pigments produced by chemical synthesis from coal or petroleum, while natural dyes are those extracted from plant or animal sources. The industrial preference for artificial dyes is mainly due to their low cost to obtain and their high stability in different media and processing conditions (Feketea & Tsabouri, 2017). The use of these additives is, however, one of the most controversial advances in food industry, since their use is often justified only to dietary habits (Gebhardt et al., 2020).

In recent years, an increasing concern about the safety and possible health hazards of food artificial dyes has emerged, mainly because most of them are incorporated in children's products (Ahmed et al., 2020; Lemoine et al., 2020; Lehmkuhler et al., 2020). In this context, tartrazine (INS102/Yellow n. 5) is a synthetic dye belonging to the class of azo colorants. Its structure has a naphthalene ring and a benzene ring linked by an azo type bond (N=N) as illustrated in Fig. 1.1a. It is an additive widely used in products such as snacks and candies and, despite having excellent stability to light, acidic media and high temperatures, its consumption has been linked to adverse reactions such as hives, asthma, anaphylaxis, irritability, sleep disturbances and hyperactivity in children (McCann et al., 2007). The biggest concern about azo colorants is related to the secondary products originated after the breakdown of the azo bond (amino-azobenzenes), structures with high carcinogenic potential (Drake et al., 1975).

Figure 1.1. Chemical structure of (a) tartrazine and (b) curcumin, and (c) visual aspect of crystalline curcumin and turmeric plant

(a)   (b)   (c)
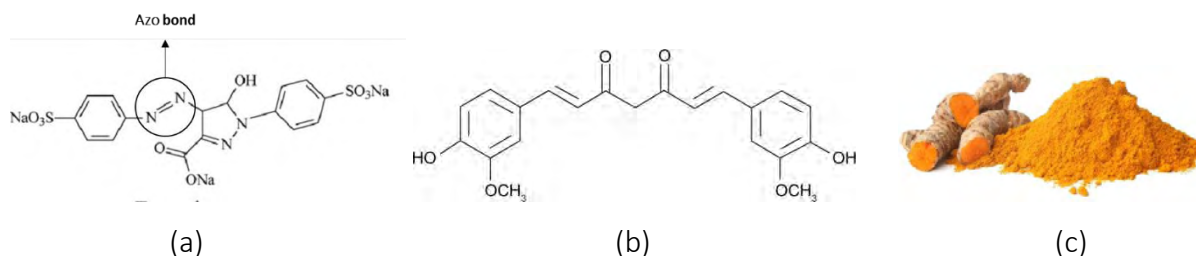
Reference: Own source

Although it has been banned from countries such as Norway and Austria, tartrazine (CAS 1934-21-0) continues to be used in other countries of the European Union, besides the United States and Brazil, in which a daily intake (ADI) of 7.5 mg/kg body weight is acceptable (ANVISA, 1999). To replace tartrazine in food formulations, curcumin appears as a potential substitute.

Curcumin (diferuloilmethane) is a natural polyphenol with low molecular weight found in the rhizome of the herbaceous plant *Curcuma longa L*, also known as turmeric or "açafrão-da-terra" in Brazil. Its chemical structure and appearance are seen in Figs. 1.1b-c, respectively. It is a crystalline powder with intense yellow color, and for this reason, it has been used in food industry as a colorant (CAS 458-37-7) in products such as macaroni, mustards, ice cream, cheese, sauces, chips, popcorn, cereals, cookies, and margarine. This condiment originated of southern Asian regions is also used as preservative and flavoring agent (Jiang et al., 2021). Several studies suggest that curcumin has anticarcinogenic, antiviral, antiarthritic, antioxidant, and anti-inflammatory activities. The hydroxyl functional groups present in benzene rings, the double bonds present in alkene chains, and its diketone portion are believed to have key roles in the pharmaceutical activities of curcumin (Liu et al., 2015).

Although its pharmaceutical properties, the direct incorporation of curcumin in water-based food formulations is hindered due its hydrophobicity and natural instability. Moreover, curcumin is easily degraded in alkaline media (pH > 7) and after light and/or oxygen exposure. Its low water solubility (11 ng/mL, 25 °C) leads to low oral bioavailability, low absorption rate in the gastrointestinal tract, besides a rapidly elimination from the body through urine (Aditya et al., 2013). Also, the direct incorporation of curcumin into foods may promote undesirable

changes in the organoleptic properties, such as appearance, odor, and flavor (Aditya et al., 2015).

The encapsulation of curcumin in lipid carriers arises as an alternative to increase its stability in aqueous media, besides promoting an increase in oral bioaccessibility and solubility (Sabet et al., 2021). Several colloidal systems have been to encapsulate curcumin, including micelles, emulsions/nanoemulsions, Pickering emulsions, hydrogels, phytosomes, solid lipid microparticles/nanoparticles, nanocrystals, oil bodies, protein nanoparticles, and liposomes/ nanoliposomes (Dai et al., 2019; Demirci et al., 2017; McClements, 2020; Zheng et al., 2019).

1.2 VITAMIN D_3: Definition and overview about its deficiency

Vitamins are organic lipophilic compounds that are essential for the body to function properly. They play key roles in growth and help to prevent diseases. However, a great amount of these vitamins must be acquired through food or supplementation as they are not naturally produced by the human body (Katouzian & Jafari, 2016).

Vitamin D is a pro-hormone molecule found in two forms, ergocalciferol (vitamin D_2) and cholecalciferol (vitamin D_3). Vitamin D_2 is synthesized from the incidence of ultraviolet (UV) radiation on ergosterol molecules found in plants. Vitamin D_3, on the other hand, is synthesized from UV radiation on 7-dehydrocholesterol molecules presented in human epidermis (Ložnjak & Jakobsen, 2018). Fig. 1.2 shows the chemical structure of vitamins D_2 and D_3.

Figure 1.2. Chemical structure of (a) vitamin D_2 and (b) vitamin D_3

(a)　　　　　(b)
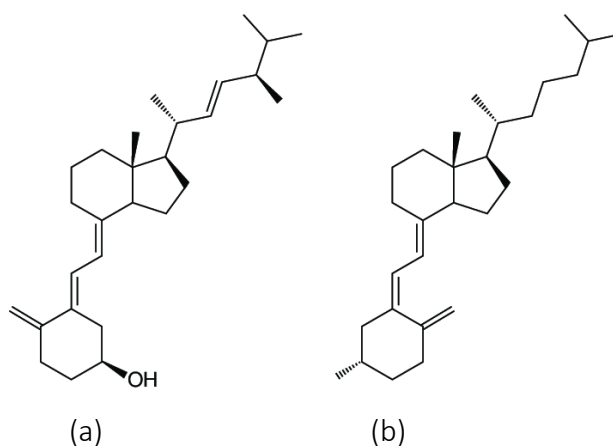
Reference: Own source

Several health benefits are attributed to vitamin D intake, among them: (I) the increased absorption of calcium in the intestine, which contributes to the formation and mineralization of bones, (II) the proper functioning of the cardiovascular system, (III) the strengthening conferred to the immune system, (IV) anticancer effect and (V) antioxidant capacity (Holick, 2007). Even though both forms of vitamin D are known to have antiradical effects, vitamin D_3 is substantially more potent than vitamin D_2 (Armas, Hollis & Heaney, 2004).

Vitamin D deficiency is recognized as a pandemic (Holick, 2017). Insufficient vitamin D intake (<30 ng/mL) is related to risk of onset of cancers, autoimmune diseases, hypertension, infections, as well as early osteoporosis in adults and rickets in children (Holick, 2007). The main cause for such deficiency is lack of exposure to sunlight. Holick & Chen (2008) reported that any factor that decreases the transmission of UV radiation to Earth's surface or blocks the penetration of this radiation in the skin affect directly the cutaneous production of vitamin D_3. In this context, people who spend most of their time indoors, or those who live in high latitude regions, black people (melanin absorbs much of the UV radiation), and even those who have the habit of always use sunscreen before leaving home, all are susceptible to VD3 deficiency. In these cases, it is recommended a supplementation with about 800-1000 IU for children or adults to obtain the 30 ng/mL daily needed for proper functioning of the body.

Unfortunately, few foods naturally contain this vitamin. Examples include oils extracted from the livers of fat fish such as salmon, tuna, and cod, mushrooms, and egg yolk in small amounts. The fortification of products with vitamin D emerges as a possible key to reverse this situation (McCourt et al., 2020; Zahedirad et al., 2019). Commercially available foods such as cereal bars, orange juice and dairy products, including pasteurized milk, cheese, margarine and yogurt, are examples of products already fortified with this vitamin. It is important to highlight that these foods are most often fortified with the most active form of vitamin D, vitamin D_3 (Holick, 2007). The bioactive in these cases is added in the form of oil, in order to promote its better incorporation into the food matrix (Gomes et al., 2015).

To assess an optimized VD3 fortification process, a stricter control of the processing conditions is necessary, since this vitamin is highly unstable in the presence of UV radiation, oxygen or under high temperatures. However, conflicting information is found concerning the stability of vitamin D_3 in fortified foods. Some studies report high stability under controlled storage conditions (Bajaj & Singhal, 2021), while others report severe losses over storage time (Kazmi et al., 2007). In order to increase the stability of vitamin D_3 in food formulations, its

incorporation in lipidic carrier systems can be considered. As presented for curcumin, this practice leads to an increase in solubility of this vitamin, as well as in its oral bioavailability. Among the colloidal systems, those already used to encapsulate vitamin D_3 include solid lipid nanoparticles, emulsions, complexes, and liposomes (Maurya, Bashir, & Aggarwal, 2020).

1.3 LIPOSOMES: Definitions and characterization techniques

In general, encapsulation technologies have emerged with the purpose of increasing the stability and bioavailability of bioactive substances. In this context, liposomes appear as one of the most studied carrier systems in the pharmaceutical area for the transport of hydrophilic and hydrophobic molecules, due to the amphiphilic structure of their main constituents, the phospholipids. Compared to other traditional carrier systems, liposomes present some advantages including non-toxicity, flexibility, biocompatibility, biodegradability, and non-immunogenicity (Akbarzadeh, 2013). Liposomes were developed for medical purposes and were later applied by the pharmaceutical industry in cosmetics and in the transport of vaccines, hormones, enzymes, and vitamins into the body (Emami et al., 2016; Liu, Bravo & Liu., 2021; New, 1990).

By definition, liposomes are spherical structures formed by one or more phospholipid bilayers that can encapsulate in their interior part of the aqueous medium in which they are dispersed (Lasic, 1998). Phospholipids are the main amphiphilic "building blocks" molecules of liposomes. Generally, phospholipids are derived from glycerol, where the 1- and 2- positions are acylated by fatty acids while 3- position is esterified with phosphoric acid forming the phosphatidyl group. If the phosphate group remains free the molecule is a phosphatidic acid, if not, it can be substituted with groups as choline, ethanolamine or inositol, for example. They present amphipathic properties due to the presence of a polar headgroup and an apolar region (generally composed of two fatty acid acyl chains) in the same molecule (Pokorný, 2003). Due to their poor solubility in water, phospholipids tend to self-assemble into bilayers fragments when dispersed in excess aqueous media, which causes the formation of hydrophobic tail edges exposed to the water. Such edges have energy proportional to the perimeter of the structure, which can be minimized by eliminating the exposition of phospholipids hydrophobic portion to the water (Patil & Jadhav, 2014). Figure 1.3 shows the formation scheme of a liposome.
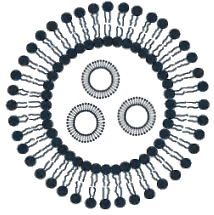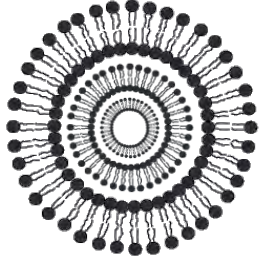
Figure 1.3. Schematic illustration of phospholipid self-assembly involved in liposome formation. After adding phospholipids in an aqueous medium (a), they tend to associate with each other forming lipid bilayers (b). The unfavorable interaction between fatty acid molecules and water is then eliminated after introducing a sufficient amount of energy into the system (c), which causes the bilayers to arrange themselves in their organized form (vesicle) (d). During this process, liposomes can incorporate hydrophilic actives present in the hydration medium into their aqueous core, as well as hydrophobic actives in internal regions of the lipid bilayer
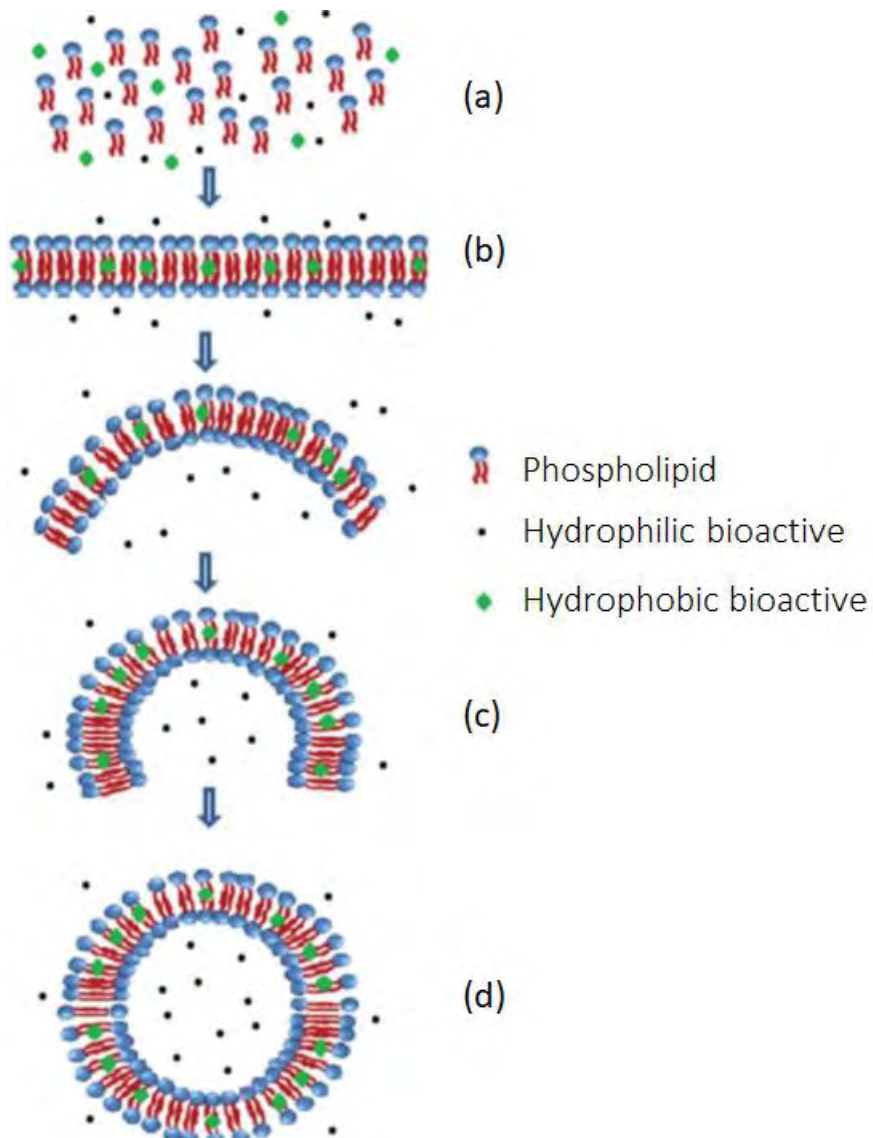
Reference: Adapted from Emami et al. (2016)

Lipid bilayers may grow in size with the addition of other phospholipid molecules in order to form the vesicles. It is possible that destabilizing forces, as hydrodynamic forces caused by high shear devices, may lead to the fragmentation of the bilayers, resulting in smaller liposomes (Payne et al., 1986). The self-closing in water excess occurs due to the attraction between hydrophobic groups to minimize the interactions with water, and the repulsion between polar headgroups due to their ionic, hydrophilic or steric characteristics (Israelachvili & Sornette, 1985). Depending on the number of phospholipid bilayers (lamellarity) and the diameter of the vesicles, the liposomes are classified as shown in Table 1.1.

Table 1.1. Classification of liposomes based on structural parameters

Type of liposomes	Diameter	Characteristic	Abbreviation	Schematic
Small unilamellar vesicles	20 to 200 nm	Small unilamellar vesicle	SUV	
Large unilamellar vesicles	above 200 nm	Unilamellar liposomes, but with average diameters higher than SUV	LUV	
Giant unilamellar vesicles	than 1 μm	Unilamellar liposomes, but with average diameters higher than LUV	GUV	
Multivesicular vesicle	higher than 1 μm	Vesicles with many vesicles inside it	MVV	
Multilamellar vesicles	0.5 to 5 μm	Consist of five or more concentric lamellae	MLV	

References: Adapted from Rashidinejad et al. (2014)

In general, the mean diameter of liposomes varies from 100 nm to about 5 μm, and it strongly depends on the production method and lipid composition. The size of liposomes is a compromise among liposome stability (decreases with increasing size), bioactive loading efficiency (increases with increasing size) and capacity to extravagate its content (decreases with increasing size). Typical liposomes are not thermodynamically stable, and, therefore, they do not form spontaneously. Thus, energy must be applied to obtain liposomes in the desired size. In addition, after their formation, they are not colloidal stable systems and it tends to aggregate or fuse into larger structures with lower curvature degree along time (Lasic, 1998; McClements, 2005). SUVs, LUVs and MVVs present a greater ability to encapsulate hydrophilic molecules, whereas lipophilic actives are commonly transported using MLVs (Laouini et al., 2012).

The first liposome production method was developed by Bangham, Standish & Watkins (1965), where basically lipids were dissolved in an organic solvent (chloroform), dried to form a thin lipid film on the walls of a flask and then hydrated with water or water-based medium under agitation. Typically, when dry lipid films are hydrated, the lamellae swell and grow into myelin figures (thin lipid tubules) but in general they do not detach so easily from a support. Although it is an accepted conception that liposomes are spontaneously formed when water is added to dry lipid films, it is an equivocated view (Lasch, Weissig, & Brandl, 2003). During hydration, required mechanical agitation can be provided by shaking, vortexing or swirling, and it causes the random breaking of myelin structures and the reseal of the exposed hydrophobic edges, leading to the self-closing and, hence, in the formation of liposomes. This random procedure generates liposomes with a wide size range. In many cases, therefore, post processing is required to reduce size and lamellarity.

Liposomes can be prepared using a wide variety of phospholipids. Most common are beneficial to the human body and can be extracted from safe and natural sources, including egg-yolk, soy, and milk (Thompson, Mozafari, & Singh, 2007). Phosphatidylcholines (lecithins) are the most abundant phospholipids in nature and also the most widely used for liposome production (Koynova & Caffrey, 1998). These structures comprise a phosphocholine grouping (hydrophilic) and two hydrocarbon chains (hydrophobic). Besides phosphatidylcholine, other phospholipids as phosphatidylserine, phosphatidylinositol and phosphatidylethanolamine can also be used for such purpose (Brandl, 2001). Chemical structures of the mentioned species are shown in Fig. 1.4.

Figure 1.4. Chemical structure of main phospholipids used for liposome production: (a) phosphatidylcholine (PC), (b) phosphatidylethanolamine (PE), (c) phosphatidylinositol (PI), and (d) phosphatidylserine (PS)
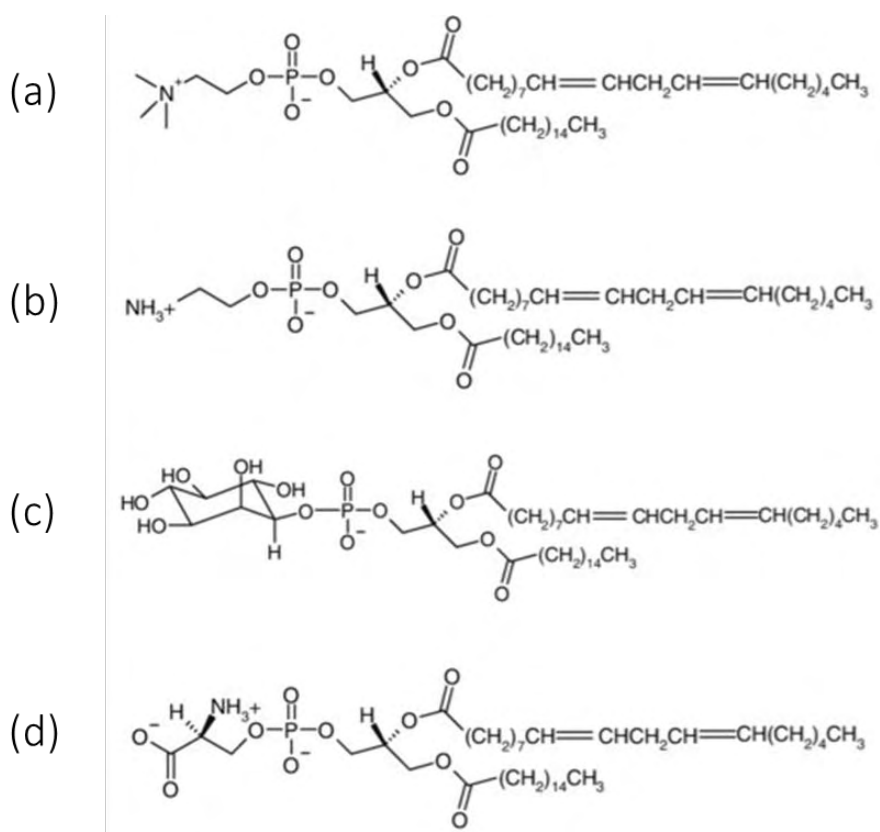
Reference: Adapted from Yip, Ashraf-Khorassani & Taylor (2007)

Phospholipids found in nature as the obtained from soy and egg-yolk contain certain polyunsaturated fatty acids such as linolenic acid (omega-3) and linoleic acid (omega-6) (Marsanasco, Chiaramon, & Alonso, 2017). Both are essential fatty acids that are not synthesized by the body and must therefore be obtained from the diet. Health benefits attributed to these fatty acids include the prevention of cardiovascular diseases, cancer, and schizophrenia, besides antihypertensive, anti-atherothrombotic, and vasodilatory activities (Hadian, 2016). In turn, choline group from phosphatidylcholine acts in neurotransmitters synthesis and is responsible for lipid transport and communication between cells and membranes (Penry & Manore, 2008).

A complete characterization of the liposomal systems, in aqueous or dried form, is quite important to evaluate its suitability for quality control and to evaluate their feasibility to be

used for a specific application in food. The physical stability of liposomes can be assessed with respect to changes in their hydrodynamic diameter (due to aggregation of vesicles) and from the quantification of the encapsulated material over time (Anderson & Omri, 2004). Another indicator of stability is the zeta potential value, a parameter that analyzes the magnitude of repulsion or electrostatic attraction between vesicles. Moreover, liposomes are susceptible to oxidation and hydrolysis. Therefore, an increase in the shelf life of liposomes can be conferred by avoiding the oxidation of unsaturated acyl chains, through the use of antioxidants and by controlling storage conditions (Grit & Crommelin, 1993). The most important experimental techniques to analyze liposomes are shown in Table 2.

Table 1.2 (Continued). Examples of techniques used for the characterization of aqueous liposome dispersions and lyophilized liposomes

Experimental technique	Measurement
Dynamic light scattering (photon correlation spectroscopy; Doppler shift spectroscopy)	Particle size distribution (diluted dispersions)
Electrical pulse courting (electrozone sensing or Coulter counter)	Particle size distribution (diluted and concentrated dispersions)
Diffusion wave spectroscopy	Particle size distribution (concentrated dispersions)
Ultrasonic spectrometry	Particle size and concentration of droplets (can be used as an on-line sensor)
Small angle X-ray scattering (SAXS) Small angle neutron scattering (SANS)	Thickness of interface layers, microstructural analyses
Electrical conductivity	Disperse volume fraction
Differential scanning calorimetry	Phase transitions (gel-liquid crystalline)
Particle electrophoresis	Zeta potential
Rheology	Droplet interactions
Transmission electron microscopy Atomic force microscopy	Morphological characteristics of aqueous dispersions of liposomes

Table 1.2. Examples of techniques used for the characterization of aqueous liposome dispersions and lyophilized liposomes

Scanning electron microscopy	Morphological characteristics of lyophilized liposomes
Electron paramagnetic resonance	Microstructural analyses
Magnetic nuclear resonance	Interactions between the cryoprotectants and phospholipids in the bilayers
Infrared spectroscopy	Interactions among chemical groups in lyophilized liposomes
Fluorescence spectroscopy	Microviscosity

Reference: Own source

The nature of bioactive compounds to be encapsulated plays an important role in the design of the carrier system. Due to the amphiphilic nature of liposomes, which are lipid bilayer vesicles with aqueous core, lipophilic and hydrophilic compounds can be encapsulated. The amount of compound inside the liposome is described in literature as encapsulation/ entrapment efficiency. Usually the entrapment efficiency is obtained after the removal of nonencapsulated bioactive, assuming that the remaining bioactive is located inside the vesicles (Taylor et al., 2005). Different methods to achieve it can be used, such as centrifugation and ultrafiltration. The release can be carried out by adding organic solvents (such as ethanol) or surfactants (such as sodium dodecyl sulfate, SDS). The bioactive quantifying method depends basically the investigated type of molecule.

1.4 APPLICATIONS of liposomes in food

Encapsulation techniques have been set up in the food technology field with different objectives, including (I) to bioactive released control, ensuring availability after a specific time, (II) to control the interaction between ingredients and the food matrix, (III) to mask odors and unpleasant flavors of some molecules and (IV) to protect some actives from adverse conditions of temperature, humidity, and chemical and/or biological degradations during processing and storage (Taylor et al., 2005). In the specific case of liposomes, they have been used for the carriage of food bioactives such as enzymes, proteins, vitamins, and antioxidants in water-

based foods such as milk, yogurts, cheeses and juices (Marsanasco et al., 2015; Mozafari et al., 2008). Table 1.3 summarizes some recent studies involving the use of liposomes to food purposes.

Table 1.3. Examples of applications of liposomes in food

Bioactive (or class of bioactives)	Lipid composition	Reference
Quercetin and fish oil	Soy lecithin	Frenzel & Steffen-Heins (2015)
Peptides	Milk fat globule phospholipids	Li, Paulson & Gill (2015)
Vitamin C	Soy PC	Liu et al. (2016)
Sericin protein	Soy PC	Suktham et al. (2016)
Grape-seed extract	Soy lecithin	Gibis, Ruedt, & Weiss (2016)
Eugenol	Soy PC	Sebaaly et al. (2016)
Black mulberry extract	Soy lecithin	Gültekin-Özgüver et al. (2016)
Grape pomace extract	Soy lecithin	Manconi et al. (2016)
Fish oil	Soy lecithin	Ghorbanzade et al. (2017)
Docosahexaenoic acid/ Eicosapentaenoic acid	Dipalmitoyl-PC	Sahari et al. (2017)
Olive pomace extract	Egg PC	Trucillo et al. (2018)
Nerolidol	Egg PC and PE	Azzi et al. (2018)
Black carrot extract	Soy lecithin	Guldiken et al. (2019)
Sea fennel	Soy PC	Alemán et al. (2019)
Bitter Gourd fruit extract		Erami, Amiri & Jafari (2019)
Coenzyme Q10	Soy lecithin	Villanueva-Bermejo & Temelli (2020)
Nisin	Soy lecithin	Pinilla et al. (2020)
Linseed oil and quercetin	PC	Huang et al. (2020)
Lactoferrin	Rapeseed phospholipids	Vergara et al. (2020)
Rutin	Soybean lecithin	Lopez-Polo et al. (2020)
Propolis	Soy PC	Ramli et al. (2021)
Curcumin	Soy PC	Li et al. (2021)
Nitroxyl	Soy lecithin	Liu et al. (2021)
Egg-yolk immunoglobulin	Soy PC and egg-yolk PC	Dong et al. (2022)

Reference: Own source

Compared to other methodologies used for encapsulation, such as extrusion, fluidized bed and spray drying, liposomes promote an increase in solubility of bioactives in high-water activity foods (Desai & Park, 2005). Incorporation into liposomes also contributes to increased stability of molecules under processing conditions typically found in industrial processes, besides providing additional protection against chemical and enzymatic changes (Mozafari et al., 2008). Liposomes were also used in studies involving the development of new packaging materials with antimicrobial properties and nanosensors capable of detecting the degree of preservation of foods during storage (Taylor et al., 2005).

Liposomes produced from phosphatidylcholine confer an increase in the nutritional value of foods due to the high content of polyunsaturated fatty acids and residual tocopherol present in their structure (Taladrid et al., 2017). In addition, these structures can modify the digestion kinetics of bioactives, increasing their bioavailability and biostability after contact with fluids present in the gastrointestinal tract (Liu et al., 2015).

Despite their numerous advantages, some problems should be highlighted regarding the effective application of liposomes in industrial processes, including (I) the difficulty to scale-up, (II) the cost of phospholipids and (III) the lack of studies and researches on the use of liposomes in industrial large-scale (Toniazzo et al., 2014; Carvalho et al., 2015). High-cost synthetic phospholipids and purified natural phospholipids used in the pharmaceutical field are the base of most of the studies investigating the use of liposomes for food. Alternatively, non-purified soy phospholipids are nearly 20% cheaper than hydrogenated phospholipids (Yokota, Moraes & Pinho, 2012). However, the presence of unsaturated fatty acids in non-purified phospholipids may confer higher permeability/higher fluidity and lower stability to lipid bilayers (Tai et al., 2020). Also, unsaturated phospholipids are more susceptible to form hydroperoxides and other secondary oxidation products, which can enhance rancidity and reduce the shelf life of food products (Ahmed et al., 2016). Therefore, the production of phospholipid-mixed liposomes containing purified and non-purified phospholipids may promote the formation of increased stable vesicles with reduced price.

With respect to coencapsulation technique, it consists in a practice often used in the pharmaceutical field and aims to include, in the same carrier, two or more bioactives (Tardi et al., 2007). Its main objective is to promote increased activity of one or more compounds and thus increased functionality of the whole structure (Halwani et al., 2008). In medical area, the

coencapsulation is performed to prolong the circulation time of actives into the body, as well as to coordinate their targeted release (Wong & Chiu, 2011).

On the other hand, this technique is little exploited in food area. Pinilla and Brandelli (2016) produced nanoliposomes coencapsulating nisin and garlic extract aiming to reduce the proliferation of bacteria in milk. Tavano et al. (2014) encapsulated phenolic acids and flavonoids (ascorbic acid/quercetin, gallic acid/curcumin) in nanoliposomes aiming increased synergistic antioxidant effect for further application in dairy products. Marsanasco et al. (2015) produced vesicles containing omega-3, omega-6 and vitamin E aiming to fortify orange juice. Kamezaki et al. (2016) incorporated astaxanthin and tocotrienol in liposomes also aiming to verify a possible antioxidant synergistic effect between both. Lopes, Pinilla & Brandelli (2019) encapsulated both lysozyme and nisin into liposomes to produce a carrier with increased antimicrobial activity. Finally, Liu et al. (2020) coencapsulated beta-carotene and vitamin C into liposomes targeting a higher protection of the pigment over storage time.

1.5 METHODS for the production of liposomes

After the first proof of concept by Bangham, Standish & Watkins (1965), demonstrating the membrane properties of liposomes and the production in laboratory scale using the dried lipid film method, different production protocols have been investigated (Patil & Jadhav, 2014). The conventional liposome production methods can be usually divided into three steps (Woodle & Papahadjopoulos, 1989):

1. Preparation of the aqueous and lipid phases;

2. Primary processing involving lipid hydration;

3. Secondary processing (size reduction after liposome formation).

The first step, the preparation of the molecular mixtures of components, include (i) the production of the aqueous phase (buffering, pH changes, ionic strength, addition of hydrophilic compounds) or/and (ii) the production of molecular lipid mixtures (usually in organic solvents). In many cases, the organic solvent is removed from the system, to produce a dry lipid mixture in the form of a powder or a film (Lasch, Weissig, & Brandl, 2003).

After that, the primary processing follows the hydration of the dry lipid mixture, or the liposome formation itself. Such a hydration can be carried out hydrating the powder or film by replacement of organic solvent with aqueous phase, or replacement of miscible organic solvent

with aqueous phase (Woodle & Papahadjopoulos, 1989). A schematic representation is showed in Fig. 1.5.

Figure 1.5. Schematic representation of liposome formatting using the hydration of dried film lipid method
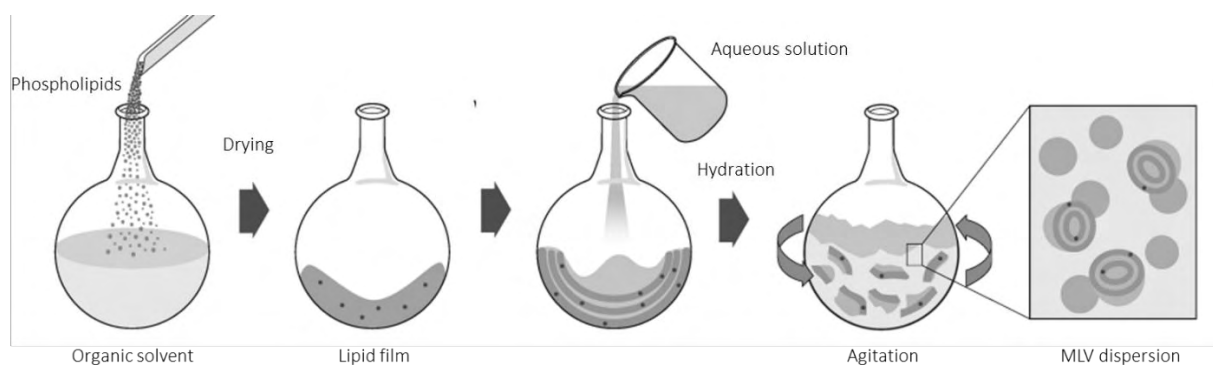
Since hydration results in liposomes with high polydispersity, then requiring a post-processing step. In this case, the changes in size observed after liposome formation are always related to a decrease in average diameter and to an increase in homogeneity, which narrows the size distribution and decrease polydispersity index. These processes normally involve input of energy for mechanical disruption such as high-pressure homogenization, microfluidization, sonication, extrusion, and dehydration-rehydration cycles (Lasic, 1998).

However, in modern approaches of liposome production, processes are not necessarily divided into three steps as described above. These modern approaches are based on the bottom-up principles, or rely on the components self-assembly. For food applications, the production method is of high concern, as the amounts of vesicles needed are massive. Some of the scalable processes are described as it follows.

(A) Solvent-injection techniques: The method was initially studied by few authors in the 70s (Batzri & Korn, 1973). It can be considered a simple and easy technique for both laboratory and industrial scale applications. A schematic representation is illustrated in Fig. 1.6. Firstly, the lipids are solubilized in an organic phase, normally a short-chain alcohol (ethanol or isopropanol, for example), and this mixture is continuously incorporated to an aqueous phase under controlled conditions (temperature, ethanol flow rate and stirring rate). The addition of

48

the organic phase into the aqueous phase provides instantaneous liposome formation, generally small unilamellar vesicles (Charcosset et al., 2015; Gouda et al., 2021). The use of ethanol as organic solvent is ideal for food applications, as it is considered to be food-grade, whereas its residue can be removed through dialysis, reverse osmosis or diafiltration (Lasic, 1998). If the liposomes will be incorporated in food, a thermal process appears as a suitable option to remove the residual ethanol. Another alternative is by using a subsequent lyophilization step.

Figure 1.6. Schematic representation of liposome formation using the ethanol injection method
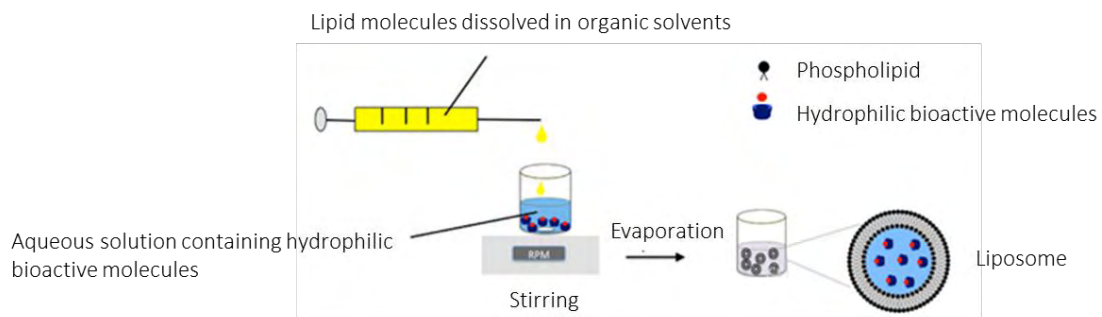
Reference: Adapted from Gharib et al. (2015)

(B) <u>Membrane contactors</u>: This technique can be easily adapted for food industry, and it is based on the ethanol injection method coupled with a membrane contactor module (Jaafar-Maalej, Charcosset, & Fessi, 2011; Pham et al., 2012). First, phospholipids are first dissolved in ethanol. Then, the alcoholic solution is pressured across a membrane (tubular porous glass) to the inner tubular direction. Aqueous phase flows in the tangential direction, allowing liposome formation as can be observed in Fig. 1.7. Process parameters that influence the vesicle characteristics are the pressure for organic phase permeation, lipid composition, aqueous-phase flow rate and membrane type (Laouini et al., 2011).

Figure 1.7. Schematic representation of liposome formation using membrane contactors
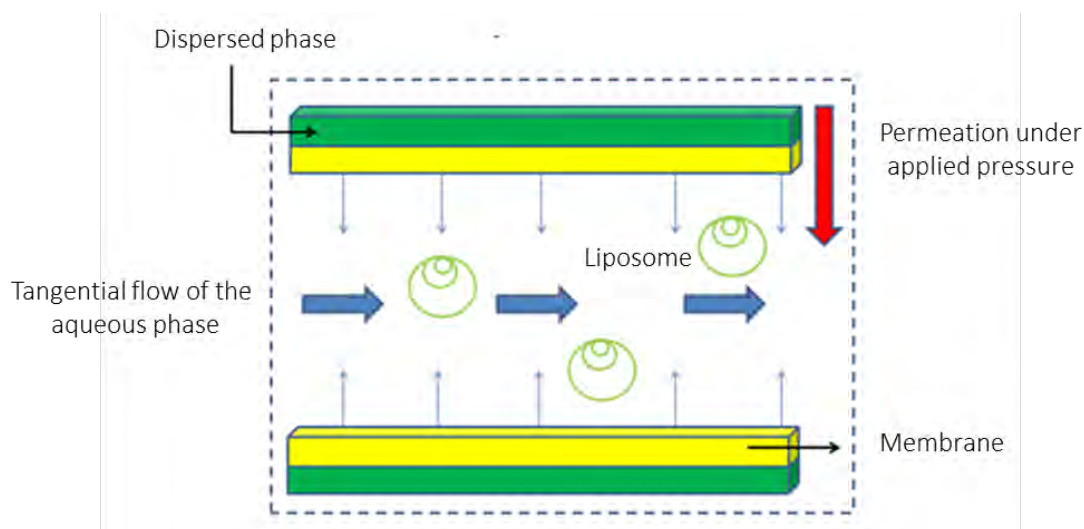
(C) <u>Hydration of proliposomes</u>: In this production method, it is necessary to first obtain a mixture of dry phospholipids and bioactives (a powder) named proliposomes. These powders can be obtained using many techniques, such as fluidized bed (Gala et al., 2015), spray drying (Toniazzo et al., 2014), freeze drying (Marín et al., 2018), coating of micronized sugars (Xu et al., 2009), milling (Ye & Liang, 2002) and supercritical techniques (Jia et al., 2019). These dry phospholipid particles are soluble in water and when hydrated (under appropriate conditions of temperature and stirring), they result in multilamellar liposomes.

The idea of "proliposomes" started with Payne et al. (1986), who defined them as dry, free-flowing particulate systems that contain in their matrix the bioactive to be encapsulated. Liposome dispersions are then obtained upon hydration. This hydration must to occur at temperatures above the phase transition temperature of the constituent phospholipids (Khan et al., 2015). The solid state of these structures ensures their stability without compromising their intrinsic activity, besides presenting advantages such as improved transport convenience, storage, distribution, and dosage, thus industrially ideal (Yan-Yu et al., 2006). Additionally, the use of proliposomes not only eliminates the stability problems of liquid liposomes, but also promotes an increase in the oral bioavailability of bioactives (Wang et al., 2018). Compared to other liposome production methods, proliposomes can be obtained in tablet or capsule form in easily industrialized procedures (Wang et al., 2018). However, some limitations surround some of these methods as, for example, cryoprotectants are required in freeze drying, whereas

others need high-cost equipment such as high-pressure homogenizers and microfluidizers (Xia et al., 2012). Also, spray drying process occurs at high temperatures, which can lead to the destruction of the phospholipid membrane of liposomes, causing a pronounced decrease in encapsulation efficiency (Gradon & Sosnowski, 2014). Moreover, this technique should be avoided to encapsulate thermosensitive bioactives (Xia et al., 2012).

A modification in the proliposome production method was suggested by Elhissi et al. (2012) and consists to drip an ethanolic solution containing phospholipids and the hydrophobic bioactive to be encapsulated onto a micronized carrier. Liposomes are also formed from the hydration of the resulting powder. Also, Elhissi et al. (2012) found that using sucrose as the micronized carrier allowed the formation of more stable liposomes than those obtained by dry lipid film hydration method. On the other hand, Elhissi et al. (2010) found that using sucrose as carrier was more efficient to minimize the size after rehydration than trehalose and lactose. Authors justified this effect to the cryoprotectant activity of sucrose. Finally, other advantages attributed to this method include the use of milder temperatures, which enables its use for the encapsulation of thermosensitive bioactives, and the higher yield obtained at the end of the process when compared to that obtained by spray drying (Silva et al., 2017). A schematic representation is illustrated in Figure 1.8.

Figure 1.8. Schematic representation of liposome formation using the hydration of proliposomes method
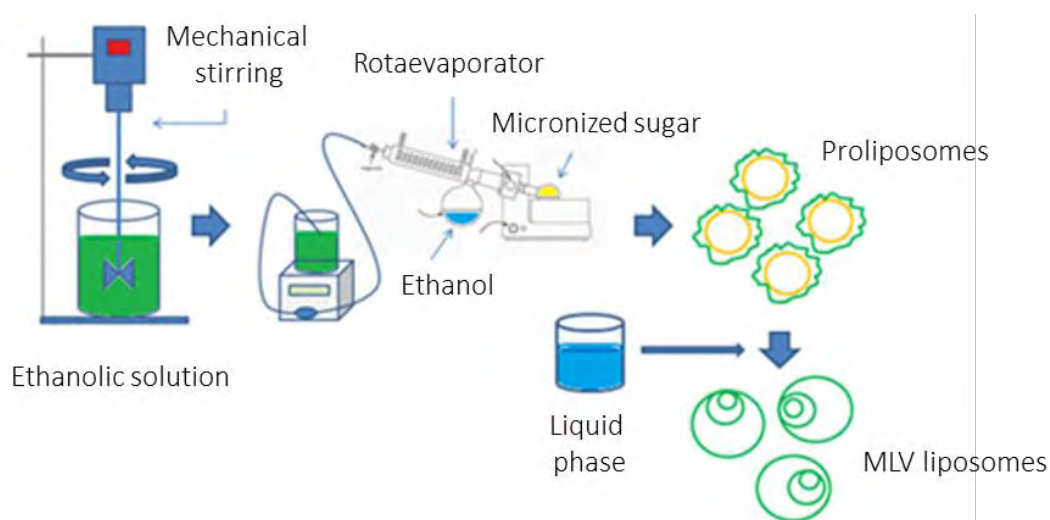
(D) <u>High-pressure homogenizers, microfluidizers and ultrasonic homogenizers</u>: These processes are commonly used to reduce the size and polydispersity of liposomes. First, it is necessary to obtain MLV dispersions and then submit these dispersions to a high shear process to decrease their size (Chung et al., 2014; Schuh et al., 2018). High-pressure homogenizers are based on pumping the liposomes dispersion at high pressure through impact valves with different configurations. This pumping at high pressure through small orifices promotes the reduction in size. Alternatively, microfluidizers also consist in pumping liposomes dispersion at high pressures, but now the dispersion flows in interaction chambers through microchannels. In this case, the high pressure (up to 275 bar) through interaction chambers promote the high shear and homogenization process, reducing particle size. Lastly, the ultrasonic homogenizers generate intense shear and pressure gradients through high intensity ultrasonic waves. The disruption of liposomes occurs due to turbulent and cavitational effects; to create ultrasonic waves, piezoelectric transducers can be used in bench-scale, whereas liquid jet generators are used in industrial scale (Canselier et al., 2002; McClements, 2005). Schematic representations of these processes are illustrated in Figure 1.9.

Figure 1.9. Schematic representation of liposome formation using (A) high-pressure homogenization, (B) microfluidization, and (C) ultrasonication

Reference: Own source
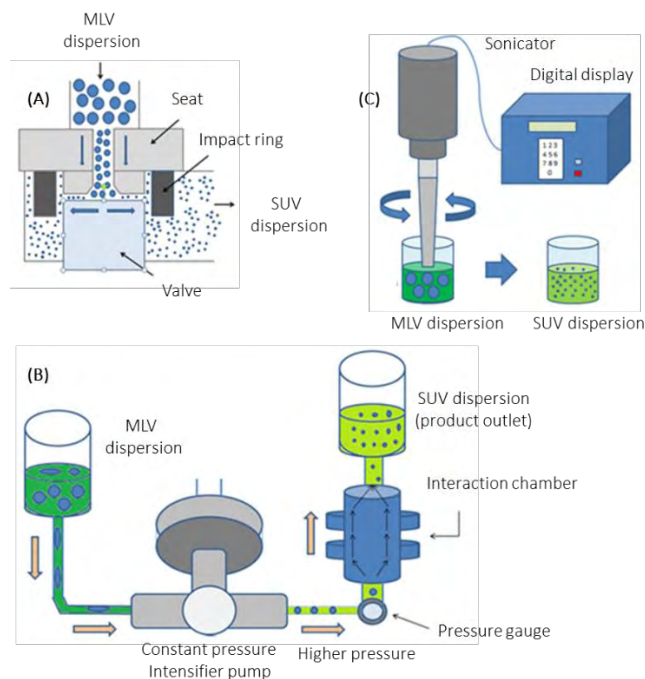
(E) <u>Supercritical fluid technology</u>: This consists as an alternative technology to the use of conventional organic solvents. Basically, fluids such as CO_2 at supercritical condition are used as the main solvent. In some cases, ethanol or other solvents can be used as co-solvents. The first reported supercritical fluid process, which is represented in Fig. 1.10, involved the mixture of lipids, co-solvent and supercritical fluid were injected into an aqueous media through a nozzle (Castor, 1994). Another strategy is the decompression method, where all materials (water, CO_2 at supercritical conditions, ethanol and lipids) flow through a nozzle allowing the intense mixing of lipids and water to form liposomes. The parameter that control liposome size is depressurization rate and the proper liposome formation depends on lipid solubilization into the solvents (supercritical CO_2 and co-solvent) (Meure, Foster, & Dehghani, 2008). In order to improve drug encapsulation or lipid solubility, different technique variations were reported (McClements, 2005). Also, the lack of mechanical stress is an alternative for labile molecules (Okate et al., 2001). Most of these processes were investigated in batch mode. Recently, efforts have demonstrated the viability to operate in continuous model (Espírito-Santo et al., 2014; Lesoin et al., 2011).

Figure 1.10. Schematic representation of liposome formation using supercritical CO_2 injection technology where (1) gas bottle, (2) cooler, (3) pump, (4) heater, (5) cosolvent, (6) lipid chamber, (7) in-line mixer, (8) nozzle, and (9) aqueous solution
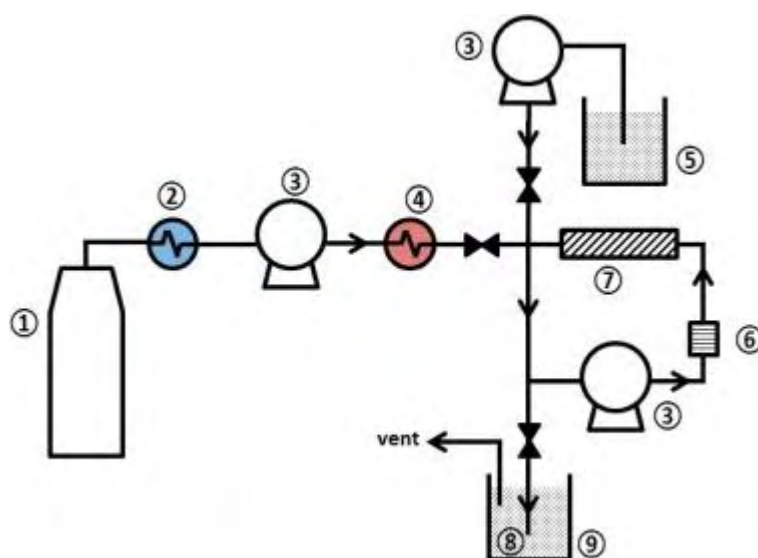
Reference: Castor (2005)

(F) <u>Microfluidic devices</u>: Microfluidic processes have deserved the attention of liposome researchers, as the main characteristic of this process is the production of phospholipid vesicles with narrow size distribution and low polydispersity. This technique explores the flow inside channels in micron dimension, which leads to laminar flow characteristics and enabling the control in space and time (Hussain et al., 2020, Jahn et al., 2010). A schematic representation of this method is illustrated in Fig. 1.11. Basically, this technique is based on a modification of ethanol injection method. First, lipids are solubilized or dispersed in an organic solvent that is soluble in water. The mixture is continuously hydro-dynamically compressed by two aqueous streams. The laminar flow across the microchannel allows a reproducible diffusion process. The lipid miscibility in organic solvent decreases, leading the formation of bilayer fragments that aggregates later in vesicles. Microfluidic allows the formation of unilamellar liposomes (Schianti et al., 2013). Its main drawback is the lack of studies regarding the scaling-up. However, the increased production can be performed by amplification techniques in which similar flow-focusing microfluidic devices are displayed in parallel configuration (Akashi et al., 1996).

Figure 1.11. Schematic representation of liposome formation using microfluidics
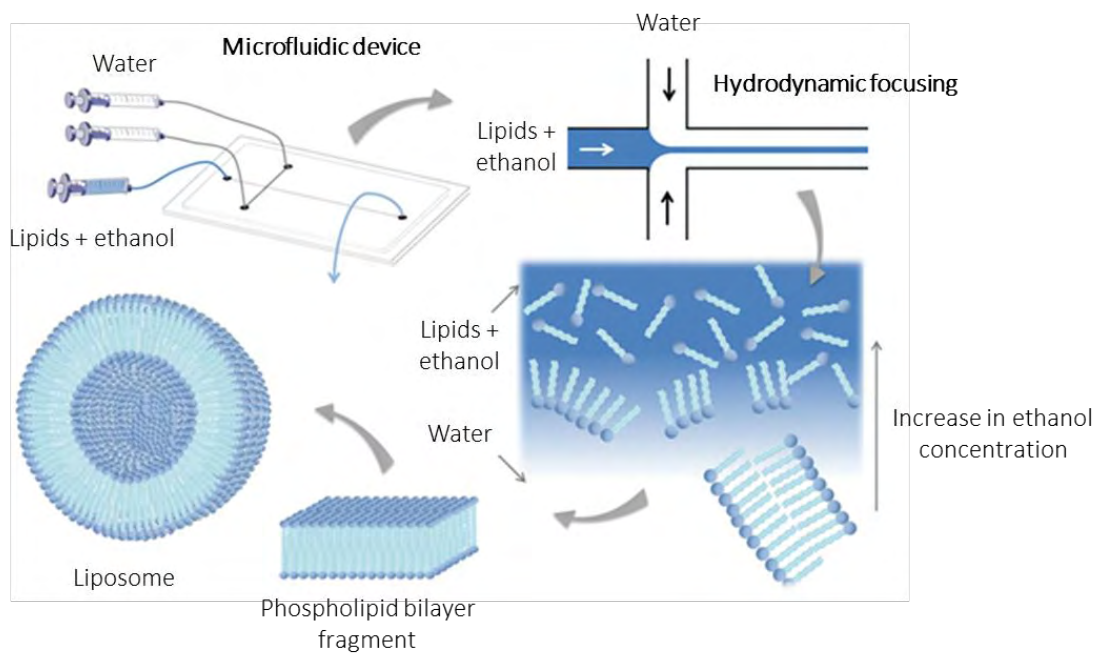
Reference: Adapted from Balbino et al. (2013)

1.6 LYOPHILIZATION: Definition and operative advantages

Lyophilization is a process widely used in food industry for the production of powdered foods (Barbosa-Canóvas et al., 2005). This practice consists of removing water from a medium, after freezing, from sublimation. Lyophilization can also be used to increase the stability of liposomes (Chen, Han, & Tang, 2010). In this context, this technique can help to prevent the hydrolysis of phospholipids and physical degradation during storage (Van Winden & Crommelin, 1999).

However, lyophilization of liposomes presents an operational problem that needs to be overcome for its effective application. It is known that lipid membranes from liposomes can be easily ruptured during the drying process due to factors such as ice crystal formation and phase transition of phospholipids (Chen, Han, & Tang, 2010). The disruption of the membrane can promote an early release of the encapsulated material, as well as aggregation and melting processes of vesicles, which results in phase separation (Sun et al., 1996).

In order to protect liposome membranes from cold damage, cryoprotectant molecules should be added to formulations (Crowe et al., 1984). Some molecules including disaccharides such as sucrose, trehalose, lactose and maltose are commonly added to liposome dispersions for such purpose (Chaudhury et al., 2012, Toniazzo et al., 2017a). Two main hypotheses have been proposed to explain the protective effect of disaccharides on membranes: the water replacement hypothesis and the vitrification model (Chen, Han, & Tang, 2010; Doxastakis., Sum, & Pablo, 2005). The water substitution hypothesis was proposed by Crowe et al. (1984) and is based on the idea that cryoprotectant molecules associate with the polar heads of phospholipids and thus maintain the lateral spacing between them in the dry state, similar to found in dispersions (Toniazzo & Pinho, 2016). Fig. 1.12. illustrates a schematic representation of mechanism depicted by water substitution hypothesis. The image shows the replacement of water molecules of the hydrophilic portion of lipid bilayer by cryoprotectant molecules, as well as eventual changes in the membrane phase transition (Doxastakis, Sum, & Pablo, 2005). The presence of disaccharides, in particular sucrose and trehalose, prevents the deleterious release of bioactives through the bilayer (Koster et al., 2000).

Figure 1.12. Schematic representation of water substitution hypothesis

Freezing → Drying →

Lyophilization with cryoprotectant ↓

Rehydration ↓

Rehydration →

▮ —— Water

⬬ —— Cryoprotectant

○ —— Head group of phospholipids

—— Acyl chain of phospholipids
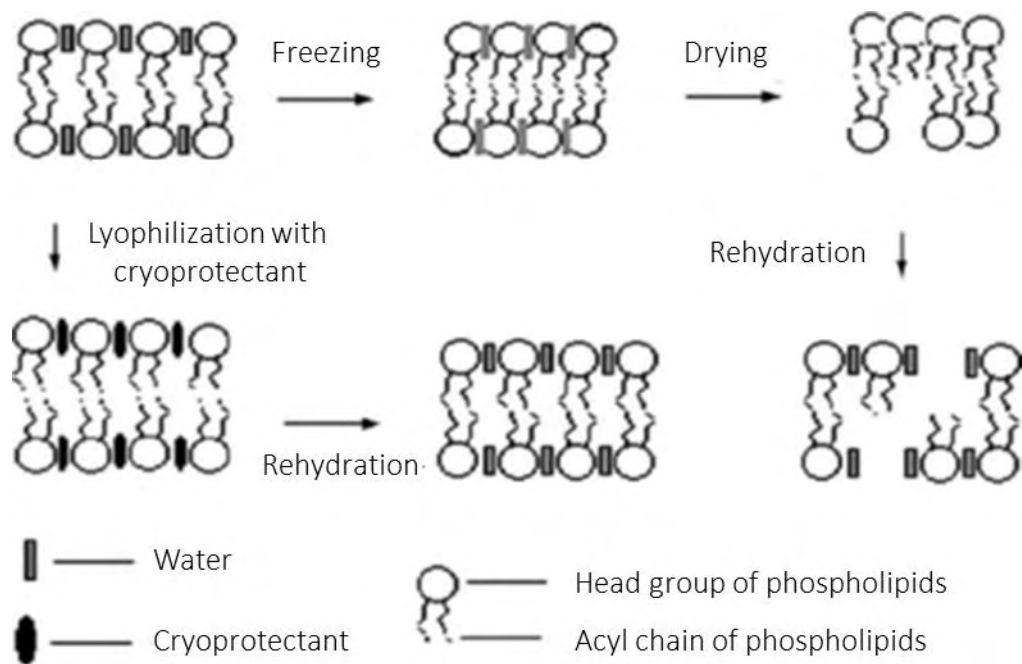
Reference: Adapted from Chen, Han, & Tang, (2010)

The second approach is based on the reduction of transition temperature of liposomes and their subsequent vitrification. In this case, the dehydrated membranes are stabilized by cryoprotectant vitrification (Ohtake et al. 2004). Carbohydrates may exist in thermodynamically unstable amorphous glassy state, possessing low molecular mobility and high viscosity (Roos, 1993). During lyophilization, the solution of sugars becomes more and more concentrated, reaching a glassy state, and trapping part of the surrounded dry material (Chen, Han, & Tang, 2010). Aggregation or melting of liposomes is prevented due to the protection provided by the glassy state of sugars, which protects liposomes from ice crystals (Wolfe & Bryant, 1999). In addition, lipid phase transition can be delayed by the action of vitrified carbohydrates (Toniazzo & Pinho, 2016).

The composition of lipid bilayer can influence the stability of vesicles after lyophilization, since phospholipids can interact differently with cryoprotectants (Toniazzo & Pinho, 2016). The type of phospholipid has a considerable effect on the cryoprotective abilities of a molecule due to the dependence between the melting temperature (T_m) and both size and unsaturation degree of the acyl chains. The retention of bioactives is also affected by lyophilization as it is related to the fluidity of lipid bilayer (Chen, Han, & Tang, 2010). Most studies conducted in the

area of liposomes lyophilization use dipalmitoylphosphatidylcholine to produce stable vesicles with minimal bioactive losses during storage (Chen, Han, & Tang, 2010). Then, little has been investigated regarding the production of lyophilized liposomes using natural phospholipids, such as lecithins obtained from egg-yolk and soybeans (Toniazzo & Pinho, 2016).

Generally, lyophilization of liposomes involves three steps (Franks, 1998):

1. Formation of ice crystals by nucleation;

2. Removal of free water by sublimation;

3. Removal of desorbed water from the dried material

In the case of liposomes, the freezing rate and osmotic pressure are factors that directly influence membrane stiffness (Chen, Han, & Tang, 2010). Thus, protocols for the sublimation and water desorption steps should be well established and should ensure that lyophilized vesicles have adequate porosity to ease hydration. Also, parameters as temperature, pressure, time, and annealing steps must to be well defined and controlled (Toniazzo & Pinho, 2016).

1.7 CORNSTARCH: Definition and applications in food

Starch is the main source of carbohydrates in vegetables. It consists in a biodegradable, renewable, and low-cost raw material that can be extracted by non-polluting methods from cereals such as corn, wheat, rice, potato, sweet potato, tapioca, and cassava. Physicochemical and functional properties of starch can vary depending on its source of obtainment (Li, Li, & Zhu, 2018). This polysaccharide is naturally found in plant cells as granules, presenting a semi-crystalline character. The crystallinity of starch grains is around 15-45% and depends on factors such as the source, composition and size of the granule populations (Matignon & Tecante, 2017).

Starch granule is mainly composed of two glucose polymers: amylose and amylopectin, whose structures are shown in Fig. 1.13. Amylose has a linear chain composed of glucopyranose units linked from α-1,4 glycosidic bond. Amylopectin presents a branched structure composed of α-D-(1,4)-glucopyranose units joined by α-1,6-type glycosidic bonds (Bahaji et al., 2014). Generally, a starch grain has about 20-25% amylose and 75-80% amylopectin. In addition to the amylose/amylopectin ratio, other factors affecting starch granule properties include the size of the amylose/amylopectin chains and the form of the latter when present in the semi-crystalline domain of the granules (Vanier et al., 2017).

Figure 1.13. Chemical structure of (A) amylose and (B) amylopectin
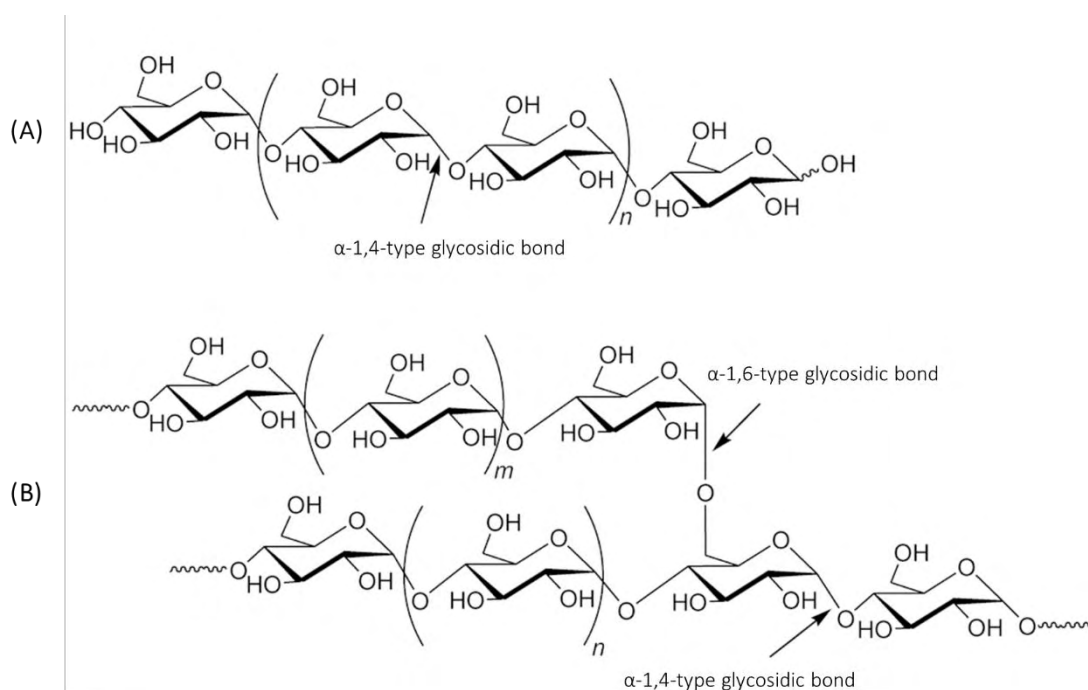
Starch granules have diameters ranging from 1 to 100 μm and the most diverse shapes (polygonal, spherical or lenticular). The internal architecture of granules is characterized by the presence of concentric growth rings arising from the hilum (Naguleswaran et al., 2014). Each growth ring (120-500 nm) is composed of blockers (20-50 nm), and each blocker is composed of semi-crystalline lamellae containing amylose and amylopectin chains (0.1-1 nm) (Le Corre, Bras, & Dufresne, 2010). In inner regions of the lamellae, crystalline areas are mainly formed by amylopectin chains, whereas the amorphous regions contain amylose and amylopectin, both attached to amylopectin branch points in disordered configuration (Naguleswaran et al., 2014).

Depending on the source, distinct properties are imparted to starch, such as viscosity, thermal stability, and retrogradation (Mahmood et al., 2017). The choice of starch should be based on the desired applications. In the food industry, starch has numerous functionalities, such as gelling agent, thickener, adhesive, and colloidal stabilizer, as well as in the control of water retention and volume increase (Singh et al., 2003). Applications in food include bakery products, sauces, soups, confectionery, sugar syrups, ice cream, snacks, beer, meat products, baby foods, and also as fat substitute (Copeland et al., 2009).

Starch contributes with about 50 to 70% of the energy obtained by the human diet as it acts as a direct source of glucose, which is an essential substrate for brain health and for the metabolic energy by red blood cells (Copeland et al., 2009). Although they appear in smaller amounts, lipids can play a significant role in determining the properties of starch. Lipids may be present on the surface of the granules in the form of triglycerides or as free fatty acids, glycolipids, and phospholipids. The lipid content of starches is related to the amylose content present in the granules: the more amylose, the greater the amount of lipids, thus the greater the amount of energy provided to the body after ingestion (Morrison & Azudin, 1987).

The native form of starch is insoluble in cold water, has a high dehydration index, a low emulsification capacity, and great instability in acidic media; hampering its direct incorporation into some food formulations (Li, Li, & Zhu, 2018). Water insolubility, the major problem, is due to the large amount of hydrogen bonds that hold chains tightly together. However, starch solubility can be increased with increased temperature to 55-70 °C in a procedure known as gelatinization (Mahmood et al., 2017). In this process, granules swell, leading to the disruption of amylopectin structure and to a consequent leaching of amylose. This process provides an increase in starch viscosity, forming a gel (Coultate, 2006). When temperature is reduced, the amylose chains rearrange themselves, increasing gel viscosity.

Retrogradation is the main factor affecting the quality of starch-based food products. Amylose retrogradation has effects in viscosity, water absorption capacity and digestibility, whereas amylopectin retrogradation leads undesirable changes in bakery products (Copeland et al., 2009). During retrogradation, amylose crystallizes rapidly, whereas amylopectin takes longer to reorganize, due to the complicated arrangement of its branched structure. Also, a high percentage of amylopectin in starch can slow down retrogradation processes during freezing and thawing (Mahmood et al., 2017). Figure 1.14 presents a schematic representation of the gelatinization and retrogradation (recrystallization) processes in starch.

Figure 1.14. Phase diagram showing the state and phase transition of starch when applying a temperature profile. Starch undergoes a transition from a crystalline to an amorphous structure when heated and a subsequent recrystallization when cooled and during storage (Tg, gelatinization temperature; AM, amylose; AP, amylopectin)
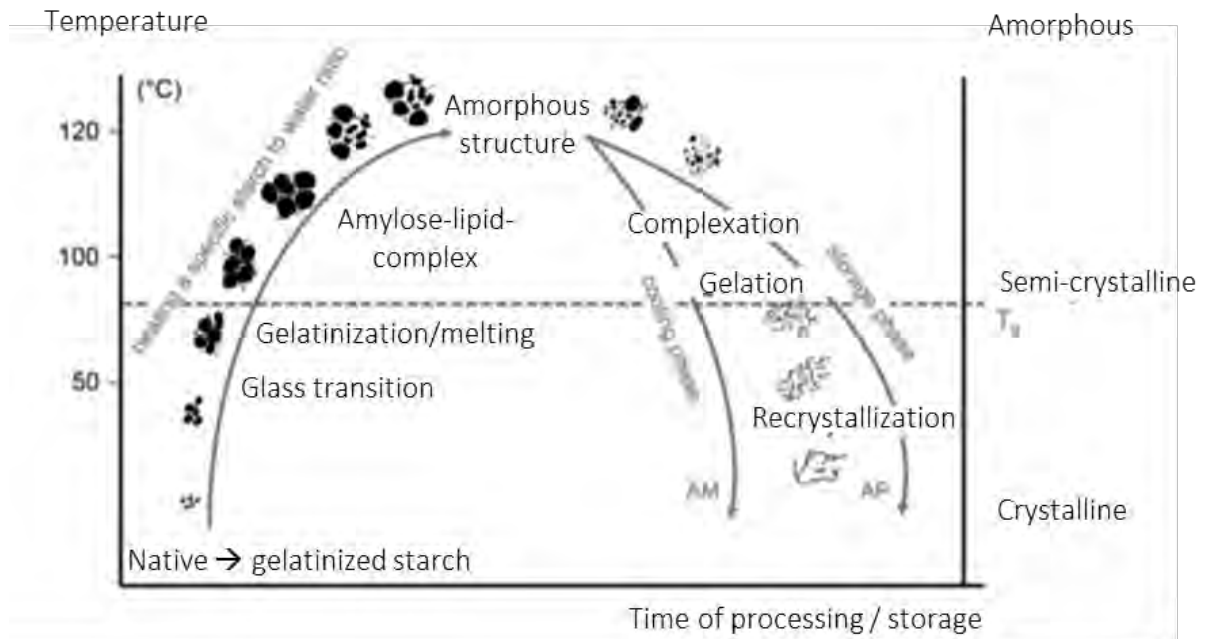
Reference: Adapted from Schirmer, Jekle, & Becker (2015)

Pasting properties are defined as those acquired after onset gelatinization temperature and include the morphological modifications from swelling to rupture of starch granules, mainly related to changes in amylose structure after leaching. Different combinations of these events, granule swelling and leaching, define the characteristics of the resulting starch dispersions, called pastes (Matignon & Tecante, 2017). The characteristics of granules after water addition are related to their swelling capacity and size. The interior of granules under these conditions has distinct phases, consisting of amylose and amylopectin. After leaching, amylose disperses in the continuous medium (Gallant, Bouchet, & Baldwin, 1997). This process occurs due to the porosity of the granules and the incompatibility between amylose and amylopectin (Svegmark & Hermansson, 1991). The pasting properties are important to understand the changes in texture or to predict retrogradation properties of products in which starch is incorporated (Lin et al., 2013).

1.8 AGGLOMERATION: Definition and applications in food

Agglomeration is a unit operation used to improve certain properties of powders, such as flowability, solubility, and porosity, from an increase in average particle diameter (Cuq, Rondet, & Abecassis, 2011). In food industry, it is mainly carried out with the aim of producing instant foods, which reconstitute rapidly in the presence of water or milk (Ji et al., 2016). Agglomeration process can be divided into three steps, as illustrated in Fig. 1.15 (Iveson et al., 2001):

1. Wetting and nucleation: stage in which the binder solution comes into contact with the dried powder, forming granules. Nucleation occurs when a particle adheres to another through the binding agents present on its surface;

2. Consolidation and coalescence: stage in which the particle diameter increases due to the contact between granules. In coalescence, the porous surface of the granule is saturated with binder forming malleable granules that are able to deform and, consequently, to unite;

3. Attrition and breakage: stage in which the granules break apart due to impacts, wears or handling processes.

Figure 1.15. Schematic representation of wet agglomeration process.

(1) Wetting and nucleation

(2) Consolidation and coalescence

(3) Attrition and breakage
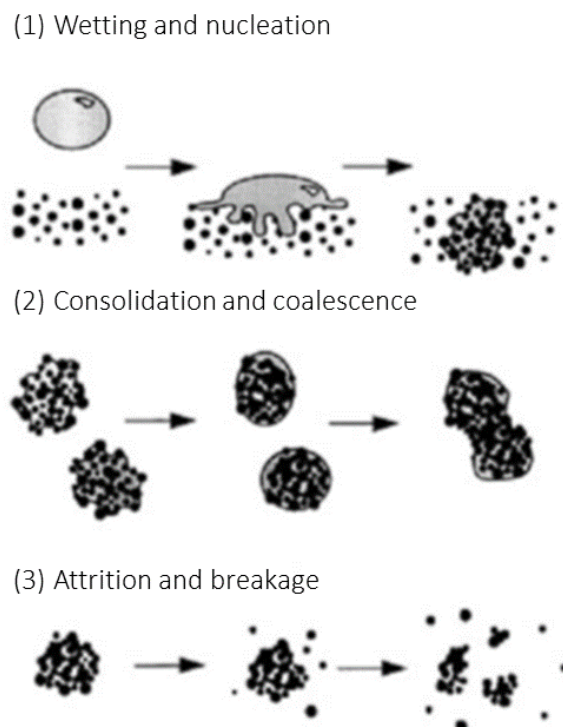
Reference: Adapted from Iveson et al. (2001)

It is common knowledge that part of the powdered foods, such as starches, flours and other particulates obtained by milling are usually characterized as fine, i.e., they have particles with diameters lower than 50 μm, mostly cohesive and difficult to fluidize. This class of powders is characterized as group C by Geldart (Masters, 1991). Therefore, there is a need to increase fluidity and decrease cohesiveness of food powders to improve their handling properties. In this context, wet agglomeration provides better particle homogenization, besides increased flowability (Reyes, Moyano, & Paz, 2007).

Wet agglomeration is used to increase the average particle size by the addition of a binder solution and mechanical action of a high shear equipment, in order to promote collisions and particle adhesion (Iveson et al., 2001) This process is used on a large scale in numerous industrial processes because of its simplicity, low operating costs and easy scaling-up (Cheng, Hsiau, & Liao, 2011; Mandato et al., 2013). The main advantages assigned to wet agglomeration include the reduction of unfavorable properties of fine powders, the increase in flowability, higher compactness and higher homogeneity (Cheng, Hsiau, & Liao., 2012; Nalesso et al., 2015). Among the wet agglomeration processes, the high shear method requires shorter processing time, lower amounts of binder solution, shorter post-processing drying time, and versatility, since it can be used to agglomerate very cohesive powders (Toniazzo et al., 2017b).

The agglomeration process is generally developed in four steps:

1. Homogenization of the dry food powders;

2. Addition of a binder solution;

3. Constant stirring of the resulting wet mass;

4. Drying of the granules.

The use of high shear equipment (mixers) contributes to the homogeneous breakdown of particles into small and cohesive aggregates, improving the dispersion of liquid around the particle surface, and thus resulting in better consolidation (Cavinato et al., 2010). The solid character of the granules enables increased chemical and microbiological stability and help to reduce transportation costs (Murrieta-Pazos et al., 2012).

In pharmaceutical area, the use of mixers for agglomeration was extensively studied by the research group of Schaefer and Kristensen (Schaefer, Holm, & Kristensen, 1992a; Schaefer, Holm, & Kristensen, 1992b; Schaefer et al., 1993a; Schaefer et al., 1993b). Since then, researchers have been successfully using high shear mixers to agglomerate particulate systems in order to increase the dissolution rate of drugs that are poorly soluble in water (Ferreira et

al., 2018; Passerini et al., 2002; Toniazzo et al., 2017b). Alternatively, in food area, most studies are focused on fluidized beds (Chemache, Kehal, & Namoune, 2021; Dacanal, Hirata, & Menegalli 2013, Fuchs et al., 2006; Jinapong, Suphantharika, & Jamnong, 2008).

1.9 References

Aditya, N.P. et al. (2013). Curcumin and genistein coloaded nanostructured lipid carriers: in vitro digestion and antiprostate cancer activity. **Journal of Agricultural and Food Chemistry**, 61(8), 1878-1883.

Aditya, N.P. et al. (2015). Co-delivery of hydrophobic curcumin and hydrophilic catechin by a water-in-oil-in-water double emulsion. **Food Chemistry**, 173, 7-13.

Ahmed, M. A. et al. (2021). Dietary intake of artificial food color additives containing food products by school-going children. **Saudi Journal of Biological Sciences**, 28(1), 27-34.

Ahmed, M. et al. (2016). Oxidation of lipids in foods. **Sarhad Journal of Agriculture**, 32(3), 230-238.

Akashi, K. I. et al. (1996). Preparation of giant liposomes in physiological conditions and their characterization under an optical microscope. **Biophysical Journal**, 71, 3242-3250.

Akbarzadeh, A. et al. (2013). Liposome: classification, preparation, and applications. **Nanoscale Research Letters**, 8, 102.

Alemán, A. et al. (2019). Encapsulation of antioxidant sea fennel (*Crithmum maritimum*) aqueous and ethanolic extracts in freeze-dried soy phosphatidylcholine liposomes. **Food Research International**, 119, 665-674.

Anderson, M., & Omri, A. (2004). The effect of different lipid components on the in vitro stability and release kinetics of liposome formulations. **Drug Delivery**, 11(1), 33-39.

ANVISA (1999). Agência Nacional de Vigilância Sanitária. Resoluções N° 382 a 389. Aprova o **Regulamento técnico que aprova o uso de Aditivos Alimentares, estabelecendo suas Funções e seus Limites Máximos para a Categoria de Alimentos 19 - Sobremesas**". DOU de 05/08/1999, n. 151. Diário Oficial da União, Brasília, DF, Brasil.

Armas, L. A., Hollis, B. W., & Heaney, R. P. (2004). Vitamin D_2 is much less effective than vitamin D_3 in humans. **The Journal of Clinical Endocrinology & Metabolism**, 89(11), 5387-5391.

Azzi, J. et al. (2018). First evaluation of drug-in-cyclodextrin-in-liposomes as an encapsulating system for nerolidol. **Food Chemistryi** 255, 399-404.

Bahaji, A. et al. (2014). Starch biosynthesis, its regulation and biotechnological approaches to improve crop yields. **Biotechnology Advances**, 32(1), 87-106.

Bajaj, S. R., & Singhal, R. S. (2021). Fortification of wheat flour and oil with vitamins B_{12} and D_3: Effect of processing and storage. **Journal of Food Composition and Analysis**, 96, 103703.

Bangham, A. D., Standish, M. M., & Watkins, J. C. (1965). Diffusion of univalent ions across lamellae of swollen phospholipids. **Journal of Molecular Biology**, 13, 238-252.

Barbosa-Canóvas, G. V. et al. (2005). Drying. In **Food Powders – Physical Properties, Processing and Functionality** (1ed). New York: Kluwer Academic/Plenum Publishers, 271-304.

Batzri, S., & Korn, E. D. (1973). Single bilayer liposomes prepared without sonication. **Biochimica et Biophysica Acta**, 298, 1015-1019.

Brandl, M. (2001). Liposomes as drug carriers: A technological approach. **Biotechnology Annual Review**, 7, 59-85.

Canselier, J. R. et al. (2002). Ultrasound emulsification – an overview. **Journal of Dispersion Science and Technology**, 23, 333-349.

Carvalho, J. M. P. et al. (2015). Physico-chemical stability and structural characterization of thickened multilamellar beta-carotene-loaded liposome dispersions produced using a proliposomes method. **Colloid and Polymer Science**, 293, 2171-2179.

Castor, T. P. (1994). **Methods and apparatus for making liposomes**. Patent WO1994027581.

Castor, T. P. (2005). Phospholipid nanosomes**. Current Drug Delivery**, 2, 329-340.

Cavinato, M. et al. (2010). Formulation design for optimal high-shear wet granulation using on-line torque measurements. **International Journal of Pharmaceutics**, 387, 48–55.

Charcosset, C. et al. (2015). Preparation of liposomes at large scale using the ethanol injection method: Effect of scale-up and injection devices. **Chemical Engineering Research and Design**, 94, 508-515.

Chaudhury, A. et al. (2012). Lyophilization of cholesterol-free PEGylated liposomes and its impact on drug loading by passive equilibration. **International Journal of Pharmaceutics**, 430(1-2), 167-175.

Chemache, L., Kehal, F., & Namoune, H. (2021). Wet agglomeration of barley flour-wheat semolina blends into couscous: Effects on rheological, culinary and sensory properties. **International Journal of Gastronomy and Food Science**, 26, 100412.

Chen, C., Han, D., Tang, X. (2010). An overview of liposome lyophilization and its future potential. **Journal of Controlled Release**, 142, 299-311.

64

Cheng, H. J., Hsiau, S. S., & Liao, C. C. (2012). Influence of the initial volume fill ratio of the granulator on melt agglomeration behavior in a high-shear mixer. **Advanced Powder Technology**, 23, 46-54.

Cheng, H. J., Hsiau, S. S., & Liao, C. C. (2011). Influence of the interaction between binder and powders on melt agglomeration behavior in a high-shear mixer. **Powder Technology**, 211, 165-175.

Chung, S. K. et al. (2014). Factors influencing the physicochemical characteristics of cationic polymer-coated liposomes prepared by high-pressure homogenization. **Colloids and Surfaces A: Physicochemical and Engineering Aspects**, 454, 8-15.

Copeland, L. et al. (2009). Form and functionality of starch. **Food Hydrocolloids**, 23(6), 1527-1534.

Coultate, T. P. (2006). **Food: The Chemistry of Its Components.** London: The Royal Society of Chemistry, Polytechnic of the South Bank, London.

Crowe, J. H. et al. (1984). Interaction of phospholipids monolayers with carbohydrate. **Biochimica et Biophysica Acta**, 769, 151-159.

Cuq, B., Rondet, E., & Abecassis, J. (2011). Food Powders engineering, between knowhow and science: Constraints, stakes and opportunities. **Powder Technology**, 208(2), 244-251.

Dacanal, G. C., Hirata, T. A. M., & Menegalli, F. C. (2013). Fluid dynamics and morphological characterization of soy protein isolate particles obtained by agglomeration in pulsed-fluid bed. **Powder Technology**, 247, 222-230.

Dai, L. et al. (2019). Curcumin encapsulation in zein-rhamnolipid composite nanoparticles using a pH-driven method. **Food Hydrocolloids**, 93, 342-350.

Demirci, M. et al. (2017). Encapsulation by nanoliposomes. **Nanoencapsulation technologies for the food and nutraceutical industries**, Academic Press, 74-113.

Desai, K. G. H., & Park, H. J. (2005). Recent developments in microencapsulation of food ingredients. **Drying Technology**, 23(7), 1361-1394.

Dong, W. et a. (2022). Preparation and characterization of egg yolk immunoglobulin loaded chitosan-liposome assisted by supercritical carbon dioxide. **Food Chemistry**, 369, 130934.

Doxastakis, M., Sum, A. K., & Pablo, J. J. (2005). Modulating membrane properties: The effect of trehalose and cholesterol on a phospholipid bilayer. **The Journal of Physical Chemistry B**, 109(50), 24173-24181.

Drake. J. J-P. (1975). Food colours – harmless aesthetics or epicurean luxuries? **Toxicology**, 5(1), 3-42.

Elhissi, A. et al. (2010). Development and characterisation of freeze-dried liposomes containing two-asthma drugs. **Micro & Nano Letters**, 5(3), 184-188.

Elhissi, A. M. A. et al. (2012). A study of size, microscopic morphology, and dispersion mechanism of structures generated on hydration of proliposomes. **Journal of Dispersion Science and Technology**, 33(8), 1121-1126.

Emami, S. et al. (2016). Liposomes as carrier vehicles for functional compound in food sector. **Journal of Experimental Nanoscience**, 11(9), 737-759.

Erami, S. R., Amiri, Z. R., & Jafari, S. M. (2019). Nanoliposomal encapsulation of Bitter Gourd (Momordica charantia) fruit extract as a rich source of health-promoting bioactive compounds. **LWT**, 116, 108581.

Espírito-Santo, I. et al. (2014). Liposomes preparation using a supercritical fluid assisted continuous process. **Chemical Engineering Journal**, 249, 153–159.

Feketea, G.; Tsabouri, S. (2017). Common food colorants and allergic reactions in children: Myth of reality? **Food Chemistry**, 230, 578-588.

Ferreira, L. S. et al. (2018). Wet agglomeration by high shear of binary mixtures of curcumin-loaded lyophilized liposomes and cornstarch: Powder characterization and incorporation in cakes. **Food Bioscience**, 25, 74-82.

Franks, F. (1998). Freeze-drying of bioproducts: putting principles into practice. **European Journal of Pharmaceutics and Biopharmaceutics**, 45, 221-229.

Frenzel, M., & Steffen-Heins, A. (2015). Impact of quercetin and fish oil encapsulation on bilayer membrane and oxidation stability of liposomes. **Food Chemistry**, 185, 48-57.

Fuchs, M. et al. (2006). Encapsulation of oil in powder using spray drying and fluidised bed agglomeration. **Journal of Food Engineering**, 75, 27-35.

Gala, R. P. et al. (2015). A comprehensive production method of self-cryoprotected nano-liposome powders. **International Journal of Pharmaceutics**, 486(1-2), 153-158.

Gallant, D. J., Bouchet, B., & Baldwin, P. M. (1997). Microscopy of starch: evidence of a new level of granule organization. **Carbohydrate Polymers**, 32(3-4), 177-191.

Gebhardt, B. (2020). Assessing the sustainability of natural and artificial food colorants. **Journal of Cleaner Production**, 260, 120884.

Gharib, R. et al. (2017). Hydroxypropyl-ß-cyclodextrin as a membrane protectant during freeze-drying of hydrogenated and non-hydrogenated liposomes and molecule-in-cyclodextrin-in- liposomes: Application to trans-anethole. **Food Chemistry,** 267, 67-74.

Ghorbanzade, T. et al. (2017). Nano-encapsulation of fish oil in nano-liposomes and its application in fortification of yogurt. **Food Chemistry**, 216, 146-152.

Gibis, M., Ruedt, C., & Weiss, J. (2016). In vitro release of grape-seed polyphenols encapsulated from uncoated and chitosan-coated liposomes. **Food Research International**, 88(A), 105-113.

Gomes, F. P. et al. (2015). Simultaneous quantitative analysis of eight vitamin D analogues in milk using liquid chromatography-tandem mass spectrometry. **Analytica Chimica Acta**, 891, 211-220.

Gouda, A. et al. (2021). Ethanol injection technique for liposomes formulation: An insight into development, influencing factors, challenges and applications. **Journal of Drug Delivery Science and Technology**, 61, 102174.

Gradon, L.., & Sosnowski, T. R. (2014). Formation of particles for dry powder inhalers. **Advanced Powder Technology**, 25, 43-44.

Grit, M., & Crommelin, D. J. (1993). Chemical stability of liposomes: Implications for their physical stability. **Chemistry and Physics of Lipids**, 64(1-3), 3-38.

Guldiken, B. et al. (2019). Formation and characterization of spray dried coated and uncoated liposomes with encapsulated black carrot extract. **Journal of Food Engineering**, 246, 42-50.

Gültekin-Özgüver, M. et al. (2016). Fortification of dark chocolate with spray dried black mulberry (*Morus nigra*) waste extract encapsulated in chitosan-coated liposomes and bioaccessability studies. **Food Chemistry**, 201, 205-212.

Hadian, Z. (2016). A review of nanoliposomal delivery system for stabilization of bioactive omega-3 fatty acids. **Electron Physician**, 8(1), 1776-1785.

Halwani, M. et al. (2008). Co-encapsulation of gallium with gentamicin in liposomes enhances antimicrobial activity of gentamicin against *Pseudomonas seruginosa*. **Journal of Antimicrobial Chemotherapy**, 62, 1291-1297.

Holick, M. F. (2007). Vitamin D deficiency. **The New England Journal of Medicine**, 357(3), 266-281.

Holick, M. F. (2017). The vitamin D deficiency pandemic: Approaches for diagnosis, treatment and prevention. **Reviews in Endocrine & Metabolic Disorders**, 18(2), 153-165.

Holick, M. F., & Chen, T. C. (2008). Vitamin D deficiency: a worldwide problem with health consequences. **The American Journal of Clinical Nutrition**, 87(4), 1080S-1086S.

Huang, J. et al. (2020). Liposome-chitosan hydrogel bead delivery system for the encapsulation of linseed oil and quercetin: Preparation and in vitro characterization studies. **LWT**, 117, 108615.

Hussain, M. T. et al. (2020). Freeze-drying cycle optimization for the rapid preservation of protein-loaded liposomal formulations. **International Journal of Pharmaceutics**, 573, 118722.

Israelachvili, J. N., & Sornette, D. (1985). The interdependence of intra-aggregate and inter-aggregate forces, **Journal de Physique Archives**, 46(12), 2125-2136.

Iveson, S. M. et al. (2001). Nucleation, growth and breakage phenomena in agitated wet granulation processes: a review. **Powder Technology**, 117(1-2), 3-39.

Jaafar-Maalej, C., Charcosset, C., & Fessi, H. (2011). A new method for liposome preparation using a membrane contactor. **Journal of Liposome Research**, 21, 213-220.

Jahn, A. et al. (2010). Microfluidic mixing and the formation of nanoscale lipid vesicles. **ACS Nano**, 4, 2077-2087.

Ji, J. et al. (2016). Rehydration behaviors of high protein dairy powders: The influence of agglomeration on wettability, dispersibility and solubility. **Food Hydrocolloids**, 58, 194-203.

Jia, J. et al. (2019). Berberine-loaded solid proliposomes prepared using solution enhanced dispersion by supercritical CO_2: Sustained release and bioavailability enhancement. **Journal of Drug Delivery Science and Technology**, 51, 356, 363.

Jiang, T., Ghosh, R., & Charcosset, C. (2021). Extraction, purification and applications of curcumin from plant materials-A comprehensive review. **Trends in Food Science & Technology**, 112, 419-430.

Jinapong, N., Suphantharika, M., & Jamnong, P. (2008). Production of instant soymilk powders by ultrafiltration, spray drying and fluidized bed agglomeration. **Journal of Food Engineering**, 84, 194-205.

Kamezaki, C. et al. (2016). Synergistic antioxidative effect of astaxanthin and tocotrienol by co-encapsulated in liposomes. **Journal of Clinical Biochemistry and Nutrition**, 59(2), 100-106.

Katouzian, I., & Jafari, S. M. (2016). Nano-encapsulation as a promising approach for targeted delivery and controlled release of vitamins. **Trends in Food Science & Technology**, 53, 34-48.

Kazmi, S. A., Vieth, R., & Rousseau, D. (2007). Vitamin D_3 fortification and quantification in processed dairy products. **International Dairy Journal**, 17(7), 753-759.

Khan, I et al. (2015). Proliposome powders prepared using a slurry method for the generation of beclomethasone dipropionate liposomes. **International Journal of Pharmaceutics**, 496(2), 342-350.

Koster, K. L. et al. (2000). Effects of vitrified and nonvitrified sugars on phosphatidylcholine fluid-to-gel phase transitions. **Biophysical Journal**, 78(4), 1932-1946.

Koynova, R., & Caffrey, M. (1998). Phases and phase transitions of the of the phosphatidylcholines. **Biochimica et Biophysica Acta**, 1376(1), 91-145.

Lakshmi, C. G. (2017). Food Coloring: The Natural Way. **Research Journal of Chemical Sciences**, 4(2), 87-96.

Laouini, A. et al. (2011). Liposome preparation using a hollow fiber membrane contactor - Application to spironolactone encapsulation. **International Journal of Pharmaceutics**, 415, 53-61

Laouini, A. et al. (2012). Preparation, characterization and applications of liposomes: State of the art. **Journal of Colloidal Science and Biotechnology**, 1, 147-168.

Lasch, J., Weissig, V., & Brandl, M. (2003). Preparation of liposomes, in: **Liposomes: A Practical Approach** 2nd ed, Oxford University Press, 24-25.

Lasic, D. D. (1998). Novel applications of liposomes, **Trends in Biotechnology**, 16(7), 307-321.

Le Corre, D., Bras, J., & Dufresne, A. (2010). Starch nanoparticles: A review. **Biomacromolecules,** 11(5), 1139-1153.

Lehmkuhler, A. L. et al. (2020). Certified food dyes in over the counter medicines and supplements marketed for children and pregnant women. **Food and Chemical Toxicology**, 143, 111499.

Lemoine, A. et al. (2020). Adverse reactions to food additives in children: A retrospective study and a prospective survey. **Archives de Pédiatrie**, 27(7), 368-371.

Lesoin, L. et al. (2011). Development of a continuous dense gas process for the production of liposomes. **The Journal of Supercritical Fluids**, 60, 51-62.

Li, J. et al. (2021). Ascorbyl palmitate effects on the stability of curcumin-loaded soybean phosphatidylcholine liposomes. **Food Bioscience**, 41, 100923.

Li, M.., Li, J., & Zhu, C. (2018). Effect of ultrasound pretreatment on enzymolysis and physicochemical properties of corn starch. **International Journal of Biological Macromolecules**, 111, 848-856.

Li, Z., Paulson, A. T., & Gill, T. A. (2015). Encapsulation of bioactive salmon protein hydrolysates with chitosan-coated liposomes. **Journal of Functional Foods**, 19(A), 733-743.

Lin, J-H. et al. (2013). Effect of granular characteristics on pasting properties of starch blends. **Carbohydrate Polymers**, 98(2), 1553-1560.

Liu, W. et al. (2015). Behavior of liposomes loaded with bovine serum albumin during in vitro digestion. **Food Chemistry**, 175, 16-24.

Liu, W. et al. (2016). Multilayered vitamin C nanoliposomes by self-assembly of alginate and chitosan: Long-term stability and feasibility application in mandarin juice. **LWT - Food Science & Technology**, 75, 608-615.

Liu, X. et al. (2020). Co-encapsulation of Vitamin C and β-Carotene in liposomes: Storage stability, antioxidant activity, and *in vitro* gastrointestinal digestion. **Food Research International**, 136, 109587.

Liu, Y. et al, (2015). Temperature-dependent structure stability and in vitro release of chitosan-coated curcumin liposome. **Food Research International**, 74, 97-105.

Liu, Y. et al. (2021). Improvement in storage quality of postharvest tomato fruits by nitroxyl liposomes treatment. **Food Chemistry**, 359, 129933.

Liu, Y., Bravo, K. M. C., & Liu, J. (2021). Targeted liposomal drug delivery: a nanoscience and biophysical perspective. **Nanoscale Horizons**, 6, 78-94.

Lopes, N. A., Pinilla, C. M. B., & Brandelli, A. (2019). Antimicrobial activity of lysozyme-nisin co-encapsulated in liposomes coated with polysaccharides. **Food Hydrocolloids,** 93, 1-9.

Lopez-Polo, J. et al. (2020). Effect of lyophilization on the physicochemical and rheological properties of food grade liposomes that encapsulate rutin. **Food Research International**, 130, 108967.

Ložnjak, P., & Jakobsen, J. (2018). Stability of vitamin D_3 and vitamin D_2 in oil, fish and mushrooms after household cooking. **Food Chemistry**, 254, 144-149.

Mahmood, K. et al. (2017). A review: Interaction of starch/non-starch hydrocolloid blending and the recent food applications. **Food Bioscience**, 19, 110-210.

Manconi, M. et al. (2016). Polymer-associated liposomes for the oral delivery of grape pomace extract. **Colloids and Surfaces B: Biointerfaces**, 146, 910-917.

Mandato, S. et al. (2013). In-line monitoring of durum wheat semolina wet agglomeration by near infrared spectroscopy for different water supply conditions and water addition levels. **Journal of Food Engineering**, 119, 533-543.

Marín, D. et al. (2018). Freeze-dried phosphatidylcholine liposomes encapsulating various antioxidant extracts from natural waste as functional ingredients in surimi gels. **Food Chemistry**, 245, 535-535.

Marsanasco, M. et al. (2015). Bioactive constituents in liposomes incorporated in orange juice as new functional food: thermal stability, rheological and organoleptic properties. **Journal of Food Science and Technology,** 52(121), 7828-7838.

Marsanasco, M., Chiaramon, N. S., & Alonso, S. V. (2017). Liposomes as matrices to hold bioactive compounds for drinkable food: Their ability to improve heath and future prospects. In: **Functional Food – Improve health through Adequate Food**. InTech Open, 2017.

Masters, K. (1991). **Spray drying handbook** (5th ed). Essex, UK: Longman Scientific & Technical.

Matignon, A., & Tecante, A. (2017). Starch retrogradation: From starch components to cereal products. **Food Hydrocolloids,** 68, 43-52.

Maurya, V. K., Bashir, K., & Aggarwal, M. (2020). Vitamin D microencapsulation and fortification: Trends and technologies. **The Journal of Steroid Biochemistry and Molecular Biology**, 196, 105489.

McCann, D. et al. (2007). Food additives and hyperactive behavior in 3-year-old and 8/9-year-old children in the community: a randomized, double blinded, placebo-controlled trial. **The Lancet**, 370, 9598, 1560-1567.

McClements, D. J. (2020). Advances in nanoparticle and microparticle delivery systems for increasing the dispersibility, stability, and bioactivity of phytochemicals. **Biotechnology Advances**, 38, 107287.

McClements, D.J. (2005). **Food emulsions: principles, practice and techniques**. New York: CRC Press.

McCourt, A. et al. (2020). Efficacy and safety of food fortification to improve vitamin D intakes of older adults. **Nutrition**, 75-76, 110767.

Meure, L. A, Foster, N. R. & Dehghani, F. (2008). Conventional and dense gas techniques for the production of liposomes: a review. **AAPS PharmSciTech**, 9, 798-809.

Morrison, W. R., & Azudin, M. N. (1987). Variation in the amylose and lipid contents and some physical properties of rice starches. **Journal of Cereal Science**, 5(1), 35-44.

Mozafari, M.R. et al. (2008). Nanoliposomes and their applications in food technology. **Journal of Liposome Research**, 18(4), 309-327.

Murrieta-Pazos, I et al. (2012). Food powders: Surface and form characterization revisited. **Journal of Food Engineering**, 112, 1-21.

Naguleswaran, S. et al. (2014). Amylolysis of amylopectin and amylose isolated from wheat, triticale, corn and barley starches. **Food Hydrocolloids**, 35, 686-693.

Nalesso, S. et al. (2015). Texture analysis as a tool to study the kinetics of wet agglomeration processes. **International Journal of Pharmaceutics**, 485, 61-69.

New, R.R.C. (1990). **Liposomes: A practical approach**, New York: IRL Press.

Ohtake, S. et al. (2004). Effect of sugar-phosphate mixtures on the stability of DPPC membranes in dehydrated systems. **Cryobiology**, 48, 81-89.

Okate, K. et al. (2001). Development of a new preparation method of liposomes using supercritical carbon dioxide. **Langmuir**, 17, 3898-3901.

Passerini, N. et al. (2002). Preparation and characterisation of ibuprofenpoloxamer 188 granules obtained by melt granulation. **European Journal of Pharmaceutical Sciences**, 15, 71–78.

Patil, Y. P, & Jadhav, S. (2014). Novel methods for liposomes preparation. **Chemistry and Physics of Lipids,** 177, 8-18.

Payne, N. I. et al. (1986). Proliposomes: A novel solution to an old problem. **Journal of Pharmaceutical Sciences**, 75(4), 325-329.

Penry, J. T., & Manore, M. M. (2008). Choline: an important micronutrient for maximal endurance-exercise performance. **International Journal of Sport Nutrition and Exercise Metabolism**, 18(2), 191-203.

Pham, T-T. et al. (2012). Liposome and niosome preparation using a membrane contactor for scale-up. **Colloids and Surfaces B: Biointerfaces**, 94, 15-21.

Pinilla, C. M. B. et al. (2020). Structural features of myofibrillar fish protein interacting with phosphatidylcholine liposomes. **Food Research International**, 137, 109687.

Pinilla, C. M. B., & Brandelli, A. (2016). Antimicrobial activity of nanoliposomes co-encapsulating nisin and garlic extract against gram-positive and Gram-negative bacteria in milk. **Innovative Food Science & Emerging Technologies**, 36, 287-293.

Pokorný, J. (2003). Phospholipids. In **Chemical and Functional Properties of Food Lipids**. Z.E. Sikorski, A. Kołakowska (Eds.). CRC Press: Boca Raton. London, New York, Washington, D.C, 79-92.

Ramli, N. A. et al. (2021). Physicochemical characteristics of liposome encapsulation of stingless bees' propolis. **Heliyon**, 7(4), e06649.

Rashidinejad, A. et al. (2014). Delivery of green tea catechin and epigallocatechin gallate in liposomes incorporated into low-fat hard cheese. **Food Chemistry**, 156, 176-183.

Reyes, A., Moyano, P., & Paz, J. (2007). Drying of potato slices in a pulsed fluidized bed. **Drying Technology**, 25, 581-590.

Sabet, S. et al. (2021). Recent advances to improve curcumin oral bioavailability. Trends in **Food Science & Technology**, 110, 253-266.

Sahari, M. A. et al. (2017). Physicochemical properties and antioxidant activity of α-tocopherol loaded nanoliposome's containing DHA and EPA. **Food Chemistry**, 215, 157-164.

Schaefer, T. et al. (1993a). Melt pelletization in high shear mixer. IV. Effects of process variables in a small laboratory scale mixer. **European Journal of Pharmaceutical Sciences**, 1, 125–131.

Schaefer, T. et al. (1993b). Melt pelletization in high shear mixer. V. Effects of apparatus variables. **European Journal of Pharmaceutical Sciences**, 1, 133–141.

Schaefer, T., Holm, P., & Kristensen, H. G. (1992a). Melt pelletization in high shear mixer. I. Effects of process variables and binder. **Acta Pharmaceutica Nordica**, 4, 133–140.

Schaefer, T., Holm, P., Kristensen, H. G. (1992b). Melt pelletization in high shear mixer. II. Power consumption and granule growth. **Acta Pharmaceutica Nordica**, 4, 141–148.

Schianti, J. N. et al. (2013). Scaling up of rifampicin nanoprecipitation process in microfluidic devices. **Progress in Nanotechnology and Nanomaterials**. 2, 101-107.

Schirmer, M., Jekle, M., & Becker, T. (2014). Starch gelatinization and its complexity for analysis. **Starch – Stärke**, 67(1-2), 30-41.

Schuh, R. S. et al. (2018). Physicochemical properties of cationic nanoemulsions and liposomes obtained by microfluidization complexed with a single plasmid or along with an oligonucleotide: Implications for CRISPR/Cas technology. **Journal of Colloid and Interface Science,** 530, 243-255.

Sebaaly, C. et al. (2016). Effect of composition, hydrogenation of phospholipids and lyophilization on the characteristics of eugenol-loaded liposomes prepared by ethanol injection method. **Food Bioscience,** 15, 1-10.

Silva, G. S. et al. (2017). Characterisation of curcumin-loaded proliposomes produced by coating of micronized sucrose and hydration of phospholipid powders to obtain multilamellar liposomes. **International Journal of Food Science & Technology**, 52(3), 772-780.

Singh, N. et al. (2003). Morphological, thermal and rheological properties of starches from different botanical sources. **Food Chemistry**, 81(2), 219-231.

Suktham, K. et al. (2016). Physical and biological characterization of sericin-loaded copolymer liposomes stabilized by polyvinyl alcohol. **Colloids and Surfaces B: Biointerfaces**, 148, 487-495.

Sun, W. Q. et al. (1996). Stability of dry liposomes in sugar glasses. **Biophysical Journal**, 70, 1769-1776.

Svegmark, K., & Hermansson, A. M. (1991). Distribution of amylose and amylopectin in potato starch pastes: effects of heating and shearing. **Food Structure,** 10(2), 117-129.

Tai, K. et al. (2020). Stability and release performance of curcumin-loaded liposomes with varying content of hydrogenated phospholipids. **Food Chemistry**, 326, 126973.

Taladrid, D. et al. (2017). Effect of chemical composition and sonication procedure on properties of food-grade soy lecithin liposomes with added glycerol. **Food Research International**, 100, Part 1, 541-550.

Tardi, P. G. et al. (2014). Coencapsulation of irinotecan and floxuridine into low cholesterol-containing liposomes that coordinate drug release in vivo. **Biochimica et Biophysica Acta**, 1768, 678-687.

Tavano, L. et al. (2014). Co-encapsulation of antioxidants into niosomal carriers: gastrointestinal release studies for nutraceutical applications. **Colloids and Surfaces B: Biointerfaces**, 114, 82-88.

Taylor, T.M. et al. (2005). Liposomal nanocapsules in food science and agriculture. **Critical Reviews in Food Science and Nutrition**, 45(7-8), 587-605.

Thompson, A. K., Mozafari, M. R., & Singh, H. (2007). The properties of liposomes produced from milk fat globule membrane material using different techniques. **Le Lait**, 87(4-5), 349-360.

Toniazzo, T. et al. (2014). β-carotene-loaded liposome dispersions stabilized with xanthan and guar gums: Physico-chemical stability and feasibility of application in yogurt. **LWT – Food Science and Technology**, 59(2), 1265-1273.

Toniazzo, T. et al. (2017a). Encapsulation of quercetin in liposomes by ethanol injection and physicochemical characterization of dispersions and lyophilized vesicles. **Food Bioscience**, 19, 17-25.

Toniazzo, T. et al. (2017b). Production of cornstarch granules enriched with quercetin liposomes by aggregation of particulate binary mixtures using high shear process. **Journal of Food Science**, 82(11), 2626-2633.

Toniazzo, T., & Pinho, S. C. (2017). Lyophilized liposomes for food applications: Fundamentals, processes, and potential applications. In: **Encapsulation and Controlled Release Technologies in Food Systems**. Lakkis, J. M. (ed.). New York: John Wiley & Sons, 78-96.

Trucillo, P. et al. (2018). Supercritical assisted process for the encapsulation of olive pomace extract into liposomes. **The Journal of Supercritical Fluids**, 135, 152-159.

Van Winden, E. C., & Crommelin, D. J. (1999). Short term stability of freeze-dried, lyoprotected liposome. **Journal of Controlled Release**, 58, 69-86.

Vanier, N. L. et al. (2017). Molecular structure, functionality and applications of oxidized starches: A review. **Food Chemistry**, 221, 1546-1559.

Vergara, D. et al. (2020). An *in vitro* digestion study of encapsulated lactoferrin in rapeseed phospholipid–based liposomes. **Food Chemistry** 321, 126717.

Villanueva-Bermejo, D., & Temelli, F. (2020). Optimization of coenzyme Q10 encapsulation in liposomes using supercritical carbon dioxide. **Journal of CO_2 Utilization**, 38, 68-76.

Wang, Q. et al. (2018). A novel formulation of [6]-gingerol: proliposomes with enhanced oral bioavailability and antitumor effect. **International Journal of Pharmaceutics**, 535(1-2), 308-315.

Wolfe, J., & Bryant, G. (1999). Freezing, drying, and/or vitrification of membrane-solute-water systems. **Cryobiology**, 39, 103-129.

Wong, M. Y., & Chiu, G. N. (2011). Liposomes formulation of co-encapsulated vincristine and quercetin enhanced antitumor activity in a trastuzumab-insensitive breast tumor xenograft model. **Nanomedicine**, 7(6), 834-840.

Woodle, M. C., & Papahadjopoulos, D. (1989). Liposome preparation and size characterization. **Methods in Enzymology**, 171, 193-217.

Xia, F. et al. (2012). Preparation of lutein proliposomes by supercritical anti-solvent technique. **Food Hydrocolloids**, 26(2), 456-463.

Xu, H. et al. (2009). Optimized preparation of vinpocetine proliposomes by a novel method and in vivo evaluation of its pharmacokinetics in New Zealand rabbits. **Journal of Control Release**, 140(1), 61-68.

Yan-Yu, X. et al. (2006). Preparation of silymarin proliposome: a new way to increase oral bioavailability of silymarin in beagle dogs. **International Journal of Pharmaceutics**, 319(1-2), 162-168.

Ye, Z. W., & Liang, W. Q. (2002). Preparation of interferon-containing liposomes by the powder bed grinding method. **Journal of Zhejiang University**, 31, 433-436.

Yip, H. S. H., Ashraf-Khorassani, M., & Taylor, L. T. (2007). Feasibility of phospholipids separation by packed column SFC with mass spectrometric and light scattering detection. **Chromatographia**, 65, 655-665.

Yokota, D., Moraes, M., & Pinho, S. C. (2012). Characterization of lyophilized liposomes produced with non-purified soy lecithin: a case study of casein hydrolysate microencapsulation. **Brazilian Journal of Chemical Engineering**, 29(2), 325-335.

Zahedirad, M. et al. (2019). Fortification aspects of vitamin D in dairy products: A review study. **International Dairy Journal**, 94, 53-64.

Zheng, B. et al. (2019). Impact of curcumin delivery system format on bioaccessibility: Nanocrystals, nanoemulsion droplets, and natural oil bodies. **Food & Function**, 10(7), 4339-4349.

Chapter 2. CURCUMIN-LOADED PROLIPOSOMES PRODUCED BY THE COATING OF MICRONIZED SUCROSE: INFLUENCE OF THE TYPE OF PHOSPHOLIPID ON THE PHYSICOCHEMICAL CHARACTRERISTICS OF POWDERS AND ON THE LIPOSOMES OBTAINED BY HYDRATION

Chapter 2. Curcumin-loaded proliposomes produced by the coating of micronized sucrose: Influence of the type of phospholipid on the physicochemical characteristics of powders and on the liposomes obtained by hydration

Abstract

The feasibility of producing proliposomes containing curcumin, as well as liposome dispersions, using different mixtures of purified and nonpurified soybean phospholipids was studied. Proliposomes were produced through coating of micronized sucrose and physicochemically characterized over 30 days of storage. In addition, the possible interactions among the components were investigated using X-ray powder diffraction (XRD) and Fourier transform infrared spectroscopy (FT-IR). The proliposomes demonstrated a low propensity of water adsorption and low hygroscopicity. In addition, the curcumin content retained in the powders ranged from 67 to 92%. The liposomes were produced following proliposome hydration. Atomic force microscopy indicated the vesicles presented spherical shapes and photon correlation spectroscopy detected that their hydrodynamic diameters ranged from 207 to 222 nm. Finally, the curcumin-loaded liposomes preserved up to 63% of the bioactive compound but remained stable for only 15 days of storage.

Keywords: microencapsulation; curcuminoid; mixed liposomes nonpurified phospholipids; phospholipid vesicles;

2.1. Introduction

Color is considered to be one of the most important attributes in the judgment of food quality and the acceptance of food products by consumers along with flavor, texture and aroma. In this context, synthetic colorants have been applied in food industries for several purposes, including maintaining the color lost during the processing and standardizing the color among different food product batches. However, studies have linked the intake of synthetic yellow dyes, such as tartrazine (E102), to adverse health effects in children, including allergies, attention deficit, irritability, restlessness and sleep disturbance. In this context, the natural yellow colorant curcumin (E100) appears to be a suitable natural alternative to tartrazine (Arango-Ruiz et al. 2018).

Curcumin (diferulomethane) is the primary natural polyphenol found in the rhizome of the herbaceous plant Curcuma longa L., also known as turmeric. Curcumin is currently used in the food industry as a coloring, flavoring and preservative agent in several products, including cheeses, margarine, curry, soups, mustard and ice cream (Borrin et al., 2016). In addition, curcumin exhibits several medicinal properties, including antioxidant, anti-inflammatory, anticancer, and antimicrobial activities, all suggested to be related to its chemical structure, which includes hydroxyl groups linked to benzene rings, double bonds in the alkene portion, and a central β-diketone moiety (Liu et al., 2017). However, the direct incorporation of curcumin into aqueous-based food formulations is hampered due to its low solubility in water (11 ng/mL at 25 °C), high photosensitivity and instability in the presence of chemical oxidants (Aditya et al., 2013). To overcome these disadvantages, the encapsulation of curcumin in lipid carriers as liposomes appears to be an alternative to increase its aqueous solubility, in addition to increasing its oral bioavailability (Chaves et al., 2018).

Liposomes are colloidal spherical vesicles with an internal aqueous core formed by the self-assembly of amphiphilic phospholipids in aqueous media (Lasic, 1998). These systems have been applied to improve the bioavailability of hydrophobic bioactive compounds and to promote a controlled release in food formulations (Taylor et al., 2005). Phosphatidylcholines are the most abundant phospholipids in nature and are also used the most frequently in liposome productions. In addition, other phospholipids, such as lysophosphatidylcholine, phosphatidylinositol, and phosphatidylethanolamine, can also be used to produce liposomes. These lecithins can provide nutritional value to liposomes due to their high polyunsaturated fatty acid composition (Laye, McClements, & Weiss, 2008).

However, there are two major disadvantages about the encapsulation of bioactives in liposomes: the cost of phospholipids and the difficulty of scaling up (Taylor et al., 2005). Liposomes for food purposes are usually produced using the same phospholipids applied by the pharmaceutical industry, such as expensive synthetic phospholipids and highly purified natural phospholipids, which are cheaper than the synthetics but are still expensive if a large-scale production is considered (Michelon et al., 2016). Alternatively, nonpurified soybean lecithins cost nearly 20% less than hydrogenated phospholipids (Yokota, Moraes, & Pinho, 2012). However, it is known that unsaturated phospholipids are more susceptible to oxidation. To overcome this disadvantage, the production of liposomes containing molecules with antioxidant properties, such as curcumin, may contribute to the reduction of undesirable oxidation products (Chaves et al., 2018).

The hydration of proliposomes is one of the most cost-effective and easily scalable techniques of the liposome production methods to produce considerable amounts of liposomes (Wagner & Vorauer-Uhl, 2011). Proliposomes are defined as dry, free-flowing phospholipid particulate systems, which contain the bioactive to be encapsulated in their lipid matrix. Liposome vesicles are obtained after the hydration of these powders under controlled conditions of temperature and agitation (Payne et al., 1986). The solid-state of the proliposomes ensures their higher stability and is also convenient for transportation, storage, distribution and dosage, rendering them suitable for industrial processes. Finally, some advantages are related to the production of proliposomes using a coating of micronized sucrose (CMS), such as the use of milder temperatures, which do not compromise the integrity of the bioactive compound to be encapsulated, and the higher process yield obtained at the end of the process when compared to other processes, such as spray drying (Silva et al., 2017).

In this context, this study aimed to verify the feasibility of producing curcumin-containing proliposomes by a coating of micronized sucrose using mixtures of purified and nonpurified phospholipids. The particulate systems were characterized in terms of morphology, water activity, moisture content, solubility, hygroscopicity, moisture adsorption isotherms and content of the incorporated curcumin over 30 days of storage. In addition, possible interactions among the proliposome components were evaluated using Fourier transform infrared spectroscopy (FT-IR) and X-ray diffraction (XRD). Liposome vesicles were obtained using proliposome hydration and characterized in terms of morphology, hydrodynamic diameter, size distribution, zeta potential, amount of encapsulated curcumin and instrumental colorimetry.

The results obtained by this study will be useful to (i) verify the feasibility of the substitution of high-cost purified soy lecithins for lower-cost nonpurified phospholipids in liposome production for food applications and to (ii) stabilize curcumin in the liposomes using a simple method that can be scaled up.

2.2. Material and methods

2.2.1. Chemicals and reagents

Proliposomes were produced using two types of food-grade soybean lecithins purchased from Lipoid GmbH (Ludwigshafen, Germany): purified hydrogenated soy phosphatidylcholine Phospholipon 90H (P90H), containing a minimum of 90% w/w phosphatidylcholine (PC), a maximum of 4% w/w lysophosphatidylcholine (LPC), and 2% w/w triglycerides (TG) and fat-free powder lecithin Lipoid S40 (LS40), containing a minimum of 40% w/w phosphatidylcholine, 15% w/w phosphatidylethanolamine (PE), 4% w/w lysophosphatidylcholine and 3% w/w phosphatidylinositol (PI). Crystalline and purified curcumin was obtained from Sigma-Aldrich (St. Louis, MO, USA). Xanthan gum (XG) (Grindsted Xanthan 80) was donated by DuPont (Cotia, SP, Brazil), and guar gum (GG) was obtained from Êxodo Científica (Hortolândia, SP, Brazil). Sucrose, dimethyl sulfoxide (DMSO) and sodium benzoate were purchased from Synth (Diadema, SP, Brazil). All of the chemicals used in this study were reagent grade. Deionized water (from a Direct Q3 system, Millipore, Billerica, MA, USA) was used throughout the experiments.

2.2.2. Production of the curcumin-containing proliposomes

Proliposomes were produced using the coating of micronized sucrose method as described by Silva et al. (2017). Briefly, 100 mL of ethanolic solutions containing 3.2 g of total phospholipids and curcumin (when added) were produced using the formulations described in Table 1. The ethanolic solution was added as drops at a flow rate of 4 mL.min−1 using a peristaltic pump (Masterflex 7528-30, Cole-Parmer, Vernon Hills, IL, USA) onto 2 g of sucrose previously micronized in a ball mill (CE500, CIENLAB, Campinas, SP, Brazil). The solutions were maintained under sonication until the end of the dripping to maintain the dispersion of Lipoid S40 in ethanol. The injection process occurred in a rotary evaporator (MA120, Marconi, Piracicaba, SP, Brazil) in which the rotary flask was maintained at 55 ± 2 °C to vaporize the ethanol. The rotary flask was also covered to avoid early degradation of the curcumin. The

proliposomes were stored in vacuum desiccators protected from light at room temperature (25 °C) prior to their hydration.

Table 2.1. Formulations used for the production of curcumin-loaded proliposomes

Formulation	Phospholipon 90H (g)	Lipoid S40 (g)	Curcumin (mg)	Ethanol (mL)
F50	1.6	1.6	-	100
F50C	1.6	1.6	25	100
F70	0.96	2.24	-	100
F70C	0.96	2.24	25	100
F100	-	3.2	-	100
F100C	-	3.2	25	100

Reference: Chaves & Pinho (2019)

2.2.3. Characterization of the proliposomes

2.2.3.1. Water activity and moisture content

The water activity values were determined using an AquaLab (Decagon Devices, Pullman, WA, USA). Powders were transferred to a sample cup and filled to approximately ½ full and then placed in the instrument sample drawer. The values were obtained using the continuous mode. The moisture content values of samples were determined using a moisture analyzer with infrared radiation (MB35 Halogen, Ohaus, Switzerland). Briefly, 0.5 g of samples were placed in aluminum plates and then heated at 105 °C in AUTO configuration. The results were obtained after the complete removal of moisture from the samples.

2.2.3.2. Hygroscopicity

Hygroscopicity analyses were conducted as described by Cai and Corke (2006) with some modifications. Briefly, 0.2 g of proliposomes were placed in weighing filters and maintained for one week in desiccators at 25 °C containing a saturated sodium chloride solution (relative humidity 62%). The analyses were performed in triplicate, and the hygroscopicity values were expressed as g H2O adsorbed/100 g dry matter.

2.2.3.3. Solubility

The solubility analyses were performed as described by Eastman and Moore (1984) with modifications. First, 0.5 g of proliposome was added to an Erlenmeyer flask containing 50 mL of deionized water and homogenized using an orbital shaker (Marconi, Piracicaba, SP, Brazil) for 5 min at 200 rpm at 25 °C. The samples were centrifuged (5430R, Eppendorf, Hamburg, Germany) at 1057×g for 5 min at 25 °C. Finally, aliquots of 25 mL of the supernatant were transferred to a previously weighed Petri dish and maintained in a convection oven at 105 °C until the water had completely evaporated. The solubility was calculated based on the initial mass of the sample solubilized in the 25 mL of the supernatant, and the result was expressed as a percentage of the solubilized powder in water.

2.2.3.4. Moisture sorption isotherms

The sorption isotherms of the proliposomes were obtained using the static gravimetric method described by Labuza (1985). One-gram samples were placed in weighing filters and stored in desiccators containing different salt solutions with water activities ranging from 0.143 to 0.845. The desiccators were stored for 4 weeks at 25 °C, and the amount of adsorbed water was determined by the gain in weight at regular intervals. The equilibrium moisture was calculated using the ratio between the total mass of water and the dry mass of the sample. The moisture sorption isotherms were obtained by fitting the values of the equilibrium moisture to the BET model as shown in Eq. (1):

BET model: $X = (X_m * C * a_w)/[(1 - a_w) * (1 + (C - 1)) * a_w]$ (1)

where X represents the moisture content on a dry weight basis (g water/g dry matter), X_m is the monolayer of water (g water/g dry matter), a_w is the water activity and C is a constant.

2.2.3.5. Curcumin content analysis

The curcumin in the proliposomes was quantified using spectrophotometry based in Silva et al. (2017) with modifications. First, a mass of 0.1 g of proliposomes was diluted in 10 mL of anhydrous ethanol and centrifuged at 1878 × g for 5 min at 4 °C. The supernatant was transferred to a volumetric flask, and the centrifugation was repeated until curcumin could not be detected in the upper phase. The curcumin concentration was calculated from the absorbance measurements at 425 nm using a spectrophotometer (Genesys 10S, Thermo

Scientific, Waltham, MA, USA). Pure anhydrous ethanol was used as the blank. The bioactive compound was quantified using an analytical curve of pure curcumin (≥94%) in anhydrous ethanol ($R^2 = 0.9996$). Limits of detection (LOD) and quantification (LOQ) were calculated directly from the analytical plot. LOD and LOQ were calculated as 3.3σ/S and 10σ/S, respectively, where σ is the standard deviation of intercept and S is the slope of the analytical plot.

2.2.3.6. Morphology

The morphology of the proliposomes was obtained using scanning electron microscopy (SEM) in a TM-300 microscope (Hitachi, Tokyo, Japan). The samples were placed on double-faced carbon tapes (without any previous preparation) and fixed to aluminum stubs. The micrographs were captured using a voltage of 15 kV and 100x magnification.

2.2.3.7. X-ray powder diffraction (XRD)

X-ray diffraction analyses were conducted using a MiniFlex600 (Rigaku, Tokyo, Japan) with a copper anode tube with λ = 1.5418 Å and a graphite monochromator in the diffracted beam. The scanning angle 2θ ranged from 5° to 40°, and the data were obtained in steps of 0.2° using a 2°/min rate.

2.2.3.8. Fourier transform infrared (FT-IR) spectroscopy

FT-IR spectroscopy analyses were performed using a PerkinElmer FT-IR Spectrometer (Waltham, MA, USA). Samples (0.01 g) were deposited in KBr pellets, and the spectra were obtained in the wavenumber region between 4000 and 400 cm^{-1}. The resolution used was 4 cm^{-1} with 20 scans in total. The data were analyzed using the software included in the equipment (Spectrum One, v. 5.3.1., PerkinElmer, Waltham, MA, USA).

2.2.4. Production of the curcumin-loaded liposomes

Curcumin-loaded liposome dispersions were produced as described by Chaves et al. (2018). Briefly, 100 mL of deionized water was added to 2 g of proliposomes containing curcumin and subjected to ultra-agitation at 13,000 rpm for 5 min at 65 °C. Subsequently, the dispersions were immediately cooled to 25 °C for the addition of the polysaccharides. Xanthan gum (0.01% w/v) and guar gum (0.09% w/v) were added in a 10:90 (XG:GG) ratio under

84

magnetic stirring (3600 rpm). Sodium benzoate (0.02% w/v) was added as an antimicrobial agent. Finally, the dispersions were transferred to amber flasks and stored in a refrigerated incubator at 10 °C.

2.2.5. Physicochemical characterization of the curcumin-loaded liposomal dispersions

2.2.5.1. Morphology

The morphology of the vesicles was visualized by atomic force microscopy (AFM) using a NT-MDT microscope (Solver Next, Zelenograd, Russia) as described by Ruozi et al. (2015) with modifications. The analyses were performed at a scanning velocity of 0.7 Hz using the intermittent contact mode. The resonance frequency for the cantilever (Tap 150AI-G, Budget Sensors) was 150 kHz, and the force constant was 5 N/m. To improve the visualization of the liposomes, the dispersions were diluted 100x in ultrapure water. Samples of 40 μL of the diluted liposomes were placed on the surface of a mica disk and left stationary for 2 min. Finally, the excess of the diluted liposomes was removed using a paper filter.

2.2.5.2. Hydrodynamic diameter, size distribution and zeta potential

The hydrodynamic diameter and size distribution of the dispersions were obtained by photon correlation spectroscopy (PCS) at 25 °C using a ZetaPlus analyzer (Brookhaven Instruments Company, Holtsville, NY, USA). The analyses were performed using a He-Ne laser at 627 nm and 90° as the angle of incidence. The samples were previously diluted 100x in deionized water to avoid the multiple scattering of light phenomena. The zeta potential was also determined in the ZetaPlus analyzer after diluting one drop of the dispersion in 1 mM potassium chloride solution. The conductivity of the samples after dilution was 50 mS/cm. Finally, the Helmoltz-Smoluchowski equation was used to calculate the zeta potential using the electrophoretic mobility data obtained for the liposome dispersions. The ZetaPlus equipment performed 10 readings for each sample before displaying the mean and standard deviation values. The data for these parameters were obtained using the software included with the system and are presented as the mean ± standard deviation.

2.2.5.3. Curcumin content analysis

The curcumin in the liposomes was quantified using spectrophotometry as described by Borrin et al. (2016). The dispersions were diluted in DMSO in a 1:25 (v/v) ratio, and their

absorbance values were measured at 425 nm. Pure DMSO was used as a blank. The bioactive concentration in the samples was obtained using an analytical curve previously obtained from pure curcumin (≥94%) in DMSO (R^2 = 0.9996). Limits of detection (LOD) and quantification (LOQ) were calculated directly from the analytical plot. LOD and LOQ were calculated as 3.3σ/S and 10σ/S, respectively, where σ is the standard deviation of intercept and S is the slope of the analytical plot.

2.2.5.4. Determination of instrumental color

Parameters of the tristimulus color system (L*, a* and b*) were obtained using a Miniscan XE (HunterLab, Reston, VA, USA). CIE (Commission Internationale de l'Eclairage) was used as the output reading system. The illuminator was D65 with the observer at 10°. Liposome dispersions (5 mL) were transferred to a transparent Petri dish, and the measurements were obtained after the colorimeter had been pressed against the Petri dish surface. Chroma (C*) and hue angle (h°) were also calculated using Eqs. (2), (3), respectively. The changes in color can be visualized when the three parameters L*, a* and b* are related to the total color difference (ΔE) calculated using Eq. (4).

$$C^* = [(a^*)^2 + (b^*)^2]^{1/2} \tag{2}$$
$$h^\circ = \tan^{-1}(b^*/a^*) \tag{3}$$
$$\Delta E = [2 * \Delta L^* + 2 * \Delta a^* + 2 * \Delta b^*]^{1/2} \tag{4}$$

2.2.6. Statistical analyses

Statistical analyses of the results were performed by a Tukey's test at a 5% significance level ($p < 0.05$) using SAS Software version 9.2 computer program (Statistical Analyses Systems, Cary, NC, USA). All the analyses were performed in triplicate with the mean values unless otherwise stated, and the error bars shown represent the mean ± standard deviation.

2.3. Results and discussions

2.3.1. Characterization of the curcumin-containing proliposomes

2.3.1.1. Powder properties

The micrographs obtained for the curcumin-containing proliposomes using scanning electron microscopy are shown in Figs. 2.1a-c. The material had a very irregular shape with many agglomerates. The images revealed that the micronized sucrose was efficiently coated by the phospholipids, since a thin layer of phospholipids can be distinguished on the surface of the sucrose granules.

Figure 2.1. Micrographs obtained by scanning electron microscopy (SEM) for proliposomes containing curcumin produced with different concentrations of Phospholipon 90H (P90H) and Lipoid S40 (LS40): (a) 50:50 P90H:LS40 (F50C), (b) 30:70 P90H:LS40 (F70C), and (c) 0:100 P90H:LS40 (F100C). Error bars: 1 mm. Magnification: 100×. (d) Moisture adsorption isotherms (at 25 °C) obtained by fitting adsorption data using the BET model (---) for the formulations (■) 50:50 P90H:LS40, (●) 70:30 P90H:LS40, and (▲) 50:50 P90H:LS40
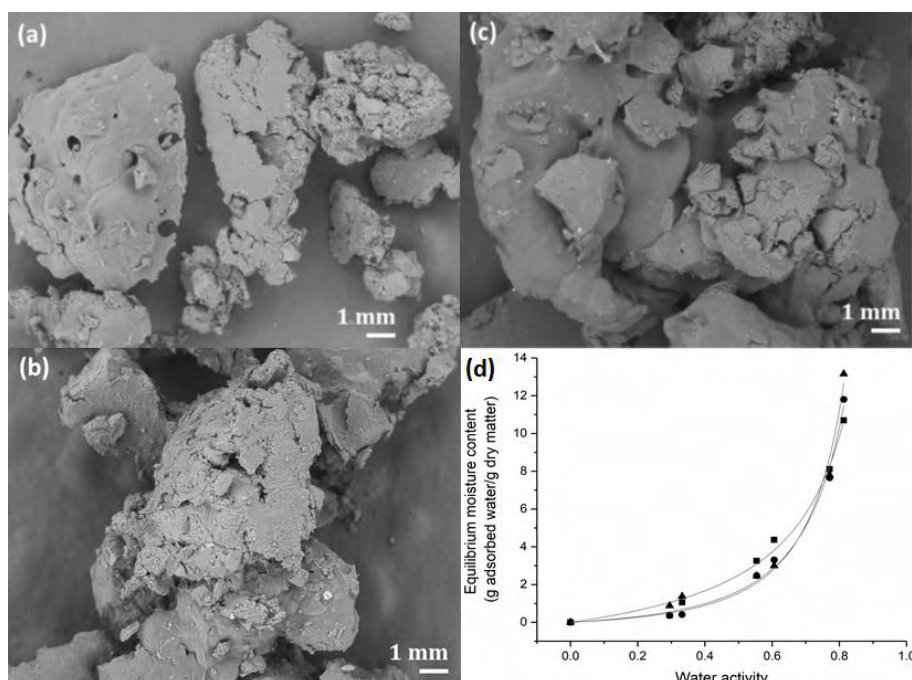
Reference: Chaves & Pinho (2019)

Some characteristics of the proliposomes are summarized in Table 2.2. As observed, the values of the water activity (A_w) ranged from 0.20 to 0.25. Low values of A_w are required for

food powders to decrease the chance of microbial survival and growth (Beuchat et al., 2013). Similarly, the moisture content obtained for the proliposomes was also low, ranging from 1.61 to 2.03%, which are considered excellent results, since higher-moisture powders cause more transport and storage difficulties, as well as a decrease in the handling properties (Juarez-Enriquez et al., 2017). In addition, the increase in the amount of LS40 added did not result in significant changes in both parameters among the formulations, even though the LS40 was a highly hygroscopic phospholipid.

The hygroscopicity values obtained ranged from 6.74 to 8.65 g adsorbed water/100 g of dry matter. It is worth noting that the values were low even in the presence of a highly hygroscopic polysaccharide, such as sucrose. A low value of this parameter is also required to extend the shelf life of the powders, since it contributes to maintaining their physicochemical characteristics even in high relative humidity environments (Silva et al., 2017). The low capacity to adsorb water even at high relative humidity conditions can also be observed in the moisture adsorption isotherms shown in Fig. 2.1d. The isotherms showed that the proliposomes adsorb low amounts of water from the environment when stored under an $A_w < 0.6$, which are typical conditions in the storage of food powders, since deterioration due to microbial growth does not easily occur (Roos, 2001). The parameters obtained by fitting the experimental data to the BET model are shown in Table 2.2. This model is widely used to predict the moisture data of food powders and is based on the kinetics for the formation of a monolayer of water. The moisture content in the monolayer (X_m) for the proliposomes ranged from 2.44 to 6.14 g adsorbed water/100 g of dry matter indicating the safety humidity values in which the powders must be stored without any loss of quality. The values obtained for the C constant are within the range established for food powders (Timmermann, Chifre, & Iglesias, 2001).

Alternatively, the solubility of the proliposomes ranged from 32.1 to 46.7%, which is considerably lower than the 98% obtained by Silva et al. (2017) that produced solely curcumin-proliposomes using P90H. Such a decrease in solubility was probably due to the presence of other phospholipids than the purified and hydrogenated phosphatidylcholine in the vesicles, such as phosphatidylethanolamine, that are not able to absorb water in similar quantities (McIntosh, 1996). In addition, low solubility may be related to the coating process used for the proliposome production (Silva et al., 2017). According to Zhang et al. (2016), the higher the number of phospholipid molecules coating the carrier, the lower the area available for contact between the carrier and water, which results in low solubility rates. In addition, as previously

shown in Fig. 2.1a-c, the sucrose granules were fully coated by the phospholipids, which substantiates the previous statement.

The curcumin concentrations in the proliposomes on the 1st and the 30th day of storage are also presented in Table 2.2. The representative linear equation of curcumin in ethanol was $y = 0.1425x - 0.0053$, calculated by the least square methods. The limit of quantification (LOQ) was found as $0.864 \pm 0.079\ \mu g/mL$. The limit of detection (LOD) was found as $0.285 \pm 0.026\ \mu g/mL$. As seen, the amount of bioactive compound remained constant only in the F50C formulation, differently from the others, in which a slight decrease was observed. However, despite the high sensitivity of curcumin to oxidation, from 78 to 92% of its initial amount was preserved in the proliposomes in the F70C and F50C formulations, respectively, which is an excellent result, since the storage conditions were not modified.

Table 2.2. Powder characteristics of curcumin-loaded proliposomes

Powder properties		Formulations		
		F50C	F70C	F100C
Water activity (A_w)		$0.20^A \pm 0.01$	$0.21^A \pm 0.01$	$0.25^A \pm 0.10$
Moisture content (%)		$2.03^A \pm 0.50$	$1.90^A \pm 0.28$	$1.61^A \pm 0.77$
Solubility (% solubilized powder)		$46.7^A \pm 2.51$	$41.5^A \pm 1.54$	$32.1^B \pm 5.15$
Hygroscopicity (g adsorbed water/100g dry matter)		$6.93^A \pm 0.76$	$6.74^A \pm 0.86$	$8.65^A \pm 2.78$
Curcumin concentration (mg/g of proliposome)	1st day	$3.42^{ABa} \pm 0.21$	$3.85^{Aa} \pm 0.15$	$2.98^{Ba} \pm 0.30$
	30th day	$3.16^{Aa} \pm 0.44$	$3.01^{Ab} \pm 0.18$	$2.00^{Bb} \pm 0.08$
% curcumin preserved		92.4	78.2	67.1
Parameters fitted using BET model	X_m (g water/g dry matter)	2.44 ± 0.10	4.09 ± 0.8	6.14 ± 3.0
	C	1.05 ± 0.35	0.25 ± 0.10	0.14 ± 0.1
	R^2	0.9913	0.9934	0.9847

Means followed by the same uppercase letter in the same line and by the same lowercase letter in the same column were not significantly different ($p > 0.05$) by Tukey's test.

Reference: Chaves & Pinho (2019)

2.3.1.2. Fourier transform infrared spectroscopy (FT-IR)

The FT-IR technique can be used to explain the mechanism of coating by exploring the interactions among the proliposome components. The FT-IR spectra obtained for the pure components and proliposomes are shown in Fig. 2.2. It can be observed from the spectra that most peaks related to the curcumin (from 818 to 1616 cm^{-1}) did not appear in the spectra of curcumin-containing proliposomes, probably due to the low amount of the bioactive compound added than the other ingredients in the formulations. According to Lewis and McElhaney (2007), the asymmetric stretching vibration of the P=O group can be identified by a peak near 1200 cm^{-1}. Thus, in the spectra obtained for P90H and LS40, this peak was determined at 1266 and 1224 cm^{-1}, respectively. In addition, the position of the P=O stretching peak is sensitive to hydrogen bonding, shifting to lower wavenumbers with the increase in these types of bonds (Popova & Hincha, 2003). Therefore, in the mixed proliposomes (F50, F50C, F70, and F70C), this peak was located at 1240 cm^{-1} between the wavenumbers found for the P=O stretching in the spectra of pure phospholipids. Therefore, the hydrogen-bonding interactions probably led to a slight shifting in the P=O peak primarily in the P90H, indicating an increase in the hydration state of the polar head group region of this phospholipid (Popova & Hincha, 2003). In addition, the drying of the phosphatidylcholine membranes in the presence of sucrose seems to result in a similar shift (Tsvetkova et al., 1998). Otherwise, the carbonyl stretching vibration C=O was identified at 1730 cm^{-1} in P90H and 1737 cm^{-1} in LS40. Considering the spectra obtained for the proliposomes, a decrease in the intensity of this peak was observed (1726 cm^{-1}), indicating a strengthening of the hydrogen bonds or even the formation of a new hydrogen bond (Liu et al., 2013). In this context, it can be assumed that an interaction between the hydroxyl group of sucrose and the polar head of the phospholipids may have occurred in a manner similar to that reported in the freeze-drying process, in which sucrose acts as a cryoprotectant molecule (Doxastakis, Sum, & Pablo, 2005). In addition, very intense peaks at 2842/2854 and 2930 cm^{-1} are present in the spectra of the pure phospholipids, as well as in the spectra of empty and curcumin-loaded proliposomes with almost no modifications (2854 and 2912 cm^{-1}). These peaks are related to the symmetric and asymmetric CH_2 stretching vibrations, and an increase in their intensity indicates that the acyl chains of the phospholipids in the dry state are more ordered (Frías et al., 2006). As can be observed, an increase in the LS40 concentration led to a decrease in the intensities of these peaks. Therefore, it can be concluded that the proliposomes produced with solely LS40 (F100

and F100C) are more likely to result in less ordered acyl chains when in the dry state. In addition, the presence of curcumin in the proliposomes appeared to affect the intensity of these peaks in the F70C and F100C formulations, since lower intensity values were obtained in comparison with those obtained for the unloaded F70 and F100 formulations.

Figure 2.2. Infrared spectra obtained for pure components: (i) curcumin, (ii) Lipoid S40, (iii) Phospholipon 90H, (iv) sucrose and for proliposomes produced with different concentrations of Phospholipon 90H (P90H) and Lipoid S40 (LS40): (A) 50:50 P90H:LS40 (F50), (B) 50:50 P90H:LS40 + curcumin (F50C), (C) 30:70 P90H:LS40 (F70), (D) 30:70 P90H:LS40 + curcumin (F70C), (E) 0:100 P90H:LS40 and (F) 0:100 P90H:LS40 + curcumin (F100C)
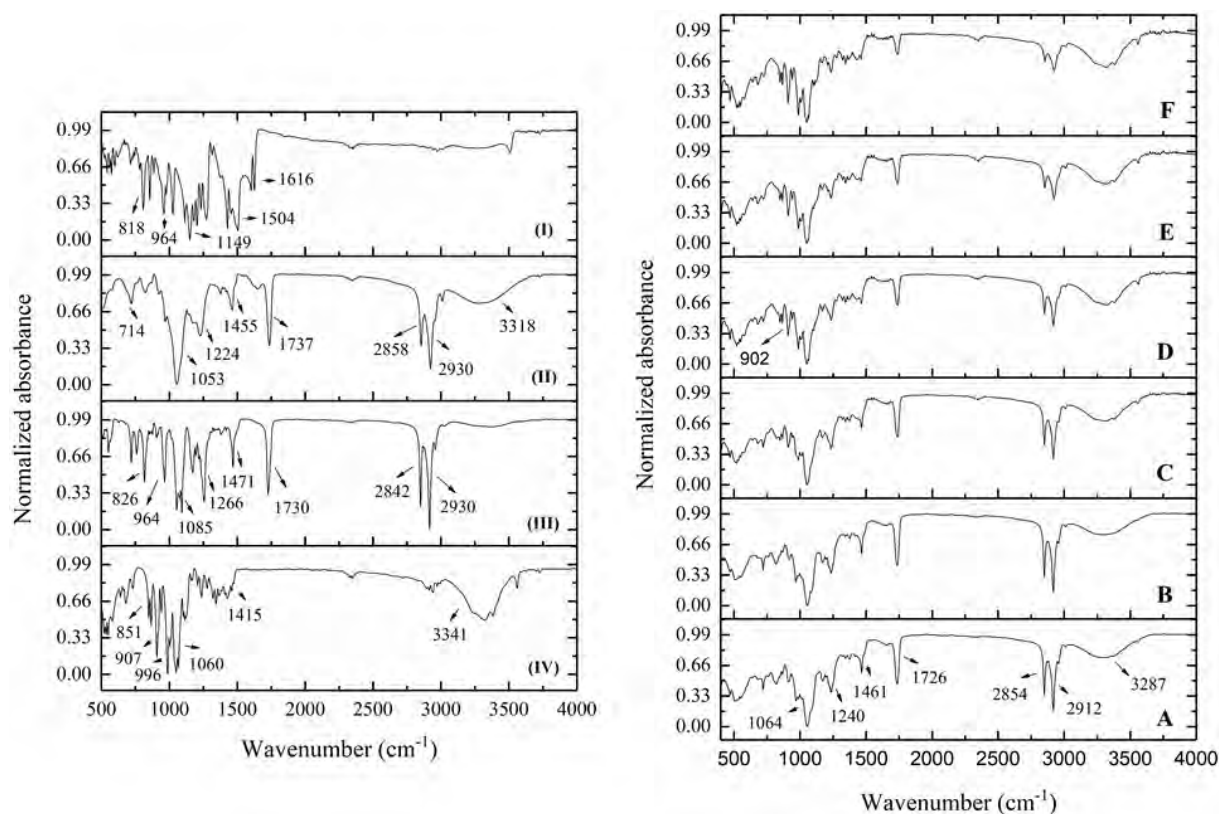
Reference: Chaves & Pinho (2019)

2.3.1.3. X-ray diffraction (XRD)

The X-ray diffraction analysis allowed to determinate the crystalline properties of the raw materials (sucrose, phospholipids, curcumin) and proliposome formulations. The XRD diffraction patterns obtained are shown in Fig. 2.3. As sucrose presented a high crystalline

pattern, it was necessary to verify if its bounds would amorphized after the proliposomes production. Clearly, the diffraction patterns obtained for the proliposomes consisted of an overlap of the spectra obtained for the pure components. In addition, all the patterns demonstrated an increase in the curve approximately 2θ = 15°, indicating the presence of amorphous regions. Crystallinity percentages were calculated and are shown as follows: 52% for F50, 41% for F50C, 54% for F70, 37% for F70C, 23% for F100 and 94% for F100C. Since a substantial number of amorphous regions is needed to assure a good hydration of powders, it can be assumed that F50C and F70C would be more easily hydrated than F100C (Silva et al., 2017).

Figure 2.3. X-ray diffraction patterns obtained for pure components: (i) curcumin, (ii) Lipoid S40, (iii) Pholipon 90H, (iv) sucrose and for proliposomes produced with different concentrations of Pholipon 90H (P90H) and Lipoid S40 (LS40): (A) 50:50 P90H:LS40 (F50), (B) 50:50 P90H:LS40 + curcumin (F50C), (C) 30:70 P90H:LS40 (F70),(D) 30:70 P90H:LS40 + curcumin (F70C), (E) 0:100 P90H:LS40 and (F) 0:100 P90H:LS40 + curcumin (F100C)

Reference: Chaves & Pinho (2019)

2.3.2. Physico-chemical stability of the curcumin-loaded liposomes

2.3.2.1. Size distribution, zeta potential and morphology

The results obtained for the physicochemical characterization of the curcumin-loaded liposomes on the first and the 15th day of storage are summarized in Table 2.3. It is important to note that the samples did not remain stable for more than 20 days. As can be observed, the dispersions showed average hydrodynamic diameters typically obtained for large unilamellar vesicles, since the values ranged from 207 to 222 nm. Interestingly, this is an unprecedented result, since the vesicles produced using the hydration of the proliposomes method are usually multilamellar (≥500 nm) (Wagner & Vorauer-Uhl, 2011). Indeed, this result was probably related to the sonication step needed to maintain the LS40 in dispersion. It is known that the sonication of phospholipid suspensions results in the fragmentation of the particles but does not influence the lamellar arrangement of the individual molecules (Papahadjopoulos & Miller, 1967). In this study, the formation of nanoliposomes might be related to a more uniform sucrose coating with the phospholipids during the proliposome production, facilitating the hydration of the powders upon the addition of the aqueous phase (Khan et al., 2015). In addition, as can be observed in Table 2.3, only the F100C formulation did not demonstrate significant changes in size after 15 days of storage, a behavior that can be confirmed by visualizing the size distribution curves as shown in Fig. 2.4.

Figure 2.4. Size distribution curves of curcumin-loaded liposomes produced with different concentrations of Phospholipon 90H (P90H) and Lipoid S40 (LS40): (a) 50:50 P90H:LS40 (F50C), (b) 30:70 P90H:LS40 (F70C), (c) 0:100 P90H:LS40 (F100C) obtained at the 1st day (black lines) and at the 15th day (red lines) of storage. Right below, micrographs obtained by atomic force microscopy for formulations (A) F50C, (B) F70C, and (C) F100C
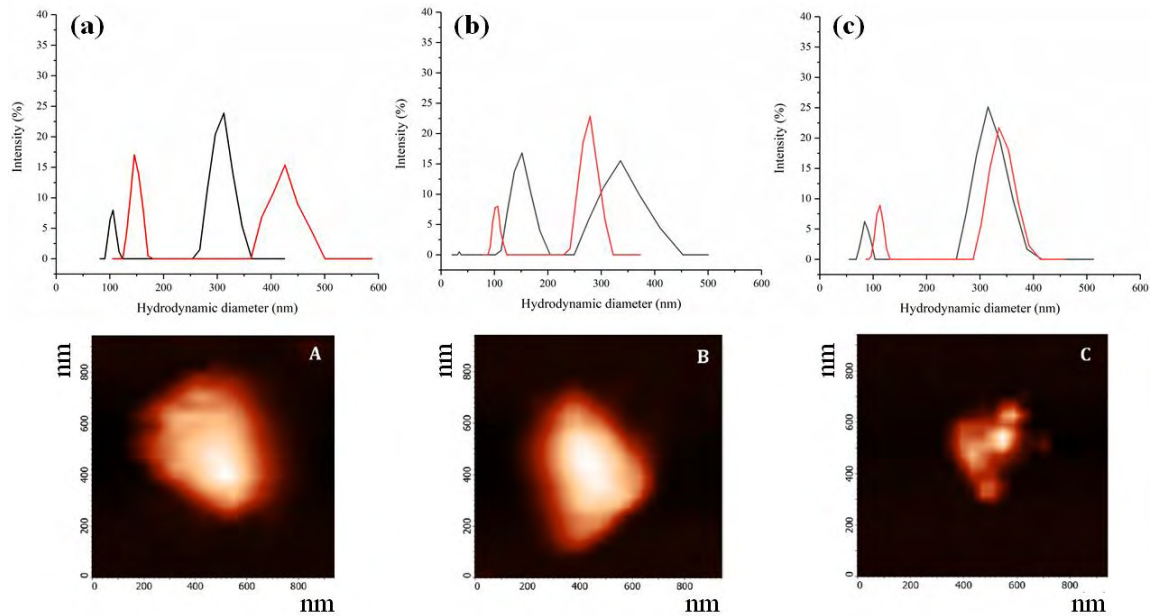
Reference: Chaves & Pinho (2019).

Table 2.3. Physicochemical parameters obtained (at 25 °C) for curcumin-loaded liposome dispersions over storage time

Formulation/Time		F50C		F70C		F100C	
		1st day	15th day	1st day	15th day	1st day	15th day
Average hydrodynamic diameter (nm)		$218^A \pm 1.6$	$214^B \pm 1.2$	$207^C \pm 0.9$	$215^{AB} \pm 1.5$	$222^D \pm 1.2$	$222^D \pm 0.6$
Zeta potential		$-142^A \pm 13$	$-132^{ABC} \pm 9$	$-111^B \pm 11$	$-105^B \pm 11$	$-149^{AC} \pm 10$	$-126^{AB} \pm 5$
Curcumin concentration (mg/L)		$73^A \pm 4$	$46^B \pm 7$	$58^{AB} \pm 6.5$	$48^B \pm 6$	$70^{AB} \pm 9.5$	$54^{AB} \pm 16$
% curcumin preserved			63		82.7		77.1
Colorimetric parameters	L*	$48.6^{AC} \pm 0.5$	$50^A \pm 0.3$	$46.6^B \pm 0.9$	$49.4^A \pm 1.5$	$45.5^B \pm 0.5$	$47.4^{BC} \pm 0.7$
	a*	$-5.1^{AC} \pm 0.2$	$-7.2^B \pm 0.5$	$-3.8^{AE} \pm 0.5$	$-6.1^{BC} \pm 0.6$	$-1.3^D \pm 0.2$	$-3.5^E \pm 0.8$
	b*	$63.9^A \pm 0.4$	$60.6^{AB} \pm 1.2$	$61.2^{AB} \pm 2.9$	$59.8^B \pm 1.2$	$61.9^{AB} \pm 0.3$	$59.1^B \pm 0.2$
	C*	$64.1^A \pm 0.4$	$61^{AB} \pm 1.2$	$61.3^{AB} \pm 2.9$	$60.1^B \pm 1.3$	$61.9^{AB} \pm 0.3$	$59.2^B \pm 0.2$
	h°	$94.6^{AC} \pm 0.2$	$96.8^B \pm 0.6$	$93.5^C \pm 0.3$	$95.8^{AB} \pm 0.5$	$91.2^D \pm 0.2$	$93.4^C \pm 0.8$
	ΔE	-	$4.2^A \pm 1.1$	-	$4.1^A \pm 1.1$	-	$4.0^A \pm 1.1$

Means followed by the same uppercase letter in the same line were not significantly different ($p > 0.05$) by Tukey's test.

Reference: Chaves & Pinho (2019)

In addition, the reasons for the instability of the dispersions were investigated. First, the presence of highly unsaturated fatty acids in PE is usually related to more permeable and less stable membranes (Biltonen & Lichtenberg, 1993). Otherwise, PE possess a smaller polar head group than PC and a large area occupied by its hydrocarbon chains, which produces an overall cone shaped molecule that contributes to a tighter packing in the membranes containing PC, thus, decreasing the vesicle size (Litzinger & Huang, 1992). However, the curvature increases as the size decreases, which contributes to the faster kinetics of water absorption, as well as aggregation and phase separation (Rovira-Bru, Thompson, & Szleifer, 2002). Finally, unlike PC, PE did not form lamellae alone, preferring nonlamellar phases to reverse hexagonal H_{II} phases, and possesses a poorly hydrated head group (Israelachvili, 1992).

The values of the zeta potential obtained for all the liposomes ranged from -105 to -149 mV as can also be seen in Table 2.3. The high values obtained could be considered to be indicative of "excellent stability", since the line between stable and unstable dispersions is generally taken at either $+30$ or -30 mV (Greenwood & Kendall, 1999). However, this was not consistent with the results obtained, since all the dispersions were already unstable on the 20th day of storage. In this context, it is important to note that the colloidal stability does not depend exclusively on the zeta potential value. According to the DLVO theory, this stability is due to the sum of the electrostatic repulsive forces, resulting from the double electric layer, and the attracting van der Waals forces. Although the zeta potential provides information about the repulsive forces, this parameter does not provide any information about the van der Waals attracting forces. In addition, for nanoliposomes, other forces as hydrophobic and hydration forces have an even more significant action in stability than the van der Waals forces (Sabín et al., 2006). Therefore, the early instability of the liposomes produced in this study may be related to the action of these forces, and none of them are measured by the zeta potential. Finally, the negative values obtained by this parameter can be attributed to (i) the orientation of the phosphatidylcholine polar heads on the surface of the liposomes with the phosphate group located above the plane of the choline group (Ascenso et al., 2013) or to (ii) the presence of negative charges in phosphatidic acid, phosphatidylinositol and phosphatidylethanolamine in the lecithins (Nongonierma et al., 2009).

The micrographs obtained using atomic force microscopy for the liposome dispersions are shown in Fig. 2.5. As can be visualized, the vesicles displayed a smooth spherical or near-

spherical shape. In addition, the values of size obtained by the AFM are consistent with the nanometric values measured using photon correlation spectroscopy.

2.3.2.2. Incorporation and protection of curcumin

Curcumin concentrations preserved in the liposomes over the 15 days of storage are also shown in Table 2.3. The representative linear equation of curcumin in DMSO was $y = 0.1184x - 0.0006$, calculated by the least square methods. The limit of quantification (LOQ) was found as 0.798 ± 0.106 µg/mL. Limit of detection (LOD) was found as 0.263 ± 0.035 µg/mL. As can be observed, similar amounts of the bioactive were retained in the formulations on the first day of storage regardless of the LS40/P90H ratio used. However, on the 15th day of storage, the F50C formulation showed a significant decrease in curcumin content, a behavior that was not seen in the formulations produced with higher amounts of LS40. The tighter packing in the formulations containing higher amounts of PE may have contributed to this result, since the highly packed structures may have more efficiently protected the bioactive compound over storage time. In addition, the curcumin concentrations obtained from the vesicles produced with the mixed phospholipids were at least 27% higher than those obtained by Chaves et al. (2018) who produced curcumin-loaded multilamellar vesicles using P90H. Interestingly, the liposomes obtained in this study were unilamellar and theoretically more susceptible to the action of oxidizing agents (Almog, Forward, & Samsonoff, 1991).

2.3.2.3. Instrumental colorimetry

The colorimetric parameters obtained using instrumental colorimetry are also summarized in Table 2.3. As can be observed, an increase in the amount of LS40 added to the dispersions led to a decrease in the luminosity parameter L* even on the first day of storage, which can be related to the brownish characteristic of LS40. Considering the values obtained for Chroma (C*) and hue angle (h°), it can be deduced that the dispersions demonstrated an intense yellow color according to the CIEL*A*B* color space, which reinforces the high coloring effect of the encapsulated curcumin. Finally, all of the liposomes showed some color variation over the storage time, since the values of ΔE were all higher than 2 (Francis & Clydesdale, 1975). This result can be related to the instability of the dispersions, since the phase separation results in visual changes in color.

2.4. Conclusions

The results obtained in this study revealed that it is feasible to produce curcumin-containing proliposomes by the coating of micronized sucrose method using mixtures of purified and nonpurified phospholipids. The amount of the nonpurified phospholipids did not influence the parameters obtained for the powders, with the exception of solubility. The proliposomes produced were stable even under highly relative humidity conditions, which is a highly desirable characteristic for food powders. Curcumin was efficiently preserved in the proliposomes for 30 days, but significantly higher amounts were obtained for samples containing a lesser content of nonpurified phospholipids. Otherwise, the presence of the same nonpurified phospholipids was deleterious for the higher amounts of curcumin encapsulated in the liposomal vesicles. Finally, the short storage time observed for the dispersions suggests the need for a more intensive study considering the optimization of the process parameters.

2.5. Acknowledgements

2.6. References

Aditya, N. P. et al. (2013). Curcumin and genistein coloaded nanostructured lipid carriers: in vitro digestion and antiprostate cancer activity. **Journal of Agricultural and Food Chemistry**, 61, 1878-1883.

Almog, R., Forward, R., Samsonoff, C. (1991). Stability of sonicated aqueous suspensions of phospholipids under air. **Chemistry and Physics of Lipids**, 60, 93-99.

Arango-Ruiz, A. et al. (2018). Encapsulation of curcumin using supercritical antisolvent (SAS) technology to improve its stability and solubility in water. **Food Chemistry**, 258, 156-163.

Ascenso, A. et al. (2013). Novel trtinoinformulatios: a drug-in-cyclodextrin-in-liposome approach. **Journal of Liposome Research**, 23, 211-219.

Beuchat, L. R. et al. (2013). Low-water activity foods: increased concern as vehicles of foodborne pathogens. **Journal of Food Protection**, 76, 150-172.

Borrin, T. R. et al. (2016). Curcumin-loaded nanoemulsions produced by the emulsion inversion point (EIP) method: An evaluation of process parameters and physico-chemical stability. **Journal of Food Engineering**, 169, 1-9.

Cai, Y.Z., & Corke, H. (2006). Production and properties of spray-dried Amaranthus betacyanin pigments. **Journal of Food Science**, 67, 1248-1252.

Chaves, M. A. et al. (2018). Structural characterization of multilamellar liposomes coencapsulating curcumin and vitamin D_3. **Colloids and Surfaces A: Physicochemical and Engineering Aspects**, 549, 112-121.

Doxastakis, M., Sum, A. K., & Pablo, J. J. (2005). Modulating membrane properties: The effect of trehalose and cholesterol on a phospholipid bilayer. **The Journal of Physical Chemistry**, 109, 24173-24181.

Eastman, J. E., & Moore, C. O. (1984). Cold water-soluble granular starch for gelled food composition. **U.S. Patent 4465702**, 14 ago. 1984.

Francis, J. F., & Clydesdale, F. M. (1975). **Food colorimetry, theory and application**. New York: Van Nostrand Reinhold/AVI. ISBN: 978-0-8705-5183-3.

Frías, M. A. et al. (2006). FTIR analysis of the interaction of arbutin with dimyristoyl phosphatidylcholine in anhydrous and hydrated states. **Biochimica et Biophysica Acta (BBA) – Biomembranes**, 1758, 1823-1829.

Greenwood, R., & Kendall, K. (1999). Selection of suitable dispersants for aqueous suspensions of zirconia and titaniapowdersusing acoustophoresis. **Journal of the European Ceramic Society,** 19, 478-488.

ICH – Harmonised Tripartity Guideline. (2005). **Validation of Analytical Procedures: Text and Methodology Q2**(R1). IFMPA: Geneva.

Israelachvili, J.N. (1992). Fluid-like structures and self-assembling systems: micelles, bilayers and biological membranes. In: **Intermolecular and Surface Forces**. Academic Press: London, 2nd ed, 366-394.

Juarez-Enriquez, E. et al. (2017). Effect of water content on the flowability of hygroscopic powders. **Journal of Food Engineering**, 205, 12-17.

Khan, I. et al. (2015). Proliposome powders prepared using a slurry method for the generation of beclometasone dipropionate liposomes. **International Journal of Pharmaceutics**, 496, 342-350.

Labuza, T. P. (1985). Moisture sorption: Practical aspects of isotherm measurement and use. Saint Paul, MN: American Association of Cereal Chemists. ISBN: 978-1-8911-2718-2.

Lasic, D. D. (1998). Novel applications of liposomes, Trends in Biotechnology, 16, 307-321.

Laye, C., McClements, D. J., & Weiss, J. (2008). Formation of biopolymer-coated liposomes by electrostatic deposition of chitosan. Journal of Food Science, 73, N7-N15.

Lewis, R. N, & McElhaney, R. N. (2007). Fourier transform infrared spectroscopy in the study of lipid phase transitions in model and biological membranes: practical considerations. Methods in Molecular Biology, 400, 207-226.

Litzinger, D. C., & Huang, L. (1992). Amphipathic poly(ethylene glycol) 5000-stabilized dioleoylphosphatidylethanolamine liposomes accumulate in spleen. Biochimica et Biophysica Acta (BBA) - Lipids and Lipid Metabolism, 1127, 249-254.

Liu, W. et al. (2013). Improved physical and in vitro digestion stability of a polyelectrolyte delivery system based on layer-by-layer self-assembly alginate-chitosan-coated nanoliposomes. Journal of Agricultural and Food Chemistry, 61, 4133-4144.

Liu, Y. et al. (2017). Improved antioxidant activity and physicochemical properties of curcumin by adding ovalbumin and its structural characterization. Food Hydrocolloids, 72, 304-311.

McIntosh, T. J. (1996). Hydration properties of lamellar and non-lamellar phases of phosphatidylcholine and phosphatidylethanolamine. Chemistry and Physics of Lipids, 81, 117-131.

Michelon, M. et al. (2016). Structural characterization of β-carotene-incorporated nanovesicles produced with non-purified phospholipids. Food Research International, 79, 95-105.

Nongonierma, A. B. et al. (2009). Evaluation of two food grade proliposomes to encapsulate an extract of a commercial enzyme preparation by microfluidization. Journal of Agricultural and Food Chemistry, 57, 3291-3297.

Papahadjopoulos, D., & Miller, N. (1967). Phospholipid model membranes. I. Structural characteristics of hydrated liquid crystals. Biochimica et Biophysica Acta (BBA) – Biomembranes, 135, 624-638.

Payne, N. I. et al. (1986). Proliposomes: A novel solution to an old problem. Journal of Pharmaceutical Sciences, 75, 325-329.

Popova, A. V., & Hincha, D. K. (2003). Intermolecular interactions in dry and rehydrated pure and mixed bilayers of phosphatidylcholine and digalactosyldiacylglycerol: A Fourier transform infrared spectroscopy study. Biophysical Journal, 85, 1682-1690.

Roos, Y. H. (2001). Water activity and plasticization. In Eskin, N. A. M. & Robinson, D. S. **Food Shelf Life Stability**. London: CRC Press, 3-36.

Rovira-Bru, M., Thompson, D. H., & Szleifer, I. (2002). Size and structure of spontaneously forming liposomes in lipid/PEG-lipid mixtures. **Biophysical Journal**, 83,2419-2439.

Ruozi, B. et al. (2005). Atomic force microscopy and photon correlation spectroscopy: Two techniques for rapid characterization of liposomes. **European Journal of Pharmaceutical Sciences**, 25, 81-89.

Sabín, J. et al. (2006). Size and stability of liposomes: A possible role of hydration and osmotic forces. **The European Physical Journal**, 20, 401-408.

Silva, G. S. et al. (2017). Characterisation of curcumin-loaded proliposomes produced by coating of micronised sucrose and hydration of phospholipid powders to obtain multilamellar liposomes. **International Journal of Food Science & Technology**, 52, 772-780.

Tanford, C. (1980). **The hydrophobic effect: Formation of micelles and biological membranes** (2nd ed.). New York, NY: Wiley-Interscience, pp. 233.

Taylor, T. M. et al. (2005). Liposomal nanocapsules in food science and agriculture. **Critical Reviews in Food Science and Nutrition**, 45, 587-605.

Timmermann, E. O., Chirife, J., & Iglesias, H.A. (2001). Water sorption isotherms of foods and foodstuffs: BET or GAB parameters? **Journal of Food Engineering**, 48, 19-31.

Tsvetkova, N. M. et al. (1998). Effect of sugars on headgroup mobility in freeze-dried dipalmitoylphosphatidylcholine bilayers: Solid-State 31P NMR and FTIR studies. **Biophysical Journal**, 75, 2947-2955.

Wagner, A., & Vorauer-Uhl, K. (2011). Liposome Technology for Industrial Purposes. **Journal of Drug Delivery**, 2011, 1-9.

Yokota, D., Moraes, M., & Pinho, S. C. (2012). Characterization of lyophilized liposomes produced with non-purified soy lecithin: a case study of casein hydrolysate microencapsulation. **Brazilian Journal of Chemical Engineering**, 29, 325-335.

Zhang, K. et al. (2016). Development of quercetin-phospholipid complex to improve the bioavailability and protection effects against carbon tetrachloride-induced hepatotoxicity in SD rats. **Fitoterapia**, 113,102-109.

Chapter 3. UNPURIFIED SOYBEAN LECITHINS IMPACT ON THE CHEMISTRY OF PROLIPOSOMES AND LIPOSOME DISPERSIONS ENCAPSULATING VITAMIN D_3

Chapter 3. Unpurified soybean lecithins impact on the chemistry of proliposomes and liposome dispersions encapsulating vitamin D$_3$

Abstract

Vitamin D$_3$ (VD3)-loaded proliposomes using the micronized sucrose coating (MSC) technique and mixtures of soybean lecithins with variable degrees of purity were prepared. The phospholipid powders were characterized in terms of water activity, moisture content, solubility, hygroscopicity, moisture adsorption isotherms and the retained amount of VD3. X-ray diffraction and Fourier transform infrared spectroscopy were the techniques applied to investigate molecular interactions among the ingredients during the coating process, as well as the crystalline structure of the phospholipid powders. Liposome dispersions were produced by hydration of the proliposomes. The liposomal systems were analyzed in terms of hydrodynamic diameter, size distribution, zeta potential and the amount of encapsulated VD3. The morphologies of proliposomes and liposomes were observed using scanning electron microscopy and atomic force microscopy, respectively. The VD3-proliposomes showed low values for water activity, moisture content and solubility as well as high values for hygroscopicity. Liposome dispersions were in the nanometer range and showed high values for zeta potential, but remained stable for only 15 days, probably due to the high concentrations of unpurified lecithin used throughout the process (≥50% w/w). However, the content of VD3 in proliposomes and in loaded-liposome dispersions reached 81.4 and 90.2%, respectively. The results suggested that it was feasible to prepare VD3-entrapped proliposomes using the MSC method, but storage conditions must be better controlled to maintain their stability.

Keywords: nanoencapsulation; cholecalciferol; non-purified phospholipids; nanoliposomes; mixed liposomes.

3.1. Introduction

Vitamins have several fundamental roles, including the promotion of normal body growth, and the prevention and treatment of several disorders. Vitamin D (VD), which comprises vitamin D_2 (VD2, ergocalciferol) and vitamin D_3 (VD3, cholecalciferol), is a prohormone with different biological effects, including the control of calcium and phosphorus metabolism (Wiseman, 1993). VD3 is the most active form of VD, and it can be synthesized after the exposure to light of 7-dehydrocholesterol molecules present in the human epidermis (Lee et al., 2008). Nevertheless, VD3 deficiency is now recognized as a pandemic (Holick, 2017). The main cause for such deficiency is the lack of sunlight exposure due to several reasons, such as (a) staying indoors for long periods of time, (b) some geographic conditions at higher latitudes, and (c) the loss of 7-dehydrocholesterol reserves in the epidermis throughout the years (Holick, 2017).

Unfortunately, only a few foods naturally contain VD3. Examples include fresh salmon, cod liver oil, and egg yolk (Holick, 2007). The fortification of food products with VD3 appears to be a possible solution to overcome this drawback (Gomes et al., 2015). However, to optimize the fortification process, tighter control of processing conditions is necessary, as this vitamin is susceptible to degradation, especially when exposed to light, oxygen, elevated temperatures and humidity (Jakobsen & Knuthsen, 2014). Several colloidal systems are already being studied for the delivery of VD3, such as micelles (Desmarchelier et al., 2017), nanoemulsions (Ozturk et al., 2015), polymeric nanospheres (Ramezanli et al., 2017), water-in-oil-in-water double emulsions (Dima & Dima, 2020) and liposomes (Chaves et al., 2018). The incorporation of VD3 into lipid carrier systems as liposomes may create a barrier against prooxidant agents, in addition to increasing its bioavailability (Chaves et al., 2018).

Liposomes are amphipathic spherical-shaped vesicles that contain an internal aqueous phase surrounded by one or more concentric phospholipid bilayers. These systems are applied for encapsulation because of their capacity to entrap both lipophilic and hydrophilic functional compounds (Emami et al., 2016). When compared to other carrier systems, liposomes have numerous advantages, including biodegradability, biocompatibility, non-immunogenicity and non-toxicity (Tai et al., 2018). In the food industry, these carriers can be used to deliver flavor compounds, enzymes, vitamins, proteins and antioxidants in foods such as milks, yogurts, cheeses and juices (Marsanasco et al., 2015; Mozafari et al., 2008). Liposomes were successfully

studied as delivery systems for vitamin A (Sachaniya et al., 2018), vitamin C (Parhizkar et al., 2018), vitamin E (Laouini et al., 2013) and vitamin K1 (Campani et al., 2014).

Various phospholipids, such as phosphatidylcholine (PC), phosphatidylethanolamine (PE), phosphatidylinositol (PI) and lysophosphatidylcholine (LPC), are commonly used in different types of liposome formulations. All of them can be isolated from natural sources and purified to different extents, and the more purified, the higher their price (Paltauf & Hermetter, 1990). Natural soybean phospholipids are preferably used instead of synthetic ones, as they are derived from renewable sources, are produced with more ecologically friendly processes, have a higher nutritional polyunsaturated fatty acid profile, and are available in larger scale at relatively low costs (Van Hoogevest & Wendel, 2014). However, the degree of lipid unsaturation is a parameter used to describe membrane susceptibility to oxidation (Rudolphi-Skórska et al., 2017). VD3 is a membrane antioxidant that can possibly prevent lipid peroxidation (Talebi et al. 2019). VD3 acts by regulating proteins that can reduce oxidative stress and by increasing glutathione, which is the molecule responsible for protecting neurons from oxidative degenerative diseases (Jain et al., 2018).

Improving the stability of liposomes with storage remains a challenge. Liposomal dispersions have problems related to vesicle instability, such as hydrolysis and phospholipid oxidation. A loss of the encapsulated material may occur as well as vesicle fusion and/or aggregation (Yan-Yu et al., 2006). An effective way to overcome these problems is formulating liposomes as proliposomes (Kumar et al., 2001). This idea was originally developed by Payne et al. (1986), who defined proliposomes as free-flowing dry particulate systems in which the lipid matrix contains the bioactive compound to be encapsulated. Furthermore, proliposomes can also be obtained in the form of pellets or capsules using easy industrial procedures such as extrusion/spheronization, simple compressing, and cogrinding/wet granulation (Luo et al., 2013; Tantisripreecha et al., 2011; Zhang et al., 2016).

The proliposomes obtained in this study were produced using the micronized sucrose coating (MSC) method. Elhissi et al. (2006) showed that the use of sucrose as a micronized carrier led to the formation of more stable liposomes after the hydration of proliposomes than those obtained using the dry-lipid film method. The use of sucrose also contributes to the homogeneity in the size of vesicles when compared to the size obtained using other carbohydrate carriers, such as trehalose and lactose (Elhissi et al., 2010). Another advantage of

MSC is the use of lower temperatures, making it suitable for the incorporation of thermolabile bioactive compounds, such as vitamins (Chaves et al., 2018).

The present study produced vitamin D_3 (VD3)-incorporated proliposomes using the micronized sucrose coating method (MSC) by exploring the possibility to replace part of the purified phospholipids by unpurified lecithins during production. The proliposomes were characterized for 30 days of storage using analyses and techniques commonly applied for particulate systems, such as the determination of their water activity (aw), moisture content, solubility, hygroscopicity and the retained VD3. Powders were also characterized using scanning electron microscopy (SEM), Fourier transform infrared spectroscopy (FT-IR) and X-ray diffraction (XRD). Liposome dispersions were produced after the hydration of proliposomes and characterized for 15 days in terms of the morphology, particle size, zeta potential and the amount of encapsulated VD3.

3.2. Materials and methods

3.2.1. Chemicals and reagents

Vitamin D_3 (VD3, cholecalciferol, >98% purity, analysis of standard) was purchased from Sigma-Aldrich Co. (St. Louis, MO, USA). Purified soy phosphatidylcholine (Phospholipon 90H, P90H, >90% w/w PC, >4% w/w LPC, and >2% w/w triglycerides (TG)) and fat-free powdered lecithin (Lipoid S40, LS40, >40% w/w PC, >15% PE, >4% LPC, and >3% w/w PI were obtained from Lipoid GmbH (Ludwigshafen, Germany). Xanthan gum (XG) (Grindsted Xanthan 80) was kindly supplied by DuPont (Cotia, SP, Brazil), and guar gum (GG) was obtained from Êxodo Científica (Hortolândia, SP, Brazil). Sucrose and sodium benzoate were purchased from Synth (Diadema, SP, Brazil). For vitamin D_3 quantification, methanol and acetonitrile (HPLC-grade) were obtained from Merck (Darmstadt, Germany) and Êxodo Científica Sumaré, SP, Brazil, respectively. Water was purified with a Milli-Q system (Millipore Corp., Billerica, MA, USA) and used throughout the experiments. The other chemicals and reagents used in this study were of analytical grade and mainly from Dinâmica Química Contemporânea (Indaiatuba, SP, Brazil).

3.2.2. Production of VD3-containing proliposomes

The micronized sucrose coating method used to produce proliposomes was described in Chaves and Pinho (2019). Briefly, a VD3 stock solution was prepared using 0.01 g of powder in 100 mL methanol (which corresponded to a final solution containing almost 400,000 IU of

VD3) using a magnetic stirring at 3,200 rpm at 25 °C for 30 min. The formulations used for proliposome production are summarized in Table 3.1. Briefly, the phospholipids and 20 mL (~80,000 IU) of the VD3 stock solution were added to 100 mL absolute ethanol (Dinâmica) and the resulting mixture was homogenized using ultra-agitation (T25 Ultra-Turrax, IKA, Staufen, Germany) at 13,000 rpm at 25 °C for15 min. Then, the ethanolic solution was dripped with the aid of a peristaltic pump (4 mL/min, Masterflex 7528-30, Cole-Palmer, Vernon Hills, IL, USA) onto 2 g of sucrose previously micronized in a ball mill (CE500, CIENLAB, Campinas, SP, Brazil). As LS40 is not easily dispersed in ethanol, the solutions were maintained using sonication (40 kHz/135 W) (Ultra Cleaner 1400 bath, Unique, Indaiatuba, SP, Brazil) until the end of the dripping process. The ethanol was all removed using a rotary evaporator (MA120, Marconi, Piracicaba, SP, Brazil) at 55 ± 2 °C. The resulting powders were stored in amber flasks and kept in vacuum desiccators at room temperature (25 ± 2°) for a maximum of two wk.

Table 3.1. Formulations used for the production of VD3-loaded proliposomes

Formulation	Phospholipon 90H (g)	Lipoid S40 (g)	Vitamin D_3 (IU)	Ethanol (mL)
F50V	1.6	1.6	80,000	100
F70V	0.96	2.24	80,000	100
F100V	-	3.2	80,000	100

Reference: Chaves & Pinho (2020)

3.2.3. Characterization of the proliposomes

3.2.3.1. Morphology

The morphology of the proliposomes was measured using SEM (TM-300, Hitachi, Tokyo, Japan) operated at 15 kV. The samples were placed on double-faced carbon tapes and fixed to aluminum stubs. No pre-treatment was done. The micrographs were obtained at 100 × magnification.

3.2.3.2. Water activity (a_w) and moisture content (X_w)

The a_w of samples was obtained using an AquaLab instrument (Decagon Devices, Pullman, WA, USA). The equipment was calibrated using pure water at room temperature. Samples were placed in sample cups and filled to ~½ full and aw was measured at 25 °C using

the instrument drawer. The values were obtained using the continuous mode. The Xw was measured using a moisture analyzer with infrared radiation (MB35 Halogen, Ohaus, Nänikon, Switzerland) until constant weight.

3.2.3.3. Solubility

Solubility analysis was done as described by Chaves and Pinho (2019) based on Eastman and Moore (1984). Briefly, 50 mL of deionized water was added to 0.5 g of proliposomes and homogenized at 200 rpm at 25 °C for 20 min using an orbital shaker (Marconi). Then, the sample was centrifuged at $1.10 \times 10^3 \times g$ at 25 °C for 30 min using a high-speed refrigerated centrifuge (5430R, Eppendorf, Hamburg, Germany). Aliquots of 25 mL of the supernatant were placed in previously weighed Petri dishes and dried at 105 °C for 24 h in an oven. The solubility results were expressed as percentage of solubilized powder in the water considering the initial mass of sample that would be represented by the 25 mL.

3.2.3.4. Hygroscopicity

The analysis of hygroscopicity was done as described by Chaves and Pinho (2019) based on Cai and Corke (2000). Briefly, 0.2 g of sample was placed in a glass vessel and stored for 1 wk at 25 °C in a desiccator containing a saturated sodium chloride solution (relative humidity: 62%). Hygroscopicity was obtained using Eq. (1). The values previously measured for moisture content were used to obtain the mass of samples on a dry weight (dw) basis (MD):

$$Hygroscopicity\ (g\ H_2O\ adsorbed/100\ g\ dry\ matter) = WG\ (g)/MD\ (g) * 100 \qquad (1)$$

where WG = water gain after 1 wk.

3.2.3.5. Moisture adsorption isotherms

The gravimetric method described by Labuza (1984) was applied to obtain the sorption isotherms of the proliposomes. Briefly, powder samples were placed in glass vessels and stored in desiccators for 4 wk at 25 °C, including salt solutions with different aw (Chaves & Pinho, 2019). Periodically, the amount of adsorbed water was measured as the gain in weight. The moisture sorption isotherms were assessed by fitting the values of the equilibrium moisture to the Oswin and Halsey models showed in Eqs. (2), (3)), respectively.

$Oswin\ model: X = a * [A_w/(1 - A_w)]\char`^b$ (2)

$Halsey\ model: X = [(-A_w)/(\ln(A_w)]\char`^(1/b)$ (3)

where X represents the moisture content on dw basis and a and b are constants.

3.2.3.6. XRD

The crystalline structure of the proliposomes was analyzed using XRD with a copper anode tube, λ = 1.5418 Å and a graphite monochromator in the diffracted beam (MiniFlex600, Rigaku, Tokyo, Japan). The measurements were done using a few mg of each sample and a scan speed of 2°/min between 5° and 35° (2θ).

3.2.3.7. FT-IR

The infrared spectra of the samples were obtained on a spectrophotometer (Spectrum One, v. 5.3.1, PerkinElmer, Waltham, MA, USA) using a 100:1 KBr to sample ratio (by weight), a speed of 0.2 cm/s, 20 scans, 4 cm^{-1} of resolution and spectral range from 4000 to 400 cm^{-1} (PerkinElmer).

3.2.3.8. VD3 content in the proliposomes

The quantification of VD3 in the proliposomes was done using the method of Staffas and Nyman (2003). Sample (300 mg) was diluted in 5 mL methanol and Vortexed (IKA) at 1250 rpm at 25 °C for 5 min. Then, the resulting solutions were sonicated at 25 °C for 10 min and centrifuged at 7.40 x 10^3 × g at 4 °C for 5 min to separate the vitamin from the lipid matrix. The supernatant was brought to 10 mL methanol to enhance the extraction. The methanolic extracts were filtered using nylon syringe filters (0.45 μm, Ø = 13 mm, LCR Científica, Americana, SP, Brazil), transferred to 2 mL vials and measured using high-performance liquid chromatography (HPLC, Shimadzu Prominence System, Kyoto, Japan). The separation was done using a Shim-Pack VP-ODS column (4.6 μm, 0.46 × 25 cm, Shimadzu) maintained at 35 °C. Methanol and acetonitrile were used for sample separation at a ratio of 9:1 (v/v) and a constant flow of 1.6 mL.min-1. Aliquots of 10 μL were analyzed at 265 nm for 10 min. VD3 was identified based on its retention time (7.3 min), and the concentrations of the VD3 standard were plotted against the values of the area under the curve (AUC) obtained using the software with the

equipment. The predictive equation (R^2 = 0.9946) was obtained over the concentration range 0.3–12 µg/mL (Chaves et al., 2018).

3.2.4. Production of VD3-loaded liposome dispersions

VD3-loaded liposome dispersions were produced as described by Chaves et al. (2018) and Chaves and Pinho (2019). Briefly, 2 g of proliposomes was hydrated with 100 mL deionized water and homogenized using ultra-agitation at 13,000 rpm at 65 °C for 5 min. The dispersions were cooled to 25 °C before the addition of xanthan gum (0.01% w/v) and guar gum (0.09% w/v) as stabilizers and sodium benzoate (0.02% w/v) as the antimicrobial agent. The resulting systems were mixed using magnetic stirring at 3,600 rpm at 25 °C for 20 min, transferred to amber flasks and refrigerated at 10 °C for a maximum of 4 wk.

3.2.5. Physicochemical characterization of the VD3-loaded liposome dispersions

3.2.5.1. Particle size and zeta potential

The particle size of the vesicles was measured using photon correlation spectroscopy (PCS) at 25 °C using a ZetaPlus analyzer (Brookhaven Instruments Co., Holtsville, NY, USA). Samples were diluted 100 × in their original solvent and measured at 627 nm. The zeta potential was also determined in the ZetaPlus analyzer after diluting the dispersions (1:5 v/v) in a 1 mM KCl solution. Both sets of results were calculated by the software with the instrument.

3.2.5.2. Morphology

Atomic force microscopy (AFM) images of liposomes were obtained using an NT-MDT microscope (Solver Next, Zelenograd, Russia). Dispersions were diluted 100 × in deionized water prior to visualization. The conditions used were as follows: force constant, 5 N.m-1; resonance frequency for the cantilever, 150 kHz; and scanning velocity, 0.7 Hz. The diluted liposomes were placed on the surface of a mica disk and left stationary for 2 min. Filter paper was used to remove excess diluted liposomes when necessary.

3.2.5.3. VD3 content in the liposome dispersions

The amount of encapsulated VD3 in the liposome dispersions was determined using high-performance liquid chromatography (HPLC) with the same conditions as showed in section

2.3.8. In this case, sample (2 g) of liposome dispersion was diluted in 5 mL methanol before starting the analysis.

3.2.6. Statistical analyses

All analyses were done in triplicate, and the results are expressed as the average ± standard deviation. One-way analyses of variance were done using SAS Software version 9.2 (Statistical Analysis Systems, Cary, NC, USA). Differences among samples were measured using Tukey's test with a significance level of $p \leq 0.05$.

3.3. Results and discussion

3.3.1. Characterization of VD3 proliposomes

3.3.1.1. Morphology

The surface morphology of the VD3 proliposomes studied using SEM is shown in Fig. 3.1a–c. The micrographs showed that the particles were coarse and porous and showed various shapes. An increase in the amount of LS40 in the proliposome formulation apparently led to the formation of particles with a narrower shape. The size of the particles produced with formulation F50V ranged from 2 to 3 mm, and the particles were more homogenously rounded than the particles of the other formulations. On the other hand, particles produced with only LS40 (F100V) showed sizes that ranged from 4 to 8 mm, and they were more agglomerated than those in F50V. Therefore, it could be inferred that proliposomes produced with less LS40 could be more hydrated. F50V showed more porous particles than those of the other formulations, which facilitated their further hydration (Chaves & Pinho, 2019). The surface of the proliposomes produced with more LS40 showed a more uniform coating compared to that of the others, probably due to a more effective deposition of phospholipids on the sucrose granules. However, this aspect can hamper the contact between the water and the sucrose granules, decreasing their potential for hydration (Elhissi et al., 2012). The smaller the proliposomes are, the larger their specific area and, consequently, more easily hydrated (Xia et al., 2012).

Figure 3.1. Micrographs obtained by scanning electron microscopy (SEM) for the proliposomes containing vitamin D_3 produced with different concentrations of Phospholipon 90H (P90H) and Lipoid S40 (LS40): (A) 50:50 w/w P90H:LS40 (F50V), (B) 30:70 w/w P90H:LS40 (F70V), and (C) 0:100 w/w P90H:LS40 (F100V). Error bars: 1 mm. Magnification: 100 ×. Moisture adsorption isotherms (at 25 °C) obtained by fitting adsorption data using (D) the Oswin model (−) and (E) the Halsey model (−) for the formulations (■) F50V, (●) F70V, and (▲) F100V
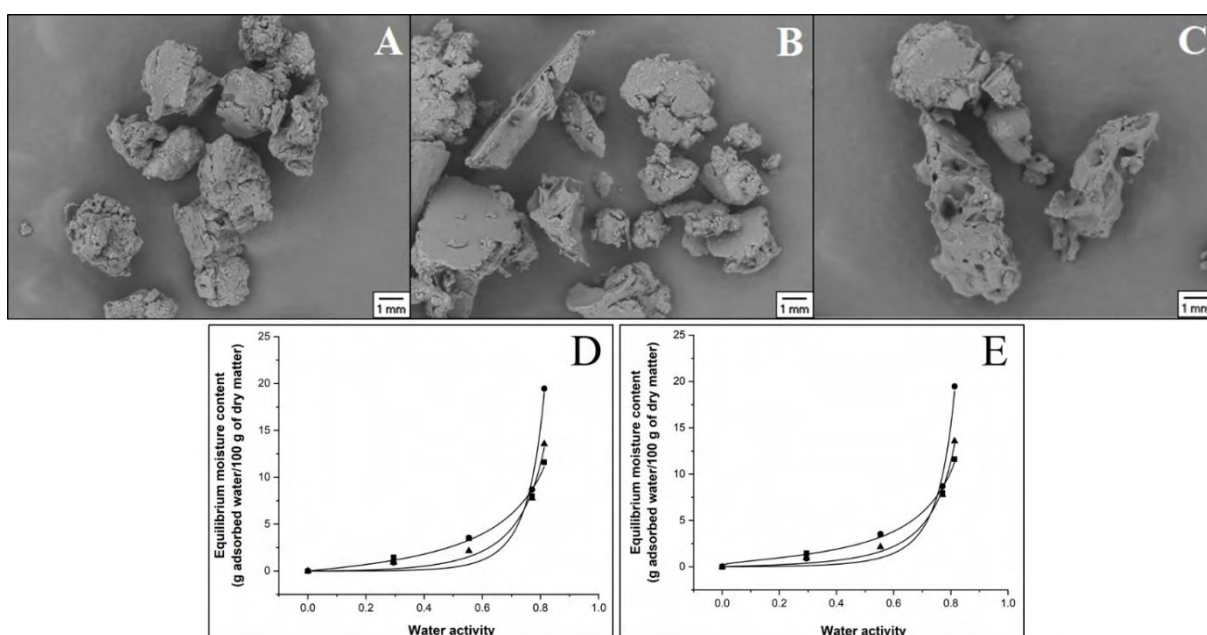
Reference: Chaves & Pinho (2020)

3.3.1.2. Water activity (a_w) and moisture content

Water activity measurements provide information on how water binds to the powder matrix, while moisture content measures the total amount of water (Juarez-Enriquez et al., 2011). The values obtained for both parameters are shown in Table 3.2. The results obtained for a_w were considered to be good, as low values lead to the desirable handling of food powders (Cuq et al., 2011). The growth of microorganisms is delayed in environments with a_w <0.60 and most bacteria in media with a_w <0.87 (Beuchat et al., 2013). Otherwise, food powders with low water activities are more susceptible to lipid oxidation (Labuza et al., 1970; Vu et al., 2020). Lipid oxidation tends to be minimized when the water content corresponds to a monomolecular layer (Smith et al., 2002). However, the addition of VD3 to liposomal membranes may be helpful to inhibit the lipid oxidation rate, as this bioactive compound may

have antioxidant properties (Wiseman, 1993). On the other hand, the moisture content values can also be a good indicator of long stability, as microbial growth is significantly decreased when this parameter is <10% (Mercer, 2008). The increase in the amount of unpurified phospholipids did not result in significant differences in either parameter.

Table 3.2. Powder properties obtained for the vitamin D_3 proliposomes

Powder properties		Formulations		
		F50V	F70V	F100V
Water activity (A_w)		$0.17^{AB} \pm 0.02$	$0.13^{B} \pm 0.01$	$0.19^{A} \pm 0.02$
Moisture content (%)		$1.93^{A} \pm 0.26$	$1.98^{A} \pm 0.20$	$2.22^{A} \pm 0.30$
Solubility (% solubilized powder)		$46.4^{A} \pm 1.02$	$46.8^{A} \pm 1.00$	$42.6^{B} \pm 1.36$
Hygroscopicity (g adsorbed water/100g dry matter)		$7.24^{A} \pm 0.23$	$8.43^{A} \pm 0.72$	$6.78^{A} \pm 1.48$
Vitamin D_3 concentration (µg/g of proliposome)	1st day	$250.5^{Ba} \pm 10.9$	$277.8^{Aa} \pm 4.50$	$257.8^{Ba} \pm 6.55$
	30th day	$267.1^{Aa} \pm 8.61$	$266.4^{Aa} \pm 12.3$	$209.9^{Bb} \pm 7.10$
% vitamin D_3 preserved		100	95.9	81.4
Parameters fitted using the Oswin model	A	2.67 ± 0.40	0.40 ± 0.44	1.06 ± 0.40
	B	0.97 ± 0.11	2.62 ± 0.75	1.72 ± 0.27
	R^2	0.9907	0.9608	0.9882
Parameters fitted using the Halsey model	A	1.57 ± 0.27	0.58 ± 0.16	0.76 ± 0.12
	B	0.84 ± 0.08	0.35 ± 0.10	0.50 ± 0.06
	R^2	0.9939	0.9648	0.9918

Means followed by the same uppercase letter in the same line and by the same lowercase letter in the same column were not significantly different ($p > 0.05$) by Tukey's test.

Reference: Chaves & Pinho (2020)

3.3.1.3. Solubility

The results for the solubility of the proliposomes are also shown in Table 3.2. The powders showed solubility values similar to those obtained by Chaves and Pinho (2019), in which curcumin-containing proliposomes were produced using the same phospholipids. Elhissi et al. (2012) proposed that the low solubilities with proliposomes produced using the MSC method might be related to the number of phospholipids that effectively cover the carrier molecule. According to the authors, the higher this number, the lower the area available for

contact between the water and the carrier, which explains the lower solubility rates. These results are consistent with those obtained from SEM images (Fig. 1a–c). Some phospholipids, such as PE, are not as easily hydrated as PC when added to an aqueous medium, which might be the cause of the decreased solubility of the proliposomes produced with higher amounts of unpurified phospholipids (McIntosh, 1996).

3.3.1.4. Hygroscopicity and moisture sorption isotherms

The results for the hygroscopicity of proliposomes are shown in Table 3.2. The values measured can be considered low since sucrose was used as the carrier, and this molecule has an amorphous structure. Additionally, moisture sorption isotherms are shown in Fig. 3.1d-e. The understanding of moisture sorption isotherms for food powders is used for the design and optimization of several processes such as packaging and the prediction of moisture changes during drying (Jamali et al., 2006). The isotherms obtained for proliposomes are consistent with the Type III isotherm proposed by Brunauer et al. (1969). For this type of isotherm, an increase in aw led to an increase in the moisture content, a behavior frequently observed for solids soluble in water, e.g., sugars, and described by formulae based on Raoult's Law (Blahovec & Yanniotis, 2009). Adsorption data also suggested that proliposomes showed microbiological stability (a_w <0.60) at moisture contents <7.5 g of adsorbed water/100 g of dm. Some protective measures (e.g., vacuum storage or refrigeration) must be taken to ensure the stability of the systems, as the values obtained for hygroscopicity (considering the standard deviations) were >7.5 g of adsorbed water/100 g of dm for all the formulations (Samborska et al., 2019). Additionally, it is possible to infer that sample F70V will be the most hygroscopic during storage, as it showed a more pronounced inflection point at a_w >0.60. In general, the high values obtained for hygroscopicity are consistent with sugar-high, amorphous, metastable powders with low aw (Roos and Karel, 1991; Samborska et al., 2019). The adsorption by carbohydrates occurs due to the links between hydrogen atoms present in water and hydroxyl groups present in the amorphous regions of the substrate (Samborska et al., 2019; Shi et al., 2013). The parameters obtained by fitting the experimental data to the Oswin and Halsey models are shown in Table 3.2. From the values of the coefficient of determination (R^2), the Halsey model fit the experimental data slightly better than the Oswin model. However, a good fit is ensured if the value of R^2 >0.99. The Oswin method is mathematically consistent when the values for "a" and for "b" are >0 and <1, respectively (Blahovec, 2004). From this perspective, the Oswin

model was only effective in fitting F50V data. On the other hand, the Halsey model fit the data for F50V and F100V. This model has been used to adjust moisture values obtained from meat and dairy foods as well as seeds (Ghayal et al., 2013). The literature concerning the fitting of moisture sorption data for proliposomes is still limited.

3.3.1.5. XRD

XRD patterns of VD3-entrapped proliposomes are shown in Fig. 3.2. For the patterns obtained for the pure ingredients used during proliposome production (Fig. 3.2a–d), intense peaks were obtained in the diffractograms of sucrose and VD3, suggesting a crystalline structure. On the other hand, both LS40 and P90H showed an amorphous "halo" pattern in the range of 10° < 2θ < 30°. Characteristic diffraction peaks of VD3 were observed at 15.5°, 17.9° and 21.8°. Sucrose peaks were observed at 11.7°, 18.9°, 19.6° and 24.8°. Moreover, the peaks related to VD3 did not appear in the proliposome patterns (Fig. 3.2e–g), as the low concentration of VD3 added to the formulations (2 mg, ~0.04% w/w) may not have been sufficient to be detected by XRD. The results suggested that the bioactive compound was dispersed homogenously in the proliposome matrix in an amorphous or noncrystalline form (Karn et al., 2014). The patterns obtained for the proliposome formulations overlapped with the diffractograms of the pure components. At this point, all of the characteristic peaks obtained for sucrose, as well as the same amorphous halo region showed for phospholipids, appeared in the diffractograms obtained for the powders (Fig. 3.2e–g). The decrease in the amorphous halo region seen in the diffractogram of the F100V formulation suggested a more crystalline structure than that of the F50V and F70V formulations. The higher number of unhydrated phases observed in the F100V diffractogram was expected as this formulation showed more deposition of material covering the carrier as observed in the SEM image (Fig. 3.1c). As mentioned before, this characteristic can hamper the hydration of the amorphous regions of the sucrose granules. The peaks observed in the proliposome patterns confirm that the crystallinity of sucrose was not completely lost throughout the procedure. The changes observed in the diffractograms obtained for the samples in relation to those obtained for the pure components may suggest some interactions among all the components during the coating process (Rojanarat et al., 2011).

Figure 3.2. XRD patterns obtained for (a) vitamin D$_3$ (VD3), (b) Phospholipon 90H (P90H), (c) Lipoid S40 (LS40), (d) sucrose and for the proliposomes prepared using the formulations: (e) 50:50 w/w P90H:LS40 (F50V), (f) 30:70 w/w P90H:LS40 (F70V) and (g) 0:100 w/w P90H:LS40 (F100V). Characteristic peaks obtained for sucrose are highlighted with blue dot lines and peaks obtained for VD3 are highlighted with red continuous lines

Reference: Chaves & Pinho (2020)
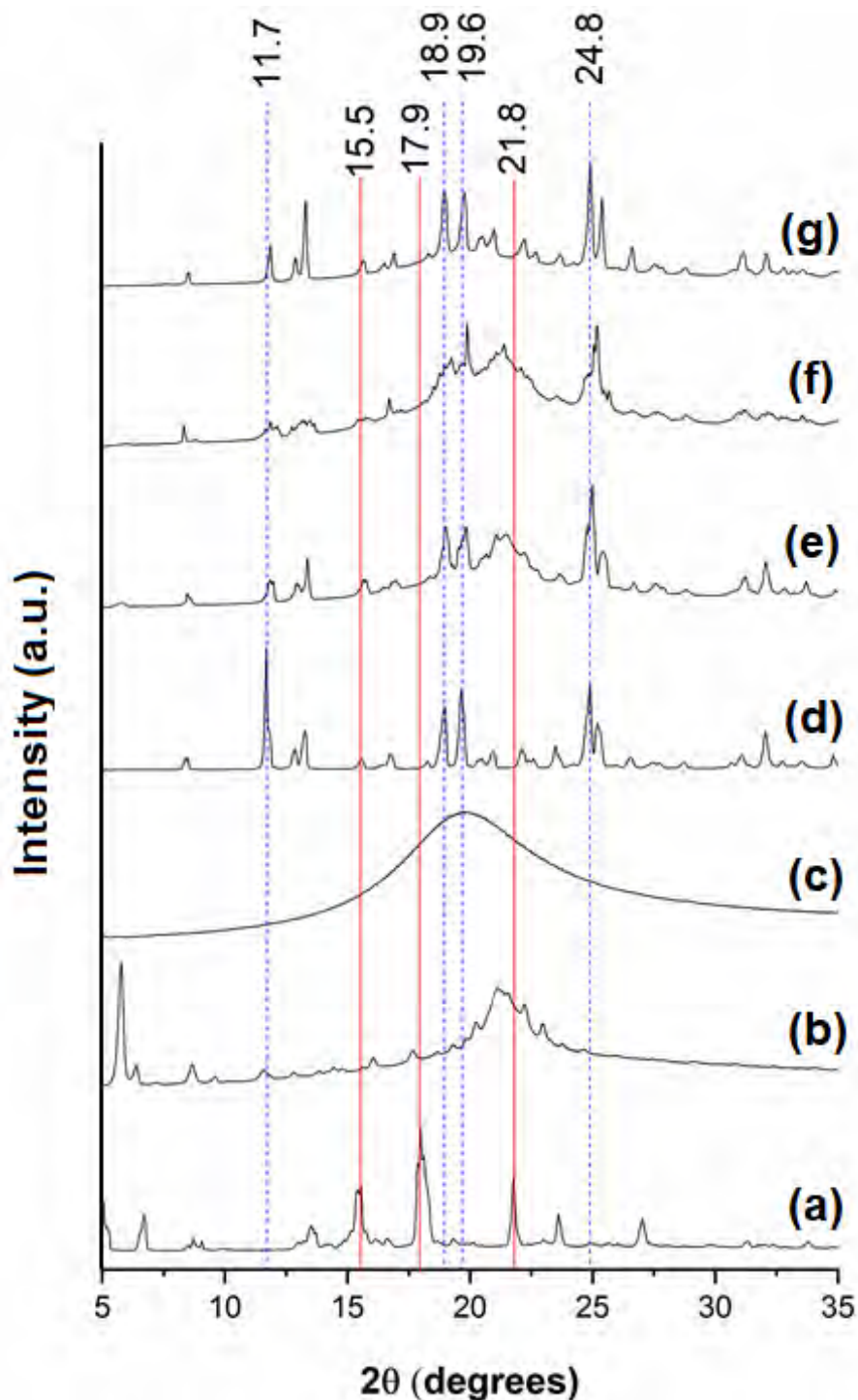
3.3.1.6. FT-IR

Infrared spectroscopy can be applied to investigate structural and conformational changes in the typical absorption bands of the entrapped VD3 since any shifts are indicative of intermolecular interactions between the molecule and the lipid matrix of proliposomes. FT-IR spectra obtained for the pure components (VD3, P90H, LS40 and sucrose) and for the proliposomes produced with different concentrations of phospholipids are shown in Fig. 3.3. The detailed wavenumbers of the relevant bands are also shown in Fig. 3. The peaks related to VD3 (Fig. 3.3a) are characterized by CH3 asymmetric stretching and CH_2 symmetric stretching in the region from 3082 to 2736 cm^{-1} (Ignjatović et al., 2013). The O–H stretching of VD3 is located at a band within the region from 3499 to 3082 cm^{-1} (Braithwaite et al., 2017). As expected, CH_2 and CH_3 stretches are also seen in the spectra of both phospholipids (Fig. 3.3b and c), and the O–H stretch was most prominent in the spectrum obtained for sucrose (Fig. 3.3d). The same peaks observed in the spectra of the formulations (Fig. 3.3e–g) were related to these components, as VD3 was added to samples at a relatively low concentration. However, it was possible to confirm that VD3 was successfully entrapped in the lipid matrix, as no new chemical bonds appeared in the proliposome spectra. This behavior suggested a combination of physical interactions (Pinilla et al., 2019). The "saccharide bands" related to the presence of sucrose were observed in the range of 1200–900 cm^{-1} in the proliposome spectra, which correspond to the stretching of C–C and C–O and to the bending of C–H (Rodriguez-Rosales & Yao, 2020). On the other hand, the spectra of P90H and LS40 showed peaks at 1051 and 1252 cm^{-1} corresponding to the symmetric and asymmetric vibrations of PO_2- groups (Depciuch, Sowa-Kućma, Nowak, et al., 2016), and the 1733 cm^{-1} peak is related to the stretching vibrations of the lipid group (Depciuch, Sowa-Kućma, Misztak, et al., 2016). All peaks were also verified for the formulations but at lower intensities, which suggested some interactions between the phospholipids and the other ingredients. Additionally, the F100V formulation (Fig. 3.3g) showed even lower intensities for CH_2, CH_3 and lipid group stretches, which implied that more interactions may occur when the amount of unpurified phospholipids is increased. The decrease in the intensities of these peaks is related to less ordered acyl chains in dried systems (Chaves & Pinho, 2019).

Figure 3.3. Infrared spectra of (a) vitamin D$_3$ (VD3), (b) Phospholipon 90H (P90H), (c) Lipoid S40 (LS40), (d) sucrose and of proliposomes prepared using the formulations: (e) 50:50 w/w P90H:LS40 (F50V), (f) 30:70 w/w P90H:LS40 (F70V) and (g) 0:100 w/w P90H:LS40 (F100V)
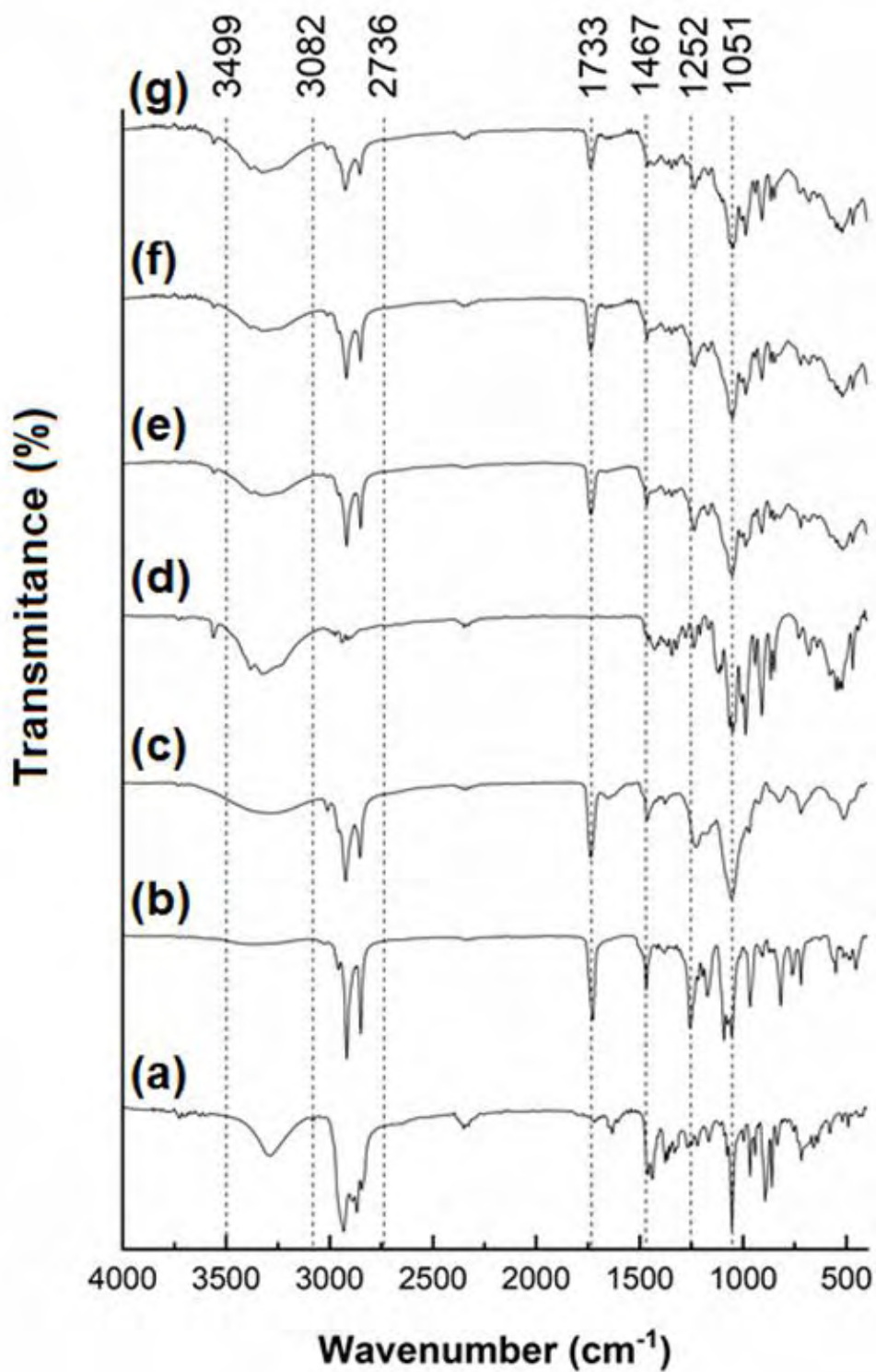
3.3.1.7. VD3 content in the proliposomes

VD3 concentrations in the proliposomes were quantified on the 1st and 30th days of storage, and the results are summarized in Table 3.2. The amount of VD3 increased in the F50V formulation, which was different from the other two formulations, where a slight but not significant decrease was observed. However, the amount of the bioactive compound in all formulations was up to 80%, which is a relatively good result, as VD3 is highly sensitive to several environmental factors, such as light, oxygen, temperature and humidity (Lalloz et al., 2018). Since the proliposomes produced were stored in the dark in vacuum desiccators, no external prooxidant factors were considered deleterious to the VD3 loss observed in either the F70V or F100 formulations. Chu et al. (2011) attributed an increase in the viscosity and a sharp loss of dehydrosilymarin from proliposomes produced using the film dispersion-freeze drying method to excessive amounts of phospholipids in the formulation. In this context, as shown by the SEM micrograph of the F100V formulation (Fig. 1c), the excessive deposition of phospholipids on the surface of the sucrose granules may have been harmful to the entrapment of VD3 in this formulation. Otherwise, proliposomes with this characteristic can be applied as good carriers to deliver VD3 if presented as tablets or pellets since they have relatively high resistance to water penetration (Khan et al., 2018). Alternatively, proliposomes produced using the MSC method are heterogeneous (Elhissi et al., 2011), which may have contributed to some differences in VD3 quantification. Nevertheless, the high percentages of the preservation of the bioactive compound obtained for all formulations were probably related to the high lipophilic characteristic (logP = 9.09) of VD3 (Ramezanli et al., 2017).

3.3.2. Physicochemical characterization of the VD3-loaded liposomal dispersions

3.3.2.1. Hydrodynamic diameter, size distribution and zeta potential

The values measured for hydrodynamic diameter and zeta potential for the VD3-loaded liposomes are shown in Table 3.3. Liposomes showed bimodal distributions even on the 1st day of storage, as shown in Fig. 3.4. The hydrodynamic diameters obtained were in the nanometer region, characteristic of large, unilamellar vesicles (New, 1990). This was unexpected as the hydration of proliposomes usually results in multilamellar vesicles. The sonication step used to maintain the LS40 dispersed in ethanol during the coating process was probably responsible for this reduction in size as previously reported (Chaves & Pinho, 2019). However, even nanoliposomes tend to be stable for longer periods of time than multilamellar vesicles yet, the

dispersions produced remained stable for only 15 days. The cause for such an instability could have been due to the presence of PE, which has a high amount of unsaturated fatty acids in its composition. Therefore, its presence in lipid membranes is usually related to an increase in the permeability of bilayers and a physical instability of liposome dispersions (Biltonen & Lichtenberg, 1993). In addition, PE has a smaller polar head group than that of PC and a larger area occupied by its hydrocarbon chains, which leads to an overall cone-shaped molecule that contributes to tighter packing in the membranes containing PC, thus decreasing the size of the vesicles (Litzinger & Huang, 1992). Curvature increases with decreasing size, which leads to aggregation and phase separation due to the fast kinetics of water absorption (Rovira-Bru et al., 2002). Zeta potential values obtained could be considered to be indicative of "excellent stability", as the limits between stable and unstable dispersions are generally taken as either +30 or −30 mV (Greenwood & Kendall, 1999). The resultant decrease of zeta potential from the 1st to the 15th day for all formulations is indicative of a reduction in the electrostatic repulsion with storage time due to the tendency of nanoformulations to agglomerate because of interparticle adhesion forces (Mahbubul, 2019). Most likely, the unexpected instability observed for the dispersions may be due to the presence of free radicals in the proliposomes that appeared during the sonication step due to the collapse of bubbles by cavitation. Therefore, these radicals can promote the hydrolysis and/or oxidation of phospholipid membranes (Silva et al., 2010).

Table 3.3. Physicochemical parameters obtained (at 25 °C) for vitamin D_3-loaded liposome dispersions over storage time

Formulation/Time	F50V		F70V		F100V	
	1st day	15th day	1st day	15th day	1st day	15th day
Average hydrodynamic diameter (nm)	$270^A \pm$ 2.7	$270^A \pm$ 1.9	$256^B \pm$ 1.2	$259^B \pm$ 1.2	$246^C \pm$ 1.5	$250^C \pm 1.2$
Zeta potential	$-138^{AB} \pm$ 7	$-73^C \pm 10$	$-144^A \pm 6$	$-107^{BC} \pm$ 18	$-143^A \pm$ 17	$-114^{AB} \pm$ 14
VD3 concentration (µg/mL)	$7.60^A \pm$ 1.98	$7.75^A \pm$ 1.80	$8.42^A \pm$ 2.03	$7.60^A \pm$ 1.07	$8.66^A \pm$ 1.64	$8.72^A \pm$ 1.19
% VD3 preserved		100		90.2		100

Means followed by the same uppercase letter in the same line were not significantly different ($p > 0.05$) by Tukey's test.

Reference: Chaves & Pinho (2020)

3.3.2.2. Morphology

The morphologies of the VD3-liposomes were visualized on the 1st day of storage using atomic force microscopy (AFM). As seen in Fig. 3.4, the vesicles showed a spherical shape and a smooth surface. The values of particle size obtained using AFM for F50V and F70V agreed with the values obtained using PCS. However, the value obtained for F100V was higher than that determined using PCS. This deviation could have been related to the interaction of the smooth surface of vesicles with the surface of mica due to lipid spreading or flattening of liposomes (Sriamornsak et al., 2008). Different tendencies can be observed after the adsorption of liposomes on the mica surface in relation to their lipidic composition due to their elastic properties and interaction with the tip (Ruozi et al., 2007). Even with these differences, the AFM and PCS results can be correlated, as the AFM-determined diameters can be recalculated and measured as spheres or hemispheres (Kanno et al., 2002). F100V showed a bimodal size distribution on the 1st day of storage (Fig. 3.4c). The sample analyzed using AFM may have been collected from the second population of liposomes in the higher-diameter region.

Figure 3.4. Size distributions curves of vitamin D$_3$-loaded liposomes produced with different concentrations of Phospholipon 90H (P90H) and Lipoid S40 (LS40): (a) 50:50 P90H:LS40 (F50V), (b) 30:70 P90H:LS40 (F70V), (c) 0:100 P90H:LS40 (F100V) obtained at the 1st day (black lines) and at the 15th day (blue lines) of storage. In detail, micrographs obtained by atomic force microscopy at the 1st day of storage for formulations (A) F50V, (B) F70V, and (C) F100V. Scale: 200 nm
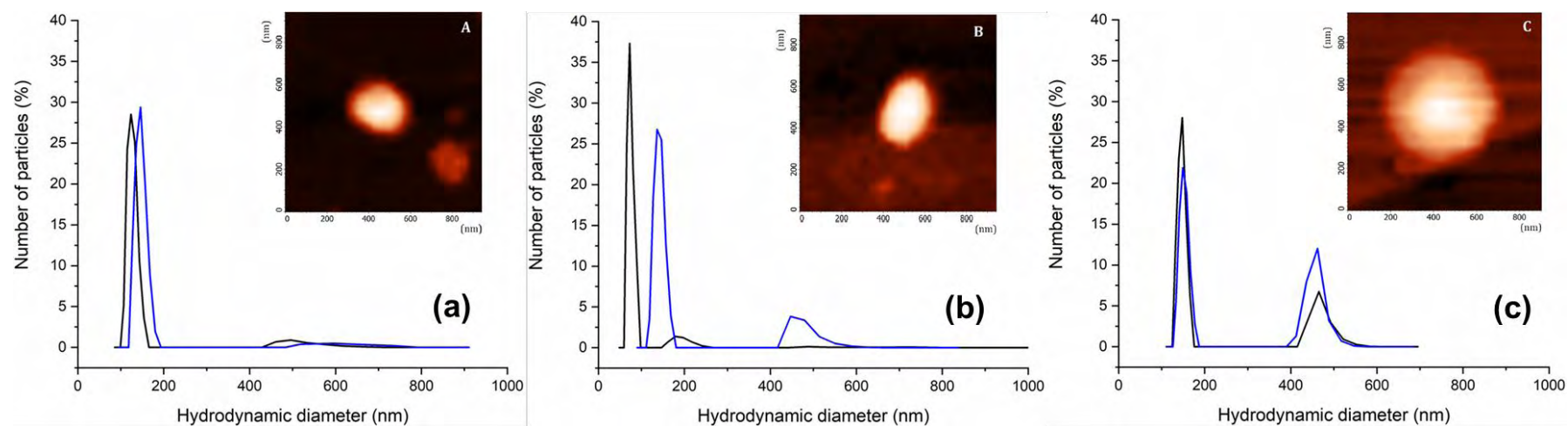
Reference: Chaves & Pinho (2020)

3.3.2.3. VD3 content in the liposome dispersions

The VD3 concentration in the liposome dispersions over 15 days of storage time is shown in Table 3.3. No significant decreases in the concentration of the bioactive compound were observed for any of the formulations. The large standard deviations obtained may be a reflection of liposome heterogeneity. VD3 has been efficiently incorporated into bilayers produced with PC (Chaves et al., 2018; Dalmoro et al., 2019; Merz & Sternberg, 1994; Mohammadi et al., 2014). In Bondar and Rowe (1995), the authors discussed that high concentrations of VD3 retained in liposomes over the storage time must reflect the strong association between this molecule and saturated phospholipids. On the other hand, the results by Tuckey et al. (2008) showed that VD3 can migrate quickly between phospholipid membranes due to its weak association with the bilayers, hindering the action of pro-oxidizing agents. Recently, Dalmoro et al. (2019) obtained an entrapment efficiency of ~88.4% for VD3 encapsulated in nanoliposomes and related the capacity of interchange suggested by VD3 and its high miscibility with PC to a disorder in the structure of lipid membranes, a consequent decrease in their fluidity and a resultant higher retention in vesicles. This can be correlated to the intercalation of VD3 molecules between the hydrocarbon chains of phospholipids and thus to a disturbance of the gel-liquid crystalline phase transition of the vesicles (Merz & Sternberg, 1994).

3.4. Conclusions

VD3-containing proliposomes were successfully prepared using the micronized sucrose coating method. The powders produced can be considered microbiologically safe according to the low values measured for a_w and X_w. The results for hygroscopicity suggested that the powders must be stored in low-humidity conditions to prolong their physicochemical stability. Additionally, the presence of unpurified phospholipids in the proliposome formulations was unfavorable to the solubility of the proliposomes. On the other hand, the bioactive compound was efficiently entrapped in the lipid matrix of the proliposomes, as no new bonds were observed in either the XRD or FT-IR profiles. High retentions of VD3 were observed after 30 days of storage. The crystallinity peaks in the XRD profiles for the proliposomes corroborated the low values obtained for solubility. Otherwise, the amount of unpurified phospholipids was also an important factor regarding the stability of liposome dispersions, suggesting that 50% (w/v) unpurified lecithin was too high for the purpose. Lipid oxidation analysis could be done

to verify the stability of low-saturated phospholipids during storage. Also, measurements of the antioxidant activity of VD3 in the liposomal systems could be helpful to define its potential scavenger capacity.

3.5. Acknowledgements

3.6. References

Biltonen, R. L., & Lichtenberg, D. (1993). The use of differential scanning calorimetry as a tool to characterize liposome preparations. **Chemistry and Physics of Lipids**, 64(1-3), 129-142.

Blahovec, J. (2004). Sorption isotherms in materials of biological origin mathematical and physical approach. **Journal of Food Engineering**, 65, 489-495.

Blahovec, J., & Yanniotis, S. (2009). Modified classification of sorption isotherms. **Journal of Food Engineering**, 91(1), 72-77.

Bondar, O.P., & Rowe, E.S. (1995). Differential scanning calorimetric study of the effect of vitamin D_3 on the thermotropic phase behavior of lipids model systems. **Biochimica et Biophysica Acta**, 1240(2), 125-132.

Braithwaite, M. C. et al. (2017). A novel multi-tiered experimental approach unfolding the mechanisms behind cyclodextrin-vitamin inclusion complexes for enhanced vitamin solubility and stability. **International Journal of Pharmaceutics**, 532(1), 90-104.

Brunauer, S., Skalny, J., & Bodor, E.E. (1969). Adsorption on non-porous solids. **Journal of Colloid and Interface Science**, 30(4), 546-552.

Cai, Y. Z., & Corke, H. (2000). Production and properties of spray-dried Amaranthus betacyanin pigments. **Journal of Food Science**, 65, 1248-1251.

Campani, V. et al. (2014). Development of a liposome-based formulation for vitamin K1 nebulization on the skin. **International Journal of Pharmaceutics**, 9, 1823-1832.

Chaves, M.A. et al. (2018). Structural characterization of multilamellar liposomes coencapsulating curcumin and vitamin D_3. **Colloids and Surfaces A: Physicochemical and Engineering Aspects**, 549, 112-121.

Chaves, M.A., & Pinho, S.C. (2019). Curcumin-loaded proliposomes produced by the coating of micronized sucrose: influence of the type of phospholipid on the physicochemical characteristics of powders and on the liposomes obtained by hydration. **Food Chemistry**, 291, 7-15.

Chu, C. et al. (2011). Proliposomes for oral delivery of dehydrosilymarin: preparation and evaluation in vitro and in vivo. **Acta Pharmacologica Sinica**, 32(7), 973-980.

Cuq, B., Rondet, E., & Abecassis, J. (2011). Food Powders engineering, between knowhow and science: Constraints, stakes and opportunities. **Powder Technology**, 208(2), 244-251.

Dalmoro, A. et al. 2019). Micronutrients encapsulation in enhanced nanoliposomal carriers by a novel preparative technology. **RSC Advances**, 9, 19800.

Depciuch, J. et al. (2016a). Phospholipid-protein balance in affective disorders: Analysis of human blood serum using Raman and FTIR spectroscopy. A pilot study. **Journal of Pharmaceutical and Biomedical Analysis**, 131, 287-296.

Depciuch, J. et al. (2016b). Olfactory bulbectomy-induced changes in phospholipids and protein profiles in the hippocampus and prefrontal cortex of rats. A preliminary study using a FTIR spectroscopy. **Pharmacological Reports**, 68(3), 521-528.

Desmarchelier, C. et al. (2017). Comparison of the micellar incorporation and the uptake of cholecalciferol, 25- hydroxycholecalciferol and 1-α-hydroxycholecalciferol by the intestinal cell. **Nutrients**, 9, 1152.

Dima, C., & Dima, S. (2020). Bioaccessibility study of calcium and vitamin D_3 co-microencapsulated in water-in-oil-in-water double emulsions. **Food Chemistry**, 303, 125416.

Eastman, J.E., & Moore, C.O. (1984). Cold water soluble granular starch for gelled food composition. U.S. **Patent 4465702**, 14 ago. 1984.

Elhissi, A., Gill, H., Ahmed, W., & Taylor, K. (2011). Vibrating-mesh nebulization of liposomes generated using an ethanol-based proliposome technology. **Journal of Liposome Research**, 21(2), 173-180.

Elhissi, A.M. et al. (2006). Formulations generated from ethanol-based proliposomes for delivery via medical nebulizers. **The Journal of Pharmacy and Pharmacology**, 58(7), 887-894.

Elhissi, A.M. et al. (2010). Development and characterisation of freeze-dried liposomes containing two anti-asthma drugs. **Micro & Nano Letters**, 5(3), 184-188.

Elhissi, A.M. et al. (2012). A study of size, microscopic morphology, and dispersion mechanism of structures generated on hydration of proliposomes. **Journal of Dispersion Science and Technology**, 33(8), 1121-1126.

Emami, S. et al. (2016). Liposomes as carrier vehicles for functional compound in food sector. **Journal of Experimental Nanoscience**, 11(9), 737-759.

Ghayal, G. et al. (2013). Moisture sorption isotherms of dietetic Rabri at different storage temperatures. **International Journal of Dairy Technology**, 66(4), 587-594.

Gomes, F.P. et al. (2015). Simultaneous quantitative analysis of eight vitamin D analogues in milk using liquid chromatography-tandem mass spectrometry. **Analytica Chimica Acta**, 891, 211-220.

Holick, M.F. (2017). The vitamin D deficiency pandemic: Approaches for diagnosis, treatment and prevention. **Reviews in Endocrine and Metabolic Disorders**, 18(2), 153-165.

Ignjatović, N. et al. (2013). Multifunctional hydroxyapatite and poly(d,l-lactide-co-glycolide) nanoparticles for the local delivery of cholecalciferol. **Materials Science and Engineering: C**, 33(2), 943-950.

Jain, S. K. et al. (2018). Glutathione stimulates vitamin D regulatory and glucose-metabolism genes, lowers oxidative stress and inflammation, and increases 25-hydroxy-vitamin D levels in blood: A novel approach to treat 25-hydroxyvitamin D deficiency. **Antioxidants & Redox Signaling,** 29(17), 1792-1807.

Jakobsen, J., & Knuthsen, P. (2014). Stability of vitamin D in foodstuffs during cooking. **Food Chemistry,** 148, 170-175.

Jamali, A. et al. (2006). Sorption isotherms of Chenopodium ambrosioides, leaves at three temperatures. **Journal of Food Engineering**, 72, 77–84.

Juarez-Enriquez, E. et al. (2017). Effect of water content on the flowability of hygroscopic powders. **Journal of Food Engineering**, 205, 12-17.

Kanno, T. et al. (2002). Size distribution measurement of vesicles by atomic force microscopy. **Analytical Biochemistry**, 309(2), 196-199.

Karn, P. R. et al. (2014). Preparation and evaluation of cyclosporin A-containing proliposomes: a comparison of the supercritical antisolvent process with the conventional film method. **International Journal of Nanomedicine**, 9, 5079-5091.

Kumar, R., Gupta, R. B., & Betageri, G. V. (2001). Formulation, characterization, and in vitro release of glyburide from proliposomal beads. **Drug Delivery**, 8(1), 25-27.

Labuza, T. P. (1985). **Moisture sorption: Practical aspects of isotherm measurement and use**. Saint Paul, MN: American Association of Cereal Chemists ISBN: 978-1-8911-2718-2.

Lalloz, A. et al. (2018). Effect of surface chemistry of polymeric nanoparticles on cutaneous penetration of cholecalciferol. **International Journal of Pharmaceutics**, 553(1-2), 120-131.

Laouini, A. et al. (2013). Preparation of liposomes: a novel application of microengineered membranes - investigation of the process parameters and application to the encapsulation of vitamin E. **RSC Advances**, 3, 4985-4994.

Lee, J. H. et al. (2008). Vitamin D deficiency an important, common, and easily treatable cardiovascular risk factor? **Journal of the American College of Cardiology**, 52(24), 1848-1956.

Litzinger, D. C., & Huang, L. (1992). Amphipathic poly(ethylene glycol) 5000-stabilized dioleoylphosphatidylethanolamine liposomes accumulate in spleen. **Biochimica et Biophysica Acta (BBA) - Lipids and Lipid Metabolism**, 1127, 249–254.

Mahbubul, I.M. (2019). **Preparation, characterization, properties and application of nanofluid**. William Andrew (Ed.). ISBN: 9780128132456.

Marsanasco, M. Et al. (2015). Bioactive constituents in liposomes incorporated in orange juice as new functional food: thermal stability, rheological and organoleptic properties. **Journal of Food Science and Technology**, 52, 121, 7828-7838.

McIntosh, T. J. (1996). Hydration properties of lamellar and non-lamellar phases of phosphatidylcholine and phosphatidylethanolamine. **Chemistry and Physics of Lipids**, 81(2), 117-131.

Mercer, D. G. (2008) Solar drying in developing countries: Possibilities and pitfalls. G.L. Robertson, J.R. Lupien (Eds.), **Using food science and technology to improve nutrition and promote national development**, International Union of Food Science & Technology. ISBN: 978-0-9810247-0-7.

Merz, K., & Sternberg, B. (1994). Incorporation of vitamin D_3-derivatives in liposomes of different lipid types. **Journal of Drug Targeting**, 2(5), 411-417.

Mohammadi, M., Ghanbarzadeh, B., & Hamihehkar, H. (2014). Formulation of nanoliposomal vitamin D_3 for potential application in beverage fortification. **Advanced Pharmaceutical Bulletin**, 4(2), 569-575.

Mozafari, M. R. et al. (2008). Nanoliposomes and their applications in food technology. **Journal of Liposome Research**, 18(4), 309-327.

New, R.R.C. (1990). **Liposomes: A practical approach**, New York: IRL Press.

Ozturk, B. et al. (2015). Nanoemulsion delivery systems for oil-soluble vitamins: Influence of carrier oil type on lipid digestion and vitamin D_3 bioaccessibility. **Food Chemistry**, 187, 499-506.

Paltauf, F., & Hermetter A. (1990). Phospholipids — Natural, Semisynthetic, Synthetic. In: Hanin I., Pepeu G. (eds) **Phospholipids**. Springer, Boston, MA.

Parhizkar, E. Et al. (2018). Design and development of vitamin C-encapsulated proliposome with improved in-vitro and ex-vivo antioxidant efficacy. **Journal of Microencapsulation**, 35(3), 301-311.

Payne, N. I. et al. (1986). Proliposomes: A novel solution to an old problem. **Journal of Pharmaceutical Sciences**, 75(4), 325-329.

Pinilla, C. M. B., Thys, R. C. S., & Brandelli, A. (2019). Antifungal properties of phosphatidylcholine-oleic acid liposomes encapsulating garlic against environmental fungal in wheat bread. **International Journal of Food Microbiology**, 293, 72-78.

Ramezanli, T. et al. (2017). Polymeric nanospheres for topical delivery of vitamin D_3. **International Journal of Pharmaceutics**, 516(1-2), 196-203.

Rodriguez-Rosales, R. J., & Yao, Y. (2020). Phytoglycogen, a natural dendrimer-like glucan, improves the soluble amount and Caco-2 monolayer permeation of curcumin and enhances its efficacy to reduce HeLa cell viability. **Food Hydrocolloids**, 100, 105442.

Rojanarat, W. et al. (2011). Isoniazid proliposome powders for inhalation-preparation, characterization and cell culture studies. **International Journal of Molecular Sciences**, 12(7), 4414-4434.

Roos, Y. H., & Karel, M. (2006). Plasticizing effect of water on thermal behavior and crystallization of amorphous food models. **Journal of Food Science**, 56(1), 38-43.

Rovira-Bru, M., Thompson, D. H., & Szleifer, I. (2002). Size and structure of spontaneously forming liposomes in lipid/PEG-lipid mixtures. **Biophysical Journal**, 83, 2419–2439.

Rudolphi-Skórska, E., Filek, M., & Zembaia, M. (2017). The effects of the structure and composition of the hydrophobic parts of phosphatidylcholine-containing systems on phosphatidylcholine oxidation by ozone. **The Journal of Membrane Biology**, 250, 493–505.

Ruozi, B. et al. (2005). Atomic force microscopy and photon correlation spectroscopy: Two techniques for rapid characterization of liposomes. **European Journal of Pharmaceutical Sciences**, 25, 81-89.

Sachaniya, J. et al. (2018). Liposomal formulation of vitamin A for the potential treatment of osteoporosis. **International Journal of Nanomedicine**, 13, 51-53.

Samborska, K. et al. (2019). Development and characterization of physical properties of honey-rich powder. **Food and Bioproducts Processing**, 115, 78-86.

Shi, Q., Fang, Z., & Bhandari, B. (2013). Effect of addition of whey protein isolate on spray-drying behavior of honey with maltodextrin as a carrier material. **Drying Technology**, 31, 1681-1692.

Silva, R. et al. (2010). Effect of ultrasound parameters for unilamellar liposome preparation. **Ultrasonics Sonochemistry**, 17(3), 628-632.

Smith, A. L., Shirazi, H. M., & Mulligan, S. R. (2002). Water sorption isotherms and enthalpies of water sorption by lysosyme using quartz crystal microbalance/heat conduction calorimeter. **Biochimica et Biophysica Acta**, 1594, 150-159.

Sriamornsak, P.et al. (2008). Atomic force microscopy imaging of novel self-assembling pectin–liposome nanocomplexes. **Carbohydrate Polymers**, 71(2), 324-329.

Staffas, A., & Nyman, A. (2003). Determination of cholecalciferol (vitamin D_3) in selected foods by liquid chromatography. NMKL Collaborative Study. **Journal of AOAC International**, 86(2), 400-406.

Talebi, V. et al. (2019). Effects of different stabilizers on colloidal properties and encapsulation efficiency of vitamin D_3 loaded nano-niosomes. **Journal of Drug Delivery Science and Technology**, 101284.

Tuckey, R. C. et al. (2008). Pathways and products for the metabolism of vitamin D_3 by cytochrome P450scc. **The FEBS Journal**, 275(10), 2585-2596.

Van Hoogevest, P., & Wendel, A. (2014). The use of natural and synthetic phospholipids as pharmaceutical excipients. **European Journal of Lipid Science and Technology**, 116(9), 1088-1107.

Wang, Q. et al. (2018). A novel formulation of [6]-gingerol: proliposomes with enhanced oral bioavailability and antitumor effect. **International Journal of Pharmaceutics**, 535(1-2), 308-315.

Wiseman, H. (1993). Vitamin D is a membrane antioxidant. Ability to inhibit iron-dependent lipid peroxidation in liposomes compared to cholesterol, ergosterol and tamoxifen and relevance to anticancer action. **FEBS Letters**, 326(1-3), 285-288.

Xia, F. et al. (2012). Preparation of lutein proliposomes by supercritical anti-solvent technique. **Food Hydrocolloids**, 26(2), 456-463.

Yan-Yu, X. et al. (2006). Preparation of silymarin proliposome: a new way to increase oral bioavailability of silymarin in beagle dogs. **International Journal of Pharmaceutics**, 319(1-2), 162-168.

Chapter 4. INFLUENCE OF PHOSPHOLIPID SATURATION ON THE PHYSICOCHEMICAL CHARACTERISTICS OF CURCUMIN/VITAMIN D_3 CO-LOADED PROLIPOSOMES OBTAINED BY THE MICRONIZED SUCROSE COATING PROCESS

Chapter 4. Influence of phospholipid saturation on the physicochemical characteristics of curcumin/vitamin D₃ co-loaded proliposomes obtained by the micronized sucrose coating process

Abstract

The effects of different food-grade saturated and unsaturated soy phospholipids ratios on the production of proliposomes with curcumin and vitamin D₃ were studied. A micronized sucrose-coating process was employed to obtain the proliposomes. The phospholipid ratio had a minor influence on their physicochemical parameters, as low values for water activity (a_w $\leq$0.26), moisture content (X_w $\leq$2.97%), hygroscopicity ($\leq$8.62 g adsorbed water/100 g dry matter), and intermediate values for solubility ($\leq$44.8% of solubilized powder) were obtained. Also, FT-IR and XRD results revealed an improvement in their amorphous structure due to sucrose. The entrapment efficiency values for curcumin and vitamin D₃ were up to 100 and 98.7%, respectively, after 60 days. Additionally, the nanoliposomes resulting from the hydration of proliposomes exhibited sizes lower than 400 nm. The results shown herein are relevant to the production of lower-cost synergistic carriers with high bioactive retention using an abundant raw material such as sucrose.

Keywords: nonhydrogenated phospholipids, cholecalciferol, curcuminoid, sugar-based carriers, food powder, saturated phospholipids

4.1. Introduction

Curcumin (CUR, 1,7-diphenyl-1,6-heptadiene-3,5-dione) is a natural crystalline polyphenol extracted from the rhizome of turmeric plants. It is often used in supplements or as a preservative and food colorant due to its strong yellow color. Its multiple biological properties include anticarcinogenic, antioxidant, anti-inflammatory and antimicrobial activities; these are mostly due to the presence of β-dione and keto-enol interconversion structures able to scavenge oxygen free radicals (Tai et al., 2020). Despite its biological activities, extremely poor solubility in aqueous solutions, very low oral bioavailability and easy degradability hinder its direct incorporation in several food products. In addition, curcumin presents a high metabolic rate and rapid excretion, which decreases its absorption in the human body (Wang et al., 2021).

Vitamin D$_3$ (VD3, cholecalciferol) is a fat-soluble bioactive substance synthesized in human skin after sunlight exposure. It presents steroid hormone function and plays important roles in calcium and phosphorus homeostasis and bone health and in the inhibition of cardiovascular diseases, different types of cancer and diabetes (Tan et al., 2019). In addition, VD3 deficiency is very common due to diets poor in this micronutrient, low sunlight exposure and/or metabolic disorders. Therefore, discussions have been raised regarding the fortification of foods and beverages with this vitamin. However, VD3 also has high susceptibility to environmental factors such as heat, pH, light, and oxidation, which hampers its direct incorporation during food processing. Additionally, like curcumin, this vitamin also exhibits poor water solubility and poor oral bioavailability (Mulrooney et al., 2021; Xiang et al., 2020).

To address the drawbacks of both bioactive substances mentioned above, encapsulation in lipid carriers has emerged as a suitable technique to protect these molecules during processing and to increase their solubility and absorption by epithelial cells, possibly increasing their bioavailability. Several delivery systems have been developed for CUR or VD3, such as micelles, emulsions, solid lipid nanoparticles, complex coacervates, hydrogels and liposomes (Santos, Carvalho, & Garcia-Rojas, 2021; Sunagawa et al., 2021; Tai et al., 2020; Xiang et al; 2020). Liposomes are spherical vesicles mainly composed of phospholipids. These structures tend to form linear aggregates called lipid bilayers when dispersed in aqueous media, and due to their thermodynamic properties, they tend to close upon themselves if there is enough energy input. During this process, liposomes can encapsulate other molecules by drawing them into their interior from the aqueous media in which they are dispersed. Due to

the amphipathic characteristics of phospholipids, liposomes can entrap both hydrophilic and/or lipophilic compounds, offering a very versatile delivery system.

To overcome the stability problems associated with liposome dispersions, the "proliposome" concept was developed by Payne et al. (1986). Proliposomes (PLs) are solid, dry, free-flowing particles that immediately form dispersions upon the addition of a hydration medium. The main advantages related to proliposomes include their improved solubility, ease of handling, and physicochemical stability (Khan et al., 2021). Different methods for PL production have been proposed in the literature, such as film deposition on the carrier, the fluidized-bed technique, spray drying, the supercritical antisolvent method and lyophilization (Chordiya et al., 2020). Among these, the micronized sucrose coating process proposed by Elhissi et al. (2006) uses this sugar as the carrier through its coating by phospholipids and bioactives after ethanol removal. Advantages of this method include the use of mild temperatures, higher process yield and relatively easy scalability (Chaves & Pinho, 2020).

The cost of phospholipids is one of the major concerns about liposome production for food. Purified saturated phospholipids are normally expensive, mainly because they require repeated hydrogenation processes. The production of lipid carriers to replace purified/saturated with unpurified/unsaturated raw materials appears to be an alternative for improving the cost-effectiveness. However, the addition of unsaturated phospholipids can promote an increase in the fluidity of the lipid bilayers and, consequently, decrease their rigidity, which may lead to early molecule diffusion from the inner core of vesicles to the aqueous environment. In this sense, a study aiming to optimize the phospholipid ratio for the production of PLs is highly required and necessary to verify the feasibility of the process regarding the production of lower-cost carriers with high potential to retain bioactives. The main objective of this study was to produce CUR-VD3 co-loaded PLs using different ratios of food-grade saturated and unsaturated phospholipids. The particulate systems were characterized using techniques and analysis commonly applied for food powders, including water activity, moisture content, solubility, hygroscopicity, sorption isotherms, morphology by scanning electron microscopy, differential scanning calorimetry, Fourier transform infrared spectroscopy and X-ray diffraction. CUR/VD3 retention was evaluated at 25 °C over a 60-day period of storage.

4.2. Material and methods

4.2.1. Chemicals and reagents

Curcumin (from *Curcuma longa*, Turmeric, powder, C1386) and cholecalciferol (>98% purity, analysis of standard, C9756) were purchased from Sigma Aldrich (St. Louis, MO, USA). Purified soy phosphatidylcholine (Phospholipon 90H, P90H, >90% w/w PC) and fat-free powdered lecithin (Lipoid S40, L40, >40% w/w PC, >15% w/w PE) were purchased from Lipoid GmbH (Ludwigshafen, Germany). Xanthan gum (Grindsted Xanthan 80) was donated by DuPont (Cotia, SP, Brazil), and guar gum was purchased from Êxodo Científica (Hortolândia, SP, Brazil). Sucrose was purchased from Synth (Diadema, SP, Brazil) and micronized in a ball mill (CE500, CIENLAB, Campinas, SP, Brazil) for 10 h at 100 rpm. For VD3 quantification, methanol and acetonitrile (HPLC-grade) were purchased from Merck (Darmstadt, Germany). Deionized water from a Direct Q3 system (Millipore, Billerica, MA, USA) was used throughout the experiments. The other chemicals and reagents used in this study were of analytical grade and used without any further purification.

4.2.2. Production of the CUR-VD3 co-loaded proliposomes

Proliposomes were produced as previously described by Chaves et al. (2018) using the formulations summarized in Table 1. Phospholipid ratios were chosen based on preliminary tests and previous studies (Chaves & Pinho, 2019; Chaves et al., 2021). First, a VD3 mother solution was produced by dissolving 0.01 g of VD3 in 100 mL methanol (final solution ~400,000 IU) using magnetic stirring at 3,200 rpm at 25 °C for 30 min. Then, 3.2 g of phospholipids, 25 mg of curcumin and 20 mL of the VD3 mother solution were mixed with 100 mL of ethanol using ultra-agitation (T25, Ultra-Turrax, IKA, Staufen, Germany) at 13,000 rpm at 25 °C for 15 min. The production of PLs was carried out using a rotary evaporator (MA120, Marconi, Piracicaba, SP, Brazil). Two grams of micronized sucrose was constantly wetted by the addition of drops of the ethanolic solution using a Masterflex 7528-30 peristaltic pump (Cole-Palmer, Vernon Hills, IL, USA) operated at 4 mL/min. Sonication at 40 kHz was used to maintain the phospholipids dispersed in ethanol. The evaporation proceeded at 65 ± 5 °C until ethanol removal, and only a thin layer of product was observed in the volumetric flask where only sucrose was first present. CUR-VD3 PLs were then scraped from the flask and stored in amber vessels in humidity-controlled desiccators for a maximum of two weeks.

Table 4.1. Formulations used for the production of CUR-VD3 proliposomes (PLs)

Formulation	Phospholipon 90H (g)	Lipoid S40 (g)	Curcumin (mg)	Vitamin D_3 (IU)
F50	1.6	1.6	25	80,000
F70	0.96	2.24	25	80,000
F100	-	3.2	25	80,000

Reference: Chaves & Pinho (2021)

4.2.3. Characterization of the proliposomes

4.2.3.1. Water activity (a_w) and moisture content (X_w)

The a_w of the samples at 25 °C was measured using a calibrated aw meter (Aqualab, Decagon Devices, Pullman, WA, USA). The moisture content (X_w) of the samples was measured using a moisture analyzer with infrared radiation (MB35 Halogen, Ohaus, Nänikon, Switzerland).

4.2.3.2. Hygroscopicity

The hygroscopicity of PLs was evaluated using the method described by Chaves & Pinho (2019) that was based on the method described by Cai and Corke (2006). In this method, 200 mg of sample was conditioned in weighing filters and maintained in desiccators containing a saturated sodium chloride solution (62% w/v) at 25 °C for one week. The values were expressed as g of adsorbed H_2O/100 g dry weight.

4.2.3.3. Solubility

Powder solubility analysis was determined using the method described by Chaves & Pinho (2019), which was based on that of Eastman and Moore (1984). First, 0.5 of PL was mixed with 50 mL of deionized water using an orbital shaker (Marconi) operated at 200 rpm at 25 °C for 20 min. The samples were submitted to centrifugation at 1,100 x g at 25 °C for 30 min (5430R, Eppendorf, Hamburg, Germany), and then 25 mL of the supernatant was collected and placed in previously weighed Petri dishes. Finally, the samples were dried in a convection oven at 105 °C for 24 h. The solubility was calculated based on the initial mass of the sample solubilized in the 25 mL aliquot. The result was expressed as a percentage of the solubilized powder in water.

4.2.3.4. Moisture adsorption isotherms

Moisture adsorption isotherms were obtained using gravimetry as described by Labuza (1985). First, 2 g of PLs was placed in weighing filters and stored in desiccators at 25 °C for a maximum of 4 weeks. Each desiccator contained a salt solution with a previously determined aw ranging from 0.143 to 0.845. The weight of the filters was then periodically measured at regular intervals. The equilibrium moisture data on a dry basis (X) were fitted to the Oswin model to obtain the isotherms. The equation that represents this model is presented in Eq. (1).

Oswin model: $X = a * [a_w/(1 - a_w)]\text{\textasciicircum}b$ (1)

where "a" and "b" are constants.

4.2.3.5. CUR content analysis

The curcumin in the PLs was quantified using spectrophotometry as described by Chaves & Pinho (2019). The concentration was calculated from the absorbance values at 425 nm using a Genesys 10S spectrophotometer (Thermo Scientific, Waltham, MA, USA). Quantification was carried out using an analytical curve of pure curcumin (≥94%) in anhydrous ethanol (R^2 = 0.9996).

4.2.3.6. VD3 content analysis

The vitamin D_3 in the PLs was quantified using high-performance liquid chromatography as previously described by Chaves & Pinho (2020). The separation was performed using a Shim-Pack VP-ODS column (4.6 µm, 0.46 × 25 cm, Shimadzu, Kyoto, Japan) at 35 °C and an HPLC apparatus (Shimadzu). The mobile phase was composed of methanol and acetonitrile at a 9:1 ratio (v/v) and was pumped at a 1.6 mL/min flow rate. Samples were analyzed at 265 nm for 10 min, and VD3 was identified based on its retention time (7.3 min). Quantification was carried out using an analytical curve of pure VD3 in the mobile phase (R^2 = 0.9946).

4.2.3.7. Morphology

Scanning electron microscopy (SEM) was used to observe the morphology of the PLs. A TM-300 apparatus (Hitachi, Tokyo, Japan) was employed and operated at 15 kV. The samples were placed on double-faced carbon tape and fixed to aluminum stubs. The images were obtained at 100x magnification.

4.2.3.8. Fourier transform infrared (FT-IR) spectroscopy

A PerkinElmer FT-IR spectrometer (Waltham, MA, USA) was employed to obtain the infrared spectra of raw materials and proliposomes. A mass of 0.01 g of each sample was placed onto KBr pellets, and the spectra were obtained between 4000 and 400 cm^{-1} at 0.2 cm/s. The resolution used was 4 cm^{-1} with 20 scans in total.

4.2.3.9. X-ray powder diffraction (XRD)

A Miniflex600 apparatus (Rigaku, Tokyo, Japan) was employed to obtain the XRD spectra of pure ingredients and proliposomes. The instrument was equipped with a copper anode tube and a graphite monochromator in the diffracted beam and was operated at a wavelength of 1.5418 Å. The measurements were performed at a rate of 2°/min with a 2θ angle ranging from 5° to 35°.

4.2.3.10. Differential scanning calorimetry (DSC)

Thermal analysis was performed by DSC using a DSC-TA2010 instrument (TA Instruments, New Castle, DE, USA). The PLs (20 mg) were placed over hermetically sealed aluminum pans and heated from 40 °C to 80 °C using a heating ramp of 10 °C/min and an inert atmosphere (45 mL/min N2). The phase transition temperatures were calculated using Universal Analyzer Software (v.7, TA Instruments, New Castle, DE, USA).

4.2.4. Hydration of proliposomes and formation of liposomes

Liposome dispersions were produced from the hydration of proliposomes as described by Chaves et al. (2021). First, 100 mL of dispersion was produced by hydrating 2 g of proliposomes with deionized water under ultragitation (T25, IKA, Staufen, Germany) at 13,000 rpm at 65 °C. Xanthan and guar gums were added (0.02% w/v) at 25 °C using magnetic stirring at 3,600 rpm at a 10:90 ratio. The resulting dispersions were stored at 10 °C for a maximum of 4 weeks. Thereafter, the size and morphology of CUR-VD3-loaded liposomes were determined using atomic force microscopy with an NT-MDT microscope (Solver Next, Zelenograd, Russia). The method applied was described by Ruozi et al. (2005) with some modifications. The analyses were carried out at 0.7 Hz using the intermittent contact mode; the resonance frequency was

150 Hz, and the force constant was 5 N/m. The dispersions were previously diluted 100x in ultrapure water, and the excess was removed using a paper filter prior to observation.

4.2.5. Statistical analysis

The experiments were performed in triplicate. The obtained data are herein shown as the mean values ± standard deviations. Analysis of variance was performed using Tukey's test at a 5% significance level ($p < 0.05$) using SAS Software (v. 9.4, Cary, NC, USA).

4.3. Results and discussions

4.3.1. Characterization of the CUR-VD3 co-loaded PLs

4.3.1.1. Powder properties

The visual aspect and micrographs obtained using SEM for the CUR-VD3 co-loaded PLs are shown in Fig. 4.1. It is clear that the increase in LS40 content led to a more agglomerated aspect of the PLs and a brownish color that is characteristic of nonhydrogenated phospholipids. Saturated phospholipids, such as those mostly found in P90H, are more stable as powders, whereas unsaturated phospholipids are extremely hygroscopic and absorb water from the environment, developing a gummy texture (Jin et al., 2008). SEM images revealed that the PLs presented a nonrounded and rough surface. The dented appearance is a consequence of ethanol removal throughout the processing (Murrieta-Pazos et al., 2012). The brighter aspect observed for F100 reflected a higher surface fat content in this sample and, therefore, a more uniform coating of sucrose granules by the phospholipids. However, this higher surface fat content may compromise other parameters, such as the wettability, flowability and storage stability of powders, due to fat oxidation (Jones et al., 2013). The powder properties of the PLs are summarized in Table 2. None of the parameters exhibited significant changes, i.e., they were independent of the phospholipid composition. In this context, samples presented a very low content of bound water, as confirmed by the aw and Xw values. Low moisture food powders with low aw (<0.85) are considered low-risk because they are less prone to microbial growth, including foodborne pathogens (FDA, 2015; Quinn et al., 2021).

The solubility of powders tends to increase with the addition of highly hydrophilic excipients such as sugars. However, the PLs produced herein are mostly composed of phospholipids (61% w/w) against 38% w/w sucrose and 1% w/w bioactive ingredients. Food powders with a higher content of lipids are likely to be less soluble. In this context, Felix da Silva

et al. (2017) attributed a limitation on the hydration of particles to a higher surface roughness due to the higher presence and surface activity of fat. Therefore, the intermediate solubility of the PLs is mostly due to the presence of sucrose that contains a high number of -OH polar groups. In addition, the dissolution enhancement of the molecules can also be achieved by increasing surface area of the bioactive substances exposed to the larger-size molecules of sucrose (Das et al., 2011). Although the hygroscopicity of the PLs tended to increase with higher LS40 incorporation, the results obtained for the samples did not differ significantly considering the standard deviations, and all of them exhibited low values for this parameter. Highly hygroscopic ingredients may be considerably harmful to the final product, as they directly affect some manufacturing steps, such as collection, transportation and handling (Sobulska & Zbicinski, 2020). The similarity of the values found for the samples is probably due to the similar number of hydrophilic groups appearing in each structure. Additionally, the lack of significant difference among the hygroscopicity values can be correlated with the same lack of difference in the moisture content, as the highly hygroscopic nature of a food powder can be a result of higher water absorption from the environment (Adetoro, Opala, & Fawole., 2020).

Figure 4.1. Visual aspect of CUR-VD3 co-loaded proliposomes (PLs) produced with Phospholipon 90H (P90H) and Lipoid S40 (S40) at different ratios (P90H:LS40): (A) 50:50 (F50), (B) 30:70 (F70) and (C) 0:100 (F100). Micrographs imaged using SEM for formulations (D) F50, (E) F70 and (F) F100. Magnification: 100 x. Scale: 1 mm

Reference: Chaves & Pinho (2021)
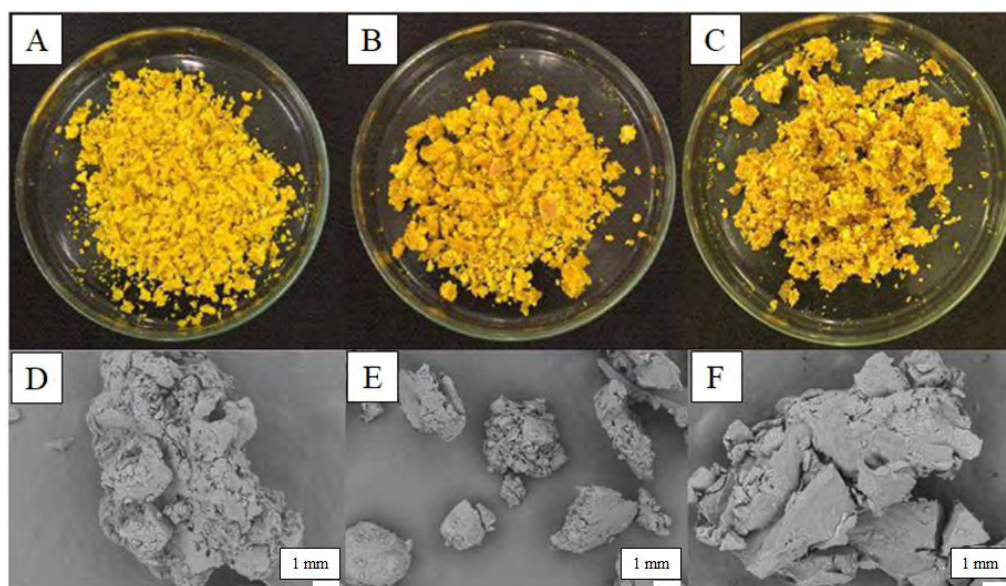
Table 4.2. Powder properties of CUR-VD3 co-loaded proliposomes

Powder properties		Formulations		
		F50	F70	F100
a_w		$0.26^A \pm 0.11$	$0.26^A \pm 0.04$	$0.22^A \pm 0.08$
X_w (%)		$2.97^A \pm 1.13$	$2.59^A \pm 0.11$	$2.44^A \pm 0.61$
Solubility (% solubilized powder)		$44.4^A \pm 0.84$	$44.8^A \pm 1.92$	$42.5^A \pm 2.15$
Hygroscopicity (g adsorbed water / 100 g d.m)		$5.90^A \pm 0.30$	$7.50^A \pm 2.04$	$8.62^A \pm 2.03$
CUR concentration (mg/g PL)	1st day	$3.35^{Aa} \pm 0.16$	$3.67^{Aa} \pm 0.06$	$3.59^{Aa} \pm 0.18$
	60th day	$3.49^{Aa} \pm 0.17$	$3.48^{Aa} \pm 0.14$	$3.78^{Aa} \pm 0.21$
% CUR preserved		100	94.8	100
VD3 concentration (IU/g PL)	1st day	$9.72^{Aa} \pm 0.02$	$10.21^{Aa} \pm 0.60$	$9.83^{Aa} \pm 0.33$
	60th day	$8.93^{Bb} \pm 0.14$	$8.69^{Bb} \pm 0.06$	$9.70^{Aa} \pm 0.12$
% VD3 preserved		91.9	85.1	98.7
Parameters fitted using the Oswin model	a	4.56 ± 0.48	3.78 ± 0.60	2.40 ± 0.21
	b	0.65 ± 0.09	0.81 ± 0.13	1.20 ± 0.06
	R^2	0.9617	0.9516	0.9952

Means followed by the same uppercase letter in the same line and by the same lowercase letter in the same column were not significantly different ($p > 0.05$) by Tukey's test

Reference: Chaves & Pinho (2021)

Fig. 4.2 presents the moisture sorption isotherms obtained for the PLs as well as the thermograms obtained using DSC. The Oswin model fit the experimental data well, with R^2 ranging from 0.9516 to 0.9952. The parameters A and B are also shown in Table 4.2. The two-parameter empirical Oswin model has been successfully applied to fit experimental moisture data from food powders, including starchy, highly proteinic and sugar-rich powders (Muzaffar and Kumar, 2016; Marques et al., 2020; Stępień, Witczak, & Witczak (2020). The isotherms revealed for the samples can be included in the Type III characterization described by Brunauer, which has been reported for other sugar-rich and high-fat powders (Stępień, Witczak, & Witczak, (2020). Regarding DSC thermograms, F50 presented the highest melting temperature (T_m), whereas F100 did not show any thermal phenomenon in the temperature range studied

(40 to 80 °C). Higher values for T_m are required for powder quality stability to avoid problems such as stickiness. Therefore, it is reasonable to state that the incorporation of unpurified phospholipids led to a decrease in the T_m of PLs. Otherwise, it is known that environments with higher moisture content lead to a decrease in the T_m of food powders (Sobulska & Zbicinski, 2020). Therefore, as no significant changes were observed regarding the moisture content of the samples and all of them were stored under the same conditions, the absence of a T_m suggests that F100 may have presented a glass transition below 40 °C. Additionally, nonhydrogenated phospholipids have mono- and polyunsaturated fatty acids with phase transitions mainly below 0 °C, which explains the reduction seen when only LS40 was used to produce the PLs (van Hoogevest, 2017). Consequently, more attention is needed when storing samples containing higher amounts of unpurified phospholipids, as a lower T_m may increase the plastifying/rubbery effect of powders.

Figure 4.2. (a) Moisture adsorption isotherms at 25 °C determined by fitting adsorption data using the Oswin model (—) for the formulations (■) F50, (●) F70, and (▲) F100. (b) Thermograms assessed by DSC for formulations (A) F50, (B) F70 and (C) F100.
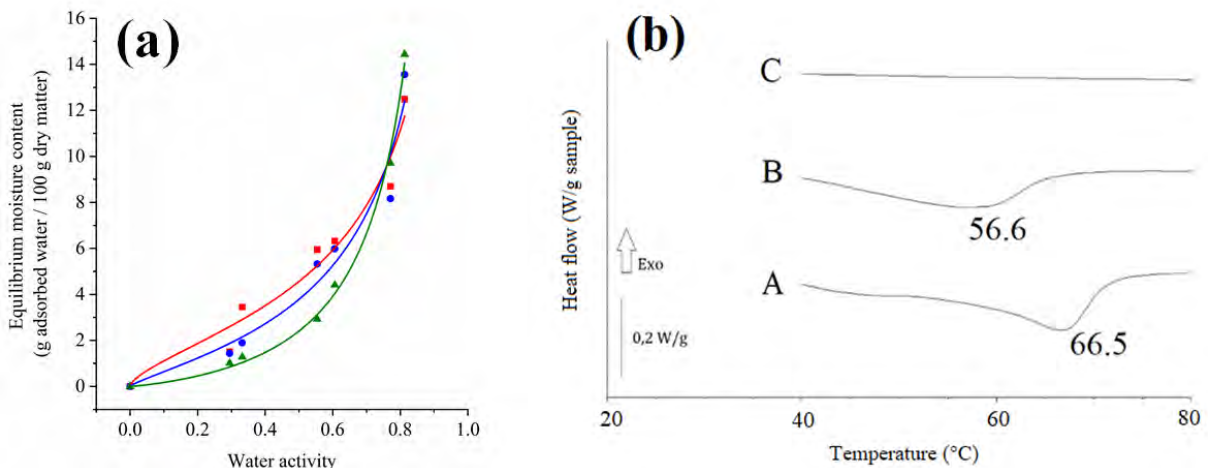
Regarding the preservation of bioactive ingredients, the CUR concentration remained constant over 60 days of storage for all the samples, as shown in Table 4.2. A retention up to 100% indicated that CUR was efficiently entrapped in the lipid matrix of the powders, regardless of the phospholipid ratio. Interestingly, F100 was produced with LS40 alone and did not show

a reduction in CUR content even with the higher content of nonhydrogenated phospholipids, which are theoretically more susceptible to oxidation. However, it is important to emphasize that storage under controlled conditions may clearly contribute to the reduced oxidation. Additionally, CUR has well-known antioxidant activity that may have helped to maintain the integrity of phospholipids (Chaves & Pinho, 2019). In turn, VD3 retention slightly decreased in F50 and F70 over the same period. As curcumin was added at higher concentrations than VD3 (0.78% and 0.06% w/w drug-to-lipid ratio, respectively), it is possible that some of the vitamin molecules were not coated onto sucrose during the process and were then carried out with ethanol during evaporation. Nonetheless, VD3 retention was up to 98.7%, which is an excellent result considering the high sensitivity of this bioactive compound.

4.3.1.2. FT-IR and XRD results

Fig. 4.3 shows the spectrum obtained using FT-IR and the diffractograms acquired using XRD for both the pure ingredients and CUR-VD3 co-loaded PLs. Regarding the FT-IR results, the absorbance bands of the functional groups showed signals at the following frequencies: between 3620 and 3073 cm^{-1} (stretching vibration of O–H groups), 2913 cm^{-1} (methylene, – CH_2, asymmetric stretching vibration), 2849 cm^{-1} (methylene, –CH_2, symmetric stretching vibration) and 1733 cm^{-1} (amide, C=O, stretching vibration). The fingerprint region of the PLs contained other relevant groups: 1468 cm^{-1} (C-H bending), 1235 cm^{-1} (C-O-C stretching vibration) and 1051 cm^{-1} (C-O stretching vibration). By observing the PL spectrum (f-h), it can be seen that all presented a band between 3620-3073 cm^{-1} due to the presence of sucrose (c) and VD3 (e); in addition, the frequencies at 2913 cm^{-1} and 2849 cm^{-1} were due to P90H and LS40 (a-b) and VD3, and that at 1733 cm^{-1} was due to the phospholipids (Popova & Hincha, 2003; Tsvetkova et al., 1998). The peaks at 1500 cm^{-1} and 1139 cm^{-1} related to CUR (d) appeared at low intensities in the PL spectrum, probably due to the lower amount added to formulations than sucrose or phospholipids. Finally, it is plausible that perhaps the hydroxyl groups found in sucrose interacted with the phosphate groups of the phospholipids at frequencies of 1421 cm^{-1} (P=O stretching) and 1053 cm^{-1} (P-O-C stretching) and exhibited wavelength shifts in a similar manner as that reported during the freeze-drying process, with sucrose acting as a cryoprotectant molecule (Doxastakis, Sum, & Pablo, 2005).

For XRD diffractograms obtained for CUR (d) and VD3 (e), sharp peaks are typical of highly crystalline molecules. The main peaks observed for CUR at 8.77° and 17.3° appeared at

lower intensities in the F50 (f) and F70 (g) spectra, suggesting interactions among it and the other components and corroborating the FT-IR results. The peak at 17.3° observed in the F100 (h) spectra presented similar intensity as pure CUR, which reveals a weaker interaction compared to the other samples. In addition, F100 exhibited the highest number of peaks, indicating more crystalline structures within the samples, which may imply a slower hydration process in the formation of liposomes. Moreover, the main peak exhibited for VD3 at 18.0° did not appear in the PL patterns. This peak probably overlapped with the broader bands of the P90H and LS40 (a-b) that occurred at the same 2θ angles, as VD3 was added in a smaller amount than the other ingredients. Furthermore, the broad band between 15° and 25° in the phospholipid patterns indicates an amorphous structure. This band was also present in the PL diffractograms, mostly in F50, which indicates the presence of more amorphous regions in this powder. Finally, another indication of interaction among the ingredients can be observed from the peaks related to sucrose at 11.6°, 18.9°, 19.5° and 24.8°. The reduction in the intensity of some peaks as well as all of their shifts are probably due to the effective coating process (Chaves & Pinho, 2020).

Figure 4.3. (A) FT-IR spectrum and (B) XRD diffractograms obtained for the main ingredients: (a) Phospholipon 90H (P90H), (b) Lipoid S40 (LS40), (c) sucrose, (d) curcumin and (e) vitamin D$_3$; and for the CUR-VD3 co-loaded PLs produced at different phospholipids ratios (P90H:LS40): (f) 50:50 (F50), (g) 30:70 (F70) and (h) 0:100 (F100). In the XRD diffractograms, green lines are related to sucrose, red lines to curcumin and blue lines to vitamin D$_3$
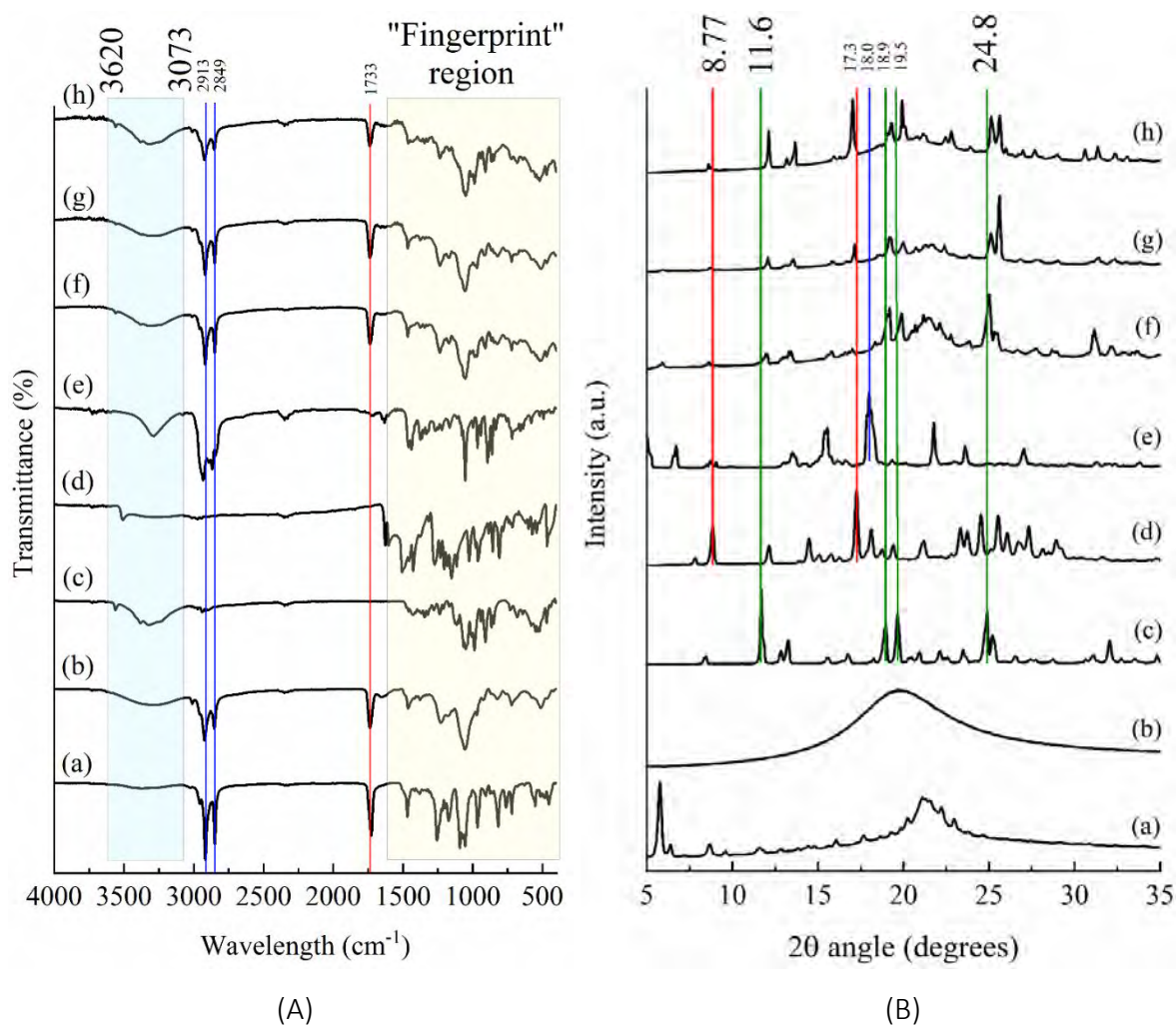
Reference: Chaves & Pinho (2021)

4.3.2. Characterization of the CUR-VD3 co-loaded liposomes

Liposome dispersions were successfully produced by the hydration of the PLs and characterized over 15 days of storage. A full characterization of these liposomes has been published elsewhere (Chaves et al., 2021). As a way to show in this study that it is feasible to produce nanoliposomes with the PLs prepared herein, the visual aspects of the nanodispersions and micrographs obtained using atomic force microscopy (AFM) are reported in Fig. 4.4. The

dispersions presented an intense yellow color typical of curcumin, and the vesicles had mean diameters ranging from 200 and 400 nm, which is consistent with values obtained by photon correlation spectroscopy (PCS) (Chaves et al., 2021). The vesicles showed spherical or quasi-spherical shapes and appeared to have smooth surfaces. The size of F100 (Fig.4.4c) was slightly higher than the mean average obtained by PCS, probably due to vesicle fusion during the drying step performed on the mica surface during sample preparation (Li et al., 2021). Overall, the addition of unsaturated phospholipids did not modify the spherical morphology of liposomes.

Figure 4.4. Visual aspect and atomic force micrographs (AFM) obtained for the CUR-VD3 co-loaded liposomes produced with Phospholipon 90H (P90H) and Lipoid S40 (S40) at different ratios (P90H:LS40): (A) 50:50 (F50), (B) 30:70 (F70) and (C) 0:100 (F100)
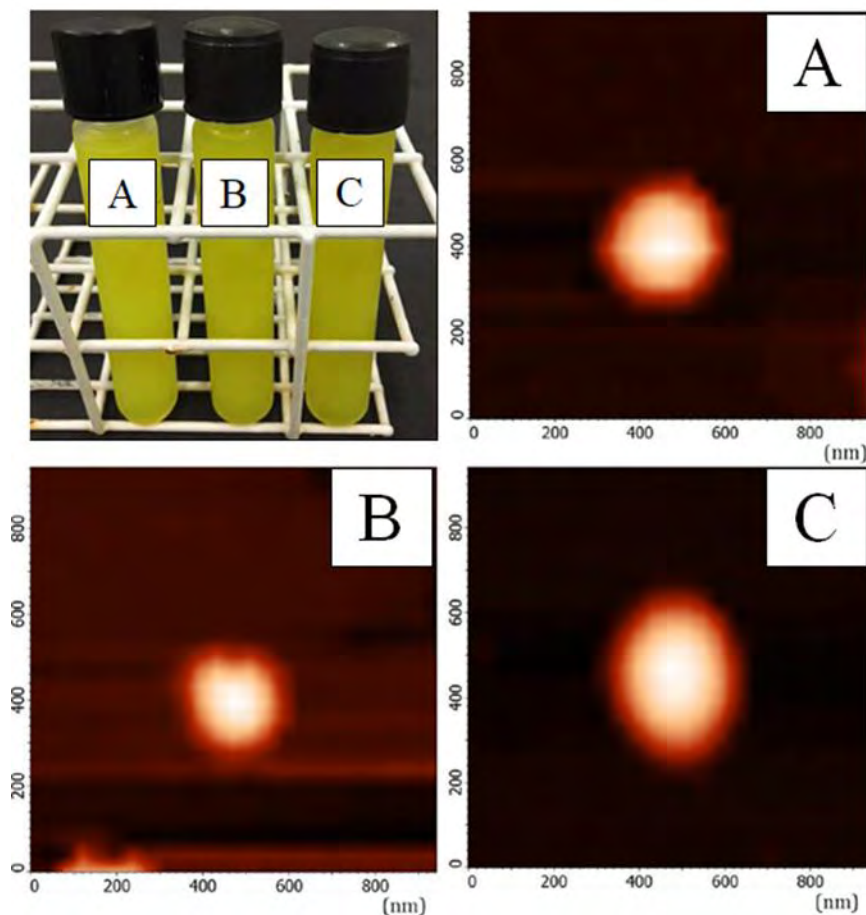
Reference: Chaves & Pinho (2021)

4.4. Conclusions

CUR-VD3 co-loaded proliposomes were efficiently produced using the micronized sucrose coating method. Powders presented low values for aw, Xw and hygroscopicity and intermediate values of solubility. The addition of unsaturated phospholipids did not affect the physicochemical properties of the PLs. The systems proved to be efficient in incorporating both curcumin and vitamin D$_3$, retaining up to 100 and 98.7% of bioactive content, respectively, over 60 days under controlled storage conditions (low humidity and light avoidance) at room temperature. The intermediate solubility of the samples was also verified by the presence of some amorphous regions in the XRD diffractograms; these regions were mainly attributed to the presence of sucrose. Additionally, the coating process was efficient, as observed in the SEM images and verified by the shifting of some peaks in the FT-IR spectra. Nanosized and spherical liposomes were produced by hydration of the PLs under controlled conditions of temperature and agitation. Finally, the results obtained in this study showed that it is feasible to produce PLs using lower-cost materials such as sucrose and unpurified phospholipids and achieve high bioactive retention potential.

4.5. Acknowledgments

4.6. References

Adetoro, A. O.; Opara, U. L.; & Fawole, O. A. (2020). Effect of carrier agents on the physicochemical and technofunctional properties and antioxidant capacity of freeze-dried pomegranate juice (Punica granatum) powder. **Foods**, 9(10), 1388.

Cai, Y. Z.; & Corke, H. (2000). Production and properties of spray-dried Amaranthus betacyanin pigments. **Journal of Food Science**, 65, 1248-1251.

Chaves, M. A.; & Pinho, S. C. (2019). Curcumin-loaded proliposomes produced by the coating of micronized sucrose: Influence of the type of phospholipid on the physicochemical

characteristics of powders and on the liposomes obtained by hydration. **Food Chemistry**, 291, 7-15.

Chaves, M. A.; & Pinho, S. C. (2020). Unpurified soybean lecithins impact on the chemistry of proliposomes and liposome dispersions encapsulating vitamin D_3. **Food Bioscience**, 37, 100700.

Chaves, M. A. et al. (2021). Nanoliposomes coencapsulating curcumin and vitamin D_3 produced by hydration of proliposomes: Effects of the phospholipid composition in the physicochemical characteristics of vesicles and after incorporation in yoghurts. **International Journal of Dairy** Technology, 74, 107-117.

Chaves, M. A. et al. (2018). Structural characterization of multilamellar liposomes coencapsulating curcumin and vitamin D_3. **Colloids and Surfaces A: Physicochemical and Engineering Aspects**, 549, 112-121.

Chordiya, D. et al. (2020). Chapter 17 - Proliposomes: a potential colloidal carrier for drug delivery applications. **The Future of Pharmaceutical Product Development and Research - Advances in Pharmaceutical Product Development and Research**, 581-608.

Das, A. et al. (2011). Solubility and dissolution enhancement of etoricoxib by solid dispersion technique using sugar carriers. **International Scholarly Research Notices**, 819765.

Doxastakis, M.; Sum, A. K.; & Pablo, J. J. (2005). Modulating membrane properties: The effect of trehalose and cholesterol on a phospholipid bilayer. **The Journal of Physical Chemistry**, 109, 24173-24181.

Eastman, J. E.; & Moore, C. O. (1984). Cold water-soluble granular starch for gelled food composition. **U.S. Patent 4465702**.

Elhissi, A. M. et al. (2006). Formulations generated from ethanol-based proliposomes for delivery via medical nebulizers. **Journal of Pharmacy and Pharmacology**, 58(7), 887-894.

Felix da Silva, D. et al. (2017). The influence of raw material added emulsifying salt and spray drying on cheese powder structure and hydration properties. **International Dairy Journal**, 74, 27-38.

Food and Drug Administration (FDA). (2015). **Water Activity (a_w) in foods**. Available in: https://www.fda.gov/ICECI/Inspections/InspectionGuides/InspectionTechnicalGuides/ucm072916.htm. Accessed in May 16 2021.

Jones, J. R. et al. (2013). Effect of processing variables and bulk composition on the surface composition of spray dried powders of a model food system. **Journal of Food Engineering**, 118, 19-30.

Khan, S. et al. 2021). Enhanced in vitro release and permeability of glibenclamide by proliposomes: Development, characterization and histopathological evaluation. **Journal of Drug Delivery Science and Technology**, 63, 102450.

Labuza, T. P. (1985). **Moisture sorption: Practical aspects of isotherm measurement and use**. 978-1-8911-2718-2, American Association of Cereal Chemists, St. Paul, MN, USA.

Li, J. et al. (2021). Ascorbyl palmitate effects on the stability of curcumin-loaded soybean phosphatidylcholine liposomes. **Food Bioscience**, 41, 100923.

Marques, R. C. D. et al. (2020). Modeling sorption properties of maize by-products obtained using the Dynamic Dewpoint Isotherm (DDI) method. **Food Bioscience**, 38, 100738.

Mulrooney, S. L. et al. Vitamin D_3 bioaccessibility: Influence of fatty acid chain length, salt concentration and l-α-phosphatidylcholine concentration on mixed micelle formation and delivery of vitamin D_3. **Food Chemistry**, 344, 128722.

Murrieta-Pazos, I. et al. (2012). Food powders: Surface and form characterization revisited. **Journal of Food Engineering**, 112(1-2), 1-21.

Muzaffar, K.; & Kumar, P. (2016). Moisture sorption isotherms and storage study of spray dried tamarind pulp powder. **Powder Technology**, 291, 322-327.

Payne, N. I. et al. (1986). Proliposomes: A novel solution to an old problem. **Journal of Pharmaceutical Sciences,** 75 (4), 325-329.

Popova, A. V.; & Hincha, D. K. (2003). Intermolecular interactions in dry and rehydrated pure and mixed bilayers of phosphatidylcholine and digalactosyldiacylglycerol: A Fourier transform infrared spectroscopy study. **Biophysical Journal**, 85, 1682-1690

Quinn, A. R. et al. (2021). Isothermal inactivation of Salmonella, Listeria monocytogenes, and Enterococcus faecium NRRL B-2354 in peanut butter, powder infant formula, and wheat flour. **Food Control**, 121, 107582.

Ruozi, B. et al. (2005). Atomic force microscopy and photon correlation spectroscopy: Two techniques for rapid characterization of liposomes. **European Journal of Pharmaceutical Sciences**, 25, 81-89.

Santos, M. B.; Carvalho, M. G.; & Garcia-Rojas, E. E. (2021). Carboxymethyl tara gum-lactoferrin complex coacervates as carriers for vitamin D_3: Encapsulation and controlled release. **Food Hydrocolloids**, 112, 106347.

Sobulska, M.; & Zbicinski, I. (2020). Advances in spray drying of sugar-rich products. **Drying Technology**, online.

Stępień, A.; Witczak, M.; & Witczak, T. (2020). Moisture sorption characteristics of food powders containing freeze dried avocado, maltodextrin and inulin. **International Journal of Biological Macromolecules**, 149, 256-261.

Sunagawa, Y. et al. (2021). A novel amorphous preparation improved curcumin bioavailability in healthy volunteers: A single-dose, double-blind, two-way crossover study. **Journal of Functional Foods**, 81, 104443.

Tai, K. et al. (2020). Stability and release performance of curcumin-loaded liposomes with varying content of hydrogenated phospholipids. **Food Chemistry**, 326, 126973.

Tan, Y. et al. (2019). Impact of an indigestible oil phase (mineral oil) on the bioaccessibility of vitamin D_3 encapsulated in whey protein-stabilized nanoemulsions. **Food Research International**, 120, 264-274.

Tsvetkova, N. M. et al. (1998). Effect of sugars on headgroup mobility in freeze-dried dipalmitoylphosphatidylcholine bilayers: Solid-State 31P NMR and FTIR studies. **Biophysical Journal**, 75, 2947-2955.

Van Hoogevest, P. (2017). Review – An update on the use of oral phospholipid excipients. **European Journal of Pharmaceutical Sciences**, 108, 1-12.

Wang, Y. et al. (2021). Curcumin-loaded liposomes with the hepatic and lysosomal dual-targeted effects for therapy of hepatocellular carcinoma. **International Journal of Pharmaceutics**, 602, 120628.

Xiang, C. et al. (2020). Development of ovalbumin-pectin nanocomplexes for vitamin D_3 encapsulation: Enhanced storage stability and sustained release in simulated gastrointestinal digestion. **Food Hydrocolloids**, 106, 105926.

Chapter 5. NANOLIPOSOMES COENCAPSULATING CURCUMIN AND VITAMIN D$_3$ PRODUCED BY HYDRATION OF PROLIPOSOMES: EFFECTS OF THE PHOSPHOLIPID COMPOSITION IN THE PHYSICOCHEMICAL CHARACTERISTICS OF VESICLES AND AFTER INCORPORATION IN YOGHURTS

Chapter 5. Nanoliposomes coencapsulating curcumin and vitamin D_3 produced by hydration of proliposomes: Effects of the phospholipid composition in the physicochemical characteristics of vesicles and after incorporation in yoghurts

Abstract

Nanoliposomes coencapsulating curcumin and vitamin D_3 (VD3) using different compositions of purified and unpurified lecithins were produced by hydration of proliposomes and characterised over 15 days of storage. The dispersions were incorporated to pineapple yoghurts produced in laboratory-scale, which were also characterised. Results showed that curcumin and vitamin D_3 were retained in the nanovesicles up to 86.1% and 94.1%, respectively. Most of the parameters assessed for the yoghurt samples were within the limits required by the Brazilian legislation and the Codex Alimentarius. Finally, the enriched product was well accepted by the panelists with the purchase intention ranging from 53 to 75%.

Keywords: dairy technology, rheology, fortification, microencapsulation, nutraceutical foods, physicochemical properties.

5.1. Introduction

Currently, the search for new functional food products has been steadily growing as people are increasingly concerned about their eating habits and pursuing healthier lifestyles. Yoghurt is one of the most biologically active foods consumed by humans as probiotic carriers, and its ingestion is currently linked to health benefits, including a reduction in cholesterol levels, the stimulation of the immune system and the supply of proteins, lipids and micronutrients (Campo et al., 2019; Abdesslem et al., 2020; Hadjimbei et al., 2020; Khaledabad et al., 2020). On the other hand, even though yoghurts are not considered rich sources of bioactives, their enrichment can be simple and effective due to their structural characteristics. In this context, nanoencapsulation has been widely reported as a successful method to improve the application and bioavailability of bioactives in water-formulated foods by preserving and protecting against harmful conditions during processing (Rostamabadi, Falsafi, & Jafari, 2019).

Nanoliposomes are the nanometric version of liposomes and consist in spherical vesicles containing one or more phospholipid bilayer membranes surrounding an aqueous core formed after an input of energy (Khorasani, Danaei, & Mozafari, 2018). Among the lipid components used in nanoliposome production, phosphatidylcholine, phosphatidylserine, phosphatidylinositol, and phosphatidylethanolamine are the most known and all can be found in lecithins extracted from both soybean or egg yolk. In this sense, unpurified soy lecithins can cost at least 20% less than hydrogenated phospholipids (Chaves & Pinho, 2019).

Curcumin is a low-molecular-weight natural polyphenolic compound found in the rhizome of the Curcuma longa L. Due to its intense yellow colour, curcumin is used by the food industry as a dye (E100), appearing to be a natural suitable substitute for artificial yellow dyes such as tartrazine (E102). However, the direct incorporation of curcumin in water-based food formulations is a technological challenge due to its oxidative instability and low hydrophilicity. Besides, an important issue is that the direct incorporation of curcumin into foods can lead to undesirable effects in the organoleptic properties, as it has a very strong spicy flavour.

Vitamin D is a prohormone that consists of ergocalciferol or vitamin D_2 (VD2) and cholecalciferol or vitamin D_3 (VD3). Several health benefits are attributed to the intake of vitamin D, including the increase in calcium absorption in the intestine, the proper functioning of cardiovascular and immune systems, and its anticancer effect (Holick, 2017). However, only a few food products contain naturally this vitamin in their composition, which reinforces the

need of enrichment. However, vitamin D_3 is also lipophilic and highly unstable in the presence of UV radiation, oxygen and under high temperatures.

In this context, the present study aimed to coencapsulate curcumin and vitamin D_3 in nanoliposomes produced using different mixtures of purified and unpurified lecithins by hydration of proliposomes, incorporate these systems into yoghurts and evaluate the eventual changes in the physicochemical characteristics of both nanoliposome dispersions and produced yoghurts during storage. The results obtained by this study will be useful for establishing the feasibility of the replacement of purified phospholipids by unpurified lecithins in the production of nanoliposomes and determining the feasibility of producing an enriched yoghurt with curcumin and vitamin D_3, aiming the replacement of artificial yellow dyes in an affordable product to deliver vitamin D_3.

5.2. Material and methods

5.2.1. Chemicals and reagents

Purified hydrogenated soy phosphatidylcholine – Phospholipon 90H (P90H) – and unpurified fat-free powdered lecithin – Lipoid S40 (LS40) – were obtained from Lipoid GmbH (Ludwigshafen, Germany). Curcumin and vitamin D_3 were purchased from Sigma-Aldrich (St. Louis, MO, USA). Xanthan gum was donated by DuPont (Grindsted Xanthan 80, Cotia, SP, Brazil), and guar gum was obtained from Êxodo Científica (Hortolândia, SP, Brazil). Whole-milk yoghurt was purchased from the Aeronautics Farm (FAYS) (Pirassununga, SP, Brazil). The other ingredients used in the production of yoghurt samples were concentrated pineapple juice (Maguary®, Araguari, MG, Brazil), refined sugar (União®, São Paulo, SP, Brazil), pineapple flavour (Arcolor®, São Paulo, SP, Brazil) and artificial tartrazine yellow colorant (Arcolor®, São Paulo, SP, Brazil). All chemicals used during this study were of analytical reagent grade. Deionised water was used throughout the experiments (Direct Q3, Millipore, Billerica, MA, USA).

5.2.2. Production of curcumin/vitamin D_3-loaded nanoliposomes

The protocol for the production of the nanoliposome dispersions was described elsewhere (Chaves & Pinho, 2019). Proliposomes were produced using the micronised sucrose coating method, and the formulations are presented in Table 5.1. The ethanolic solutions containing Lipoid S40 were submitted to sonication at 40 kHz before the dripping to maintain

the phospholipid dispersed. Aqueous liposome dispersions were obtained after the hydration of 2 g of the respective phospholipid powders with 100 mL of deionised water under ultra-agitation (T25, IKA, Staufen, Germany) at13 000 rpm at 65 °C. Xanthan and guar gums were directly added as thickeners (0.02% w/v) using magnetic stirring (3,600 rpm) at 25 °C at a ratio of 10:90. Sodium benzoate (0.02% w/v) was used as an antimicrobial agent. The dispersions were produced in triplicate and were stored in amber flasks covered with aluminum foil and maintained under refrigeration at 10 °C prior to the analyses for a maximum of 4 weeks.

Table 5.1. Formulations used for the production of CUR-VD3 proliposomes

Formulation	Phospholipid (g)		Curcumin (mg)	Vitamin D_3 (IU)
	Phospholipon 90H (P90H)	Lipoid S40 (LS40)		
L1	3.2	-	25	80,000
L2	-	3.2	25	80,000
L3	1.6	1.6	25	80,000

Reference: Chaves et al. (2021)

5.2.3. Characterisation of curcumin/vitamin D₃-loaded nanoliposomes

5.2.3.1. Hydrodynamic diameter, size distribution and zeta potential

Hydrodynamic diameter and size distribution were assessed by photon correlation spectroscopy (PCS) using a ZetaPlus analyzer (Brookhaven Instruments Company, Holtsville, NY, USA). A drop of sample was diluted in deionised water 10× to avoid the multiple scattering of light. Measurements were taken at 25 °C with a He-Ne laser at 627 nm and an angle of incidence of 90°. The same analyzer was used to measure the zeta potential. Samples were diluted 10× in 1 mM KCl, and values of zeta potential were calculated from the electrophoretic mobility data.

5.2.3.2. Morphology

The morphology of the nanoliposomes was observed using transmission electron microscopy (TEM) and carried out at the Electron Microscopy Center of the Paulista School of Medicine (Federal University of São Paulo, São Paulo, SP, Brazil). Pellets of liposomes were resuspended in 100 μL of buffer containing 2% formaldehyde (v/v) and placed on a flat-surfaced film to form var-coated nickel grids. Then, the grids were washed with 0.1 M sodium cacodylate

and negatively stained for 10 min using saturated uranyl acetate. Finally, the excess uranyl was removed using paper filters, and samples were analyzed using a JEOL 1200 EX II (JEOL Ltd., Tokyo, Japan) operating at 80 kV. The images were obtained with a GATAN 791 camera (Gatan Inc., Pleasanton, USA). Levels/contrast/brightness and resolution adjustments were performed with Adobe Photoshop 7®.

5.2.3.3. Quantification of encapsulated bioactive compounds

Curcumin was quantified using spectrophotometry as described by Chaves et al. (2018). Nanoliposomes were diluted at a 1:20 v/v ratio with anhydrous ethanol and vortexed (3600 rpm) for 20 min. The absorbance of the supernatant was measured at 425 nm (Thermo Scientific, Genesys 10S UV–Vis, Shanghai, China). Pure anhydrous ethanol was used as the blank solution. Curcumin concentrations were calculated using an analytical curve previously obtained from pure curcumin (≥ 94%) in anhydrous ethanol (R^2 = 0.9996). VD3 was quantified using high-performance liquid chromatography (Chaves et al., 2018). For the analysis, a Shim-Pack VP-ODS column (4.6 m, 0.46 × 25 cm, Shimadzu, Tokyo, Japan) was employed. Acetonitrile and methanol were used for sample separation at a 1:9 v/v ratio and a constant flow of 1.6 mL/min for 10 min, using a detection wavelength of 265 nm. VD3 was identified by comparison of the retention time (7.3 min) obtained from pure crystalline powdered VD3 (≥98%), and concentrations were calculated using an analytical curve (R^2 = 0.9946).

5.2.4. Production of pineapple yoghurts containing curcumin/vitamin D₃-loaded nanoliposomes

Pineapple yoghurts enriched with curcumin/vitamin D₃-loaded nanoliposomes were produced in laboratory-scale using the formulations shown in Table 5.2. Preliminary tests were carried out in order to obtain a similar texture to the product commonly found on the market. The nanoliposome dispersions were mixed with the other ingredients during the production of the samples. Each formulation was produced in triplicate and stored in amber flasks of high-density polyethylene and maintained under refrigeration at 10 °C.

Table 5.2. Composition of the produced yogurts

	Formulations				
	Control 1 (C1) ("blank")	Y1	Y2	Y3	Control 2 (C2)*
Whole milk plain yogurt (g)	700	700	700	700	700
Concentrated pineapple juice (mL)	56	56	56	56	56
Refined sugar (g)	56	56	56	56	56
Pineapple flavor (mL)	3.5	3.5	3.5	3.5	3.5
Artificial yellow colorant (mL)	-	-	-	-	3
Liposome dispersion – L1* (mL)	-	35	-	-	-
Liposome dispersion – L2* (mL)	-	-	35	-	-
Liposome dispersion – L3* (mL)	-	-	-	35	-

* The C2 formulation was produced only for the sensory analysis
* L1: liposome dispersion produced with only Phospholipon 90H (P90H)
* L2: liposome dispersion produced with only Lipoid S40 (LS40)
* L3: liposome dispersion produced with P90H and LS40 in a 50:50 ratio

Reference: Chaves et al. (2021)

5.2.5. Characterisation of pineapple yoghurts with curcumin/vitamin D₃-loaded nanoliposomes

5.2.5.1. Water activity (A_w) and moisture content

The water activity of the samples was assessed using an AquaLab instrument (Decagon Devices, Pullman, WA, USA), whereas moisture content was obtained using a moisture analyzer with infrared radiation (MB35 Halogen, Ohaus, Switzerland).

5.2.5.2. pH and titratable acidity

The pH of the samples was measured using a pH meter (Mater MB-10, São Paulo, SP, Brazil). The titratable acidity was obtained by titrating a solution containing 10 g of yoghurt and 10 mL of deionised water up to pH 8.2 with a 0.1 N NaOH solution (AOAC, 1995). The percentages of acidity were calculated according to Eq. (1) and expressed as g lactic acid/100 g of yoghurt.

$$\% \text{ titratable acid} = (V_{NaOH} * N_{NaOH} * 90 * 100)/m_{yoghurt} * 1000 \qquad (1)$$

where V_{NaOH} is the volume (mL) of NaOH titrant used, N_{NaOH} is the normality of the NaOH titrant (N), and $m_{yoghurt}$ is the mass (g) of the test sample.

5.2.5.3. Syneresis (%S)

A mass of 30 g of yoghurt was spread on filter paper (80 g/cm^3) in a funnel and placed on the top of a 50-mL graduated cylinder. The cylinders were stored under refrigeration (8 °C) for 5 h, and the volumes of expelled whey were measured. The percentages of syneresis (%S) were calculated according to Eq. (2) (Riener et al., 2010):

$$\%S = \text{mass of expelled whey (g) / mass of yoghurt (g)} * 100 \tag{2}$$

5.2.5.4. Rheological characterisation

The rheological characterisation of the yoghurts was analyzed according to Sah et al. (2016) with modifications. The behavior of viscosity and the determination of the flow curves were performed using a rotational rheometer (AR 2000, TA Instruments, New Castle, DE, USA), and the software was included with the equipment. The geometry applied was the parallel plate type (60 mm, gap 800 μm). All samples were analyzed at 10 °C with a relaxation time of 2 min and a shear rate of 500 s^{-1}. The data obtained were fitted using the Herschel–Bulkley model (R^2 > 0.9969) presented in Eq. (3):

$$\tau = \tau_0 + \gamma * K^n \tag{3}$$

where τ_0 is the yield stress (Pa), K is the consistency coefficient (Pa.s^n), and n is the flow behavior index (dimensionless).

Oscillatory tests were also performed with a rotational rheometer to determine the storage modulus (G′) and the loss modulus (G″) of the yoghurts. For the frequency sweep analysis, a frequency ramp ranging from 0.1 to 10 Hz and an oscillatory stress of 0.2 Pa were applied. It is worth mentioning that this value of 0.2 Pa was in the viscoelasticity region previously assessed.

5.2.5.5. Instrumental colorimetry

The coloring potential attributed to curcumin during storage was observed by instrumental colorimetry. A Miniscan XE (HunterLab, Reston, VA, USA) was used to determine the parameters of the tristimulus colour system (L*, a* and b*). The CIE (*Commission Internationale de l'Éclairage*) was used as the output reading system, D65 was used as the illuminator, and the observer angle was 10°. Samples were transferred to Petri dishes, and the

measurements were obtained after the colorimeter had been pressed against their surfaces. Other parameters, such as chroma (C*), hue angle (h*) and total colour difference (ΔE), were also calculated.

5.2.5.6. Determination of the vitamin D₃ content in the yoghurts

The determination of the VD3 content in the yoghurts was performed using HPLC. Firstly, the samples were submitted to cold saponification (Gomis, Fernández, & Gutiérrez-Alvarez, 2000). 5 mL of yoghurts was transferred to test tubes with 5 mL of ethanol and 0.025% w/v of butylated hydroxytoluene and then submitted to sonication for 5 min. Afterwards, 15 mL of hexane was added, and the mixtures were vortexed for 5 min. The organic upper phases were separated, and the process was repeated to complete the extraction. The phases were combined, filtered using nylon membrane filters (0.45 µm, Ø = 13 mm) and collected in 2-mL vials. Afterwards, hexane was removed via evaporation under a stream of nitrogen, and the residues were resuspended in 1 mL of methanol. Finally, the samples were submitted to HPLC analysis under the same conditions as described in Section 2.3.3.

5.2.5.7. Sensory evaluation

This research was approved by the Ethics Research Committee from the Faculty of Animal Science and Food Engineering (FZEA) – University of São Paulo (USP, Brazil) (code CAAE 65895417.0.0000.5421), and the 122 untrained participants signed a term of consent. The consumer acceptance of the enriched yoghurts was evaluated using a hedonic test and a category-type scale with odd number (one to nine) categories ranging from 'dislike it extremely' to 'like it extremely'. For the sensory evaluation, four samples were submitted to the panellists: the three enriched formulations (Y1, Y2 and Y3) and a control (C2) coloured with the artificial dye (tartrazine). The panellists rated the yoghurts on aroma, colour, texture, flavour and overall acceptance. They were also asked about their purchase intent. Samples were served to panellists in identified plastic cups using a monadic form along with water and salt biscuits. All samples were microbiologically tested for coliforms, yeast and mould counts before the sensory evaluation.

5.2.6. Statistical analyses

Statistical analyses of the results were performed using Tukey's test at a 5% significance level ($P < 0.05$) and the SAS software version 9.2 computer program (Statistical Analyses Systems, Cary, NC, USA). All the analyses were performed in triplicate with the mean values unless otherwise stated, and the error bars shown represent the mean ± standard deviation.

5.3. Results and discussion

5.3.1. Characterisation of curcumin/vitamin D₃-loaded nanoliposomes

The physicochemical parameters obtained for the nanoliposomes on the first and 15th day of storage are shown in Table 5.3. The size distributions and micrographs obtained by TEM are shown in Figure 5.1. As seen in Table 5.3, the values of size were significantly different among the formulations; vesicles produced with LS40 (L2 and L3) presented smaller diameters than the formulation produced with only P90H (L1). This result was probably due to the use of sonication to maintain the dispersion of LS40 in ethanol during the production of proliposomes (Chaves & Pinho, 2019). Moreover, liposomes produced by hydration of proliposomes are usually multilamellar (MLV) and present hydrodynamic diameters higher than 500 nm (Lasic 1998). Thus, the results obtained for this study were unprecedented, as the liposomes produced in this study using LS40 resulted in diameters smaller than 320 nm and were thus considered large unilamellar vesicles (LUV). Figure 5.1 shows that the liposomes exhibited bimodal size distributions, corroborating previously reported results (Chaves & Pinho, 2019). The presence of some aggregates confirmed the results obtained by size distribution, as two populations can be distinguished.

The zeta potential results obtained ranged from −146 to −41 mV, indicating good stability over the storage. The contents of bioactive compounds retained in the dispersions were up to 86.1 and 94.1% for curcumin and vitamin D₃, respectively, which could be considered an excellent result considering that both bioactive compounds are easily oxidised. Regarding colorimetric parameters, L1 presented the highest value for luminosity (L*) among the formulations, a result that was expected, as this formulation did not contain LS40, a brownish lecithin, in its composition (Chaves and Pinho 2019). In addition, the low values assessed for a* and the high values assessed for b* suggest an intense yellow coloration, characteristic of curcumin, a result corroborated by the values of Hue angle (~90°). The values

of ΔE revealed some changes in the colour of dispersions over the storage as they were higher than 2 (Francis & Clydesdale, 1975).

Figure 5.1. Size distributions curves of curcumin/vitamin D_3-loaded nanoliposomes produced with Phospholipon 90H (P90H) and Lipoid S40 (LS40) obtained for formulations: (a) L1 (100% P90H), (b) L2 (100% LS40) and (c) L3 (50% P90H + 50% LS40) at the 1st day (—) and at the 15th day (----) of refrigerated storage (at 10 °C). Right below, micrographs obtained by transmission electron microscopy for formulations (d) L1, (e) L2 and (f) L3. Scale: 2 µm.

Reference: Chaves et al. (2021)
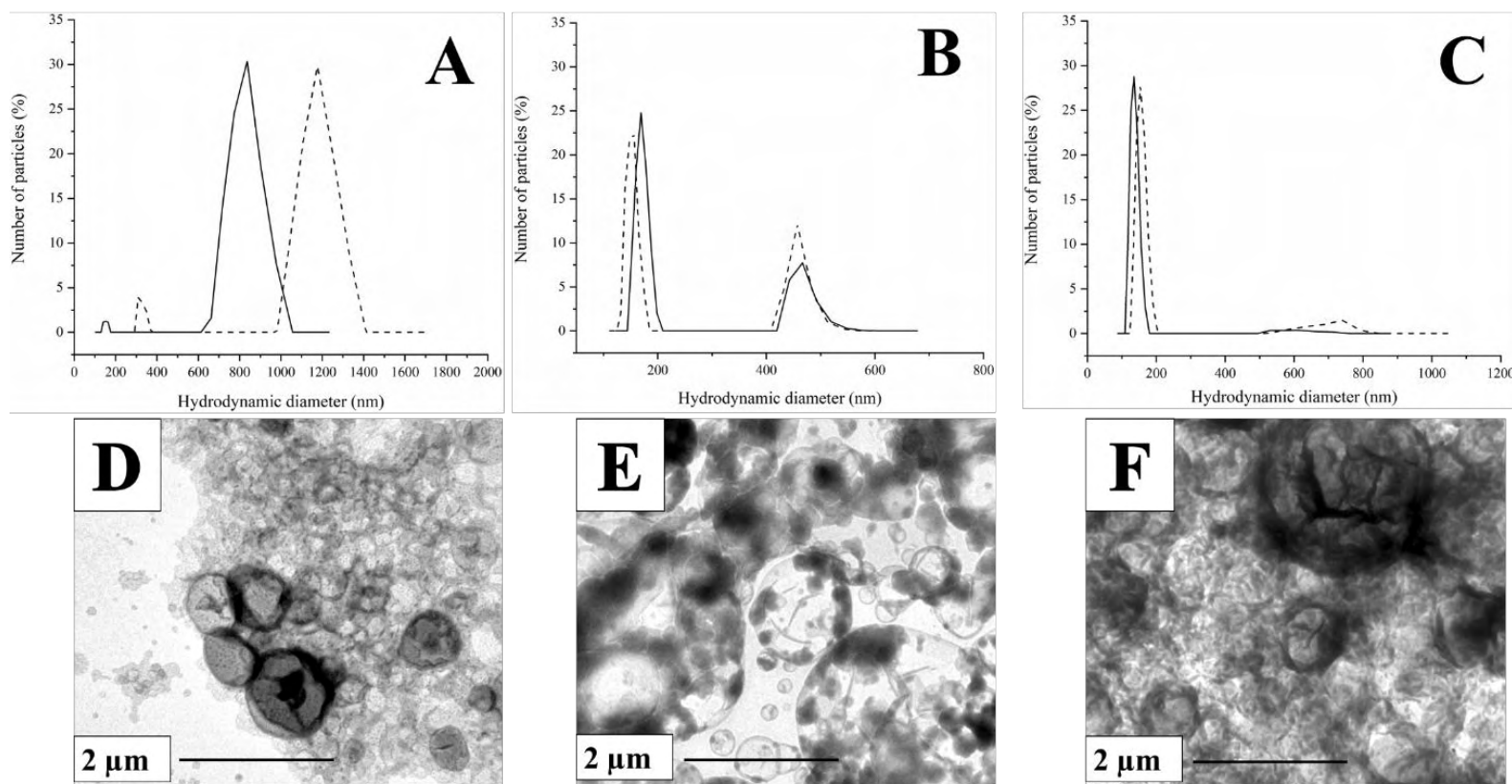
Table 5.3. Physicochemical parameters obtained (at 25 °C) for the curcumin/vitamin D$_3$-loaded liposomes over storage time

Formulation/Time		L1		L2		L3	
		1st day	15th day	1st day	15th day	1st day	15th day
Average hydrodynamic diameter (nm)		813^B ± 32.0	987^A ± 51.0	224^D ± 0.80	241^D ± 1.40	262^D ± 1.80	322^C ± 2.30
Zeta potential		-43^C ± 4.0	-41^C ± 3.0	-111^B ± 10.0	-137^A ± 14.0	-146^A ± 7.0	-41^C ± 2.0
Curcumin concentration (µg/mL)		54^B ± 5.0	56^{AB} ± 7.0	72^A ± 4.0	62^{AB} ± 12	64^{AB} ± 2.0	61^{AB} ± 1.0
% Curcumin preserved		-	100	-	86.1	-	95.3
VD3 concentration (µg/mL)		8.1^A ± 0.4	8.0^A ± 1.1	8.4^A ± 1.3	7.9^A ± 1.0	7.5^A ± 0.7	8.4^A ± 2.0
% VD3 preserved		-	98.8	-	94.1	-	100
Colorimetric parameters	L^*	57^A ± 0.1	53^{AB} ± 5.0	47^C ± 0.2	45^C ± 0.3	50^{BC} ± 0.2	48^{BC} ± 0.3
	a^*	-8.3^A ± 0.4	-8.2^A ± 0.3	-2.1^C ± 0.1	-1.5^C ± 0.3	-6.0^B ± 0.1	-6.2^B ± 0.2
	b^*	58^B ± 1.1	57^B ± 5.0	59^B ± 0.8	69^A ± 0.4	62^B ± 0.4	71^A ± 0.1
	C_{ab}^*	59^B ± 0.3	58^B ± 4.0	59^B ± 0.8	69^A ± 0.4	62^B ± 0.5	71^A ± 0.1
	h_{ab}^*	91^B ± 0.2	92^B ± 1.0	92^B ± 0.1	91^B ± 0.3	96^A ± 0.1	95^A ± 0.2
	TCD	-	5.8^A ± 3.8	-	10^A ± 0.4	-	9.4^A ± 0.3

Means followed by the same uppercase letter in the same line were not significantly different (p > 0.05) by Tukey's test.

Reference: Chaves et al. (2021)

5.3.2. Characterisation of the pineapple yoghurts containing curcumin/vitamin D₃-loaded nanoliposomes

5.3.2.1. Physicochemical aspects and morphological characterisation

The physicochemical parameters obtained for the yoghurts on the 1st and 15th day under refrigerated storage are summarised in Table 5.4. The values of pH obtained ranged from 4.02 to 4.06, which was in accordance with the requirements of Brazilian legislation (Brazil, 2007) and were not affected by storage. No significant differences were identified among the samples, indicating that the addition of unpurified phospholipids did not result in changes of pH. All samples presented water activities around 0.98, typical for this product, but the moisture content ranged from 65.9 to 70.2%, lower than commonly found for juice-enriched yoghurts (Karnopp et al., 2017). The decrease in moisture content may be related to the high content of solids (mostly sugars) present in the formulations due to the addition of refined sugar and concentrated pineapple juice, which may have led to an increase in osmotic pressure. Otherwise, it is known that this increase can have an adverse effect on the starter culture, thus hindering the growth of lactic acid bacteria, as the high hygroscopicity of sugars can decrease the level of water available for their metabolism (Vinderola, Bailo, & Reinheimer, 2000). However, the final acidity of the samples ranged from 0.69 to 0.76 g lactic acid/100 g of yoghurt, within the range stipulated by the Brazilian legislation (between 0.6 and 1.5 g lactic acid/100 g yoghurt) (Brazil, 2007) and by the Codex Alimentarius (min. 0.6%) (World Health Organization (WHO), 2011). Furthermore, the nondairy ingredients added to the plain whole-milk yoghurt during the production of the formulations represented a maximum ranging from 14.1% to 17.7% w/w, which was lower than the maximum stipulated by the Brazilian legislation (30% w/w) for 'fermented milks with additions' (Brazil, 2007) and by the Codex Alimentarius (50% w/w) for 'flavored fermented milks' (WHO, 2011).

Syneresis is one of the major undesirable defects that can appear in yoghurts and is defined as the shrinkage of the protein network that leads to the loss of the serum phase from the gel. The accumulation of whey on the surface of yoghurts contributes to a subsequent decrease in acceptability (Kiros et al., 2016). The percentages of syneresis (%S) are presented in Table 5.4. It was observed that all yoghurts showed an increase in syneresis over the storage time. However, the %S on the 1st day of storage obtained for samples Y2 and Y3 was lower than observed for the control sample. This may be due to the higher content of solids present in the enriched samples due to the addition of sugar-rich ingredients. In addition, C1 and Y1

also presented higher values of syneresis on the 15th day of storage than Y2 and Y3, suggesting that the addition of unpurified lecithins to liposomes may have contributed positively to reducing the loss of the aqueous phase. In this sense, it is known that most of the phospholipids present in P90H and LS40 are zwitterionic. Thus, it was reasonable to consider that their negative charges may interact with the positive charges presented in casein micelles, helping straighten the protein network and, consequently, reducing syneresis in a similar way as anionic polysaccharides (Campo et al., 2019). Additionally, LS40 contains phosphatidic acid and many fatty acids, as well as negatively charged molecules, which may also have contributed to such straightening.

Table 5.4 also shows the results obtained for instrumental colorimetry. Some small differences among the parameters obtained on the 1st and 15th day of storage were detected. Firstly, the decrease observed for a* (and, consequently, for C*) revealed the yoghurts presented a slight tendency to acquire a greenish yellow colour after 15 days of storage, probably due to curcumin oxidation. However, the values of ΔE obtained for the enriched samples were lower than 2, which indicated that no significant changes in colour occurred during the storage time (Francis & Clydesdale, 1975), reinforcing the suitable food colouring property attributed to curcumin. In this context, Gutierres et al. (2012) showed that curcumin when incorporated in yoghurt can contribute to the reduction of hyperglycaemia due to the stimulation of insulin production. In addition, the authors reported that this reduction may occur due to the stimulus of increased glucokinase activity or the well-known antioxidant activity of curcumin. Additionally, Dei Cas and Ghidoni (2019) showed that the combination of curcumin with lecithins in delivery systems can improve pharmacokinetic profile and the cellular uptake of curcumin up to 15- to 20-fold. Regarding the applicability in the dairy industry, the high content of curcumin retained in the yoghurt samples may contribute to the maintenance of the organoleptic properties of the product, as this molecule is a natural polyphenol capable of reducing the number of deteriorating microorganisms (Rahmatalla, Alazeem, & Abdalla, 2017).

Concerning the VD3 content, the concentrations obtained ranged from 0.31 to 0.42 μg/g yoghurt (1240 to 1680 IU/g yoghurt), as shown in Table 5.4. Mostafai et al. (2019) studied the fortification of yoghurts with VD regarding the reduction of the deficiency rates in prediabetic patients and concluded that a consumption of a daily dose of 1000 IU VD from fortified yoghurts for 3 months would be enough to improve their serum lipid indexes. The

authors also stated that yoghurt was more suitable for delivering this vitamin than oral supplements due to its low cost and higher nutritional value. In this sense, the yoghurts produced in this study could be theoretically applied with this purpose, as the obtained VD3 concentrations were up to 1240 IU/100 g yoghurt. In addition, the amounts obtained were lower than the upper limit of 4000 IU stipulated by the Institute of Medicine (IOM) to avoid hypervitaminosis. On the other hand, the decrease in the VD3 content observed in the Y2 formulation can be a result of fatty acid lipoxidation during storage due to the high content of nonhydrogenated species in this sample that may have led to the formation of reactive oxygen species that can act as prooxidation agents, causing VD3 degradation (Mahmoodani et al., 2017).

Table 5.4. Physicochemical (at 25 °C) and rheological (at 10 °C) parameters obtained for the yogurt formulations over storage time

Formulation/Time		C1		Y1		Y2		Y3	
		1st day	15th day	1st day	15th day	1st day	15th day	1st day	15th day
pH		$4.03^A \pm 0.01$	$4.03^A \pm 0.00$	$4.06^A \pm 0.01$	$4.05^A \pm 0.01$	$4.04^A \pm 0.02$	$4.04^A \pm 0.01$	$4.05^A \pm 0.03$	$4.03^A \pm 0.01$
Water activity		$0.98^A \pm 0.01$	$0.98^A \pm 0.01$	$0.98^A \pm 0.01$	$0.98^A \pm 0.01$	$0.98^A \pm 0.01$	$0.98^A \pm 0.01$	$0.98^A \pm 0.01$	$0.98^A \pm 0.00$
Moisture content (%)		$65.9^C \pm 1.25$	$69.6^{AB} \pm 0.99$	$67.0^{BC} \pm 0.38$	$69.1^{AB} \pm 0.66$	$67.9^{ABC} \pm 1.04$	$69.5^{AB} \pm 0.89$	$68.4^{ABC} \pm 1.33$	$70.2^A \pm 0.43$
Titratable acidity (g lactic acid/100 g yogurt)		$0.75^{AB} \pm 0.03$	$0.76^A \pm 0.02$	$0.69^C \pm 0.01$	$0.69^C \pm 0.01$	$0.71^{BC} \pm 0.01$	$0.71^{BC} \pm 0.02$	$0.71^{BC} \pm 0.01$	$0.69^C \pm 0.02$
Syneresis (g whey/100 g yogurt)		$39.2^{BC} \pm 0.92$	$41.2^{AB} \pm 0.24$	$37.0^{CDE} \pm 1.62$	$43.5^A \pm 0.22$	$35.9^{DE} \pm 1.16$	$39.9^{BC} \pm 0.72$	$34.4^E \pm 2.17$	$38.8^{BCD} \pm 0.76$
Vitamin D_3 concentration (µg VD3/g yogurt)		-	-	$0.33^B \pm 0.03$	$0.38^{AB} \pm 0.02$	$0.42^A \pm 0.03$	$0.31^B \pm 0.01$	$0.37^{AB} \pm 0.05$	$0.37^{AB} \pm 0.01$
Vitamin D_3 concentration (IU/100 g yogurt)		-	-	$1320^B \pm 120$	$1520^{AB} \pm 80$	$1680^A \pm 120$	$1240^B \pm 40$	$1480^{AB} \pm 20$	$1480^{AB} \pm 40$
% Vitamin D_3 preserved		-	-	-	100	-	73.8	-	100
Colorimetric parameters	L^*	$68.4^A \pm 0.03$	$68.4^A \pm 0.01$	$67.9^D \pm 0.00$	$67.6^E \pm 0.01$	$68.0^C \pm 0.01$	$68.0^C \pm 0.01$	$68.0^C \pm 0.01$	$68.2^B \pm 0.02$
	a^*	$-1.55^E \pm 0.08$	$-1.43^E \pm 0.08$	$-6.14^A \pm 0.02$	$-5.93^{BC} \pm 0.06$	$-5.92^{BC} \pm 0.09$	$-5.72^D \pm 0.03$	$-6.02^{AB} \pm 0.02$	$-5.79^{CD} \pm 0.03$
	b^*	$3.30^D \pm 0.10$	$3.18^D \pm 0.08$	$14.3^A \pm 0.12$	$14.0^B \pm 0.06$	$13.9^{BC} \pm 0.03$	$13.7^C \pm 0.04$	$14.1^{AB} \pm 0.09$	$13.9^{BC} \pm 0.02$
	C_{ab}^*	$3.65^D \pm 0.08$	$3.49^D \pm 0.11$	$15.5^A \pm 0.11$	$15.2^B \pm 0.08$	$15.1^B \pm 0.05$	$14.8^C \pm 0.05$	$15.3^{AB} \pm 0.09$	$15.1^B \pm 0.03$
	h_{ab}^*	$115^B \pm 1.60$	$114^{AB} \pm 0.66$	$113^A \pm 0.15$	$113^A \pm 0.12$	$113^A \pm 0.29$	$113^A \pm 0.05$	$113^A \pm 0.06$	$113^A \pm 0.08$
	TCD	-	$0.19^A \pm 0.09$	-	$0.39^A \pm 0.05$	-	$0.30^A \pm 0.10$	-	$0.35^A \pm 0.07$
Rheological parameters fitted by the Herschel Bulkley model	τ_0 (Pa)	$0.91^D \pm 0.11$	$2.20^{AB} \pm 0.02$	$2.08^B \pm 0.26$	$1.29^C \pm 0.07$	$2.50^A \pm 0.18$	$2.04^B \pm 0.05$	$1.29^C \pm 0.01$	$2.37^{AB} \pm 0.04$
	N	$0.63^{AB} \pm 0.04$	$0.65^{AB} \pm 0.01$	$0.62^B \pm 0.02$	$0.69^A \pm 0.02$	$0.64^{AB} \pm 0.01$	$0.65^{AB} \pm 0.03$	$0.68^{AB} \pm 0.02$	$0.66^{AB} \pm 0.01$
	k (Pa.s^n)	$0.82^B \pm 0.19$	$1.44^A \pm 0.06$	$1.61^A \pm 0.10$	$0.85^B \pm 0.06$	$1.56^A \pm 0.14$	$1.35^A \pm 0.18$	$0.87^B \pm 0.08$	$1.37^A \pm 0.07$

Means followed by the same uppercase letter in the same line were not significantly different ($p > 0.05$) by Tukey's test.

Reference: Chaves et al. (2021)

5.3.2.2. Rheological characterisation

The flow curves obtained for the yoghurt samples on the 1st and 15th day of storage are shown in Fig. 5.2a-b. The curves were fitted using the Herschel–Bulkley model, and the parameters obtained are shown in Table 5.4. All produced yoghurts presented non-Newtonian behavior as well as shear thinning or pseudoplastic behavior, in accordance with the values of flow behavior indexes obtained (n < 1.0). The flow curves indicated the enriched yoghurts exhibited stronger network structures on the 1st day than the control sample, as higher values for shear stress were obtained when higher shear rates were applied for such formulations. This statement could be corroborated by observing the higher values of yield stress obtained for the enriched samples. Van Oosten-Manski et al. (2009) stated that an increase in the fat content in yoghurts could lead to an increase in the corresponding yield stress, which would be suitable for this study, as the samples were enriched with phospholipids. On the other hand, the values of the consistency coefficient (K) were significantly different with increasing storage time except for Y2. For the C1 and Y3 formulations, the values of K increased over the storage time, which suggested an increase in viscosity, whereas the opposite was observed for Y1, indicating a weaker network of the gel (Sah et al. 2016). This behavior could also be observed by analyzing Fig. 5.2c-d, where it is possible to see that Y1 presented the lowest viscosity profile on the last day of storage. In this context, an increase in the shear rate led to a decrease in the apparent viscosities of all samples, indicating a breakage of the yoghurt structure during shearing. Otherwise, the higher values of K assessed on the 1st day for formulations Y2 and Y3 than for the control sample are in agreement with the conclusions obtained by Penna, Gurram, & Barbosa-Canóvas (2006) who stated that an increase in the solid content resulted in an increase in the value of the consistency coefficient. The disparity observed by Y1 may have been influenced by several factors during storage, such as water retention capacity, the interaction with milk proteins and the formation of microcrystals of sugar that can also retain water (Cruz et al., 2013).

Figure 5.2. Flow curves obtained on the (a) 1st and on the (b) 15th day of storage for the yoghurt samples: C1 (continuous lines), Y1 (dashed lines), Y2 (dotted lines) and Y3 (dash-dotted lines). Apparent viscosity (η) profiles assessed on the (c) 1st and on the (d) 15th day of storage for the samples: C1 (continuous lines), Y1 (dashed lines), Y2 (dotted lines) and Y3 (dash-dotted lines). Mechanical spectrum of samples on the (e) 1st and on the (f) 15th day of storage: C1 (squares), Y1 (triangles), Y2 (circles) and Y3 (diamonds). G' (elastic modulus, full symbols), G" (viscous modulus, empty symbols).
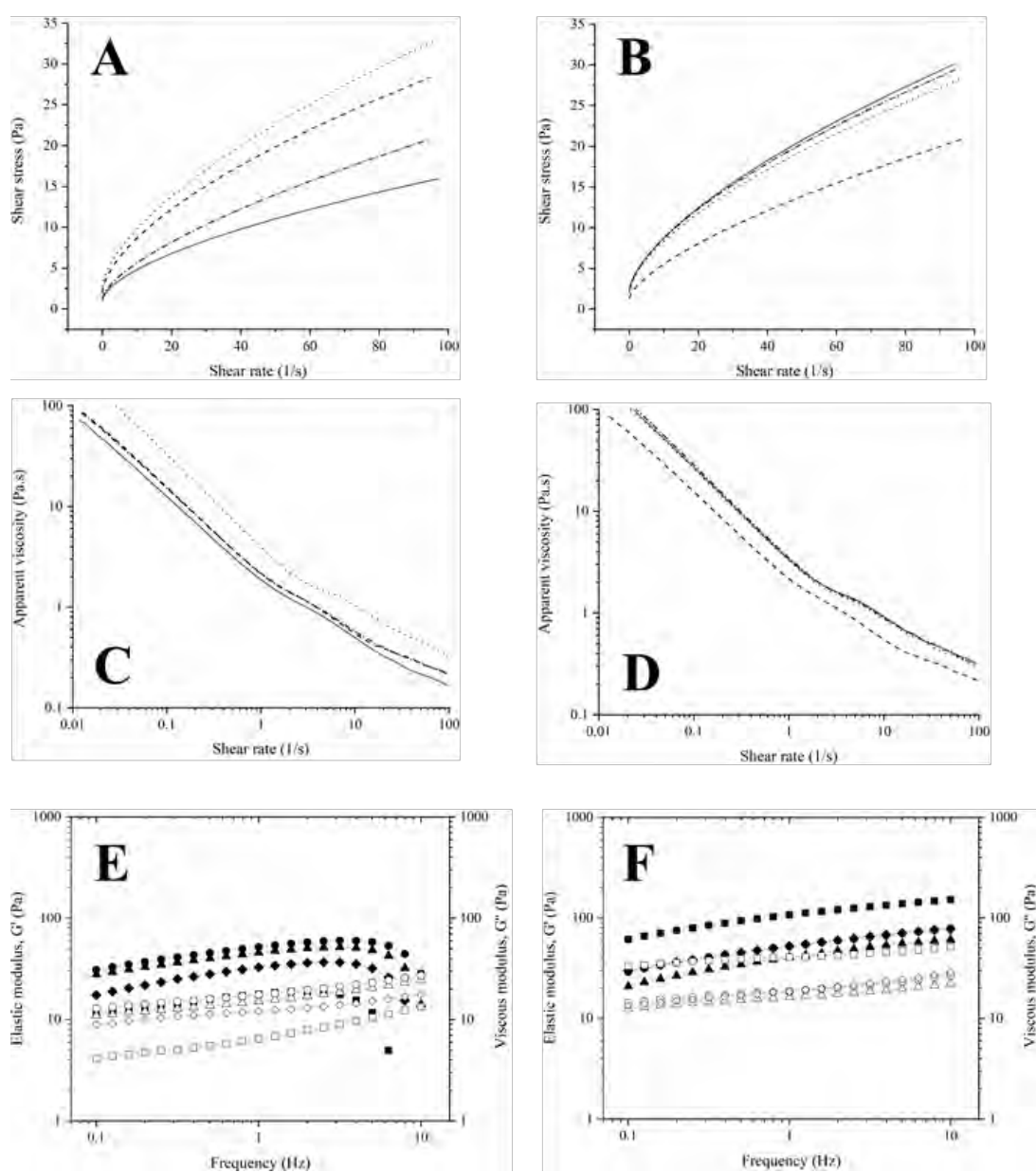
Reference: Chaves et al. (2021)

The mechanical spectra obtained within the linear viscoelastic range for the yoghurt samples are shown in Fig 5.2e-f. In general, the elastic modulus (G') values were higher than the viscous modulus (G") for all yoghurts independent of storage time, which indicated the formation of weak viscoelastic systems that could assure better stability of the samples. On the 1st day of storage (Fig. 5.2e), it was possible to observe a decay of the G' modulus at frequencies higher than 3.0 Hz, a behavior that was not seen in the profiles obtained on the 15th day (Fig. 5.2f). The absence of this decay on the 15th day can be associated with a large number of protein interactions and rearrangements during storage to a more solid-like gel (Cruz et al., 2013). Additionally, the profiles of both the G' and G" moduli obtained for the control sample were the lowest on the 1st day of storage but became the highest on the 15th day of storage. The higher profiles obtained for enriched samples on the first day suggested interactions between the liposomes and the protein network of the yoghurt gels as a result of electrostatic interactions of the phospholipids with the casein and whey proteins, which can strengthen the gel structure in a similar way as exopolysaccharide, as described by Prasanna, Grandinson, & Charalampopoulos, 2013). The weaker characteristic of the control yoghurt on the first day of storage was corroborated by the profile of apparent viscosity obtained for this sample (Fig. 5.2c), which showed that C1 presented the lowest values of viscosity through the shearing process. The increase in both moduli seen for the C1 sample on the 15th day of storage was probably a result of the increase in protein–protein interactions during storage not seen in samples containing liposomes (Doleyres, Schaub, & Lacroix, 2005).

5.3.2.3. Sensory evaluation

The scores obtained for the different attributes and the purchase intent of the yoghurts obtained in the sensory evaluation after 24 h of storage at 10 °C are shown in Figure 5.3. None of the parameters presented significant differences (P > 0.05) among the yoghurts. Additionally, no differences were perceived between the yellow colour of the yoghurts attributed to curcumin or artificial tartrazine. This result was obtained regardless of the nanoliposome formulation used. Although no significant differences were obtained among the formulations, it was possible to verify that C2 and Y1 obtained higher scores for all the parameters than those of Y2 and Y3, a result that was reflected in the positive answers concerning the purchase intention of both of the C2 and Y1 formulations (75.4% and 78.7%, respectively). In addition, the purchase intentions of C2 and Y1 would be up to 95.9% and 98.4%, respectively, if negative

answers were excluded, which reflected the excellent acceptability of Y1. Otherwise, the purchase intention of Y2 was the least accepted by the consumers, with its taste obtaining the lowest grade (6.81) among all parameters. This result may be a direct consequence of the bitter taste characteristic of LS40. Nevertheless, the overall acceptance grade of Y2 was 6.98, which corresponded to 'like moderately', which was also a positive result on the hedonic 9-point scale. Finally, when a 50:50 ratio of phospholipids was applied in liposomes to fortify the Y3 formulation, it was possible to observe a decrease of approximately 60% of the negative purchase intent answers when compared to those obtained by Y2. This result reflected that unpurified phospholipids can still be used with this purpose but in less quantity, which would still result in a reduction in production costs.

Figure 5.3. Sensory descriptive profile of yoghurt samples (Y) enriched with curcumin and vitamin D_3 coencapsulated in liposome dispersions (L): C2 (control), Y1 (enriched with L1), Y2 (enriched with L2) and Y3 (enriched with L3). L1: liposome dispersion produced with only Phospholipon 90H (P90H); L2: liposome dispersion produced with only Lipoid S40 (LS40); L3: liposome dispersion produced with P90H and LS40 in a 50:50 ratio.

Formulation	Flavor	Color	Texture	Taste	Overall Acceptance
C2	7.31[A] ± 1.03	7.42[A] ± 1.24	7.61[A] ± 0.95	7.85[A] ± 0.87	7.71[A] ± 0.82
Y1	7.58[A] ± 1.20	7.24[A] ± 1.19	7.57[A] ± 1.10	7.84[A] ± 1.55	7.73[A] ± 1.20
Y2	7.18[A] ± 1.06	7.16[A] ± 1.46	7.12[A] ± 0.98	6.81[A] ± 1.24	6.98[A] ± 1.01
Y3	7.17[A] ± 1.22	6.93[A] ± 1.08	7.49[A] ± 1.01	7.42[A] ± 0.92	7.38[A] ± 0.89

Means followed by the same uppercase letter in the same column were not significantly different ($p > 0.05$) by Tukey's test.

Purchase intent (%)	Yes	Maybe	No
C2	75.4	20.5	4.1
Y1	78.7	19.7	1.6
Y2	52.5	33.6	13.9
Y3	63.1	31.2	5.7

Reference: Chaves et al. (2021)
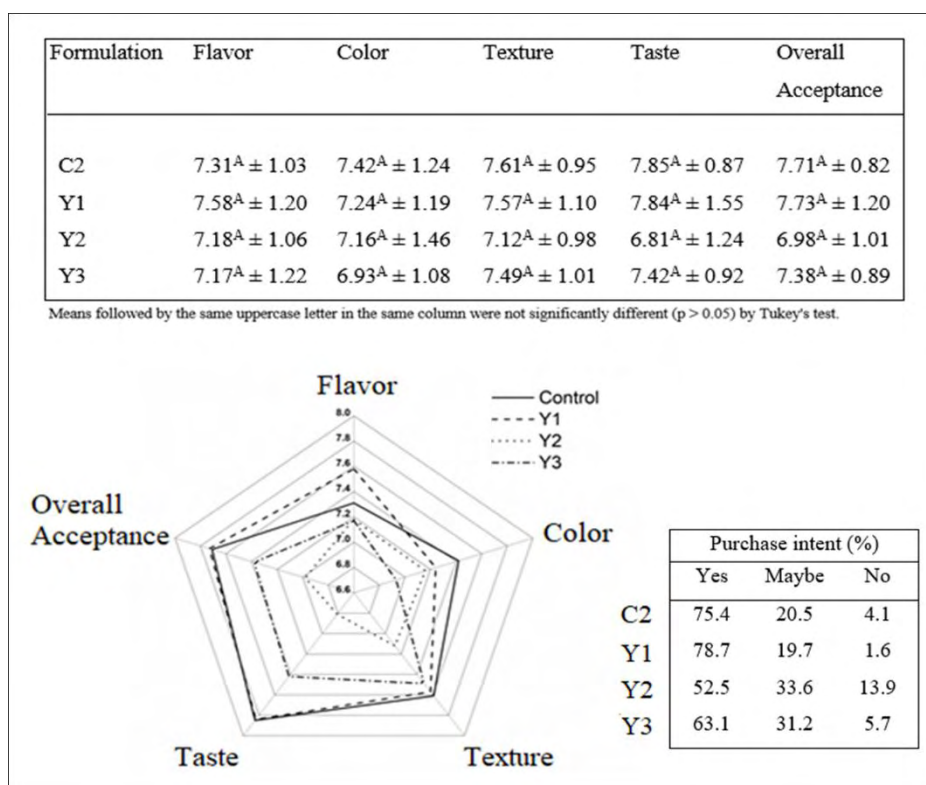
5.4. Conclusions

The resulting liposomes presented a nanometric range and good stability, as shown by zeta potential values. In addition, an increase in the content of purified hydrogenated phospholipids led to an increase in the amount of encapsulated bioactive compounds. Curcumin was successfully encapsulated in the nanoliposomes and proved to be a suitable replacer for yellow tartrazine in yoghurt, as no differences in colour were perceived by the panellists in the sensory analysis. Vitamin D_3 was not degraded after 15 days in yoghurts enriched with nanoliposomes produced with 50 and 100% purified lecithins. Values of pH, water activity and acidity obtained for yoghurts were all within the limits allowed by the Brazilian legislation and by the *Codex Alimentarius*. The incorporation of unpurified phospholipids and sugar-rich ingredients led to decreases in the moisture content and syneresis of the samples, as well as increases in their viscosities and viscoelastic properties. All yoghurts were well evaluated by the sensory panel with purchase intentions up to 63% for yoghurts enriched with liposomes produced with a 50:50 ratio of purified and unpurified lecithins and up to 78% for yoghurts produced with purified lecithins. Further studies are required to optimize the ratio of lecithins and verify the maximum amount of unpurified lecithins that can be added to yoghurt formulations.

5.5. Acknowledgments

5.6. References

Abdesslem, S. B. et al. (2020). Evaluation of the effect of fennel (*Foeniculum vulgare Mill*) essential oil addition on the quality parameters and shelf-life prediction of yoghurt. **International Journal of Dairy Technology**, 73, 403-410.

Association of Official Analytical Chemists (AOAC). (1995). **Official Methods of Analysis of the Association of Official Analytical Chemists, (method 942.15 B)**, Arlington: A.O.A.C.

Brazil. (2007). Ministério da Agricultura, Pecuária e Abastecimento. **Instrução Normativa n. 46, de 23 de outubro de 2007**. Regulamento técnico de identidade e qualidade de leites fermentados.

Campo, C. et al. (2019). Incorporation of zeaxanthin nanoparticles in yoghurt: Influence on physicochemical properties, carotenoid stability and sensory analysis. **Food Chemistry**, 301, 125230.

Chaves, M. A., & Pinho, S. C. (2019). Curcumin-loaded proliposomes produced by the coating of micronized sucrose: Influence of the type of phospholipid on the physicochemical characteristics of powders and on the liposomes obtained by hydration. **Food Chemistry**, 291, 7-15.

Chaves, M. A. et al. (2018). Structural characterization of multilamellar liposomes coencapsulating curcumin and vitamin D_3. **Colloids and Surfaces A: Physicochemical and Engineering Aspects**, 549, 112-121.

Cruz, A. G. et al. (2013). Developing a prebiotic yoghurt: Rheological, physico-chemical and microbiological aspects and adequacy of survival analysis methodology. **Journal of Food Engineering,** 114, 323-330.

Dei Cas, M. & Ghidoni, R. (2019). Dietary curcumin: Correlation between bioavailability and health potential. **Nutrients**, 11, 2147.

Doleyres, Y., Schaub, L., & Lacroix, C. (2005). Comparison of the functionality of exopolysaccharides produced in situ or added as bioingredients on yoghurt properties. **Journal of Dairy Science,** 88, 4146-4156.

Francis, J. F., & Clydesdale, F. M. (1975). **Food colorimetry, theory and application**, pp 486. Westport: AVI Publishing Company.

Gomis, D. B., Fernández, M. P., & Gutiérrez-Alvarez, Mª D. (2000). Simultaneous determination of fat-soluble vitamins and provitamins in milk by microcolumn liquid chromatography. **Journal of Chromatography A**, 891, 109-114.

Gutierres, V. O. et al. (2012). Curcumin-supplemented yoghurt improves physiological and biochemical markers of experimental diabetes. **British Journal of Nutrition**, 108, 440-448.

Hadjimbei, E. et al. (2020). Functional stability of goats' milk yoghurt supplemented with *Pistacia atlantica* resin extracts and *Saccharomyces boulardii*. **International Journal of Dairy Technology**, 73, 134-143.

Holick, M. F. (2017). The vitamin D deficiency pandemic: Approaches for diagnosis, treatment and prevention. **Reviews in Endocrine & Metabolic Disorders**, 18, 153-165.

Karnopp, A. R. et al. (2017). Optimization of an organic yoghurt based on sensorial, nutritional, and functional perspectives. **Food Chemistry**, 233, 401-411.

Khaledabad, M. A. et al. (2020). Probiotic yoghurt functionalised with microalgae and Zedo gum: chemical, microbiological, rheological and sensory characteristics. **International Journal of Dairy Technology**, 73, 67-75.

Kiros, E. et al. (2016). Effect of carrot juice and stabilizer on the physicochemical and microbiological properties of yoghurt. **LWT – Food Science and Technology**, 69, 191-196.

Khorasani, S., Danaei, M., & Mozafari, M. R. (2018). Nanoliposome technology for the food and nutraceutical industries. **Trends in Food Science & Technology**, 79, 106-115.

Lasic, D. D. (1998). Novel applications of liposomes. **Trends in Biotechnology**, 16, 307-321.

Mahmoodani, F. et al. (2017). Degradation studies of cholecalciferol (vitamin D_3) using HPLC-DAD, UHPLC-MS/MS and chemical derivatization. **Food Chemistry**, 219, 373-381.

Mostafai, R. et al. (2019). Effects of vitamin D-fortified yoghurt in comparison to oral vitamin D supplement on hyperlipidemia in pre-diabetic patients: A randomized clinical trial. **Journal of Functional Foods**, 52, 116-120.

Penna, A. L. B., Gurram, S., & Barbosa-Canóvas, G. V. (2006). Effect of high hydrostatic pressure processing on rheological and textural properties of probiotic low-fat yoghurt fermented by different starter cultures. **Journal of Food Process Engineering**, 29, 447-461.

Prasanna, P. H. P., Grandinson, A. S., & Charalampopoulos, D. (2013). Microbiological, chemical and rheological properties of low-fat set yoghurt produced with exopolysaccharide (EPS) producing Bifidobacterium strains. **Food Research International**, 51, 15-22.

Rahmatalla, S. A., Alazeem, L. A. & Abdalla, M. O. M. (2017). Microbiological quality of set yoghurt supplemented with turmeric powder (*Curcuma longa*) during storage. **Asian Journal of Agriculture and Food Sciences**, 5, ISSN: 2321 − 1571.

Riener, J. et al. (2010). A comparison of selected quality characteristics of yoghurts prepared from thermosonicated and conventionally heated milks. **Food Chemistry**, 119, 1108-1113.

Rostamabadi, H., Falsafi, S. R., & Jafari, S. M. (2019). Nanoencapsulation of carotenoids within lipid-based nanocarriers. **Journal of Controlled Release**, 298, 38-67.

Sah, B. N. P. et al. (2016). Physicochemical, textural and rheological properties of probiotic yoghurt fortified with fibre-rich pineapple peel powder during refrigerated storage. **LWT – Food Science and Technology**, 65, 978-986.

Van Oosten-Manski, J. et al. (2009). Rheology and sensory properties of stirred yoghurts. **Proceedings of the 5th International Symposium on Food Rheology and Structure**. Zurich Switzerland, Jun 15-18, 388-391.

Vinderola, C. G., Bailo, N., & Reinheimer, J. A. (2000). Survival of probiotic microflora in Argentinian yoghurts during refrigerated storage. **Food Research International**, 33, 97-102.

World Health Organization (WHO). (2011). **_Codex Alimentarius_ – Milk and Milk Products**, 2nd ed. Food and Agriculture Organization of the United Nations, Rome.

Chapter 6. CO-ENCAPSULATION OF CURCUMIN AND VITAMIN D₃ IN MIXED

NANOLIPOSOMES USING A CONTINUOUS SUPERCRITICAL CO₂ ASSISTED

PROCESS

Chapter 6. Co-encapsulation of curcumin and vitamin D_3 in mixed nanoliposomes using a continuous supercritical CO_2 assisted process

Abstract

Curcumin and vitamin D_3 (VD3) are nutraceutical compounds that exert important roles in human health. Nanoencapsulation in liposomes appears as a suitable target delivery system that can also enhance the bioavailability of these biomolecules. Vesicles were prepared using different ratios of hydrogenated and non-hydrogenated phospholipids, derived from soy and egg-yolk, respectively. A supercritical CO_2 assisted process was used to produce the nanoliposomes. The operative parameters were 40 °C and 100 bar, using a water flow rate of 10 mL/min. Nanoliposomes were characterized by scanning electron microscopy (SEM) and dynamic light scattering (DLS) to determine their morphology and stability properties; whereas release kinetics and encapsulation efficiency were measured using UV/Vis spectrophotometer. Antioxidant activity and the effect of stress-induced conditions on the nanoliposomes were also investigated. Mean diameters of the vesicles ranged from 128 to 228 nm, with encapsulation efficiencies up to 95% for curcumin and 74% for VD3. The addition of 30% w/w of saturated phospholipids to the starting formulation promoted increased vesicles size and a consequent increase in encapsulation efficiency of both biomolecules. The antioxidant activity of curcumin was preserved after processing and the co-loaded nanovesicles demonstrated a good stability under different stress conditions.

6.1. Introduction

The attention towards a healthier lifestyle is demanding new efforts from the food industry, mostly to offer clear-label products with lower levels of artificial preservatives. In this context, nutraceuticals/functional foods emerge as health-promoting products that can contribute to the prevention of some diseases due to the action of bioactive molecules present in their composition.

Nanoencapsulation technologies are extensively used to protect sensitive food nutraceuticals and to enhance their bioavailability and stability in the gastrointestinal tract (Shishir et al., 2013). These techniques consist of trapping the molecules within nanocarriers, such as nanoemulsions, nanoliposomes, solid-lipid nanoparticles and nanostructured lipid carriers, ensuring a higher efficiency of the materials and improving the optimal dosage over time (Hosseini, Ramezanzade, & McClements, 2021). Specifically, nanoliposomes are spherical vesicles consisting of one or more phospholipid bilayers, concentrically arranged, surrounded by an aqueous core after energy input (Gulzar & Benjakul, 2020). They are considered as the most promising lipid-based nanocarriers, due to their ability to encapsulate both hydrophilic and/or hydrophobic compounds, and to protect their inner bioactives from the gastric fluid (pH 5), enabling their proper absorption at the intestine (pH 7) (Kim, Kim, & Lee, 2013). Moreover, nanoliposomes can be produced from natural phospholipids known as nontoxic, biocompatible, biodegradable and non-immunogenic food-grade ingredients (Khorasani, Danaei, & Mozafari, 2018), besides to enhance the performance of molecules by improving their solubility, bioavailability, in vitro and in vivo stability (Mozafari, 2010). The nanovesicles present also a higher stability against creaming, sedimentation and aggregation than liposomes due to their smaller size (Hamadou et al., 2020). Nevertheless, despite the above-mentioned advantages, nanoliposomes are susceptible to hydrolysis and oxidation that can disrupt their phospholipid membrane and induce an early bioactive leakage (Sarabandi et al., 2019).

The conventional methods for liposome production include thin-film hydration, detergent removal, solvent injection, and reverse phase evaporation; these are multi-step methods that need additional downstream processing, as sonication or extrusion, to obtain vesicles with homogeneous size distributions. Also, the use of toxic organic solvents can be considered a relevant concern regarding the applicability of liposomes in food formulations. Alternatively, supercritical CO_2 (SC-CO_2) assisted technologies appear as suitable alternatives to the conventional methods, and have been successfully proposed in several fields (Baldino,

Scognamiglio, & Reverchon, 2020; Baldino et al., 2020; Baldino, Cardea, & Reverchon, 2019a). In particular, CO_2 is a safe and inexpensive compound with high solvation power and mass transfer rates (Gönen & Gupta, 2021). Furthermore, due to CO_2 mild critical parameters (T_c = 31.1 °C and P_c = 7.39 MPa), the degradation of heat-sensitive molecules, as pigments and vitamins, can be avoided during processing (Villanueva-Bermejo & Temelli, 2020). However, most of the high-pressure systems discussed in the literature for liposome production, such as Depressurization of an Expanded Liquid Organic Solution (DELOS) (Battista et al., 2021), Depressurization of an Expanded Solution into Aqueous Media (DESAM) (Elizondo et al., 2012), Supercritical Reverse Phase Evaporation (scRPE) (Aburai et al., 2011), and Supercritical AntiSolvent (SAS) (Lesoin et al., 2011), are characterized by semi-continuous layouts, with two or more processing steps.

Supercritical assisted Liposome formation (SuperLip) technique, instead, is a high-pressure process designed to produce nanoliposomes in a single step with an improved control of vesicles morphology and size distribution (Espírito-Santo et al., 2014; Trucillo et al., 2020). This process has been successfully used for the encapsulation of antibiotics, proteins, essential oils, dietary supplements and dyes within nanoliposomes, achieving encapsulation efficiencies up to 99% and solvent residues lower than the limits related to safety by Food & Drug Administration (Trucillo et al., 2020). Differently from the other techniques, SuperLip process consists of an inversion of the traditional liposome production steps; indeed, droplets of water are first created through spray atomization and then covered by the phospholipids. The liposomes are completely formed when the droplets reach the bottom of the formation vessel, in which a water pool is located. The continuous operative layout of SuperLip also allows a higher reproducibility of the obtained vesicles (Espírito-Santo et al., 2014).

Curcumin is a hydrophobic polyphenol molecule with several health benefits, including antioxidant, anti-inflammatory, anticancer, and antimicrobial activities (Tai et al., 2019). It is the main yellow pigment extracted from the rhizome of *Curcuma longa L.*, and it is commonly used around the world as food colorant, spice and preservative. Although its several properties, curcumin applicability in foods is hampered due to its low solubility in water (11 ng/mL at 25 °C), high sensitivity to oxygen, low absorption in the gastrointestinal tract, and rapid metabolism (Pu et al., 2019). To increase the bioavailability of curcumin, liposomes have been proposed as the lipid carrier, to enhance the gastrointestinal absorption and plasma antioxidant

activity of the bioactive compound (Tai et al., 2020; Estephan, El Kurdi, & Patra, 2021; Li et al., 2021; Wang et al., 2021).

Vitamin D_3 (cholecalciferol) is the more active form of vitamin D and can be synthetized by the human epidermis after sunlight exposure. It is a liposoluble pro-hormone molecule with an important role in calcium homeostasis and bone health (Holick, 2017). However, like curcumin, vitamin D_3 is a hydrophobic compound that cannot be easily dispersed into aqueous food formulations. Hence, the nanoencapsulation of vitamin D_3 into liposomes appears as a solution that can also increase its bioavailability in the human body, as well as to provide protection against environmental stresses as the presence of oxygen, UV radiation, or processing conditions (Holick, 2017; Mohammadi, Ghanbarzadeh, & Hamishehkar, 2014).

Based on these considerations, this study aimed to verify the feasibility of the production of nanoliposomes co-entrapping curcumin and vitamin D_3 using SuperLip technology. The idea was to produce a lipid nanocarrier capable of loading both curcumin and vitamin D_3 by using ingredients generally recognized as safe (GRAS) and an eco-friendly technology (SuperLip), in addition to characterize the vesicles using techniques commonly applied for these systems. Nanoliposomes were prepared using various concentrations of food-grade phospholipids at different degrees of hydrogenation. In this context, even though non-hydrogenated phospholipids are about 20% cheaper than hydrogenated ones, saturated phospholipids can help the stability of lipid bilayers by increasing their rigidity (Sebaaly et al., 2016; Chaves & Pinho, 2019; Chaves & Pinho, 2020). Also, it is worth-mentioning that the co-encapsulation of bioactives in nanoliposomes using a supercritical technology is not commonly found in the literature. Moreover, this technological study can open discussions about the formation of mixed membranes and its correlation with the amount of encapsulated molecules, as well as to verify the effect of the presence of vitamin D_3 in curcumin-loaded nanoliposomes.

6.2. Material, apparatus and methods

6.2.1. Chemicals and reagents

Carbon dioxide (CO_2, >99.4% purity) was purchased from Morlando Group (Naples, Italy). Curcumin (≥65% purity) and cholecalciferol (VD3, >98% purity) were purchased from Sigma Aldrich (Milan, Italy). Soy hydrogenated phosphatidylcholine (Phospholipon 90H, SPC, >90% purity) was donated by Lipoid GmbH (Ludwigshafen, Germany) and egg-yolk non-hydrogenated L-α-phosphatidylcholine (EPC, Type XVI-E, ≥99% purity) was purchased from

Sigma Aldrich (Milan, Italy). Ethanol (>99.8% purity), sodium chloride (NaCl, for analysis), sucrose (for biochemistry), 2,2-diphenyl-1-picrilhhydrazyl (DPPH), 2,2'-azino-bis(3-ethylbenzothiazoline-6-sulfonic acid) (ABTS) and potassium persulfate were purchased from Sigma Aldrich (Milan, Italy). Distilled water was produced by a lab-scale distiller, and was used throughout the experiments. All the chemicals were used as received.

6.2.2. Production of nanoliposomes using SuperLip apparatus

SuperLip apparatus was described in detail elsewhere [18]. A schematic representation of its layout is illustrated in Fig. 6.1. First, CO_2, coming from a reservoir, was delivered at 4.03 L/min to the saturator (mixing chamber) kept at 100 bar and 40 °C using a pump (LDC-M-2, Ecoflow®, Lewa, Leonberg, Germany). In the meanwhile, the ethanolic solution was prepared by mixing 500 mg of phospholipids with 100 mL of ethanol under magnetic stirring (1000 rpm/1 h). The molecule bioactives were then incorporated to the solution, which was furtherly stirred for 30 min, filtered under vacuum, and then added to a burette located next to the saturator. The solution was then pumped to the same chamber at 4.0 mL/min using a stainless-steel pump (mod. 305, Gilson, Villiers-le-Bel, France). The mixture between CO_2 and ethanol promoted the formation of a gas-expanded liquid (GXL) with a gas-to-liquid ratio of 2.39 on mass basis; whereas the mole fraction of CO_2 (x_{CO2}) was 0.714. The gas-to-liquid ratio value was chosen so that the amount of residual ethanol present in the final liposomal suspension would be less than Food and Drug Administration (FDA) limits (Trucillo et al., 2019). GXL was then delivered through a capillary tube to the liposome formation vessel, also operating at 100 bar and 40 °C. The third line, feeding water, was concomitantly delivered to the formation vessel at 10 mL/min using another pump (mod. 305, Gilson, Villiers-le-Bel, France). Before the contact with the GLX, water was atomized at the top of the formation vessel, through an 80 µm internal diameter nozzle. This choice was performed to avoid fouling and blockage problems as some deposition of material may be seen on the surface of smaller nozzles. Also, it is worth mentioning that a better control of water atomization and, consequently, of vesicle size distribution was optimized after the combination of a high pressure and the use of an 80 µm nozzle on SuperLip (Espírito-Santo et al., 2014; Trucillo et al., 2018).

Briefly, nanoliposomes were formed as it follows: first, atomized water droplets were surrounded by phospholipids in the formation vessel, resulting in inverted micelles. Next, these structures fell into the water pool located at the bottom of the vessel, where the double layer

structure was completed by the addition of a second phospholipid layer. After depressurization, ethanol and CO_2 were removed through a separator, operating at 25 °C and 10 bar. Differently from ethanol that was collected from the bottom of the separator, CO_2 passed through a rotameter (mod. 5-2500, Serval 115022, ASA, Sesto San Giovanni, Milano, Italy), to measure the gas flow rate. The nanoliposome suspensions were withdrawn from a reservoir, located below the formation vessel, and stored in Falcon tubes at 4 °C.

All formulations tested are summarized in Table 6.1. The added concentrations of curcumin and vitamin D_3 were chosen considering recommended daily intakes (Bischoff-Ferrari et al., 2009; Basnet & Skalko-Basnet, 2011). The addition of relatively higher amounts than recommended was performed to balance possible bioactive losses during processing.

Figure 6.1. SuperLip layout: (01) CO_2 reservoir; (02) burette for liquid feeding; (03) formation vessel (0.5 dm3 internal volume, 25 cm high); (04) liposome suspension reservoir; (05) separator; (06) saturator/high pressure static mixer (internal volume 0.15 dm³)

Reference: Chaves et al. (2022)
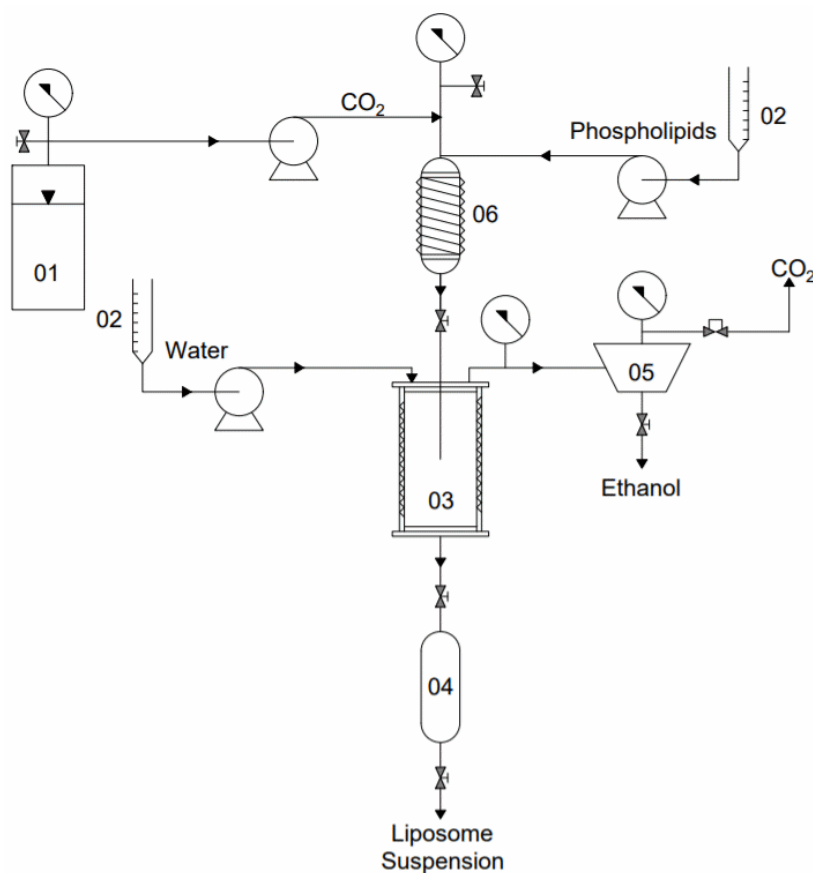
Table 6.1. Formulations used for the production of curcumin (C) and curcumin-vitamin D$_3$ (CV) co-loaded nanoliposomes, using SuperLip at 100 bar and 40 °C

Formulation	Concentration (mg/mL)				Phospholipid ratio (%)		Curcumin to lipid ratio (%)	VD3 to lipid ratio (%)
	Phospholipids		Curcumin	VD3				
	EPC	SPC			EPC	SPC		
C1	3.5	1.5	0.3	-	70	30	6	-
C2	4	1	0.3	-	80	20	6	-
C3	5	-	0.3	-	100	0	6	-
CV1	3.5	1.5	0.3	0.1	70	30	6	2
CV2	4	1	0.3	0.1	80	20	6	2
CV3	5	-	0.3	0.1	100	0	6	2

Reference: Chaves et al. (2022a)

6.2.3. Characterization of nanoliposomes

6.2.3.1. Mean diameter, ζ-potential and size distribution

Mean diameter, polydispersity index (PDI), ζ-potential and size distribution were measured using a dynamic light scattering (DLS) at 25 °C (ZetaSizer Nano S, Malvern Instruments, Worcester, UK).

6.2.3.2. Morphology

Morphology of samples was observed by a field-emission scanning electron microscope (FE-SEM, mod. LEO 1525, Carl Zeiss SMT AG, Oberkochen, Germany). Nanoliposomes were dripped onto adhesive carbon tabs, previously attached on aluminum stubs, and dried at 25 °C in fume hood for two days. Next, stubs were covered with gold using a sputter coater (mod. B7341, 250 Å, Agar Scientific, Stansted, UK) prior to the observation.

6.2.3.3. Encapsulation efficiency of curcumin (%EE$_C$)

Encapsulation efficiency of curcumin (%EE$_C$) within nanoliposomes was measured according to Cheng et al. (2019). Initially, samples were centrifuged at 6500 rpm for 1 h at -4

°C using Amicon® Ultra-15 10 kDa centrifugal filtration devices (Millipore Comp., Copenhagen, Denmark). Then, filtrates and supernatants were diluted in anhydrous ethanol (1:5 v/v) and absorbances were read at 425 nm using an UV-Vis spectrophotometer (BioSpec-nano, Shimadzu Scientific Instruments, Columbia, USA). Bioactive content was then calculated from a standard curve of ethanol solutions containing curcumin (1-6 µg/mL, Abs = 0.1792 * [Curcumin] - 0.0129, R² = 0.9998); whereas %EE$_C$ was calculated using Eq. (1):

$$\%\text{EE}_C = \left(\frac{[\text{Curcumin}]_F}{[\text{Curcumin}]_F + [\text{Curcumin}]_S} \right) * 100 \tag{1}$$

where $[Curcumin]_F$ is the concentration of curcumin in the filtrate and $[Curcumin]_S$ represents the unencapsulated amount of curcumin in the supernatant.

6.2.3.4. Encapsulation efficiency of vitamin D$_3$ (%EE$_V$)

The quantification of VD3 into nanoliposomes was performed using the method described in Chaves & Pinho (2020) with some modifications. First, 5 mL of nanoliposome dispersion were mixed with 10 mL of methanol under magnetic stirring at 1500 rpm, at 25 °C for 5 min. The samples were sonicated at 25 °C for 15 min and centrifuged (mod. IEC CL30R Thermo Scientific, Rodano, Milan, Italy) at 6500 rpm, at -4 °C for 20 min, using Amicon® Ultra-15 10 kDa centrifugal filtration devices (Millipore Comp., Copenhagen, Denmark). The filtrate was resuspended in 5 mL of methanol and filtered using nylon syringe filters (0.2 µm HA Millipore, Sigma Aldrich, Milan, Italy). The samples were analyzed by high performance liquid chromatography (mod. 1200 series, Agilent Technologies Inc., Cernusco sul Naviglio, Milan, Italy). The elution was performed using a Zorbax Eclipse Plus C18 column (GL Sciences, Torrance, Canada) maintained at 35 °C. Methanol and acetonitrile 9:1 (v/v) solution was used as the mobile phase and pumped at a constant flow rate of 1.6 mL/min. Aliquots of 10 µL were analyzed at 265 nm for 15 min, and the VD3 peak was obtained based on its retention time (4.7 min). VD3 concentration was calculated from a standard curve obtained by reading the values of area under curve (AUC) of methanol solutions containing VD3 (5-100 µg/mL). The prediction equation was AUC = 27.682 * [VD3] - 10.799, with a correlation coefficient (R²) of 0.9999. The encapsulation efficiency (%EE$_V$) was calculated using Eq. (2):

$$\%\text{EE}_V = \left(\frac{\text{VD3}_F}{\text{VD3}_F + \text{VD3}_S} \right) * 100 \tag{2}$$

where [VD3]$_F$ is the vitamin D$_3$ concentration in the filtrate and [VD3]$_S$ the unencapsulated amount in the supernatant.

6.2.3.5. DPPH scavenging activity assay

DPPH radical scavenging assay was performed using the method described by Liu et al. (2020) with some modifications. First, 15 mL of nanoliposomes were centrifuged using Amicon® Ultra-15 10 kDa centrifugal filtration devices (Millipore Comp., Copenhagen, Denmark) at 6500 rpm for 1 h at -4 °C. The filtrate was then collected and resuspended in 5 mL of ethanol. 1 mL of nanoliposome suspension was gently mixed with 3 mL of fresh DPPH 40 ppm solution and conditioned in the absence of light for 30 min. The values of absorbance were obtained at 517 nm, using a UV-Vis spectrophotometer (BioSpec-nano, Shimadzu Scientific Instruments). The percentage of the DPPH-scavenging activity was calculated using Eq. (3):

$$DPPH_{scav} (\%) = \left(1 - \frac{A_S - A_C}{A_K}\right) * 100 \tag{3}$$

where A$_S$ is the absorbance of 1 mL of nanoliposome and 3 mL of DPPH solution, A$_C$ is the absorbance of 1 mL of nanoliposome and 3 mL of ethanol, and A$_K$ is the absorbance of 1 mL of ethanol and 3 mL of DPPH solution.

6.2.3.6. ABTS scavenging activity assay

ABTS radical scavenging assay was performed using the method described by Wang, Luo, & Peng (2018) with some modifications. First, an ABTS stock solution was prepared by mixing 5 mL of 7 mM ABTS radical solution with 5 mL of 2.45 mM potassium persulfate solution. The stock solution was kept in the absence of light for 16 h at 4 °C. Then, the ABTS solution was diluted to an absorbance of 0.70 ± 0.02 (at 734 nm) before its use. The procedure was followed by the centrifugation of 15 mL of nanoliposomes using Amicon® Ultra-15 10 kDa centrifugal filtration devices (Millipore Comp., Copenhagen, Denmark) at 6500 rpm for 1 h at -4 °C. The filtrate was collected and resuspended in 5 mL of ethanol. Then, 100 µL of nanoliposome resuspension were mixed with 4 mL of the ABTS solution. The mixture was gently stirred and conditioned in the absence of light for 30 min. The absorbance was measured at 734 nm, using an UV-Vis spectrophotometer (BioSpec-nano, Shimadzu). The percentage of ABTS-scavenging activity was calculated using Eq. (4):

$$\text{ABTS}_{\text{scav}} (\%) = \left(1 - \frac{A_S - A_C}{A_K}\right) * 100 \tag{4}$$

where A_S is the absorbance of 100 μL of nanoliposome and 4 mL of ABTS solution, A_C is the absorbance of 100 μL of nanoliposome and 4 mL of distilled water, and A_K is the absorbance of 100 μL of distilled water and 4 mL of ABTS solution.

6.2.3.7. Effect of stress-induced conditions

Solutions containing different concentrations of NaCl or sucrose (100-1000 mmol/L) were mixed with the nanoliposome suspensions in a 1:9 (v/v) ratio and analyzed at 25 °C by DLS (ZetaSizer Nano S, Malvern Instruments, Worcester, UK) to obtain mean diameter, PDI and ζ-potential of vesicles under stress conditions. Also, the pH of 10 mL of each nanoliposome suspension was adjusted to 3, 7 and 12 by the addition of HCl 0.1 M and NaOH 2 M solutions and also submitted to DLS analysis.

6.2.3.8. Controlled release tests for curcumin

The release tests of curcumin from nanoliposomes were performed as described by Li et al. (2017) with minor modifications. First, 15 mL of dispersion, showing >70% entrapment of the bioactive, were centrifuged using Amicon® 10 kDa filtration devices (Millipore Comp., Copenhagen, Denmark) at 6500 rpm for 1 h at -4 °C. The filtrate was collected using a pipette and resuspended in 5 mL of distilled water. Then, 3 mL of the resuspension were transferred to a dialysis membrane (MWCO 13000 Da, Sigma Aldrich, Milan, Italy) previously bathed in an ethylene diamine tetra acetic acid (EDTA) solution at 80 °C for 30 min. The system was incubated in 300 mL of phosphate buffered saline solution (PBS, pH 7.4, 5 mM) and anhydrous ethanol at a 60:40 v/v ratio, and kept at 37 °C under constant stirring at 200 rpm for 13 h. The absorbance was monitored periodically at 425 nm using an UV-Vis spectrophotometer (BioSpec-nano, Shimadzu Scientific Instruments, Columbia, USA). Curcumin content was calculated from a standard curve obtained from absorbance measurements of 60:40 PBS: ethanol solutions containing different concentrations of the bioactive molecule (1-10 μg/mL, Abs = 0.0819 * [Curcumin] - 0.011, R^2 = 0.9996). The kinetic curves were fitted using different mathematical models as presented in Eq. (5) to (7). The adjusted coefficient of determination (R^2_{adj}) and the Akaike Information Criterion (AIC) were used to verify which model best fitted the experimental data. AIC is defined by Eq. (8) and the lower its value, the better is the fit.

First order: $\frac{M_T}{M_\infty} = a * (1 - \exp(-b * t)))$ $\qquad$ (5)

Korsmeyer $-$ Peppas: $\frac{M_T}{M_\infty} = k * t^n$ $\qquad$ (6)

Makoid $-$ Banakar: $\frac{M_T}{M_\infty} = c * t^n * \exp(-k * t)$ $\qquad$ (7)

$AIC = N * \ln\left(\frac{SS}{N}\right) + 2K$ $\qquad$ (8)

where M_T and M_∞ are the cumulative absolute concentrations of curcumin released at time "t" and at infinite time, respectively. M_T/M_∞ is the fraction of bioactive released at each time "t" and "k" is the kinetic constant. In the First-order and Makoid-Banakar models, "a", "b" and "c" are constants. In Korsmeyer-Peppas and Makoid-Banakar models, "n" is the diffusion exponent. For AIC, "N" is the number of data points, "K" is the number of parameters fit by the regression plus one and "SS" is the sum-of-squares of the vertical distances of the points from the curve.

6.2.4. Statistical analysis

All experiments were performed in triplicate and data herein shown was expressed as the mean ± standard deviation. The results were analyzed using one-way ANOVA followed by Tukey's tests at a 5% significance level ($p < 0.05$) and performed using SAS statistical software (v. 9.4, SAS Institute, Cary, NC, USA).

6.3. Results and discussion

Formulations tested in this study were prepared using two types of food-grade phospholipids: saturated soy phosphatidylcholine (SPC) and unsaturated egg-yolk L-α-phosphatidylcholine (EPC). Vesicles were loaded with curcumin alone or co-loaded with curcumin and VD3. The main objective was to obtain loaded and co-loaded nanoliposomes characterized by balanced properties between the stability of lipid bilayers due to the presence of SPC, and the increase of fluidity due to the presence of EPC. Nanoliposomes were produced by SuperLip operating at 100 bar and 40 °C, as described in section 2.2, conditions previously optimized (Trucillo et al., 2020).

6.3.1. Physicochemical properties of nanoliposomes

The results related to physicochemical properties of curcumin-loaded and curcumin-VD3 co-loaded nanoliposomes are summarized in Table 6.2. First, vesicle mean diameters were in line with those previously obtained using SuperLip under the same operating conditions (Trucillo et al., 2020), thus confirming the reproducibility of the results. Vesicle mean diameters related to the formulations CV1, CV2 and CV3 were smaller than those measured for C1, C2 and C3. In particular, vesicle mean diameter ranged from 128 ± 2 nm for CV3 to 149 ± 2 nm for C3. On the other hand, samples C1 and C2 showed the largest mean diameters among the curcumin-loaded nanoliposomes; i.e., 228 ± 6 nm and 219 ± 4 nm, respectively, suggesting the presence of hydrogenated phospholipids could lead to an increase in vesicle size. This trend was consistent with the scientific literature (Tai et al., 2020; Sebaaly et al., 2016; Azzi et al., 2018). The trend was also confirmed by the experiments carried out for co-encapsulation of curcumin and VD3 in nanoliposomes. For example, CV1, produced using 30% w/w of SPC, exhibited a mean diameter larger than CV3, produced using EPC alone (143 ± 8 nm vs. 128 ± 2 nm, respectively). Overall, the small values for size obtained are in accordance to interdigitated nanoliposomes produced with different species of phospholipids, in which their asymmetric arrangements in the lipid bilayers led to a decrease in both size and density, favoring their stability against aggregation and fusion (Adrar et al., 2021). Besides, the narrow nozzle (80 μm) used in SuperLip for water atomization and the high-shear force of CO_2 probably corroborated to the small size of the liposomes.

Table 6.2. Physicochemical parameters of curcumin and curcumin-vitamin D_3-loaded nanoliposomes, produced using SuperLip at 100 bar and 40 °C

Sample	Size (nm)	PDI	ζ potential (mV)	%EE$_C$	%EE$_V$	%DPPH$_{scav}$	%ABTS$_{scav}$
C1	228^A ± 6	0.24^{AB} ± 0.01	-12.3^{AB} ± 3.7	95^A ± 2	-	56^{AB} ± 3	68^{AB} ± 2
C2	219^A ± 4	0.18^C ± 0.01	-15.6^B ± 3.4	93^{AB} ± 1	-	49^{BC} ± 1	51^D ± 3
C3	149^B ± 2	0.15^D ± 0.01	-10.3^{AB} ± 4.0	77^{CD} ± 4	-	42^{CD} ± 4	45^D ± 8
CV1	143^B ± 8	0.25^A ± 0.01	-5.60^A ± 0.2	84^{BC} ± 5	74^A ± 9	63^A ± 5	78^A ± 3
CV2	136^{BC} ± 7	0.24^{AB} ± 0.01	-8.40^{AB} ± 0.1	75^{CD} ± 2	63^A ± 1	55^{AB} ± 1	64^{BC} ± 4
CV3	128^C ± 2	0.22^B ± 0.01	-15.5^B ± 1.0	70^D ± 5	45^B ± 2	32^D ± 8	53^{CD} ± 4

Mean values followed by the same uppercase letter in the same column do not differ significantly ($p > 0.05$) by the Tukey test.

Reference: Chaves et al. (2022)

The increase in size observed for liposomes produced with non-hydrogenated phospholipids was discussed properly in Tai et al. (2020). According to the authors, a larger diameter is related to a higher curvature frustration of vesicle membrane. Briefly, an increase in the degree of chain saturation also leads to an increase in van der Waals interactions, which results in a reduction in membrane fluidity. This reduction leads to the formation of vesicles with larger diameters and lower membrane curvatures due to an increase in rigidity. In turn, this behavior enhances the frustration of the curvature when the membranes combine to each other. On this basis, C3 and CV3 samples may have presented the lowest mean diameters among all due to the higher fluidity and lower curvature frustration of their membranes, as easier they might be bent from the use of non-hydrogenated phospholipids in their composition.

PDI values were all lower than 0.25, indicating a good size homogeneity, agreeing with the monomodal size distribution curves shown in Figure 6.2. The production of vesicles with unsaturated phosphatidylcholine alone promoted a decrease in PDI values; thus, increasing size homogeneity of the vesicles, as it can be verified for C3 and CV3. ζ-potential values were not statistically significant among curcumin-loaded vesicles, meaning that an increase in the amount of saturated phospholipids did not promote measurable changes in the surface charge of the vesicles.

Figure. 6.2. Vesicle size distribution curves obtained by DLS for (a) curcumin-loaded nanoliposomes and (b) curcumin-vitamin D$_3$-loaded nanoliposomes. Samples were produced using non-hydrogenated (EPC) and hydrogenated (SPC) phospholipids at different weight ratios (EPC:SPC): 70:30 (green lines), 80:20 (red lines) and 100:0 (blue lines)
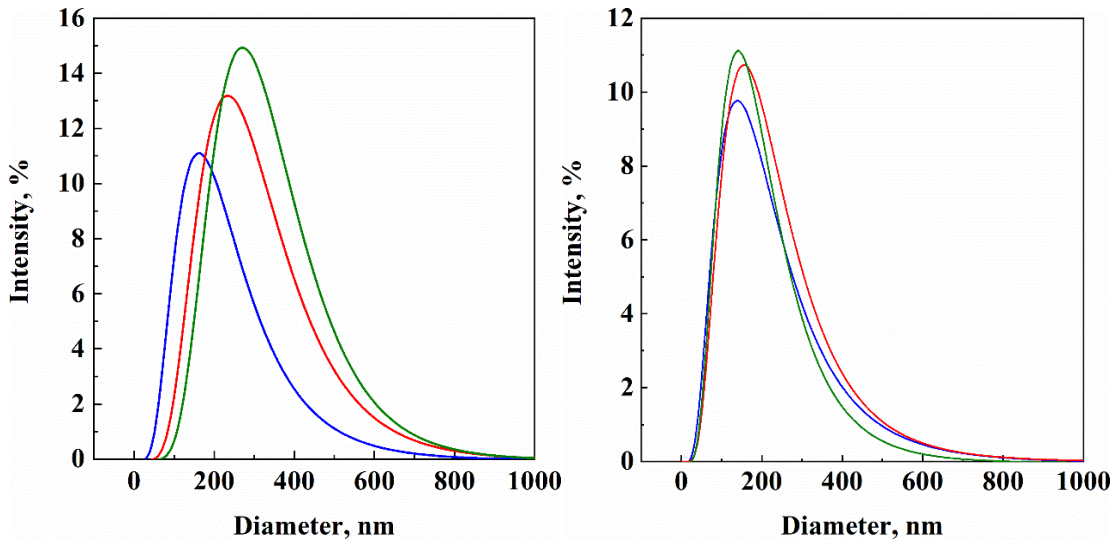
Reference: Chaves et al. (2022)

Interesting results were obtained regarding the encapsulation efficiencies for both curcumin and VD3 into the nanoliposomes (see Table 6.2). First, a decrease in %EE of the bioactives occurred with an increase in SPC amount. This trend can be directly related to the mean size of the vesicles as higher amounts of bioactive can be incorporated into larger lipid bilayers. As previously discussed, the increase in saturated phosphatidylcholine, due to the addition of SPC, promoted an increase in the mean size of vesicles, favoring the encapsulation of bioactives. However, the presence of VD3 into the lipid bilayers led to a decrease in the maximum %EE$_C$ from 95% to 84%. As curcumin and VD3 are highly hydrophobic compounds with large molecular structures, it seemed that VD3 somehow interfered in the encapsulation of curcumin, probably because both "competed" for spaces into the small sized hydrophobic region of nanoliposomes. Also, it is reasonable to believe that a reduction in both %EEC and %EE$_V$ are related to an increase in membrane fluidity due to an increase in EPC ratio. On the other hand, fat soluble vitamins are known to be better protected in smaller particles (Bajaj, Marathe, & Singhal, 2021; Salvia-Trujillo et al. 2013) so the reduction in encapsulation may perhaps be due to the higher amount of curcumin added to the formulations (6% w/w), which was three times higher than VD3 (2% w/w), which probably resulted in more free spaces filled

by the curcuminoid into the hydrophobic region of vesicles. Therefore, a reduction in the curcumin ratio or an increase in the SPC content up to 30% w/w could increase the %EE of the molecules, as larger-sized liposomes would be most likely to be formed.

Figure 6.3 shows SEM images of nanoliposomes obtained in this work. In particular, Fig. 6.3a and Fig. 6.3c refer to vesicles containing SPC; whereas Fig. 6.3b and Fig. 6.3d refer to vesicles not containing SPC. Nanoliposomes containing 30% or 20% w/w of SPC (C1 and CV1; C2 and CV2, respectively) did not exhibit significant morphological differences. Overall, all vesicles presented spherical morphology at nanometric level. However, samples containing SPC (Fig. 6.3a and Fig. 6.3c) were partly coalesced, with a rougher surface than those in which this phospholipid was not present (Figure 3b and Figure 3d). The adhesion of vesicles to form larger structures was probably due to the drying process performed before SEM analysis (Trucillo et al., 2020).

Figure 6.3. SEM images of: (a) C1, (b) C3, (c) CV1 and (d) CV3 nanoliposomes

(a)

(b)

(c)

(d)

Reference: Chaves et al. (2022)
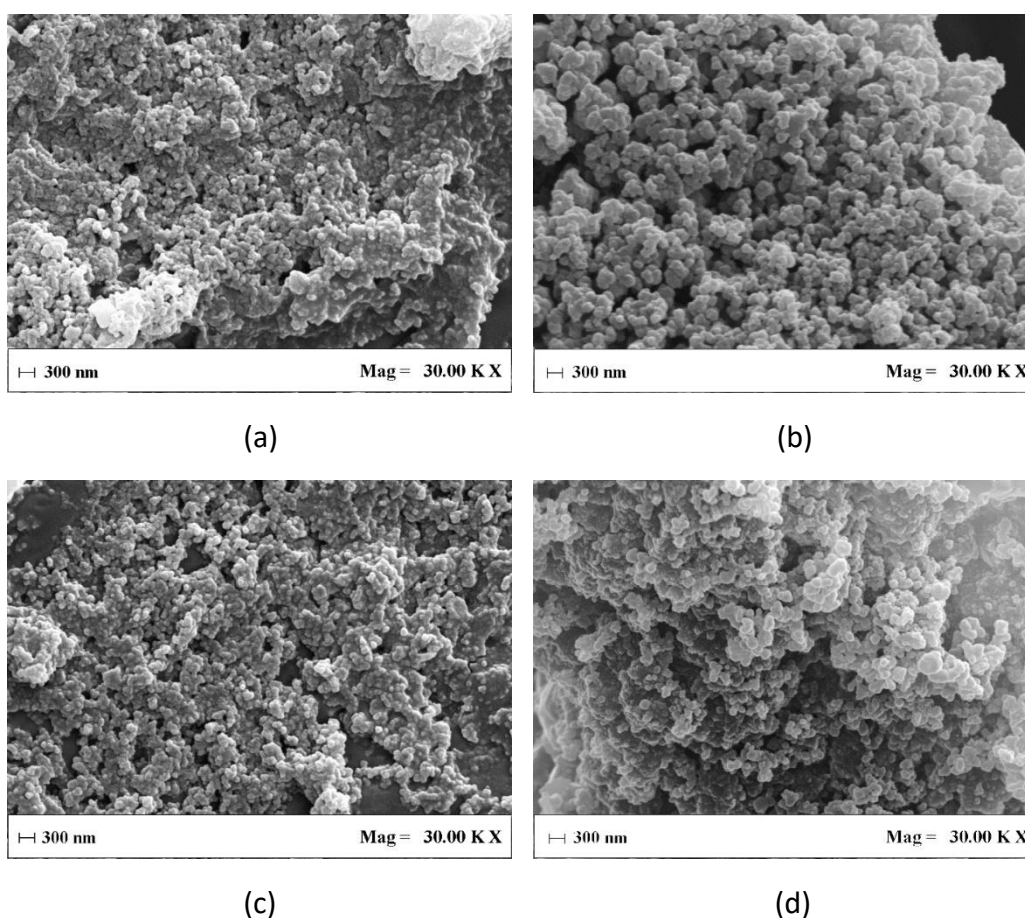
6.3.2. Antioxidant activity

The antioxidant activity of the nanoliposomes herein produced is mostly due to the presence of curcumin. To measure this property, two methods were used: DPPH and ABTS, as described in sections 6.2.3.5 and 6.2.3.6, respectively. In this context, curcumin can easily donate hydrogen atoms from its central heptadienone bond for the reduction of DPPH and ABTS radicals (Luo et al., 2021).

The values obtained for %DPPH and %ABTS radical scavenging activities are reported in Table 2. As expected, the larger values of %EE$_c$ led to higher values of radical scavenging. In this sense, the presence of SPC promoted not only the increase of loaded curcumin in the vesicles, but also the increase in their antioxidant potential. Also, the addition of phospholipids rich in saturated fatty acids (SPC), that are less sensitive to oxygen, promoted an increase in the overall antioxidant activity of the nanoliposomes (Wu et al., 2020). DPPH and ABTS methods showed similar results about the scavenging activity of curcumin-loaded vesicles; but ABTS method resulted in higher values for the co-loaded vesicles. Furthermore, the co-loaded vesicles also showed higher values of antioxidant activity than curcumin-loaded vesicles, regardless the phospholipid ratio, suggesting a sort of synergistic effect between curcuminoid and vitamin. In general, %DPPH values ranged from 32 to 63% and %ABTS from 45 to 78%, indicating the scavenging power of curcumin was well-preserved during SuperLip process, due to its mild process conditions.

6.3.3. Effect of stress-induced conditions

The loaded nanoliposomes were also submitted to different stress conditions to verify their stability range. For this purpose, parameters as mean diameter, PDI and ζ-potential were measured. The samples containing only curcumin showed similar behavior regardless the lipid ratio, as well as the vesicles co-encapsulating the bioactives. For this reason, only C2 and CV2 results are reported in Fig. 6.4.

The vesicles were stable under different concentrations of sodium chloride, as it can be observed in Fig. 6.4A. Mean diameter remained between 120 and 160 nm even at conditions of high ionic strengths. PDI values remained between 0.2 and 0.4. In turn, ζ-potential values for C2 slightly decreased with an increase in salt concentration from 100 to 200 mM (Fig. 6.4A, left). An increase in this parameter, with the addition of salt concentrations higher than 600 mM, was detected for CV2 (Figure 6.4A, right).

Similar results were found for C2 and CV2 after the addition of sucrose. Figure 6.4B shows that a decrease in size was observed after the addition of 500 mM of sucrose, followed by an increase in size at 1000 mM, for both formulations. The decrease at 500 mM may suggest that sucrose promoted an osmotically depletion of water from the lipid hydration shell or influenced in the interfacial tension of bilayers, leading to a reduction in size due to its kosmotrope characteristic (Söderlund et al., 2003). On the other hand, the increase at 1000 mM supports the interaction hypothesis related to the addition of sugar molecules into lipid membranes, which is known to result in lateral expansion of the lipid monolayers as their area is increased due to the intercalation of sugar molecules attached to the head groups of lipid membranes. Overall, the association between disaccharides and the lipid membrane can form a hydrogen bonding network with the phosphate groups, consequently replacing the water molecules located at the membrane surface, favoring the small size of vesicles and improving their stability (Roy et al., 2016). This interaction was also responsible of an increase in PDI and ζ-potential, evidencing the formation of a new population of larger vesicles in the dispersions.

A pH shift promoted an increase in size and PDI of the vesicles, as shown in Figure 6.4C. This result reflects the formation of larger vesicles in alkaline media (pH 12). Moreover, curcumin is unstable in alkaline media and undergoes to hydrolytic degradation under this condition. Therefore, the increase in size and the sharp decrease in ζ-potential may reflect the formation of negatively charged oxidation residues, such as aldehydes and carboxylic acids that can promote the formation of aggregates (Appiah-Opong et al., 2007).

Figure 6.4. Results obtained for the nanoliposomes submitted to different stress conditions: (A) addition of NaCl (100-1000 mM), (B) addition of sucrose (100-1000 mM) and (C) pH changing (3-12). On the left column, results related to the C2 formulation (80:20 EPC:SPC + curcumin). On the right column, results related to the CV2 formulation (80:20 EPC:SPC + curcumin + vitamin D₃).
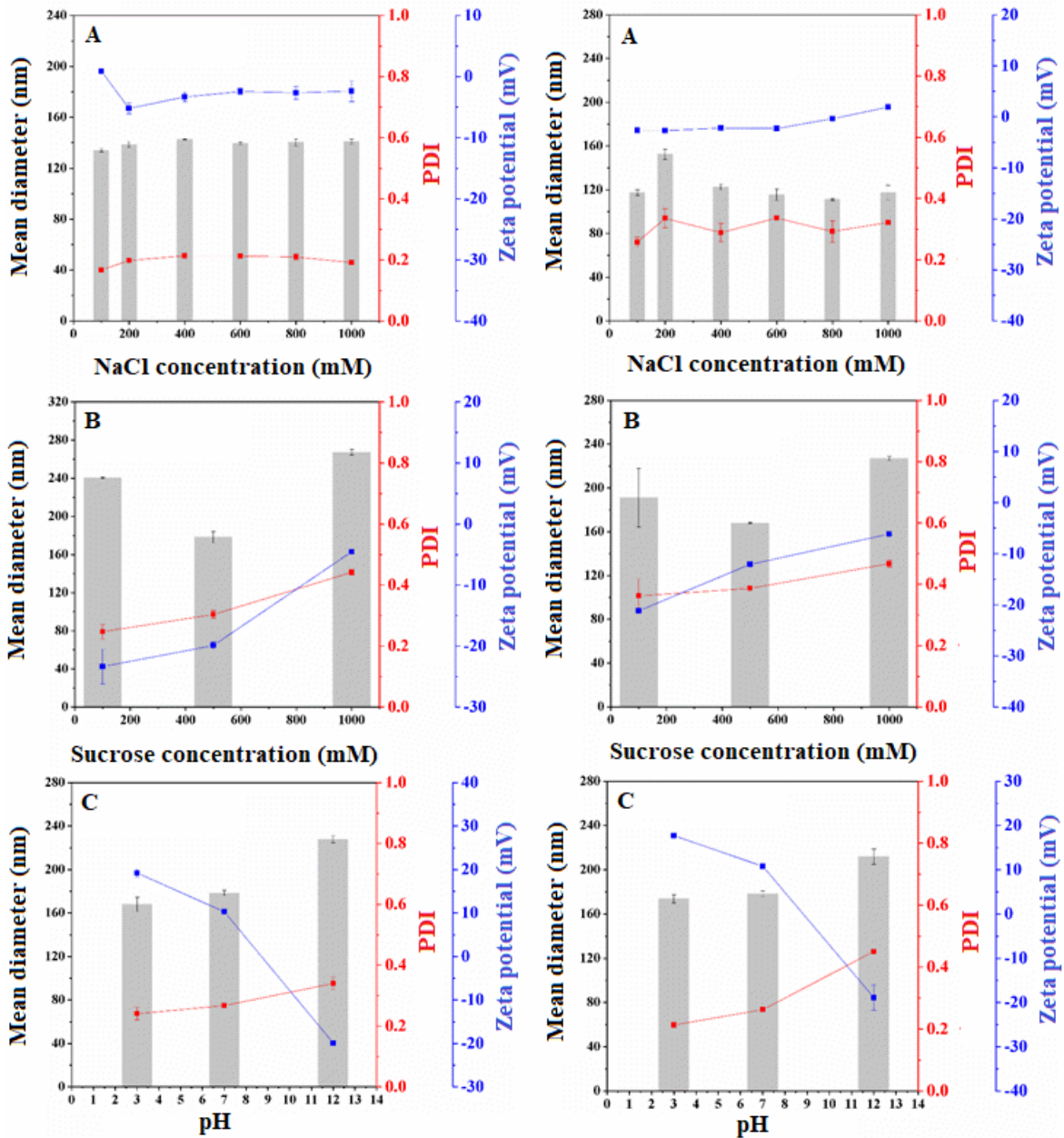
Reference: Chaves et al. (2022)

6.3.4. Release tests for curcumin

The release profiles of curcumin from nanoliposomes are presented in Fig. 6.5. Experimental data was fitted using three mathematical models, whose parameters are summarized in Table 6.3. The curves in Fig. 6.5A represent the fitting performed using the First-order model. This model best described the experimental data of curcumin release from samples C1, C2 and C3 as corroborated by the higher values for R^2_{adj} and lower values for AIC. In general, all curves were quite similar and curcumin release time from nanoliposomes was in all cases longer than the one obtained from the untreated powder, which release fitted well by both First-order and Makoid-Banakar models, with a small evident ratio of 0.03 between both (data not shown). The similarity among the kinetic release curves was a consequence of an equal similar mass transfer resistance opposed by the nanoliposomes bilayer structure to curcumin diffusion in the liquid medium, meaning that a change in phospholipid composition did not affect the type of release mechanism. Also, almost 90% of curcumin was released from all formulations after ≈ 300 min. Larger diameters observed for C1 and C2 clearly promoted a slightly longer pathway required for curcumin diffusion in the liquid medium as the bioactive from C1 was completely released after ≈ 450 min, a little sooner than others. Also, it is known that the stronger are the hydrophobic interactions between curcumin and the lipid bilayers, the slower is its diffusion (Li et al., 2018).

The experimental data related to curcumin release from the samples CV1, CV2 and CV3 were best fitted by Makoid-Banakar model as equally corroborated by the higher values for R^2_{adj} and lower values for AIC. This empirical model represents a first order process-closure of a zero-order process and its success is due to its complexity (Costa & Sousa Lobo, 2001). Interestingly, since "k" values obtained for all samples were close to zero, the Makoid-Banakar expression becomes practically identical to the Korsmeyer-Peppas model, thus enabling comparisons with the release exponent "n". In this context, the value of n = 0.41, observed for CV3, indicates a Quasi-Fickian diffusion-controlled mechanism (n <0.5); whereas the values of n = 0.77 and n = 0.64, observed for CV1 and CV2, respectively, indicate an anomalous diffusion (non-Fickian) transport (Lupina, Kowalczyk, & Drozlowska. All in all, 2020), the results showed that sustained release of curcumin was somehow influenced by the presence of vitamin D_3, which was no longer concentration-dependent after the incorporation of a second highly hydrophobic bioactive. Also, a prolonged diffusion was achieved regardless the phospholipid composition.

194

Figure 6.5. Curcumin release profiles obtained at 37 °C from (a) curcumin-loaded nanoliposomes and (b) curcumin/vitamin D_3-co-loaded nanoliposomes. Samples were produced using non-hydrogenated (EPC) and hydrogenated (SPC) phospholipids at different weight ratios (EPC:SPC): 70:30 (green), 80:20 (red) and 100:0 (blue). Release of pure curcumin in 60:40 PBS: ethanol is represented by diamonds (magenta). Symbols represent experimental data; whereas lines represent best fitting: First-order kinetic model for (a) and Makoid-Banakar model for (b). For further understanding, see R^2_{adj} and AIC values in Table 6.3

(A)
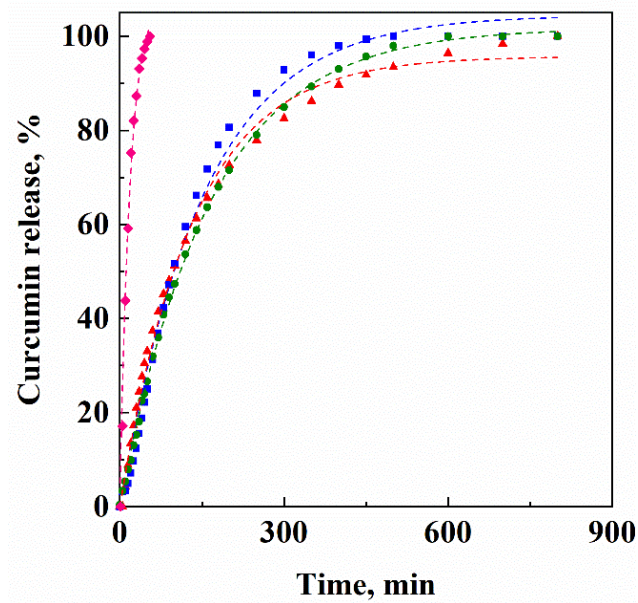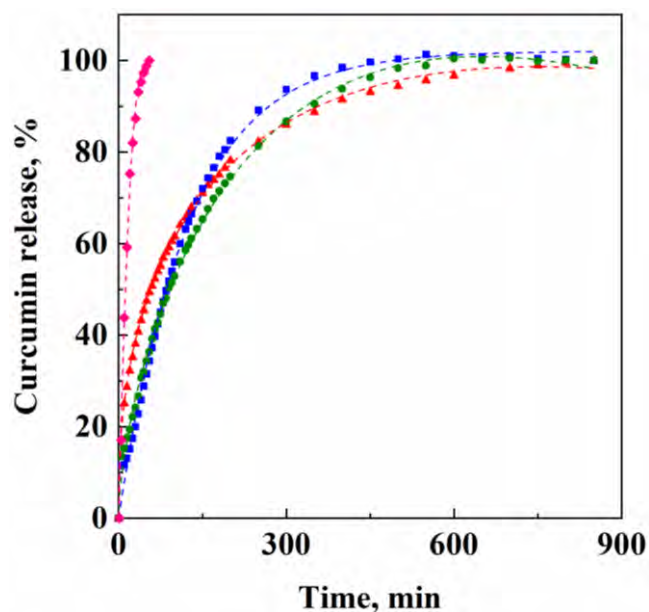
(B)   Reference: Chaves et al. (2022)

Table 6.3. Parameters obtained by fitting experimental data of curcumin release from the nanoliposomes, using different kinetic mathematical models

Formulation	Model	Equation	R^2_{adj}	AIC
Pure curcumin	First-order	$M/M\infty = 107.8 * (1-exp(-0.053*t))$	0.989	35.27
	Korsmeyer-Peppas	$M/M\infty = 13.6 * t^{0.52}$	0.936	56.56
	Makoid-Banakar	$M/M\infty = 3.71 * t^{1.15} * exp(-0.024*t)$	0.995	28.31
C1	First-order	$M/M\infty = 104.5 * (1-exp(-0.007*t))$	0.990	83.22
	Korsmeyer-Peppas	$M/M\infty = 5.312 * t^{0.47}$	0.898	153.68
	Makoid-Banakar	$M/M\infty = 0.68 * t^{0.96} * exp(-0.002*t)$	0.990	85.99
C2	First-order	$M/M\infty = 101.7 * (1-exp(-0.006*t))$	0.999	-0.94
	Korsmeyer-Peppas	$M/M\infty = 4.937 * t^{0.48}$	0.942	132.06
	Makoid-Banakar	$M/M\infty = 1.08 * t^{0.84} * exp(-0.001*t)$	0.997	46.17
C3	First-order	$M/M\infty = 95.7 * (1-exp(-0.008*t))$	0.995	53.93
	Korsmeyer-Peppas	$M/M\infty = 6.444 * t^{0.43}$	0.947	125.96
	Makoid-Banakar	$M/M\infty = 2.09 * t^{0.71} * exp(-0.001*t)$	0.992	70.89
CV1	First-order	$M/M\infty = 102.0 * (1-exp(-0.008*t))$	0.993	97.01
	Korsmeyer-Peppas	$M/M\infty = 9.424 * t^{0.38}$	0.903	210.96
	Makoid-Banakar	$M/M\infty = 1.79 * t^{0.77} * exp(-0.002*t)$	0.997	51.84
CV2	First-order	$M/M\infty = 98.9 * (1-exp(-0.008*t))$	0.989	107.07
	Korsmeyer-Peppas	$M/M\infty = 9.301 * t^{0.37}$	0.953	171.22
	Makoid-Banakar	$M/M\infty = 3.09 * t^{0.64} * exp(-0.001*t)$	0.998	20.35
CV3	First-order	$M/M\infty = 91.8 * (1-exp(-0.012*t))$	0.929	163.48
	Korsmeyer-Peppas	$M/M\infty = 16.794 * t^{0.28}$	0.971	124.72
	Makoid-Banakar	$M/M\infty = 9.71 * t^{0.41} * exp(-0.001*t)$	0.999	-30.08

Reference: Chaves et al. (2022)

6.4. Conclusions

The results presented in this study confirm that it is feasible to produce nanoliposomes loading curcumin and co-loading curcumin and vitamin D_3 by a supercritical CO_2 assisted process. The nanovesicles showed monomodal size distribution and high entrapment efficiencies for both bioactives. The operating parameters used in SuperLip (40 ºC and 100 bar) did not induce an early degradation of curcumin that also retained much of its antioxidant activity. Regarding the lipid composition of the nanoliposomes, it was found that replacing 20-30% w/w of the phospholipids for saturated species promoted an increase in the nanoliposome

size and, consequently, in the total encapsulated amount of bioactives. In turn, the addition of vitamin D_3 to the nanoliposomes determined a slight reduction in the encapsulated amount of curcumin, probably due to competition for free spaces within the lipid bilayer. In perspective, different drug-to-lipid ratios of curcumin and vitamin D_3 can be tested, in order to further increase the encapsulated molecule content, as well as different phospholipid blends can be investigated, to produce structures with the most different synergistic effects for the most different applications.

6.5. Acknowledgments

6.6. References

Aburai, K. et al. (2011). Preparation of liposomes modified with lipopeptides using a supercritical carbon dioxide reverse-phase evaporation method. **Journal of Oleo Science**, 60, 209-215.

Adrar, N. et al. (2021). Stability evaluation of interdigitated liposomes prepared with a combination of 1,2-distearoyl-sn-glycero-3-phosphocholine and 1,2-dilauroyl-sn-glycero-3-phosphocholine. **Journal of Chemical Technology & Biotechnology**, 96, 2537-2546.

Appiah-Opong, R. et al. (2007). Inhibition of human recombinant cytochrome P450s by curcumin and curcumin decomposition products. **Toxicology**, 235, 83-91.

Azzi, J. et al. (2018). Novel findings for quercetin encapsulation and preservation with cyclodextrins, liposomes, and drug-in-cyclodextrin-in-liposomes. **Food Hydrocolloids**, 81, 328-340.

Bajaj, S. R., Marathe, S. J., & Singhal, R. S. (2021). Co-encapsulation of vitamins B12 and D3 using spray drying: Wall material optimization, product characterization, and release kinetics. **Food Chemistry**, 335, 127642.

Baldino, L., Cardea, S., & Reverchon, E. (2019). Supercritical assisted electrospray: An improved micronization process. **Polymers**, 11, 244-255.

Baldino. L., Scognamiglio, M., & Reverchon, E. (2020). Supercritical fluid technologies applied to the extraction of compounds of industrial interest from *Cannabis sativa L.* and to their pharmaceutical formulations: A review. **The Journal of Supercritical Fluids**, 2020, 165, 104960.

Baldino, L. et al. (2020). Production of biodegradable superabsorbent aerogels using a supercritical CO_2 assisted drying. **The Journal of Supercritical Fluids,** 2020. 156, 104681.

Basnet, P., & Skalko-Basnet, N. (2011). Curcumin: an anti-inflammatory molecule from a curry spice on the path to cancer treatment. **Molecules**, 16, 4567-4598.

Battista, S. et al. (2021). Homogeneous and stable (+)-usnic acid loaded liposomes prepared by compressed CO_2. **Colloids and Surfaces A: Physicochemical and Engineering Aspects**, 624, 126749.

Bischoff-Ferrari, H. A. et al. (2009). Fall prevention with supplemental and active forms of vitamin D: a meta-analysis of randomised controlled trials. **BMJ**, 339, b3692.

Chaves, M. A, & Pinho, S. C. (2019). Curcumin-loaded proliposomes produced by the coating of micronized sucrose: Influence of the type of phospholipid on the physicochemical characteristics of powders and on the liposomes obtained by hydration. **Food Chemistry**, 291, 7-15.

Chaves, M. A., & Pinho, S. C. (2020). Unpurified soybean lecithins impact on the chemistry of proliposomes and liposome dispersions encapsulating vitamin D_3. **Food Bioscience**, 37, 100700.

Cheng, C. et al. (2019). Improvement on stability, loading capacity and sustained release of rhamnolipids modified curcumin liposomes. **Colloids and Surfaces B: Biointerfaces**, 183, 110460.

Costa, P., & Sousa Lobo, J. M. (2001). Modeling and comparison of dissolution profiles. **European Journal of Pharmaceutical Sciences**, 13, 123-133.

Elizondo, E. et al. (2012). Influence of the preparation route on the supramolecular organization of lipids in a vesicular system. **Journal of the American Chemical Society**, 134, 1918-2921.

Espírito-Santo, I. et al. (2014). Liposomes preparation using a supercritical fluid assisted continuous process. **Chemical Engineering Journal**, 249, 153-159.

Estephan, M., El Kurdi, R. &, Patra, D. (2021). Interaction of curcumin with diarachidonyl phosphatidyl choline (DAPC) liposomes: Chitosan protects DAPC liposomes without changing phase transition temperature but impacting membrane permeability. **Colloids and Surfaces B: Biointerfaces**, 199, 111546.

Gönen, M., & Gupta, R. B. (2021). Developments in the encapsulation of bioactives using supercritical CO_2. **Innovative Food Science and Emerging Technologies**, 678-685.

Gulzar, S., & Benjakul, S. (2020). Characteristics and storage stability of nanoliposomes loaded with shrimp oil as affected by ultrasonication and microfluidization. **Food Chemistry**, 310, 125916.

Hamadou, A. H. et al. (2020). Comparison of β-carotene loaded marine and egg phospholipids nanoliposomes. **Journal of Food Engineering**, 283, 110055.

Holick, M. F. (2017). The vitamin D deficiency pandemic: Approaches for diagnosis, treatment and prevention. **Reviews in Endocrine and Metabolic Disorders**, 18, 153-165.

Hosseini, S. F., Ramezanzade, L., & McClements, D. J. (2021). Recent advances in nanoencapsulation of hydrophobic marine bioactives: Bioavailability, safety, and sensory attributes of nano-fortified functional foods. **Trends in Food Science & Technology**, 109, 322-339.

Khorasani, S., Danaei, M., & Mozafari, M. R. (2018). Nanoliposome technology for the food and nutraceutical industries. **Trends in Food Science & Technology**, 79, 106-115.

Kim, H., Kim, Y., & Lee, J. (2013). Liposomal formulations for enhanced lymphatic drug delivery. **Asian Journal of Pharmaceutical Sciences**, 8, 96-103.

Lesoin, L. et al. (2011). Preparation of liposomes using the supercritical anti-solvent (SAS) process and comparison with a conventional method. **The Journal of Supercritical Fluids**, 57, 162-174.

Li, J. et al. Ascorbyl palmitate effects on the stability of curcumin-loaded soybean phosphatidylcholine liposomes. **Food Bioscience,** 41, 100923.

Li, R. et al. (2017). Liposomes coated with thiolated chitosan as drug carriers of curcumin. **Materials Science and Engineering: C**, 80, 156-164.
.
Li, Z-I. et al. (2018). Pluronics modified liposomes for curcumin encapsulation: Sustained release, stability and bioaccessibility. **Food Research International**, 108, 246-253.

Liu, X. et al. (2020). Co-encapsulation of vitamin C and β-carotene in liposomes: Storage stability, antioxidant activity, and in vitro gastrointestinal digestion. **Food Research International**, 136, 109587.

Luo, L. et al. (2021). Elaboration and characterization of curcumin-loaded soy soluble polysaccharide (SSPS)-based nanocarriers mediated by antimicrobial peptide nisin. **Food Chemistry**, 336, 127669.

Lupina, K., Kowalczyk, D., & Drozlowska, E. (2020). Polysaccharide/gelatin blend films as carriers of ascorbyl palmitate – A comparative study. **Food Chemistry**, 333, 127465.

Mohammadi, M., Ghanbarzadeh B., & Hamishehkar, H. (2014). Formulation of nanoliposomal vitamin D$_3$ for potential application in beverage fortification. **Advanced Pharmaceutical Bulletin**, 4, 569-575.

Mozafari, M. R. (2010). Nanoliposomes: preparation and analysis. **Methods in Molecular Biology,** 605,29-50.

Pu, C. et al. (2020). Stability enhancement efficiency of surface decoration on curcumin-loaded liposomes: Comparison of guar gum and its cationic counterpart. **Food Hydrocolloids**, 87, 29-37.

Roy, A. et al. (2016). A comparative study of the influence of sugars sucrose, trehalose, and maltose on the hydration and diffusion of DMPC lipid bilayer at complete hydration: Investigation of structural and spectroscopic aspect of lipid-sugar interaction. **Langmui**r, 32, 5124-5134.

Salvia-Trujillo, L. et al. (2013). Influence of particle size on lipid digestion and β-carotene bioaccessibility in emulsions and nanoemulsions. **Food Chemistry**, 141, 1472-1480.

Sarabandi, K. et al. (2019). Production of reconstitutable nanoliposomes loaded with flaxseed protein hydrolysates: Stability and characterization. **Food Hydrocolloids**, 96, 442-50.

Sebaaly, C et al. (2016). Effect of composition, hydrogenation of phospholipids and lyophilization on the characteristics of eugenol-loaded liposomes prepared by ethanol injection method. **Food Bioscience**, 15, 1-10.

Shishir, M. R. I. et al. (2021). Improving the physicochemical stability and functionality of nanoliposome using green polymer for the delivery of pelargonidin-3-O-glucoside. **Food Chemistry**, 337, 127654.

Söderlund, T. et al. (2003). Comparison of the effects of surface tension and osmotic pressure on the interfacial hydration of a fluid phospholipid bilayer. **Biophysical Journal**, 85:2333-2341.

Tai, K. et al. Effect of β-sitosterol on the curcumin-loaded liposomes: Vesicle characteristics, physicochemical stability, in vitro release and bioavailability. **Food Chemistry**, 293, 92-102.

Tai, K. et al. (2020). Stability and release performance of curcumin-loaded liposomes with varying content of hydrogenated phospholipids. **Food Chemistry**, 326, 126973.

Trucillo, P et al. (2018). Supercritical assisted process for the encapsulation of olive pomace extract into liposomes. **The Journal of Supercritical Fluids**, 135, 152-159.

Trucillo, P. et al. (2019). Control of liposomes diameter at micrometric and nanometric level using a supercritical assisted technique. **Journal of CO$_2$ Utilization**, 32, 119-127.

Trucillo, P. et al. (2020). Production of liposomes loaded alginate aerogels using two supercritical CO$_2$ assisted techniques. **Journal of CO$_2$ Utilization**, 39, 101161.

Villanueva-Bermejo, D., & Temelli, F. (2020). Optimization of coenzyme Q10 encapsulation in liposomes using supercritical carbon dioxide. **Journal of CO₂ Utilization**, 38, 68-76.

Wang, C. et al. (2021). Enhancing stability and anti-inflammatory properties of curcumin in ulcerative colitis therapy using liposomes mediated colon-specific drug delivery system. **Food and Chemical Toxicology**, 151, 112123.

Wang, P. P., Luo, Z. G., & Peng, X. C. (2018). Encapsulation of vitamin E and soy isoflavone using spiral dextrin: Comparative structural characterization, release kinetics, and antioxidant capacity during simulated gastrointestinal tract. **Journal of Agricultural and Food Chemistry**, 66. 10598-10607.

Wu, Y. et al. (2020). Curcumin-loaded liposomes prepared from bovine milk and krill phospholipids: Effects of chemical composition on storage stability, in-vitro digestibility and anti-hyperglycemic properties. **Food Research International**, 136, 109301.

Chapter 7. SUPERCRITICAL CO₂ ASSISTED PROCESS FOR THE PRODUCTION OF MIXED PHOSPHOLIPID NANOLIPOSOMES: UNLOADED AND VITAMIN D₃-LOADED VESICLES

Chapter 7. Supercritical CO_2 assisted process for the production of mixed phospholipid nanoliposomes: Unloaded and vitamin D_3-loaded vesicles

Abstract

In this study, SuperLip, an innovative technology assisted by supercritical carbon dioxide (SC-CO_2), was used to produce unloaded and vitamin D_3 (VD3)-loaded nanoliposomes. Vesicles were produced using hydrogenated and nonhydrogenated phosphatidylcholine from food-grade lecithins at ratios of 30:70, 20:80 and 0:100. SuperLip was operated at 100 bar and 40 °C using water flow rates ranging from 2.5 to 10 mL/min. The results showed that unloaded liposomes produced by SuperLip presented a unimodal size distribution at a water flow rate of 10 mL/min, regardless of the phospholipid ratio, and mean diameters ranging from 125 to 141 nm. VD3-loaded liposomes also presented a unimodal size distribution at this water flow rate but slightly higher diameters that ranged from 144 to 252 nm. Furthermore, the addition of 20% purified phospholipids to liposomes led to an increase in the mean size of VD3-loaded vesicles from 144 to 218 nm and an increase in the encapsulation efficiency from 66.7 to 88.9%.

Keywords: cholecalciferol; supercritical CO_2; lipid carriers; nanoencapsulation; hydrogenated phospholipids.

7.1. Introduction

Supercritical fluid technologies are receiving attention for the production of liposomes due to their advantages over conventional methods. They are green/er technologies due to the significant decrease or complete elimination of the use of organic solvents and do not require multiple steps or postprocessing downstream methods, such as sonication or extrusion, to produce nanosized vesicles (Penoy et al., 2021). Moreover, the considerable increases in reproducibility and encapsulation efficiency related to supercritical methods are advantages regarding processing time and costs (Bigazzi et al., 2020; Penoy et al., 2021), in addition to the ease of scaling up from the laboratory to industrial scale (Maqbool et al., 2019). Finally, better control of the physicochemical properties of liposomes can also be achieved using supercritical fluids (Penoy et al., 2021).

Supercritical carbon dioxide (SC-CO$_2$), an inexpensive, inert, nontoxic, nonflammable and environmentally friendly alternative to organic solvents, has been used in various fields (Baldino, Cardea, & Reverchon, 2019a; Baldino et al., 2019a; Sarno et al., 2017), including liposome production, due to its unique properties, such as high diffusivity, zero surface tension, low viscosity and high density (Zhao et al., 2017; Sharifi et al., 2019; Trucillo et al., 2020). In addition, SC-CO$_2$ exhibits mild critical parameters (Tc = 31.1 °C and Pc = 7.39 MPa), which are less likely to cause the degradation of thermosensitive molecules and can be easily achieved and controlled during industrial processes (Baldino et al., 2019b; Tanaka et al., 2020).

Briefly, liposomes are spherical vesicles composed of an aqueous compartment enclosed by one or more lipid bilayers formed by self-aggregated phospholipids. These carriers are recognized as efficient target delivery vesicles for both water-soluble and/or lipid-soluble molecules and have been extensively studied in the food area due to their nontoxicity, biodegradability and versatility (Lopes et al., 2021). Currently, several phospholipids, such as phosphatidylcholine (PC), phosphatidylethanolamine (PE) and phosphatidylinositol (PI), have been used to produce liposomes, all of which can be obtained from natural sources, such as soybean and egg yolk (Chaves & Pinho, 2020). In particular, the composition of the bilayer can regulate the intermolecular interactions and the stability of the vesicles. These interactions include hydrophilic interactions (polar head groups and water molecules), hydrogen bonding (water molecules and head groups/phosphates/carbonyl) and van der Waals interactions (hydrocarbon chains), all of which lead to the formation of closed bilayers after the supply of energy in an aqueous environment (Muñoz-Shugulí et al., 2021). Moreover, the method applied

for liposome production also influences these interactions during bilayer formation. In this sense, liposomes can be classified according to the number of bilayers as unilamellar vesicles (ULVs), oligolamellar vesicles (OLVs), and multilamellar vesicles (MLVs). MLVs are obtained when bilayer-forming lipids are dispersed in aqueous media under mild agitation, whereas ULVs and OLVs require a more substantial energy input, mostly to disrupt MLVs into these smaller structures (Emami et al., 2016). Liposomes produced using supercritical technologies are generally ULVs or MLVs with sizes up to 250 nm (Bigazzi et al., 2020).

The major drawback concerning the use of unsaturated phospholipids during liposome production is the early instability of the vesicles due to lipid oxidation. The presence of double bonds in the fatty acid chains of unsaturated phospholipids can disturb the molecular packing of the bilayer and can increase the membrane fluidity due to interspaces in the hydrophobic region (Li et al., 2015). The production of mixed liposomes containing unsaturated and saturated phospholipids appears to be a suitable alternative to reduce this drawback, as saturated/hydrogenated phospholipids present higher melting points and contribute to decreased membrane fluidity (Tai et al., 2020). However, a total replacement of nonhydrogenated phospholipids by hydrogenated phospholipids would result in an increase in the final cost of the process, as hydrogenated/purified phospholipids are more expensive due to the hydrogenation treatment (Chaves & Pinho, 2019).

SuperLip (Supercritical Assisted Liposome Formation) technology was proposed by the research group of Prof. Reverchon at the University of Salerno and consists of a one-step process to produce liposomes using supercritical carbon dioxide (Espírito-Santo et al., 2014; Trucillo et al., 2020). The idea behind the SuperLip process is to first produce atomized water drops and then to cover them with phospholipids, forming the lipid bilayer. In this context, due to the high diffusion coefficient of CO_2, the coating of water droplets by phospholipids is faster compared to conventional techniques and allows for better control of the size distribution (Trucillo, Campardelli, & Reverchon, 2019a). Furthermore, nanoliposomes produced using SuperLip reached encapsulation efficiency values up to 99% for several compounds, including dyes, antibiotics, proteins, antioxidants, dietary supplements and essential oils, proving to be a very versatile technology (Trucillo, Campardelli, & Reverchon, 2019b).

Vitamin D_3 (VD3, cholecalciferol) is a liposoluble prohormone and micronutrient that plays important roles in calcium homeostasis and bone health, as well as acting in the prevention of several diseases, such as cancer, osteoporosis, obesity, diabetes and

hypoparathyroidism (Dima & Dima, 2020). Currently, VD3 deficiency is recognized as a pandemic (Holick, 2017). The most common reasons for such deficiency include reduced sunlight exposure and low dietary intake of this vitamin, as only a few foods contain it naturally. Therefore, the production of efficient delivery systems for VD3 must be considered for further food fortification.

Therefore, the objective of the present work was to study for the first time the suitability of SuperLip technology to produce unloaded and vitamin D_3-loaded nanoliposomes using mixtures of unsaturated and saturated phospholipids. The effects of the phospholipid ratio and water flow rate used in SuperLip were both investigated. Liposomes were characterized using dynamic light scattering to calculate their mean diameter, polydispersity index, size distribution and ζ-potential, whereas their morphology was investigated using field emission scanning electronic microscopy (FE-SEM). Furthermore, VD3-loaded vesicles were also analyzed in relation to their encapsulation efficiency and size/ζ-potential under different stress conditions (salt, sugar and pH).

7.2. Materials, apparatus and methods

7.2.1. Chemicals and reagents

Carbon dioxide (CO_2, >99.4% purity) was purchased from Morlando Group (Naples, Italy). Saturated soy phosphatidylcholine (phospholipid P90H, SPC, >90% w/w PC) was kindly donated by Lipoid GmbH; unsaturated egg-yolk L-α-phosphatidylcholine (EPC, maximum of >60% w/w PC and >11% w/w PE) and cholecalciferol (VD3, vitamin D_3, >98% purity) were purchased from Sigma-Aldrich (Milan, Italy). Ethanol (>99.8% purity), sodium chloride (for analysis) and sucrose (for biochemistry) were purchased from Merck (Milan, Italy). Distilled water, used throughout the experiments, was produced in the laboratory using a homemade lab-scale distiller.

7.2.2. SuperLip: Plant and process description

A pictorial representation of the SuperLip plant is proposed in Fig. 7.1. The apparatus is formed by three feeding lines: (1) delivers CO_2 from a reservoir to the mixing chamber (M); (2) delivers water directly to the forming vessel (FV), and (3) delivers the ethanolic solution containing the phospholipids and the lipophilic molecule (in this case, vitamin D_3) to the mixing chamber. The ethanolic solutions (100 mL) were prepared under magnetic agitation at 1000

rpm for 1 h and then filtered under vacuum prior to processing. A summary of the formulations used in this study is reported in Table 7.1. Specifically, blank/empty samples were called B (from B1 to B9), whereas VD3-loaded samples were called V (from V1 to V3).

Figure 7.1. The layout of SuperLip plant
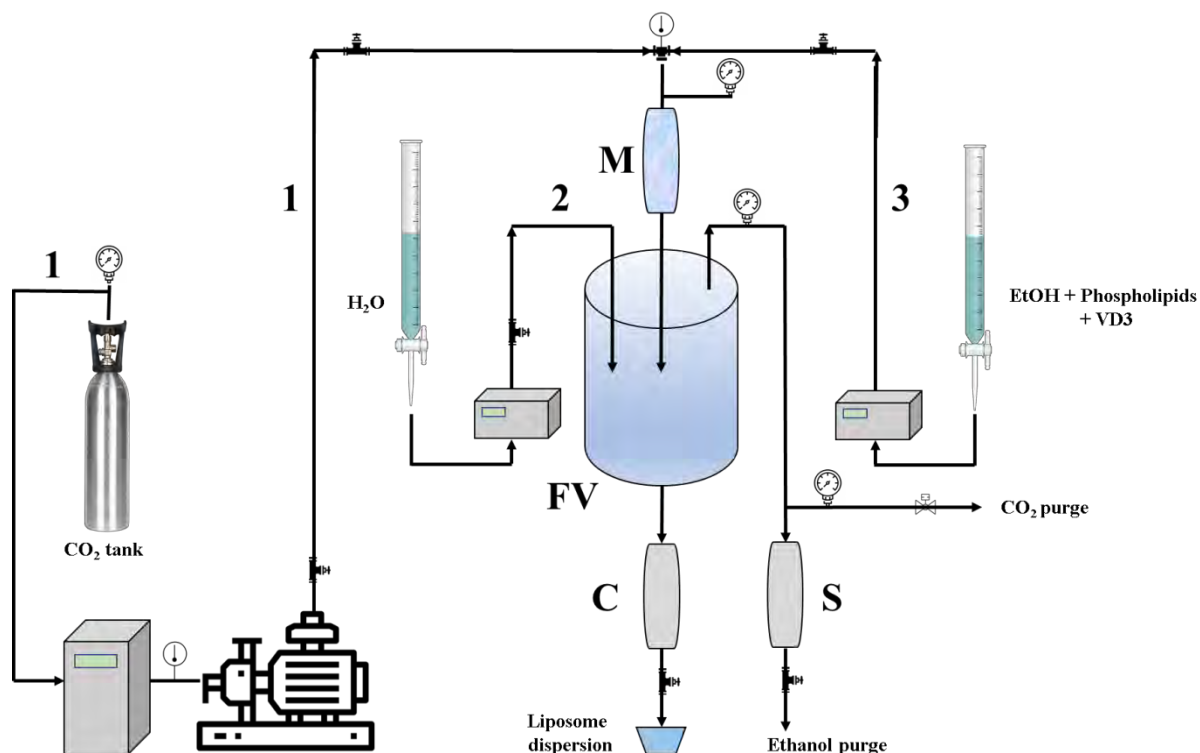
Reference: Chaves et al. (2022)

Table 7.1. (Continued) Formulations used for the production of unloaded and vitamin D_3-loaded nanoliposomes, using SuperLip at 100 bar and 40 °C

Formulation	Phospholipid ratio (%)		Water flow rate (mL/min)	Vitamin D_3 (mg)
	Phospholipon 90H (SPC)	L-α-phosphatidylcholine (EPC)		
B1	30	70	2.5	-
B2	30	70	5	-
B3	30	70	10	-
B4	20	80	2.5	-
B5	20	80	5	-
B6	20	80	10	-

Table 7.1. Formulations used for the production of unloaded and vitamin D_3-loaded nanoliposomes, using SuperLip at 100 bar and 40 °C

Formulation	Phospholipid ratio (%)		Water flow rate (mL/min)	Vitamin D_3 (mg)
	Pholpholipon 90H (SPC)	L-α-phosphatidylcholine (EPC)		
B7	0	100	2.5	-
B8	0	100	5	-
B9	0	100	10	-
V1	0	100	10	10
V2	20	80	10	10
V3	30	70	10	10

Reference: Chaves et al. (2022)

Initially, CO_2 was cooled using a refrigerated bath at -10 °C and pumped at 4.03 L/min using an Ecoflow pump (model LDC-M-2, Lewa, Leonberg, Germany) to a stainless-steel high-pressure mixing chamber, kept at 100 bar and heated at 40 °C (Trucillo et al., 2020). In parallel, the ethanolic solution was pumped using a Gilson pump (model 305, Villiers-le-Bel, France) to the same mixing chamber. Operating at these flow conditions, the GLR (gas-to-liquid ratio) obtained in the mixer is 2.4 on a mass basis. For better comprehension, the gas-to-liquid ratio is the ratio between the CO_2 and ethanol solution flow rates under the same conditions of temperature and pressure. This is the main parameter that governs the composition of the resulting expanded liquid formed in the mixing chamber (Baldino, Cardea, & Reverchon, 2019b). Subsequently, the expanded liquid was delivered through a capillary tube inside the liposome formation vessel, also operating at 100 bar and 40 °C, operative conditions that were optimized in previous papers (Trucillo, Campardelli, & Reverchon, 2019a; Trucillo, Campardelli, & Reverchon, 2019b; Trucillo et al., 2020). Concomitantly, water was pumped (2.5, 5 and 10 mL/min) using another Gilson pump (model 305, Villiers-le-Bel, France) and atomized right before the interior of the main chamber through an 80 µm nozzle.

The process of liposome formation using SuperLip consists of favorable interactions between the atomized water and the phospholipids in the expanded liquid. A scheme is illustrated in Fig. 7.2. First, the droplets of water are surrounded by phospholipids, resulting in

inverted micelle-like structures that will characterize the inner water core of the liposomes. Then, when these micelles fall in the bulk water, located at the bottom of the formation vessel, a second layer of phospholipids is formed, stabilizing the interface between the water pool and the expanded liquid and completing the double layer structure. After depressurization, ethanol was removed from the top of the formation vessel through a separator (S) operating at 25 °C and 10 bar. CO2 located in the separator then passes through a rotameter (5-2500, Serval 115022, ASA, Sesto San Giovanni, Italy) before being eliminated to the environment; this dispositive is used to measure the gas flow rate. The resulting liposomes remain stored in a reservoir (C) located at the bottom of the formation vessel and can be withdrawn using an on/off valve. Finally, the liposome dispersions were stored in Falcon tubes under refrigeration at 4 °C.

Figure 7.2. Schematic representation of liposome formation, using the SuperLip technology
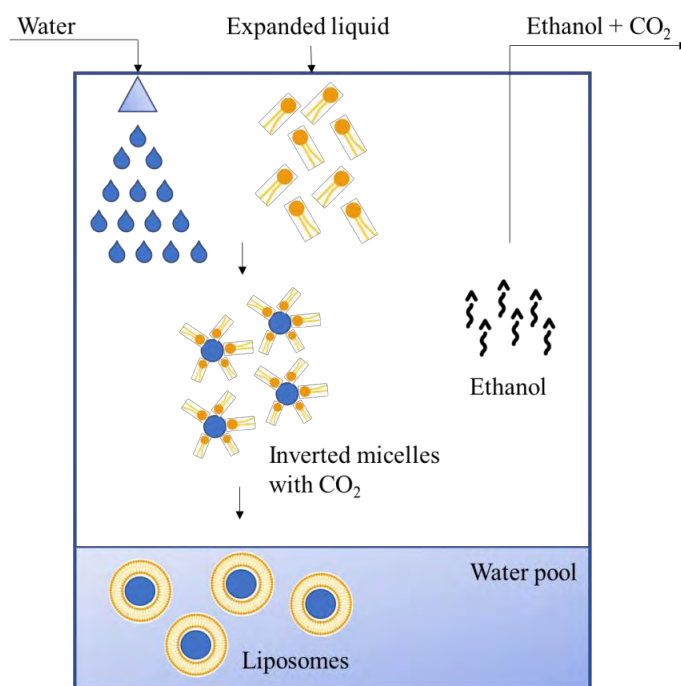
Reference: Chaves et al. (2022)

This study was divided into two parts. First, unloaded vesicles were produced by changing the phospholipid ratio and the water flow rate used in SuperLip. After establishing an optimum water flow rate of 10 mL/min, the second part consisted of producing vitamin D_3-

loaded vesicles using this water flow rate but still changing the phospholipid ratio to determine an optimal value for the encapsulation of the bioactive compound.

7.2.3. Characterization of nanoliposomes

7.2.3.1. Hydrodynamic mean diameter, ζ-potential and size distribution

Nanoliposome dispersions were characterized by dynamic light scattering (DLS) using a ZetaSizer Nano S instrument (Malvern Panalytical, Worcestershire, UK) equipped with a 5.0 mW He-Ne laser operating at 633 nm and at a scattering angle of 173°. Hydrodynamic mean diameter, polydispersity index (PDI), ζ-potential and size distributions were obtained at 25 °C using 1 mL of each sample, without any further dilution, collected immediately after the end of the process.

7.2.3.2. Morphology

The morphology of the produced liposomes was observed using a field emission scanning electron microscope (FE-SEM, mod. LEO 1525, Carl Zeiss SMT AG, Oberkochen, Germany). Briefly, a drop of each dispersion was spread over an adhesive carbon tab, previously attached to an aluminum stub, and left to dry at 25 °C in open air for two days. Then, the samples were covered with gold using a sputter coater (mod. B7341, 250 Å thickness, Agar Scientific, Stansted, UK) prior to FE-SEM observation.

7.2.3.3. Effect of stress-induced conditions

The impact on the hydrodynamic mean diameter, polydispersity index and ζ-potential of the unloaded-liposome dispersions, after the addition of different concentrations of sodium chloride and sucrose and after pH changing, was also investigated using DLS at 25 °C. Regarding the change in ionic strength, solutions containing various concentrations of NaCl or sucrose (100-1000 mmol/L) were added to the dispersions in a 1:9 (v/v) ratio. Alternatively, the pH of 10 mL of liposome dispersions was adjusted to 3, 7 and 12 using hydrochloric acid (HCl 0.1 M) and sodium hydroxide (NaOH 2 M) solutions.

7.2.3.4. Encapsulation efficiency of vitamin D$_3$

The quantification of VD3 in the nanoliposomes was performed using the method described in Chaves & Pinho (2020) and Chaves et al. (2021) with some slight modifications.

Initially, 5 mL of dispersion was diluted in 10 mL of methanol and stirred at 1500 rpm at 25 °C for 5 min. After, the samples were sonicated at 25 °C for 15 min and centrifuged (mod. IEC CL30R Thermo Scientific, Rodano, Milan, Italy) at 6,500 rpm at -4 °C for 20 min using Amicon® Ultra15 centrifugal filtration devices (10 kDa, Merck KGaA, Darmstadt, Germany). The filtrate was then resuspended in 5 mL of methanol and filtered using nylon syringe filters (0.2 µm HA Millipore, Sigma Aldrich, Milan, Italy). The resuspended filtrate and the previously obtained supernatant were transferred to 2 mL vials and analyzed separately by high-performance liquid chromatography (HPLC) (model 1200 series, Agilent Technologies Inc., Italy). The elution was performed using a Zorbax Eclipse Plus C18 (GL Sciences, Torrance, Canada) maintained at 35 °C. A methanol and acetonitrile 9:1 (v/v) solution was used as the mobile phase and pumped at a constant flow of 1.6 mL/min. Aliquots of 10 µL were analyzed at 265 nm for 15 min, and the VD3 peak was evaluated in correspondence with its retention time (4.7 min). Finally, the VD3 concentration was calculated from a standard curve, obtained by reading the absorbance values of several methanol solutions containing different concentrations of VD3 (5-100 µg/mL). The prediction equation was Abs = 27.682 * [VD3] - 10.799, with a correlation coefficient (R^2) of 0.9999. The encapsulation efficiency (%EE) was calculated using Eq. (1):

$$\%EE = \left(\frac{VD3_F}{VD3_F + VD3_S} \right) * 100 \tag{1}$$

where is the vitamin D_3 concentration retained in the filtrate, and represents the nonencapsulated amount of vitamin D_3 in the supernatant, that is, the free amount of bioactive present in the external aqueous phase of the liposome dispersion.

7.2.4. Statistical analyses

Statistical analyses of the results were performed by Tukey's test at a 5% significance level ($p < 0.05$). One-way analyses of variance (ANOVA) were performed using SAS Software version 9.4 computer program (Statistical Analyses Systems, Cary, NC, USA). Data were obtained in triplicate and are herein represented as the average ± standard deviation.

7.3. Results and discussion

7.3.1. Effect of the phospholipid composition and water flow rate

Unloaded liposomes were produced at various SPC:EPC ratios and water flow rates. The results are summarized in Table 2. Some experimental evidence can be highlighted from these data:

1. The liposome mean diameter largely depended on the water flow rate; for example, at SPC:EPC 30:70, the diameter was largely reduced from 462 nm to 139 nm, passing from 2.5 to 10 mL/min water. This trend was repeated at SPC:EPC ratio 20:80. In this case, the liposome mean diameter ranged from 310 nm to 141 nm, increasing the water flow rate from 2.5 to 10 mL/min. However, when the SPC:EPC ratio was set to 0:100 (only EPC was used to form liposomes), the smallest nanoliposomes were obtained, and the trend previously described was not observed. The size of these nanoliposomes ranged from 125 and 131 nm, showing practically constant mean diameters and limited variation in PDI.

2. Regarding ζ-potential, smaller nanoliposomes generally showed lower ζ-potential. This indication implies that smaller liposomes were more stable than larger liposomes.

3. Considering the different SPC:EPC proportions used, the liposome mean diameter largely increased with SPC content, especially at water flow rates of 2.5 and 5 mL/min.

4. Adopting a water flow rate of 10 mL/min, the smallest mean diameters were observed for the formed liposomes (from 141 to 125 nm), and their dimensions were similar regardless of the SPC:EPC ratio tested. Therefore, under this condition, the water flow rate overlapped the effect of the other process parameters. Furthermore, the ζ-potential values were the smallest.

Fig. 7.3 presents two SEM images reported and referred to as experiments B3 (Fig. 7.3a) and B9 (Fig. 7.3b), produced at a 10 mL/min water flow rate and using SPC:EPC ratios of 30:70 and 0:100, respectively. The nanometric diameter of the samples was also confirmed by their morphology.

Table 7.2. Results obtained for nanoliposomes produced using SuperLip at 100 bar and 40 °C

Formulation	Phospholipid ratio (SPC:EPC)	Water flow rate (mL/min)	Mean diameter (nm)	PDI	ζ-potential (mV)	Encapsulation efficiency (%)
B1	30:70	2.5	$462^A \pm 11$	$0.576^A \pm 0.021$	$-7.8^{AB} \pm 2.5$	-
B2	30:70	5	$425^A \pm 24$	$0.570^A \pm 0.031$	$-6.4^{AB} \pm 2.7$	-
B3	30:70	10	$139^E \pm 7$	$0.228^E \pm 0.010$	$-8.1^{AB} \pm 2.9$	-
B4	20:80	2.5	$374^B \pm 20$	$0.448^B \pm 0.030$	$-0.5^A \pm 2.8$	-
B5	20:80	5	$310^C \pm 18$	$0.500^B \pm 0.024$	$-4.5^{AB} \pm 2.8$	-
B6	20:80	10	$141^E \pm 17$	$0.224^E \pm 0.014$	$-8.1^{AB} \pm 3.3$	-
B7	0:100	2.5	$131^E \pm 4$	$0.345^C \pm 0.026$	$-8.1^{AB} \pm 2.8$	-
B8	0:100	5	$132^E \pm 1$	$0.261^{DE} \pm 0.023$	$-7.4^{AB} \pm 3.2$	-
B9	0:100	10	$125^E \pm 1$	$0.236^{DE} \pm 0.004$	$-11^B \pm 3.7$	-
V1	30:70	10	$252^D \pm 7$	$0.289^{CD} \pm 0.004$	$-6.2^A \pm 0.3$	$77.0^B \pm 1.2$
V2	20:80	10	$218^D \pm 9$	$0.253^{DE} \pm 0.016$	$-6.8^A \pm 0.4$	$88.9^A \pm 3.6$
V3	0:100	10	$144^E \pm 2$	$0.260^{DE} \pm 0.008$	$-12^B \pm 0.7$	$66.7^C \pm 2.4$

Mean diameters followed by the same uppercase letter at the same column were not significantly different ($p > 0.05$) by Tukey's test.

Reference: Chaves et al. (2022)

Figure 7.3. Micrographs obtained using FE-SEM for the vesicles produced at 10 mL/min, at different ratios of saturated Phospholipid P90H (SPC) and unsaturated L-α-phosphatidylcholine (EPC): (a) 30:70 SPC:EPC and (b) 0:100 SPC:EPC

(a)   (b)
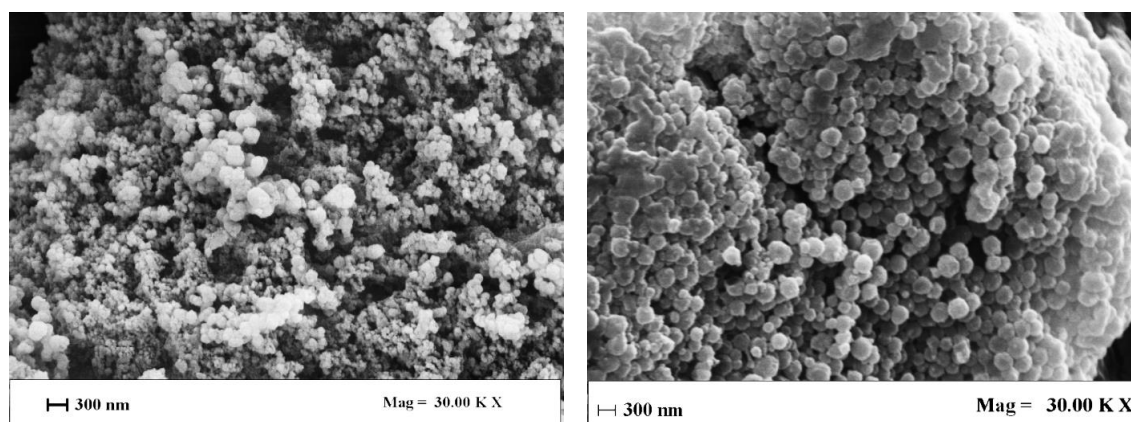
Reference: Chaves et al. (2022)

Relevant information emerged from the size distributions obtained by DLS. B1, B2, B4 and B5 liposomal distributions were bimodal, as shown in Fig. 7.4, in which the size distribution related to experiment B5 is reported as an example. This evidence demonstrated that the formation of liposomes was unfavorable under these conditions. This indication led to a substantial discard of the experiments performed at 2.5 and 5 mL/min water flow rates in the subsequent studies, in which VD3-loaded liposomes were produced.

Figure 7.4. Size distribution curve obtained for the liposomes produced at 5 mL/min, using a 20:80 ratio of Phospholipid P90H (SPC) and unsaturated L-α-phosphatidylcholine (EPC)
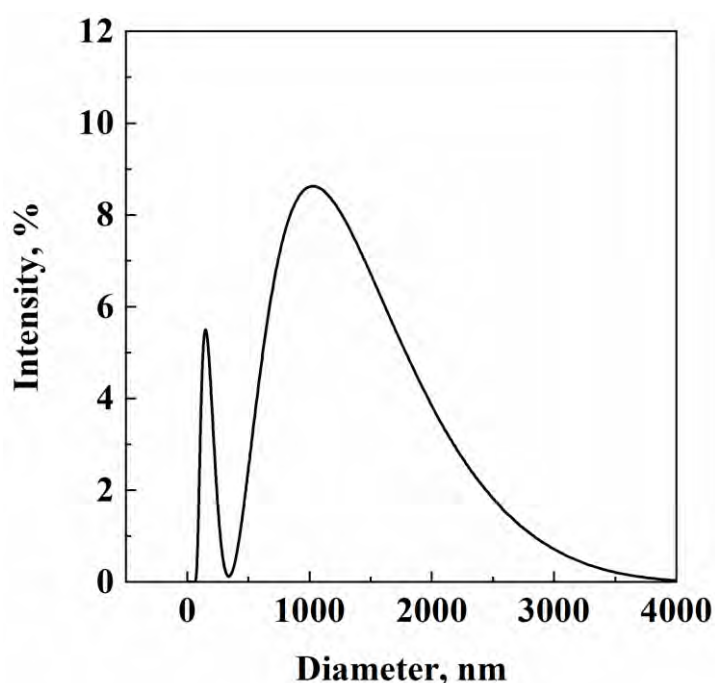
Reference: Chaves et al. (2022)

7.3.2. Effect of stress-induced conditions

For the stress condition analyses, two formulations were chosen, B6 and B9. These samples were chosen because both presented nonstatistically significant diameters and PDIs and were produced at the same water flow rate (Table 7.2). The objective here was to verify which effects could be seen in vesicles under stress conditions due to the presence of saturated phospholipids. Vesicles were stressed by incorporating, separately, amounts of NaCl or sucrose or by modifying their pH, conditions commonly found in food formulations. Therefore, how

these stresses can influence the stability of liposomes can be considered relevant. The modifications observed for mean diameter, PDI and ζ-potential are summarized in Fig. 7.5.

The addition of saline solutions led to a significant decrease in the mean diameter of liposomes (Fig. 7.5A). Indeed, after this test, the liposome mean diameter was reduced from 125 and 141 nm (Table 7.1) to values ranging from 63 to 76 nm. The addition of salt leads to the partial dehydration of vesicles and, therefore, to a reduction in size due to osmosis (Tai et al., 2020). However, an increase in NaCl concentration, from 100 to 1000 mM, only promoted a slight increase in the mean diameter of liposomes. Mouritsen (2011) attributed this effect to an increase in the density of liposomes caused by the packaging of lipids within the membranes. This process promotes stiffening of the lipid bilayer and a forced change in its curvature, which causes the appearance of structural defects. Thus, when trying to return to its lowest energy state, the bilayer tends to form larger vesicles but with smaller curvatures, which increase the tendency to instability due to flocculation (Mouritsen, 2011). Moreover, the addition of NaCl also caused a decrease in the PDI of liposomes at all concentrations: they were lower than 0.25 regardless of the salt concentration. An increase in salt concentration led to a decrease (in modulus) in ζ-potential values that can reveal a possible weakening of the electrostatic repulsion among the vesicles, especially under high ionic concentrations, thus promoting an increase in attractive interactions that may lead to early instability (Crommelin et al., 1984).

The opposite effect was observed after the addition of sucrose solutions (Fig. 7.5B). A significant increase in size was obtained even when the lowest concentration (100 mM) of the disaccharide was added to both samples. Mean diameters ranging from 175 to 360 nm were measured for the samples containing 20% SPC (Fig. 7.5B, left), whereas samples produced without SPC exhibited diameters ranging from 220 to 260 nm (Fig 7.5B, right). Interestingly, the sample produced using EPC showed a higher resistance to the addition of sucrose, as the mean size was not strongly modified by an increase in sugar concentration (Fig. 7.5B, right). In addition, the PDI remained mostly constant regardless of the sugar concentration, in contrast to the result exhibited for the B6 formulation, in which a considerable increase in PDI was observed (Fig. 7.5B, left). This result suggests that sucrose promoted the coalescence of the vesicles produced in the presence of SPC and did not have a significant influence on the stability of nanoliposomes produced using EPC alone. In this context, sucrose has been used successfully to stabilize vesicles due to the interactions between the hydroxyl radicals from the sugar and the phosphates from the phospholipid head groups, thus preventing membrane fusion by the

formation of a stable glassy state (Wolkers et al., 2004). A significant decrease in the absolute values for ζ-potential was observed for both formulations after the addition of sucrose concentrations higher than 500 mM, suggesting that higher amounts of any solute can promote a disturbance in the surface electrostatic repulsive forces of liposomes.

Changes in the pH of the dispersions induced a decrease in the liposome mean diameter under alkaline pH, as reported in Fig. 7.5C. The mean size of the vesicles produced at 20% SPC ranged from 146 to 200 nm, whereas those related to the liposomes produced using EPC alone ranged from 118 to 240 nm. At pH 3 (acidic media), the fatty acid carboxyl groups are protonated, which may cause the formation of hexagonal (H_{II}) phases in the lipid bilayer, making the liposomes unstable and easier to aggregate or fuse, explaining the higher diameters (Israelachvili, 1992). Additionally, liposomes containing PE are more susceptible to membrane fusion due to the low hydration of the polar head of this phospholipid, corroborating the higher diameter obtained for formulation B9 at this pH (Fig. 5C, right) (Li et al., 2015). PC molecules are protonated at neutral pH due to their zwitterionic nature, which enhances the reduction in size, as electrostatic repulsion is more predominant than hydrogen bonding (Roy et al., 2016). Using alkaline media, repulsive forces between the phospholipid molecules became strongly prevalent, further reducing the final size of the vesicles. Regarding PDI, the higher values obtained at pH 3 revealed the presence of aggregates due to partial coalescence (Andrade, González-Martinez, & Chiralt, 2021). Despite this fact, the PDI values for the formulations were approximately 0.30, demonstrating the stability of the systems. As expected, the ζ-potential proved to be strongly dependent on pH, increasing in the module under alkaline conditions. This effect is due to the zwitterionic characteristic of the phospholipids, which became more or less negative depending on pH (Alhakamy et al., 2015). In this context, the lower the pH is, the more positive the charge of the phospholipids. Similarly, the more alkaline the media is, the more negative the charge is (Alhakamy et al., 2015). Conclusively, the nanoliposomes appeared to present higher stability in alkaline media considering all three pH values investigated.

Figure 7.5. Parameters obtained for the unloaded nanoliposomes submitted to different stress conditions: (A) addition of NaCl (100-1000 mM), (B) addition of sucrose (100-1000 mM) and (C) pH changing (3-12). On the left column, results related to the formulation B6 (20:80 SPC:EPC). On the right column, results related to the formulation B9 (0:100 SPC:EPC)

Reference: Chaves et al. (2022)
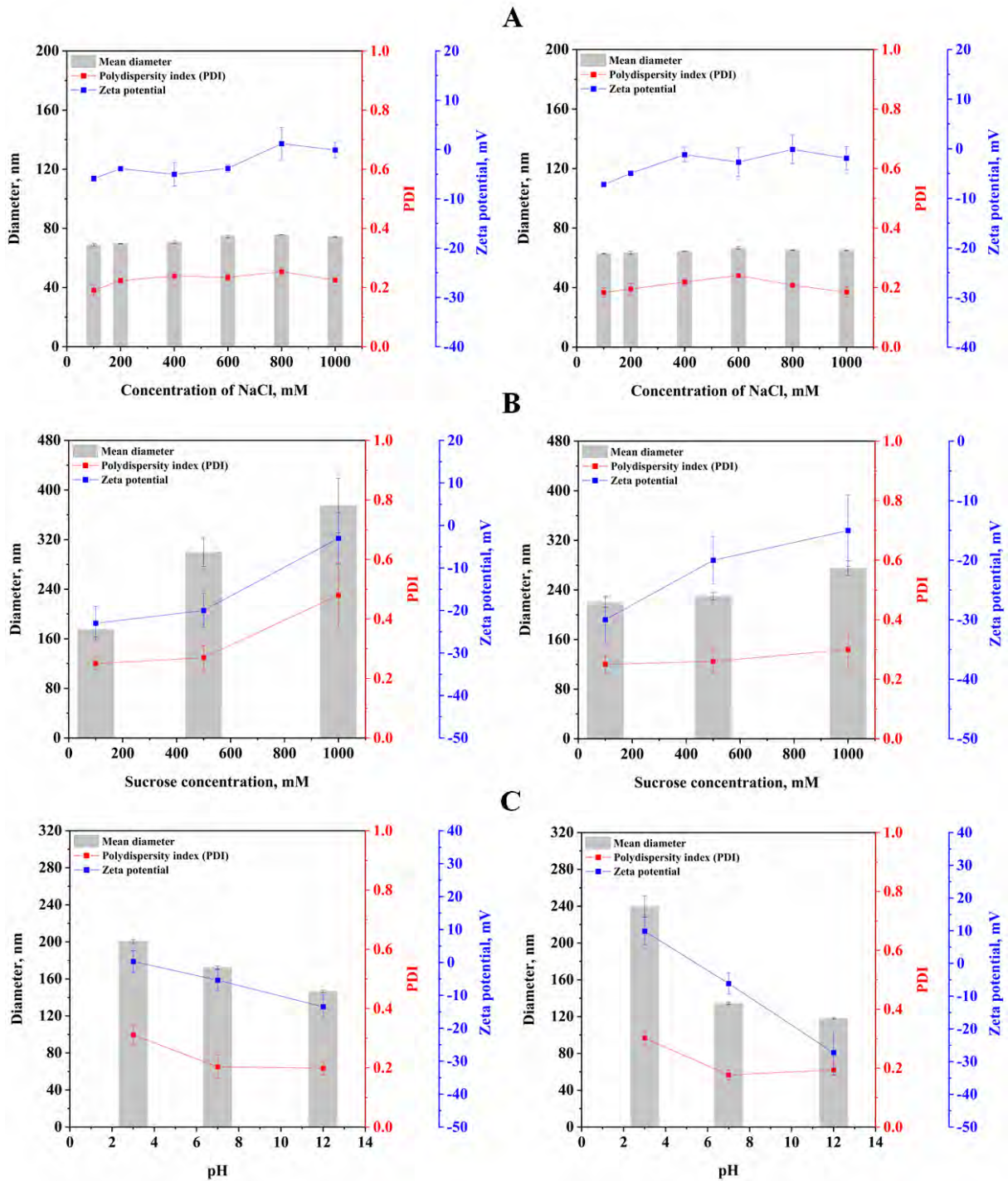
7.3.3. Characterization of vitamin D₃-loaded nanoliposomes

This series of experiments was performed in SuperLip using the same process parameters used for the unloaded samples, with the exception of the water flow rate fixed at 10 mL/min. The parameters obtained for VD3-loaded samples are also summarized in Table 7.2. Fig. 7.6a presents a photograph of these samples, in which the translucid aspect can be observed, a characteristic usually related to nanoliposome dispersions. A FE-SEM micrograph related to this sample is presented in Fig. 7.6b.

Regarding the mean diameters obtained for the VD3-loaded samples, V1 and V2 presented significantly higher values than V3, suggesting that the addition of SPC led to substantial increases in their mean sizes. This fact corroborates the findings of Tai et al. (2020), who observed that vesicles produced with hydrogenated phospholipids have larger diameters than those produced with nonhydrogenated species. This trend was not verified for the unloaded vesicles produced at the same water flow rate of 10 mL/min (B3-B6-B9), as no significant differences were detected among them. However, the incorporation of VD3 into the bilayers of mixed phospholipid nanoliposomes may have led to an increase in the mean size of the vesicles (Chaves & Pinho, 2020). Additionally, the PDIs of samples V2 and V3 did not differ from each other at a maximum SPC of 20% (w/v), and both showed a similar cumulative size distribution, as shown in Fig. 7.6c. In addition, ζ-potential was slightly higher for V3, suggesting liposomes produced with only EPCs may be slightly more stable than the others.

Interesting results were obtained for vitamin D₃ encapsulation, as efficiencies ranging from 66.7 to 88.9% were considered excellent for liposomes. The V2 sample presented the highest percentage of VD3 retention, indicating that a replacement of 20% EPC for SPC contributed to an increase of approximately 25% in the bioactive encapsulation. First, it is reasonable to assume that an increase in the average diameter was good for a higher encapsulation of a highly hydrophobic molecule such as VD3 (logP = 7.5), as the larger the lipid bilayer, the higher the amount of bioactive material that can be retained in its interior. Additionally, V3 presented the lowest %EE value. This sample was produced using only nonhydrogenated EPC and was more susceptible to oxidation due to the higher presence of unsaturated bonds, which may have led to a slight but deleterious acceleration in the degradation of VD3 caused by the action of prooxidant species.

Figure 7.6. Vitamin D$_3$-loaded nanoliposomes produced using SuperLip at 100 bar and 40 °C: (a) visual aspect of the dispersions, (b) micrograph obtained using FE-SEM at 30 KX for V3 sample and (c) cumulative size distributions. Samples were produced at a water flow rate of 10 mL/min, using different ratios of saturated Phospholipid P90H (SPC) and unsaturated L-α-phosphatidylcholine (EPC): (V1) 30:70 SPC:EPC, (V2) 20:80 SPC:EPC and (V3) 0:100 SPC:EPC
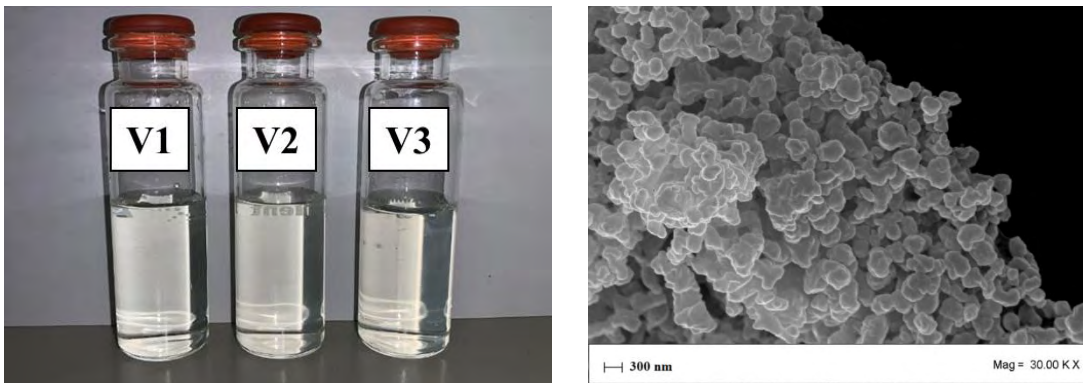
(a)   (b)

(c)
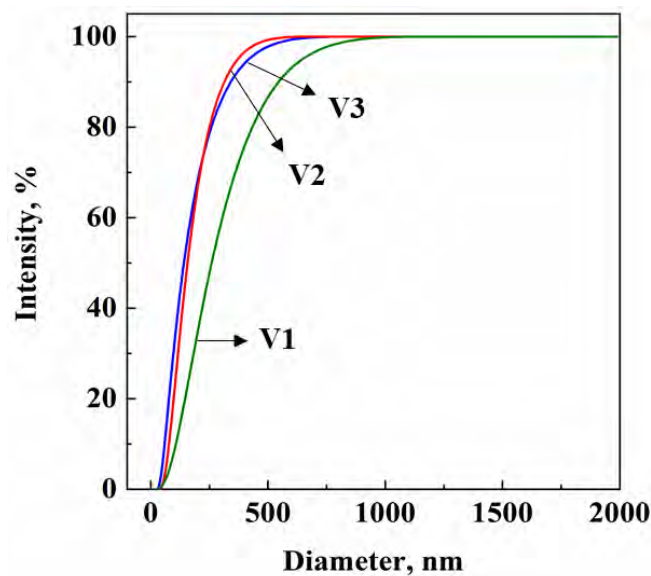
Reference: Chaves et al. (2022)

7.4. Conclusions

The results obtained in this study confirmed the feasibility of SuperLip to produce highly stable, mixed phospholipid nanoliposomes. Although the liposome dispersions produced using egg-yolk phosphatidylcholine alone presented diameters smaller than 132 nm, regardless of the water flow rate, nanosized and highly homogeneous vesicles were also produced at a

maximum of 30% soy-derived hydrogenated phospholipids when a 10 mL/min water flow rate was used. The process was considerably efficient for the production of vitamin D_3-loaded nanoliposomes, resulting in vesicles with enhanced and controlled size distributions and encapsulation efficiencies up to 88.9%.

7.5. Acknowledgments

7.6. References

Alhakamy, N. A., et al. (2015). Effect of lipid headgroup charge and pH on the stability and membrane insertion potential of calcium condensed gene complexes. **Langmuir**, 31(14), 4232-4245.

Andrade, J., González-Martinez, C., & Chiralt, A. (2021). Liposomal encapsulation of carvacrol to obtain active poly(vinyl alcohol) films. **Molecules**, 26(6), 1589.

Baldino, L., Cardea, S., & Reverchon, E. (2019a). Supercritical assisted electrospray: An improved micronization process. **Polymers**, 11(2), 244.

Baldino, L., Cardea, S., Reverchon, E. (2019b). A supercritical CO_2 assisted electrohydrodynamic process used to produce microparticles and microfibers of a model polymer. **Journal of CO_2 Utilization**, 33, 532–540.

Baldino, L. et al. (2019a). Production, characterization and testing of antibacterial PVA membranes loaded with HA-Ag3PO4 nanoparticles, produced by SC-CO_2 phase inversion. **Journal of Chemical Technology and Biotechnology**, 94, 98-108.

Baldino, L. et al. (2019b). A new tool to produce alginate-based aerogels for medical applications, by supercritical gel drying. **The Journal of Supercritical Fluids**, 146, 152-158.

Bigazzi, W et al. (2020). Supercritical fluid methods: An alternative to conventional methods to prepare liposomes. **Chemical Engineering Journal**, 383, 123106.

Chaves, M. A., & Pinho, S. C. (2019). Curcumin-loaded proliposomes produced by the coating of micronized sucrose: Influence of the type of phospholipid on the physicochemical characteristics of powders and on the liposomes obtained by hydration. **Food Chemistry**, 291, 7-15.

Chaves, M. A., & Pinho, S. C. (2020). Unpurified soybean lecithins impact on the chemistry of proliposomes and liposome dispersions encapsulating vitamin D_3. **Food Bioscience**, 37, 100700.

Chaves, M. A. et al. (2021). Nanoliposomes coencapsulating curcumin and vitamin D_3 produced by hydration of proliposomes: Effects of the phospholipid composition in the physicochemical characteristics of vesicles and after incorporation in yoghurts. **International Journal of Dairy Technology,** 74(1), 107-117.

Crommelin, D. M. (1984). Influence of lipid composition and ionic strength on the physical stability of liposomes. **Journal of Pharmaceutical Sciences**, 73(11), 1559-1563.

Dima, C., & Dima, S. (2020). Bioaccessibility study of calcium and vitamin D_3 co-microencapsulated in water-in-oil-in-water double emulsions. **Food Chemistry**, 3030, 125416.

Emami, S. et al. (2016). Liposomes as carrier vehicles for functional compounds in food sector. **Journal of Experimental Nanoscience**, 11(9), 737-759.

Espírito-Santo, I. et al. (2014). Liposomes preparation using a supercritical fluid assisted continuous process. **Chemical Engineering Journal**, 249, 153-159.

Holick, M. F. (2017). The vitamin D deficiency pandemic: Approaches for diagnosis, treatment and prevention. **Reviews in Endocrine & Metabolic Disorders**, 18(2), 153-165.

Israelachvili, J. N. (1992). Fluid-like structures and self-assembling systems: Micelles, bilayers and biological membranes. **Intermolecular and Surface Forces** (2nd ed.), Academic Press, London, pp. 366-394

Li, J. et al. (2015). A review on phospholipids and their main applications in drug delivery systems. **Asian Journal of Pharmaceutical Sciences**, 10(2), 81-98.

Lopes, N. A. et al. (2021). Nisin induces lamellar to cubic liquid-crystalline transition in pectin and polygalacturonic acid liposomes. **Food Hydrocolloids**, 112, 106320.

Maqbool, F. et al. (2019). Dispersibility of phospholipids and their optimization for the efficient production of liposomes using supercritical fluid technology. **International Journal of Pharmaceutics**, 563, 174-183.

Mouritsen, O. G. (2011). Lipids, curvature, and nano-medicine. **European Journal of Lipid Science and Technology**, 113(10), 1174-1187.

Muñoz-Shugulí, C. et al. (2021). Encapsulation of plant extract compounds using cyclodextrin inclusion complexes, liposomes, electrospinning and their combinations for food purposes. **Trends in Food Science & Technology**, 108, 177-186.

Penoy, N. et al. (2021). A supercritical fluid technology for liposome production and comparison with the film hydration method. **International Journal of Pharmaceutics**, 592, 120093.

Roy, B. et al. (2016). Influence of lipid composition, pH, and temperature on physicochemical properties of liposomes with curcumin as model drug. **Journal of Oleo Science**, 65(5), 399-411.

Sarno, M. et al. (2017). SC-CO_2-assisted process for a high energy density aerogel supercapacitor: The effect of GO loading. **Nanotechnology**, 28, 204001.

Sharifi, F. et al. (2019). Generation of liposomes using a supercritical carbon dioxide eductor vacuum system: Optimization of process variables. **Journal of CO_2 Utilization**, 29, 163-171.

Tai, K. et al. (2020). Stability and release performance of curcumin-loaded liposomes with varying content of hydrogenated phospholipids. **Food Chemistry**, 326, 126973.

Tanaka, Y. et al. (2020). Preparation of liposomes encapsulating β–carotene using supercritical carbon dioxide with ultrasonication. **The Journal of Supercritical Fluids**, 161, 104848.

Trucillo, P., Campardelli, R., & Reverchon, E. (2019a). A versatile supercritical assisted process for the one-shot production of liposomes. **The Journal of Supercritical Fluids**, 146, 136-143.

Trucillo, P., Campardelli, R., & Reverchon, E. (2019b). Antioxidant loaded emulsions entrapped in liposomes produced using a supercritical assisted technique. **The Journal of Supercritical Fluids**, 154, 104626.

Trucillo, P. et al. (2020). Production of liposomes loaded alginate aerogels using two supercritical CO_2 assisted techniques. **Journal of CO_2 Utilization**, 39, 101161.

Wolkers, W. F. et al. (2004). Preservation of dried liposomes in the presence of sugar and phosphate. **Biochimica et Biophysica Acta (BBA) – Biomembranes**, 1661(2), 125-134.

Zhao, L. et al. (2017). Encapsulation of lutein in liposomes using supercritical carbon dioxide. **Food Research International**, 100, 168-179.

Chapter 8. TERNARY BLENDS OF CORNSTARCH, MALTODEXTRIN AND
LYOPHILIZED LIPOSOMES PRODUCED BY HIGH SHEAR WET AGGLOMERATION
FOR THE COENCAPSULATION OF CURCUMIN AND VITAMIN D_3

Chapter 8. Ternary blends of cornstarch, maltodextrin and lyophilized liposomes produced by high shear wet agglomeration for the encapsulation of curcumin and vitamin D_3

Abstract

Food fortification is the most accessible way to ensure more effective micronutrient intakes by the population. Therefore, the development of new functionalities for technologies already employed by the food industry can be considered a major innovation. In this study, wet agglomeration was used to produce ternary blends of cornstarch, maltodextrin and lyophilized liposomes entrapping curcumin and vitamin D_3. The effects of unsaturated phospholipids in liposomes (0, 30, and 50% w/v) and liposome content into cornstarch (6, 8 and 10% w/w) were evaluated. Microstructure of powders was assessed using techniques as SEM, DSC, XRD and FTIR. Pasting properties of cornstarch were also investigated. Lyophilized liposomes herein produced showed low water activity (0.19-0.21) and moisture content (3.97-5.43%), high hygroscopicity (>8.5 g adsorbed water/100 g dry matter) and solubility (>65.2%), and retained up to 99.6% of curcumin and 98.8% of vitamin D_3. Cornstarch presented improved flow properties after agglomeration and even better effects after the blending with liposomes as increased diameter (> 1928 μm) and particle density (>617 kg/m³). The ternary blends also proved to be very suitable carriers for the bioactives as at least 71.9% of curcumin and 80.7% of vitamin D_3 were still available after 30 days of storage. Decreased pasting temperature (<74 °C) and viscosity (<2742 cP) of cornstarch were detected after liposome addition. Overall, the phospholipid ratio used in liposomes had a more significant impact ($p < 0.05$) on most of properties of enriched blends than liposome content added to cornstarch during agglomeration.

8.1. Introduction

Nowadays, many limiting factors associated to the direct incorporation of free hydrophobic bioactives into food formulations can be overcome with their microencapsulation into lipid-based carriers. Liposomes appear as suitable delivery systems for several bioactives due to their amphiphilic characteristic, which allows the simultaneous encapsulation of one or more hydro- and/or lipophilic molecules, besides enhancing bioavailability due to the high biocompatibility with the epithelial cells (Taylor et al., 2005). These carriers consist of vesicular structures composed of one or several phospholipid bilayer membranes displayed concentrically, enclosed by an aqueous core, and capable of encapsulate part of the medium in which they are dispersed (McClements, 2015). Liposomes can be prepared by a wide variety of techniques, some simpler, cheaper and more easily scalable than others, but all resulting in highly stable vesicles with high encapsulation efficiency. These advantages have drawn the attention of food researchers and of food industry as well, whereby the latter is constantly aiming to attempt the new consumers patterns of balanced nutrition and optimal health (Dhakal and He, 2020).

Despite their advantages, liposomes are susceptible to physical and chemical instabilities as aggregation and hydrolysis, mainly over longer storage periods. Additionally, vesicles produced with mixed phospholipids tend to destabilize more easily due to the increase of the spontaneous radius of the lipid plane curvature, this associated to the formation of non-lamellar inverted phases (Lopes et al., 2021). To extend their shelf life, lyophilization appears as a very viable option due to its common application in food industries. This process has been widely used in order to increase the stability of liposomes, particularly of those in which thermosensitive molecules have been encapsulated (Lopez-Polo et al., 2020; Vélez et al., 2019; Wang et al., 2022).

Besides the lipid-based carriers, the interest in starch-based delivery systems for encapsulation of bioactives has also been increased considerably due to their natural abundance and low cost. These polysaccharide-based systems can be used in native or modified forms and are more suitable wall materials under high temperature conditions than lipid- or protein-based carriers as they do not melt or denature to the same extent (Zhu et al., 2017). Cornstarch and maltodextrin are two polysaccharides commonly used in the food industry as ingredients, thickeners and mouthfeel improvers, due to their GRAS status, non-allergenic feature and blandness taste. Various starch systems have been used for

encapsulation as starch granule-stabilized Pickering emulsion (Marefati et al., 2015), native starch gels (Mun, Kim, & McClements, 2015), microporous starch granules (Xing et al., 2014), starch nanoparticles (Chin et al., 2014), cross-linked starch (Li et al., 2009) and hydrolyzed starch (Spada et al., 2012). Not many studies are found in the literature in which ternary blends of cornstarch, maltodextrin and lyophilized liposome are produced to confer an additional barrier protection for encapsulated bioactives (Ferreira et al., 2018; Toniazzo et al., 2017).

Wet agglomeration is a unit operation that aims to improve certain properties of powders, such as flowability, solubility, and porosity, from the increase of the average particle diameter (Cuq et al., 2013). It is mainly carried out with the aim of producing instant foods, which reconstitute rapidly in the presence of water or milk (Ji et al., 2016). This process can be divided into three steps: (i) wetting and nucleation: stage in which the binder solution comes into contact with the dry powder, initiating the formation of granules. Nucleation occurs when a particle adheres to another through the binding agents present on its surfaces; (ii) consolidation and coalescence: stage in which the particle diameter increases due to the contact between the granules. During coalescence, the porous surface of the granule is saturated with binder, leading to the formation of malleable granules that can deform and, consequently, unite; and (iii) attrition and breakage: stage in which the rupture of the granules occurs due to impacts, wearing or manipulation (Iveson et al., 2001).

Curcumin is a polyphenol present in the *Curcuma longa* (turmeric) rhizomes that has receiving considerable interest due to its many biological features. In food, this natural compound has been used as preservative, colorant, flavoring and antioxidant in dairy products, beverages, cookies, breads, cereals, mustard, food concentrates, among others. However, the direct incorporation of curcumin into food formulations is hampered by its poor solubility in water (logP = 3.2), instability at physiological pH and low oral bioavailability (Jiang et al., 2020).

Vitamin D_3 (cholecalciferol, VD3) is the most active form of vitamin D and is synthetized by the body via skin after sunlight exposure. Its recognized deficiency may be due to several reasons, including too much time indoors, geographical location, and the limitation of naturally rich foods. Mushrooms, cod liver oil, salmon and other fatty fishes, and egg yolk (in minor amounts) are some natural sources of vitamin D. Also, the enrichment of some products as milk and margarine with vitamin D is presently common practice in several countries. However, VD3 presents itself as a very hydrophobic molecule (logP = 7.5), which also hampers its incorporation into aqueous-based food formulations, alongside its high instability under high

temperatures, light exposure and oxygen presence. Nevertheless, the low bioavailability of vitamin D can also be pointed as a reason for this pandemic (Maurya, Bashir, and Aggarwal, 2020). In this context, the incorporation of curcumin and vitamin D_3 into lipid-based carriers as liposomes presents as an option to increase both their solubility and bioavailability.

The present study was designed to verify the feasibility to produce a new enriched-cornstarch product containing curcumin and vitamin D_3 coencapsulated in lyophilized liposomes, using a simple wet agglomeration process and maltodextrin solutions as the liquid binder. The outcome of this study will enable (i) to improve the knowledge with respect to new encapsulation technologies for food products, (ii) to improve the literature regarding the agglomeration of particulate systems with distinct characteristics (blends of powders), which is considered a technological challenge faded by the food industry, and (iii) to develop a new and high-value added product using low cost raw materials, with wide application range and high nutritional quality.

8.2. Material and methods

8.2.1. Chemicals and reagents

Soybean-derived phospholipids with different lengths and degrees of saturation were used throughout this study to produce liposomes. Phospholipon 90H (P90H), composed of a minimum of 90% w/w of phosphatidylcholine (PC) and a maximum of 4% w/w of lysophosphatidylcholine (LPC), and Lipoid S40 (LS40), composed of 40% w/w of PC, 15% w/w of phosphatidylethanolamine (PE), 4% w/w of LPC and 3% w/w of phosphatidylinositol (PI), were purchased from Lipoid GmbH (Ludwigshafen, Germany). Cornstarch (AMISOL® 3408) and maltodextrin (MOR REX 1910 DE 10) were kindly supplied by Ingredion TM (Mogi Guaçu, SP, Brazil). Curcumin and vitamin D_3 were purchased from Sigma-Aldrich (St. Louis, MO, USA). Stabilizers xanthan gum (XG) and guar gum (GG) were kindly donated by DuPont (Cotia, SP, Brazil). Sucrose and sodium benzoate were purchased from Synth (Diadema, SP, Brazil). Acetonitrile and methanol (HPLC-grade) acquired from Merck (Darmstadt, Germany) were used for bioactive quantification. Deionized water by means of a Milli-Q purification system (Millipore, Billerica, MA, USA) was used throughout the experiments.

8.2.2. Production of Cur-VD3-co-loaded lyophilized liposomes

Liposomes were produced by the hydration of proliposomes method following the procedure described in Chaves & Pinho (2019) and Chaves & Pinho (2020). Samples were prepared by varying the ratio between P90H and LS40 as summarized in Table 8.1. Formulations were named according to the amount of unpurified phospholipid (LS40) presented in each one. Briefly, 100 mL of an ethanolic solution containing the components of each formulation were mixed using ultragitation (T25, IKA, Staufen, Germany) at 15,000 rpm for 15 min at 25 °C and then dripped onto 2 g of micronized sucrose at a flow rate of 4 mL/min using a peristaltic pump (Masterflex 7528-30, Cole-Parmer, Vernon Hills, IL, USA). This process occurred in a rotary evaporator (MA120, Marconi, Piracicaba, SP, Brazil) in which the rotary flask was kept at 60 ± 2 °C until the complete removal of ethanol. Moreover, it is worth mentioning that samples remained under sonication at 40 kHz until the end of dripping process to maintain LS40 dispersed. Next, 2 g of the resulted proliposomes were hydrated with 100 mL of deionized water at 13,000 rpm for 5 min at 65 °C using ultragitation (IKA, Germany) to form the liposome dispersions. At this step, sucrose was added at a 2:1 sucrose-to-lipid ratio to dispersions to act as cryoprotectant during lyophilization. Samples were then cooled to 25 °C for the addition of stabilizers xanthan gum (0.01% w/v) and guar gum (0.09% w/v) under magnetic stirring at 3,600 rpm for 20 min. Lyophilization process was outsourced and performed by SublimarTM (Tatuí, SP, Brazil). Dispersions were frozen in ultra-freezer at -22 °C and submitted to lyophilization at -22 °C for 24 h. The vacuum chamber was maintained at 0.75 torr throughout the process. Samples were conditionate in laminated packaging and stored for a maximum of 4 wk in desiccators containing silica gel at 25 °C.

Table 8.1. Formulations used for the production of Cur-VD3-co-loaded lyophilized liposomes. To the formulations were added 25 mg of Cur and 80.000 IU (0.02 g) of VD3

Formulation	Phospholipid	
	Phospholipon 90H (g)	Lipoid S40 (g)
L0	3.2	-
L50	1.6	1.6
L70	0.96	2.24

Reference: Own source

8.2.3. Characterization of curcumin/VD3-co-loaded lyophilized liposomes

8.2.3.1. Water activity (a_w) and moisture content (MC)

Water activity was measured using an electronic dew point water activity meter (AquaLab 3TE, Decagon Devices, Washington, USA), whereas moisture content was measured using a moisture analyzer with infrared radiation (MB35 Halogen, Ohaus, Switzerland).

8.2.3.2. Solubility and hygroscopicity

Solubility was determined by the Eastman & Moore (1984) method with some modifications. A total of 500 mg of sample was mixed with 50 mL of deionized water in an orbital shaker (Marconi, Brazil) for 5 min at 250 rpm at 25 °C. The resulted solution was transferred to Falcon tubes and submitted to centrifugation (5430R, Eppendorf, Hamburg, Germany) at 2500 x g for 5 min at 25 °C. An aliquot of 15 mL of the supernatant was poured to pre-weighted Petri dish and maintained in a convection oven at 105 °C until constant weight. Solubility (%) value was calculated using Eq. (1):

$$\text{Solubility (\% solubilized powder)} = (MSS * (50/15) / MS) * 100 \qquad (1)$$

where MSS is the mass of suspended solids in the supernatant, MS is the initial mass of sample, and (50/15) is the dilution factor.

Hygroscopicity was measured by Cai & Corke (2006) method with modifications. Briefly, 0.2 g of sample were placed in a weighing filter and maintained in a desiccator containing a saturated solution of NaCl (UR = 70.4%) for a week. Moisture adsorption was measured by the weight gain of the sample. Hygroscopicity (g adsorbed water/100 g of dry matter) was calculated using Eq. (2):

$$\text{Hygroscopicity (g adsorbed } H_2O/100 \text{ d.m.)} = [WG \text{ (g)} / MD \text{ (g)}] * 100 \qquad (2)$$

where WG is the water gain after 1 wk and MD is the mass of the sample in dry basis.

8.2.3.3. Quantification of encapsulated curcumin

Curcumin content was determined according to the following procedure: First, 0.3 g of sample were mixed to 10 mL methanol at 1,000 rpm for 10 min at 25 °C using a mechanical laboratory shaker (Multi Reax, Heidolph Instruments, Schwabach, Germany). Then, the resulted

solution was sonicated at 40 kHz for 20 min at 25 °C and right after centrifugated at 7,000 g for 10 min at 4 °C. Supernatant was then tenfold diluted before analysis by UV-Visible spectrophotometry (Genesys 10S, Thermo Scientific, Waltham, MA, USA) at 425 nm. Pure methanol was used as the blank. Curcumin content was quantified using an analytical curve of pure curcumin (≥65%) in methanol (R^2 = 0.998). Limits of detection (LOD) and quantification (LOQ) were calculated directly from the analytical plot using Eq. (3) and (4), respectively.

$$\text{LOD} = (3.3 * \sigma)/S \tag{3}$$

$$\text{LOQ} = (10 * \sigma)/S \tag{4}$$

where σ is the standard deviation of intercept and S is the slope of the analytical plot.

8.2.3.4. Quantification of encapsulated vitamin D_3

Vitamin D_3 concentration was measured by high-performance liquid chromatography (HPLC, Shimadzu Prominence System, Kyoto, Japan). First, 0.3 g of sample were mixed to 5 mL methanol at 1,000 rpm for 5 min at 25 °C using a laboratory shaker (Multi Reax, Germany). Solutions were sonicated at 40 kHz for 10 min at 25 °C and then centrifugated at 7,000 g for 5 min at 4 °C. The supernatant was transferred to a test tube and the process was repeated to boost the vitamin extraction. The extracted was filtered using nylon filters (0.45 μm, Ø = 13 mm, LCR Científica, Americana, SP, Brazil), transferred to 2 mL vials and introduced into the HPLC system. Runs were performed under the following conditions: column (Shim-Pack VP-ODS, 4.6 μm, 0.46 x 25 cm, Shimadzu), mobile phase (methanol/acetonitrile in the ratio of 9:1 v/v), flow rate (1.6 mL/min), wavelength (265 nm), standard (cholecalciferol, 99% pure, Sigma-Aldrich, USA). VD3 concentration was quantified using an analytical curve of pure VD3 in methanol/acetonitrile 9:1 (R^2 = 0.999). Limits of detection (LOD) and quantification (LOQ) were calculated from the analytical plot using Eq. (3) and (4), respectively.

8.2.3.5. Scanning electron microscopy (SEM)

The microstructure of surface morphology of powders was observed with a scanning electron microscope (SEM model TM-300, Hitachi, Tokyo, Japan) operated at an accelerating voltage of 15 kV. Samples were placed on the double-sided adhesive carbon tapes without any previous treatment and fixed to aluminum stubs. Micrographs were observed at sample random positions.

8.2.3.6. Differential scanning calorimetry (DSC)

Thermal properties of the lyophilized liposomes were measured with a differential scanning calorimeter (DSC TA2010, TA Instruments, Delaware, USA). Powders were placed in hermetically sealed aluminum pans, and thermograms were obtained in a temperature range from 10 to 100 °C at a heating rate of 10 °C/min. The heating was performed under an inert atmosphere (45 mL/min N_2). The phase transition temperatures (T_m) were calculated using Universal Analyzes v. 7 software (TA Instruments, USA).

8.2.4. Production of Cur-VD3--enriched cornstarch

Ternary blends of cornstarch, maltodextrin and lyophilized liposomes were produced by wet agglomeration using the formulations described in Table 8.2 and based on the protocols published by Toniazzo et al. (2017) and Ferreira et al. (2018). Initially, the liquid binder solution was prepared by dispersing the maltodextrin in deionized water with the assistance of a magnetic stirrer at 1,000 rpm for 5 min at 25 °C. This solution was then dripped onto a physical mixture of cornstarch and lyophilized liposomes (when added) at a flow rate of 5 mL/min using a peristaltic pump (Cole Parmer 7528-30, Vernon Hills, Illinois, USA). Wet agglomeration occurred inside a multiprocessor (Philips, Walita RI7625, China) at an impeller rotation frequency of 1,300 rpm (21.67 Hz). Powders remained under stirring for additional 10 min after the end of maltodextrin dripping. Finally, samples were dried in a convective oven for 24 h at 60 °C. Unloaded and non-agglomerated starch was named as "NAS", whereas unloaded agglomerated cornstarch was named as "control". Other samples were named as the lyophilized formulation followed by the percentage incorporated into the cornstarch during the agglomeration process.

Table 8.2. Formulations[a,b] used for the production of curcumin/VD3-enriched cornstarch samples

Formulation	Maltodextrin (g)	Water (g)	Lyophilized liposomes (g)	Cornstarch (g)
NAS	-	-	-	100
Control	15.70	6.73	-	89.42
F0-6%	19.28	8.26	5.27 (L0)	89.42
F0-8%	23.37	10.02	5.96 (L0)	89.42
F0-10%	27.82	11.92	6.61 (L0)	89.42
F50-6%	18.75	8.04	5.44 (L50)	89.42
F50-8%	22.67	9.72	6.19 (L50)	89.42
F50-10%	26.93	11.54	6.92 (L50)	89.42
F70-6%	18.32	7.85	5.62 (L70)	89.42
F70-8%	22.10	9.47	6.43 (L70)	89.42
F70-10%	26.20	11.23	7.23 (L70)	89.42

a. The amount of each ingredient was calculated using Microsoft Excel® Solver tool.

b. The amount of ingredients took into account the moisture content of each lyophilized liposome.

Reference: Own source

8.2.5. Characterization of Cur-VD3-enriched cornstarch

8.2.5.1. Water activity and moisture content

Water activity and moisture content of samples were determined as described in section 8.2.3.1.

8.2.5.2. Solubility and hygroscopicity

Solubility of samples was determined as described in section 8.2.3.2. Hygroscopicity was also measured as described in section 2.3.2. but mass of samples used was 0.1 g.

8.2.5.3. Moisture sorption isotherms

Equilibrium moisture content of agglomerated blends was determined using the standard static gravimetric method described in Labuza (1985). To this purpose, 0.3 g of samples were weighted into glass jars and stored in desiccators above six saturated salt

solutions with water activity values ranging from 0.244 to 0.848. Desiccators were stored for 4 wks at 25 °C. Samples were weighted periodically during equilibration until no difference was observed in the gain in weight. The equilibrium moisture content data was plotted against the corresponding water activity and fitted using six mathematical models presented from Eqs. (5) to (10). To evaluate the ability of each model to fit the experimental data, the root mean square (RMS, Eq. (11)) and the coefficient of determination (R^2) were calculated.

GAB model: $X = (X_m * c * k * a_w) / [(1 - k * a_w) * (1 + (C - 1) * k * a_w)]$ (5)

Halsey model: $X = (-A / \ln a_w)^{\wedge} (1/b)$ (6)

Peleg model: $X = A * (a_w {}^{\wedge} B) + C * (a_w {}^{\wedge} D)$ (7)

Oswin model: $X = A * (a_w / 1 - a_w)^{\wedge} B$ (8)

Caurie model: $X = \exp (A + B * a_w)$ (9)

Smith model: $X = A - B * (\ln (1 - a_w))$ (10)

where "X" is the equilibrium moisture content, "X_m" is the monolayer moisture content, "a_w" is the water activity, and "c", "k", "A", "B", "C", and "D" are constants.

$$RMS = \sqrt{\sum[((u_D - u_P)/u_D)^{\wedge} 2] / N} \text{ x } 100\%$$ (11)

where "u_D" is the experimental equilibrium moisture content (g water/g dry matter), "u_P" is the equilibrium moisture content calculated from model (g water/g dry matter), and "N" is the number of fitted points.

8.2.5.4. Quantification of encapsulated curcumin and vitamin D₃

8.2.5.4. Quantification of encapsulated curcumin and vitamin D$_3$

Curcumin and vitamin D$_3$ content in agglomerated samples were determined following the methods described in sections 8.2.3.3 and 8.2.3.4., respectively, but mass of samples used was 0.5 g.

8.2.5.5. Scanning electron microscopy (SEM)

Morphology of agglomerated particles was observed by SEM following the procedure shown in section 8.2.3.5.

8.2.5.6. Mean particle size and particle size distribution

Average particle size and particle size distribution were determined using ImageJ (University of Wisconsin-Madison, Madison, Wisconsin, USA) and Origin 2020 (OriginLab Co., Northampton, Massachusetts, USA) software. SEM micrographs previously obtained for the morphology analysis were processed in ImageJ to determine the area of each particle (Dacanal et al., 2016). A minimum number of 500 particles was set for a good representation of the whole. The equivalent diameter of a circular particle of same surface area was calculated for each particle using Eq. (12). The diameters were classified into standard size intervals ranging from 0.25 to 3000 μm and frequency distributions calculated using the Analyze Data tool of Microsoft Excel® 2016 software (Redmond, WA, USA). Number-based histograms and average particle sizes were assessed using Origin. The De Brouckere mean diameter was calculated using Eq. (13), whereas the dispersion of distribution was measured as the span ratio (Eq. (14)).

$$d_{eq} = \sqrt{(4S_{eq})/\pi} \tag{12}$$

where d_{eq} is the equivalent diameter and S_{eq} is the 2-D surface area;

$$D_{[4,3]} = \Sigma \, (f_i * d_{eq}^4) \, / \, \Sigma \, (f_i * d_{eq}^3) \tag{13}$$

where f_i is the number fraction of the equivalent particle diameter;

$$\text{span} = (d_{90} - d_{10}) \, / \, d_{50} \tag{14}$$

where d_{90}, d_{10} and d_{50} are the equivalent diameters evaluated at 90%, 10%, and 50% of the size distribution, respectively.

8.2.5.7. Physical analysis

Particle density (ρ_p) was measured by pycnometry with helium as displacement medium. Bulk density (ρ_b) was calculated by measuring the volume of a known mass of powder sample poured into a graduated cylinder. Tapped density (ρ_t) analysis was conducted using a Tap Density Tester (Logan, TAP-2S, Somerset, NJ, USA) in which 30 g of sample loaded into a graduated cylinder were tapped for 1000 times. Porosity was estimated from density values previously obtained as shown in Eq. (15).

$$\varepsilon = 1 - (\rho_b/\rho_p) \tag{15}$$

Flowability and cohesiveness of the powders were evaluated in terms of Carr index (CI, %) and Hausner ratio (HR), respectively, using density values as shown in Eqs. (16) and (17). Flowability was also evaluated by FlodexTM test apparatus (Hanson Research, USA). The fluidity is reflected by the "Flodex" value, which is the minimal diameter of a disk orifice through which a powder can pass without the need of additional pressure, avoiding arch formation.

$$CI = (\rho_t - \rho_b)/\rho_t \tag{16}$$
$$HR = \rho_t/\rho_b \tag{17}$$

The wetting time (t_w) was determined according to Dacanal and Menegalli (2010). Initially, 5 g of powder were placed onto a flat surface plate located above a cylinder containing 50 mL water at 25 °C. After the removal of the flat surface, the powder came into contact with water, and the time needed for the complete wetting of the sample was recorded.

8.2.5.8. Instrumental colorimetry

Color of samples was measured using a dual-beam non-contact reflectance spectrophotometer (AerosTM, HunterLab, VA, USA). Colorimetric measurements were expressed in CIEL*a*b* color space (Commission Internationale de l'Eclairage). The light source was a D65 (day light) lamp and 10° was the viewing angle. From the results obtained for lightness (L*) and chromaticity (a* and b*), the colorfulness was estimated by calculating the Chroma (C_{ab}*) value using Eq. (18) and the vector degree of rotation by the Hue angle (h_{ab}*) using Eq. (19). Total color difference (TCD) between the 1st and 30th days of storage were also calculated using Eq. (20).

$$C_{ab}^* = \sqrt{(a^*)^2 + (b^*)^2} \tag{18}$$

$$h_{ab}^* = 180° - tan^{-1}(b^*/a^*) \tag{19}$$

$$\Delta E = \sqrt{(L^* - L_0^*)^2 + (a^* - a_0^*)^2 + (b^* - b_0^*)^2} \tag{20}$$

8.2.5.9. Pasting properties

A Rapid Visco Analyzer (RVA model 4, Newport Scientific Pty, Warriewood, New South Wales, Australia) was used to obtain the pasting properties of cornstarch samples according to the procedure described in Toniazzo et al. (2017). For the analysis, precalculated amounts of cornstarch were weighed to reach 3 g of solids adjusted to 14% moisture and mixed to 25 g of deionized water in an RVA canister. The temperature profile used was Standard 2 with 23 min heating profile. Pasting temperature, peak viscosity, time peak viscosity, breakdown viscosity, final viscosity and setback were all determined from RVA profiles by using Thermocline v 3.0 software (Newport Scientific Pty, Australia).

8.2.5.10. Structural analyses

Fourier-transform infrared spectroscopy (FTIR) of samples at 1st day was carried out using a Perkin Elmer Spectrometer (Spectrum One, USA) within range of 4000 to 650 cm^{-1} in transmission mode, and 1 cm^{-1} resolution.

X-ray diffraction (XRD) analysis was also conducted at 1st day of storage but using an X-ray diffractometer (MiniFlex 600, Rigaku, Japan), with copper anode tube with λ = 1.5418 Å and graphite monochromator in the diffracted beam. The scanning was performed within range of 5 to 40° in steps of 0.02° at 2°/min speed.

8.2.6. Statistical analysis

Differences between mean values were tested using one-way analysis of variance (ANOVA). The significance of the differences was thereafter tested with Tukey's test at $p < 0.05$. Measurements were performed at triplicate and are exhibited as mean ± standard deviation values. Statistical tests were performed using SAS version 9.4 software (SAS Institute, Cary, NC, USA).

8.3. Results and discussion

8.3.1. Production and characterization of Cur-VD3-co-loaded lyophilized liposomes

8.3.1.1. Physicochemical aspects

The visual aspect of Cur-VD3-co-loaded lyophilized liposomes is shown in Fig. 8.1a. Powders presented an intense yellow color attributed to curcumin, whereas finer particles were obtained by L0 sample produced with the pure saturated phospholipid solely (P90H).

Physicochemical parameters obtained for the samples are summarized in Table 8.3. Regarding water activity and moisture content, values obtained were <0.3 for aw and <6% for MC, which suggests an excellent stability (Tan et al., 2015). Although no significant difference was observed in aw with the increase in LS40 content, the MC of L0 sample was significantly higher (p <0.05) than L50 prepared at a 50:50 ratio of P90H and LS40. Higher MC of powders produced by drying process are usually associated to a higher viscosity of previous suspensions (Bhandari, 1993). During drying, phospholipids tend to migrate to the surface of powders due to the difference of density and eventually create a barrier contrary to moisture transfer. As mixed membranes tend to be less viscous and destabilize more easily, it is reasonable to assume that L0 sample may present the highest kinetic stability among samples as stiffer PC bilayers may be formed from the highest content of saturated phospholipids. This resistance to diffuse possibly hindered the phospholipid migration to surface, thus increasing the moisture content of this sample (Baysan et al., 2021).

Unsaturated phospholipids also promoted an increase in both solubility and hygroscopicity of lyophilized vesicles. Samples containing LS40 (L50 and L70) were highly soluble (>95%), whereas L0 exhibited moderated solubility. Values found for L50 and L70 are within the range of solubility for food powders (i.e., 67-05-99.98%) (Jaya & Das, 2004). The substantial high values of solubility may be attributed to the presence of sucrose, which presents a hydrophilic characteristic and was used as carrier molecule during proliposome production and added as cryoprotectant during lyophilization. Furthermore, it is known that lower the moisture content of a powder, the more soluble it is (Balci-Torun & Ozdemir, 2021). In this context, the higher dissolution rates of L50 and L70 samples are corroborated by their lower moisture content. Regarding hygroscopicity, the high values observed for samples were expected due to their high sugar content. L50 and L70 can be considered as hygroscopic powders as values for this parameter were higher than 10% (Bhandari, 2013). As discussed previously, the dense molecular packaging of liposomes in L0 sample may have enhanced the barrier properties towards water, thus reducing moisture absorption from the air. Overall, the increasing in hygroscopicity is resulted from decreased aw and MC values which are often related to increases in the driving forces for adsorption (Samborska, Langa & Bakier, 2015).

Curcumin content preserved in the powders are also exhibited in Table 8.3. The representative linear equation of curcumin in methanol was [Curc] = 0.2423 * Abs – 0.0007, calculated by the least square method. Limits of quantification (LOQ) and detection (LOD) were

0.791 ppm and 0.261 ppm, respectively. L0 showed the highest concentration of this bioactive on the first day after production (1180 ± 44 mg/g sample) and retained up to 99.6% over 30 days of storage. The higher saturation of P90H phospholipids may have resulted to increased van der Waals interactions and a formation of larger vesicles (Tai et al., 2020). Therefore, it is reasonable to assume that larger vesicles must have encapsulated higher amounts of curcumin. Also, the higher stiffness of saturated PC bilayers in L0 vesicles may have contributed to the higher retention of curcumin than L50 and L70, in which less rigid and more permeable membranes were formed (Tai et al., 2020). Besides the highest curcumin retention showed by L0, L50 and L70 have also proven to be efficient carriers for this compound as entrapped concentrations in these samples were up to 98.1 and 94.9%, respectively. Finally, it is also suitable to assume that embedded curcumin was most likely located in regions next to surface in L0 vesicles due to the lowest value of solubility observed for this sample. On this basis, the presence of a considerable amount of hydrophobic bioactive onto the surface of a powder may reduce its solubility (Neves et al., 2019).

Vitamin D$_3$ concentrations in the Cur-VD3-co-loaded lyophilized liposomes were also high over the 30 days of storage as reported in Table 8.3, reaching up to 98.8% in L50. Representative linear equation for this bioactive in methanol/acetonitrile 9:1 v/v was [VD3] = 1532.2 * Area + 5751.2, calculated by the least square method. Limits of quantification (LOQ) and detection (LOD) were 190.7 IU/mL and 62.9 IU/mL, respectively. Unlike curcumin, VD3 retention was significantly (p <0.05) higher in samples containing LS40. Concentrations were twice higher in L50 and L70 than L0 even on the first storage day. First, it is known that the presence of unsaturated phospholipids leads to a decrease in the fluidity and an increasing in membrane curvature "frustration" of vesicles, which results in size reduction (Tai et al., 2020). The higher VD3 content in LS40-based samples is corroborated by the small diameter displayed by vesicles produced using P90H and LS40 (Chaves & Pinho, 2020). Moreover, it is possible that VD3 filled the spaces that were formed in the lipid bilayers by the kinked tails of unsaturated phospholipids in a similar manner as cholesterol (Chaves et al., 2018). This filling may have led to a decrease in flexibility and permeability of the surrounding lipid chains, protecting the bioactive against prooxidants (Mulrooney et al., 2021).

SEM images of lyophilized liposomes are shown in Fig 8.1b. Samples presented a great variety of shapes, mostly irregular, a smooth and flattered surface, and sharped edges. Powders were mainly amorphous and did not exhibit crystalline fragments of curcumin or VD3 in their

surface. According to Kaushik and Roos (2007), an amorphous glass-like state could improve the protection over entrapped molecules from the exposure to heat and oxygen. Also, powders were very porous, which validates the high values shown for solubility.

Figure 8.1. Schematic representation of Cur-VD3-enriched cornstarch production. (A) visual aspect of Cur-VD3-co-loaded lyophilized liposomes; (B) SEM micrographs of Cur-VD3-co-loaded lyophilized liposomes (in details it is possible to observe smaller vesicles attached to the surface of dried vesicles and their porous structure); (C) visual aspect of unloaded (control) and Cur-VD3-enriched cornstarch samples produced with different concentrations of lyophilized liposomes (6, 8, and 10% w/w). Dried vesicles were produced at a 50:50 w/w saturated:unsaturated phospholipid ratio
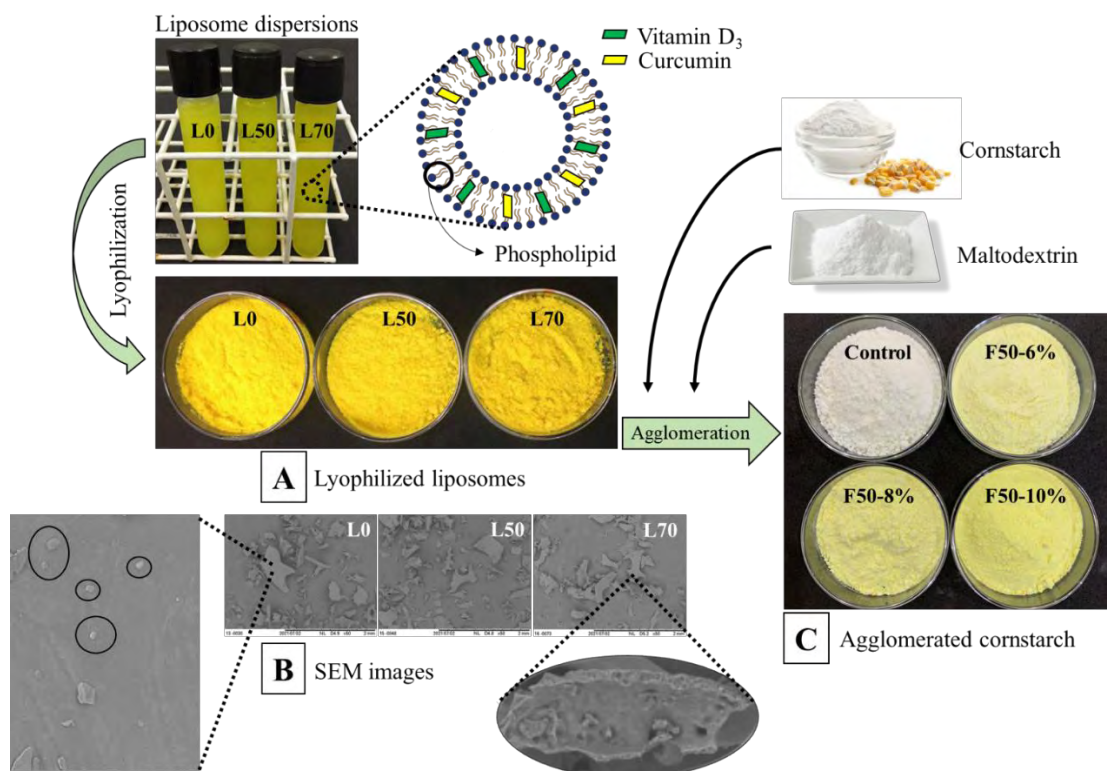
Reference: Own source

Table 8.3. Physicochemical parameters obtained for Cur-VD3-co-loaded lyophilized liposomes

Parameters		Formulations		
		L0	L50	L70
Water activity (-)		$0.21^A \pm 0.00$	$0.21^A \pm 0.01$	$0.19^A \pm 0.01$
Moisture content (%)		$5.43^A \pm 0.24$	$3.97^B \pm 0.46$	$4.51^{AB} \pm 0.44$
Solubility (% solubilized sample)		$65.2^B \pm 1.6$	$95.1^A \pm 1.3$	$95.6^A \pm 1.4$
Hygroscopicity (g adsorbed water/100 g of d.m.)		$8.5^B \pm 0.7$	$15.4^A \pm 0.5$	$14.2^A \pm 0.6$
Curcumin content (mg/g of sample)	1st day	$1180^{Aa} \pm 44$	$983^{Ba} \pm 29$	$1062^{Ba} \pm 32$
	30th day	$1175^{Aa} \pm 34$	$964^{Ba} \pm 14$	$1008^{Ba} \pm 36$
Curcumin retention (%)		99.6	98.1	94.9
Vitamin D_3 content (IU/g of sample)	1st day	$3059^{Ca} \pm 46$	$7073^{Aa} \pm 40$	$6386^{Ba} \pm 158$
	30th day	$2873^{Ca} \pm 140$	$6991^{Aa} \pm 403$	$6102^{Bb} \pm 69$
Vitamin D_3 retention (%)		93.9	98.8	95.6

Means followed by the same uppercase letter in the same line and by the same lowercase letter in the same column were not significantly different (p > 0.05) by Tukey's test.

Reference: Own source

8.3.1.2. Differential scanning calorimetry (DSC)

DSC thermograms obtained for lyophilized liposomes are depicted in Fig. 8.2. As can be seen, an increase in LS40 concentration led to a decrease in the first endothermic transition of liposomes. Unsaturated phospholipids have mono and polyunsaturated fatty acids with phase transitions mainly below 0 °C, which may have contributed to a shift in this peak to lower temperatures (van Hoogevest, 2017). Also, a higher phase transition could be the result of a

more rigid and stable membrane in L0 due to the presence of a higher number of saturated phospholipids (Yokota, Moraes & Pinho, 2012). Additionally, moisture content has also strong influence on glass transition temperatures, decreasing it to lower regions with increased moisture, thus low values for this parameter are required to increase their stability (Sepúlveda et al., 2021). In this context, L0 presented the lowest value of moisture, suggesting higher stability over storage (Table 8.2). The second endothermic peak is probably related to sucrose melting. The presence of this peak is mainly due to residual moisture content after drying or to more amorphous areas. This peak is shifted left as the higher the number of irregular particles. The occurrence of these amorphous areas may be the reason of the higher solubility values obtained for L50 and L70 (Table 8.2). Finally, the highest value of this peak obtained for L0 (170.1 °C) may be related to higher bioactive loading as they usually present higher melting temperatures (Chezanoglou & Goula, 2021).

Figure 8.2. Thermograms obtained by DSC for the Cur-VD3-co-loaded lyophilized liposomes
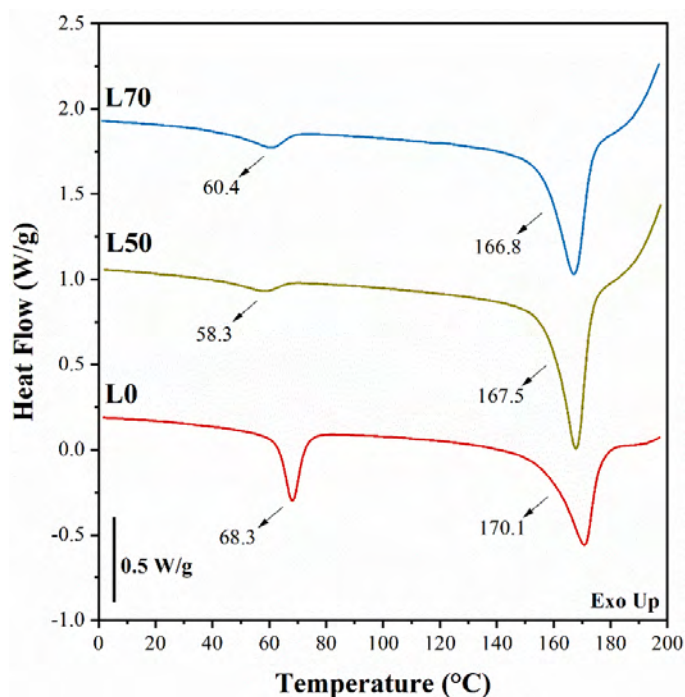
Reference: Own source

8.3.2. Production and characterization of Cur-VD3-enriched cornstarch

8.3.2.1. Powder properties

Physicochemical parameters of all cornstarch samples are given in Table 8.4. Water activity and moisture content values of agglomerated powders were lower than <0.3 and <6%, respectively, which suggests an excellent stability (Tan et al., 2015). Agglomeration led to a significant reduction (p < 0.05) in these parameters compared to non-agglomerated cornstarch, highlighting some of the advantages related to this process regarding handling simplifications and microbiological safety as most microorganisms have their development delayed in media with aw <0.6 and MC <10% (Beuchat et al., 2013). Also, maltodextrin forms a moisture-protective barrier on the surface of sugar-based powders (Chronakis, 1998). Agglomeration improved cornstarch solubility; unloaded agglomerated cornstarch (control) had solubility 10 times higher than non-agglomerated cornstarch (NAS); whereas for blended samples this value was almost 30 times higher. The higher values obtained for enriched samples than control reflected the positive effects of maltodextrin and sucrose due to their hydrophilic nature. Conversely, sucrose was also deleterious to a significant (p <0.05) increase in hygroscopicity. However, maltodextrin has been used as a solution for typical problems related to hygroscopicity by decreasing the stickiness and increasing stability of dehydrated products (Valenzuela & Aguilera, 2015).

Since cornstarch samples showed to be very hygroscopic, understanding the water adsorption behavior becomes fundamental as this property is strongly influenced by storage conditions. Sorption data were fitted to six predictive models, whose adjusted parameters are summarized in Table 8.5. High R^2 and low RMS values are desirable for a suitable model. In this context, Peleg model was the one that best fitted the values from NAS, control, F0-8%, F70-6%, F70-8%, and F70-10% samples, whereas Smith model best fitted the values obtained from F0-10%, F50-6%, F50-8%, and F50-10%. Sample F0-6% was best fitted by GAB and Caurie models. Peleg was chosen to illustrate the fit in Fig. 8.3 as it was the model that best adjusted a higher number of samples, besides exhibiting the highest values for coefficient of determination (R^2 ≥0.993) and the lowest values for root mean square (RSM ≤6.2%). Powders showed typical "J shape" according to type III Brunauer classification, a behavior often found for food rich in soluble components (Al-Muhtaseb, McMinn & Magee, 2002). In general, powders showed a sharped increase in water adsorption at a_w >0.65 but, as expected, the agglomerated blends showed higher hygroscopicity than NAS due to the presence of hydrophilic components such

as sucrose and maltodextrin. Also, native and non-hydrolyzed starch has lower hygroscopicity (Tonon et al., 2009). Conversely, the sudden increase in water adsorption at a_w >0.65 is commonly due to the prominence of solute-solvent interactions associated to sugar dissolution (Frabetti et al., 2021). Control sample showed the highest hygroscopic behavior among all, suggesting a beneficial effect of liposomes addition in reducing this property, probably due the presence of hydrophobic species. A lower hygroscopicity could be related with less surface-active sites for water interactions over particles (Soazo, Rubiolo & Verdini, 2011). Also, maltodextrin may alter the surface stickiness of sugars, acting as an effective drying aid and reducing the amount of adsorbed water (Adhikari et al., 2004). Furthermore, the increase in dried vesicles ratio did not affect the adsorption of water to a large extent, since the adsorption curves for all the samples were very similar. However, an increase in the amount of LS40 seemed to have some impact on the hygroscopic character of the blends. The increase from 6% to 10% w/w of L70 led to a slight increase in the hygroscopicity of samples as can be observed by the behavior of magenta isotherm in Fig. 8.3. Surely, this result was influenced by the higher hygroscopicity values exhibited by the LS40-based dried vesicles (Table 8.3). Finally, the results indicate that samples must to be stored at a_w <0.3 to ensure their stable glassy state.

Curcumin content among samples did not change significantly (p <0.05) on the first storage day as verified in Table 8.4. Curiously, powders containing 10% w/w of lyophilized liposomes did not present higher amounts of curcumin than those produced with 6 and 8% w/w, which suggests sample heterogeneity. However, F50-10% and F70-10% samples retained the highest amounts of the compound over the 30 days of storage with a content up to 96.7% for F50-10%. Also, an increase in LS40 content seemed to lead to an increase in curcumin retention as samples produced with L50 and L70 retained between 82.7% and 96.7% of the bioactive, whilst retentions from 57.8 to 73.3% were exhibited by those produced with L0. Here it is supposed that curcumin was located in the surface region of L0 vesicles. Thus, it is possible that part of the bioactive located in this area was lost during the drying step after agglomeration (60 °C/24 h), which did not happen in the same extent to LS40-contained samples, since probably the bioactive was situated in more internal regions. A similar trend was observed regarding VD3 retention. In this case, F50-10% was also the sample that best entrapped the vitamin throughout the 30 days of storage since day one. The increase in LS40 promoted a VD3 withholding between 89.2-98.2% against 80.7-88.1% observed for blends produced with L0. Overall, a synergistic effect on the Cur-VD3-co-encapsulation seemed promising when

liposomes produced at a 50:50 w/w P90H/LS40 ratio were incorporated into cornstarch particles after agglomeration with maltodextrin. The advantages of using sucrose and cornstarch must also be considered. First, sucrose can interact with the phosphate group of phospholipids, replacing hydrogen bounds that usually exist in water, and stabilizing dry membranes; whereas maltodextrin strengthens the glassy matrix, besides conferring protection against lipid oxidation (Kumar Lekshmi et al., 2021).

Table 8.4 (Continued). Physicochemical parameters obtained for cornstarch samples at 25 °C

Parameters		NAS	Control	F0-6%	F0-8%	F0-10%	F50-6%	F50-8%	F50-10%	F70-6%	F70-8%	F70-10%
								Formulations				
Water activity (-)		$0.44^A \pm 0.01$	$0.04^C \pm 0.00$	$0.05^A \pm 0.00$	$0.05^A \pm 0.00$	$0.05^A \pm 0.00$	$0.05^A \pm 0.00$	$0.05^A \pm 0.00$	$0.04^C \pm 0.00$	$0.06^B \pm 0.00$	$0.05^A \pm 0.00$	$0.04^C \pm 0.00$
Moisture content (%)		$11.02^A \pm 0.34$	$3.97^B \pm 0.25$	$4.67^B \pm 0.19$	$4.28^B \pm 0.26$	$3.81^B \pm 0.16$	$4.19^B \pm 0.22$	$4.18^B \pm 0.23$	$3.95^B \pm 0.41$	$4.64^B \pm 0.15$	$4.36^B \pm 0.52$	$4.04^B \pm 0.30$
Solubility (% solubilized sample)		$0.5^G \pm 0.0$	$5.1^F \pm 0.2$	$9.7^E \pm 0.6$	$11.1^D \pm 0.4$	$12.4^{BC} \pm 0.3$	$10.6^{DE} \pm 0.2$	$12.6^{BC} \pm 0.4$	$14.7^A \pm 0.6$	$11.7^{CD} \pm 0.3$	$13.1^B \pm 0.7$	$14.3^A \pm 0.2$
Hygroscopicity (g adsorbed water/100 g of d.m.)		$5.7^C \pm 1.4$	$8.2^B \pm 0.1$	$14.6^A \pm 0.4$	$14.5^A \pm 0.0$	$14.3^A \pm 0.0$	$14.5^A \pm 0.4$	$14.1^A \pm 0.4$	$13.9^A \pm 0.1$	$14.2^A \pm 0.1$	$14.7^A \pm 0.2$	$14.1^A \pm 0.5$
Curcumin content (mg/g of sample)	1st day	-	-	$54.4^{Aa} \pm 5.1$	$50.6^{Aa} \pm 4.5$	$78.0^{Aa} \pm 16.7$	$52.3^{Aa} \pm 2.1$	$60.8^{Aa} \pm 8.8$	$72.2^{Aa} \pm 3.6$	$68.2^{Aa} \pm 8.7$	$53.3^{Aa} \pm 4.3$	$68.8^{Aa} \pm 18.3$
	30th day	-	-	$39.9^{Db} \pm 0.5$	$36.4^{Db} \pm 0.9$	$45.1^{CDb} \pm 5.2$	$46.3^{BCDa} \pm 3.2$	$54.6^{BCa} \pm 8.3$	$69.8^{Aa} \pm 1.3$	$56.4^{BCa} \pm 5.3$	$48.9^{BCDa} \pm 2.3$	$58.5^{ABa} \pm 6.4$
Curcumin retention (%)		-	-	73.3	71.9	57.8	88.5	89.8	96.7	82.7	91.7	85.0
Vitamin D_3 content (IU/g of sample)	1st day	-	-	$283^{Da} \pm 11$	$300^{Da} \pm 35$	$312^{Da} \pm 13$	$381^{Ca} \pm 4$	$421^{BCa} \pm 15$	$546^{Aa} \pm 7$	$385^{Ca} \pm 20$	$411^{Ca} \pm 10$	$458^{Ba} \pm 8$
	30th day	-	-	$248^{EFb} \pm 8$	$242^{Fb} \pm 9$	$275^{Eb} \pm 5$	$357^{Db} \pm 11$	$394^{BCa} \pm 10$	$487^{Ab} \pm 5$	$378^{CDa} \pm 10$	$378^{CDa} \pm 20$	$417^{Bb} \pm 11$
Vitamin D_3 retention (%)		-	-	87.6	80.7	88.1	93.7	93.6	89.2	98.2	92.0	91.0
De Brouckere D[4,3] mean diameter (μm)		$270^C \pm 10$	$358^C \pm 23$	$1928^{AB} \pm 125$	$1874^{AB} \pm 247$	$2034^A \pm 137$	$2000^A \pm 218$	$2003^A \pm 147$	$2075^A \pm 115$	$1937^{AB} \pm 146$	$1530^B \pm 79$	$2076^A \pm 148$
d_{10} (μm)		$15^E \pm 1$	$13^E \pm 3$	$45^{BC} \pm 2$	$38^{CD} \pm 3$	$31^D \pm 6$	$64^A \pm 7$	$36^{CD} \pm 4$	$38^{CD} \pm 6$	$40^{CD} \pm 3$	$54^{AB} \pm 2$	$37^{CD} \pm 2$
d_{50} (μm)		$105^D \pm 2$	$109^D \pm 21$	$188^{BC} \pm 8$	$235^A \pm 2$	$156^C \pm 3$	$217^{AB} \pm 21$	$231^A \pm 13$	$228^A \pm 9$	$245^A \pm 9$	$222^{AB} \pm 13$	$191^B \pm 11$
d_{90} (μm)		$200^E \pm 3$	$303^D \pm 3$	$645^C \pm 13$	$1002^B \pm 71$	$1241^A \pm 52$	$1000^B \pm 16$	$1235^A \pm 42$	$1262^A \pm 15$	$1240^A \pm 14$	$1000^B \pm 32$	$1009^B \pm 16$
Span (-)		$1.8^E \pm 0.1$	$2.7^{DE} \pm 0.2$	$3.2^{CDE} \pm 0.5$	$4.1^{BCD} \pm 0.9$	$7.7^A \pm 0.7$	$4.3^{BC} \pm 0.5$	$5.2^B \pm 0.7$	$5.4^B \pm 0.3$	$4.9^B \pm 0.8$	$4.3^{BC} \pm 0.3$	$5.1^B \pm 0.1$
Bulk density (kg/m³)		$512^E \pm 10$	$540^D \pm 15$	$717^A \pm 31$	$699^{AB} \pm 16$	$644^{BC} \pm 8$	$657^{BC} \pm 16$	$662^{ABC} \pm 8$	$622^C \pm 20$	$626^C \pm 13$	$654^{BC} \pm 36$	$617^C \pm 19$
Tapped density (kg/m³)		$745^{DE} \pm 11$	$658^G \pm 22$	$813^{AB} \pm 22$	$827^A \pm 13$	$693^{FG} \pm 10$	$790^{BC} \pm 0$	$804^{AB} \pm 12$	$715^{EF} \pm 0$	$798^{ABC} \pm 12$	$805^{AB} \pm 12$	$763^{CD} \pm 11$
Particle density (kg/m³)		$656^D \pm 0$	$1071^{BC} \pm 57$	$1112^{AB} \pm 26$	$1090^{ABC} \pm 29$	$1067^{BC} \pm 4$	$1070^{BC} \pm 16$	$1067^{BC} \pm 20$	$1042^{BC} \pm 15$	$1059^{BC} \pm 8$	$1067^{BC} \pm 12$	$1061^{BC} \pm 12$
Carr's index (%)		$31^A \pm 2$	$18^{BCD} \pm 2$	$12^{DE} \pm 2$	$15^{BCD} \pm 3$	$7^E \pm 1$	$17^{BCD} \pm 2$	$18^{BCD} \pm 0$	$13^{CDE} \pm 3$	$21^B \pm 3$	$19^{BC} \pm 3$	$19^{BC} \pm 2$
Hausner ratio (-)		$1.45^A \pm 0.0$	$1.22^E \pm 0.0$	$1.13^J \pm 0.0$	$1.18^H \pm 0.0$	$1.08^K \pm 0.0$	$1.20^G \pm 0.0$	$1.21^F \pm 0.0$	$1.15^I \pm 0.0$	$1.27^B \pm 0.0$	$1.23^D \pm 0.0$	$1.24^C \pm 0.0$
Bulk porosity (-)		$0.22^C \pm 0.01$	$0.50^A \pm 0.02$	$0.37^B \pm 0.02$	$0.36^B \pm 0.04$	$0.40^B \pm 0.00$	$0.38^B \pm 0.01$	$0.38^B \pm 0.02$	$0.39^B \pm 0.02$	$0.41^B \pm 0.00$	$0.39^B \pm 0.04$	$0.42^B \pm 0.02$

Table 8.4. Physicochemical parameters obtained for cornstarch samples at 25 °C

Parameters	Formulations										
	NAS	Control	F0-6%	F0-8%	F0-10%	F50-6%	F50-8%	F50-10%	F70-6%	F70-8%	F70-10%
FLODEX index (mm)	$26^A \pm 1$	$6^{BC} \pm 1$	$5^C \pm 1$	$5^C \pm 1$	$4^C \pm 1$	$8^B \pm 1$	$6^{BC} \pm 1$	$4^C \pm 1$	$6^{BC} \pm 1$	$5^C \pm 1$	$5^C \pm 1$
Wetting time (min)	$1.9^F \pm 0.5$	$2.1^F \pm 0.3$	$22.8^{CDE} \pm 8.2$	$69.3^B \pm 2.5$	$102.3^A \pm 29$	$11.3^{CDE} \pm 2.2$	$40.9^{BCD} \pm 1.6$	$43.4^{BC} \pm 1.7$	$10.4^{DE} \pm 2.5$	$13.4^{CDE} \pm 3.3$	$11.1^{DEa} \pm 0.6$

Reference: Own source

Figure 8.3. Water sorption isotherms of cornstarch samples fitted to Peleg model. Ternary blends of cornstarch + maltodextrin + lyophilized liposomes were produced using different concentrations of dried vesicles (A) 6%, (B) 8 % and (C) 10% w/w at different phospholipid ratios of Phospholipon 90H and Lipoid S40 (P90H:LS40) - F0 (0:100), F50 (50:50), and F70 (30:70)

(a)   (b)   (c)

Table 8.5 (Continued). Predicted parameters obtained by the mathematical models used to fit the moisture sorption isotherm data of cornstarch samples at 25 °C

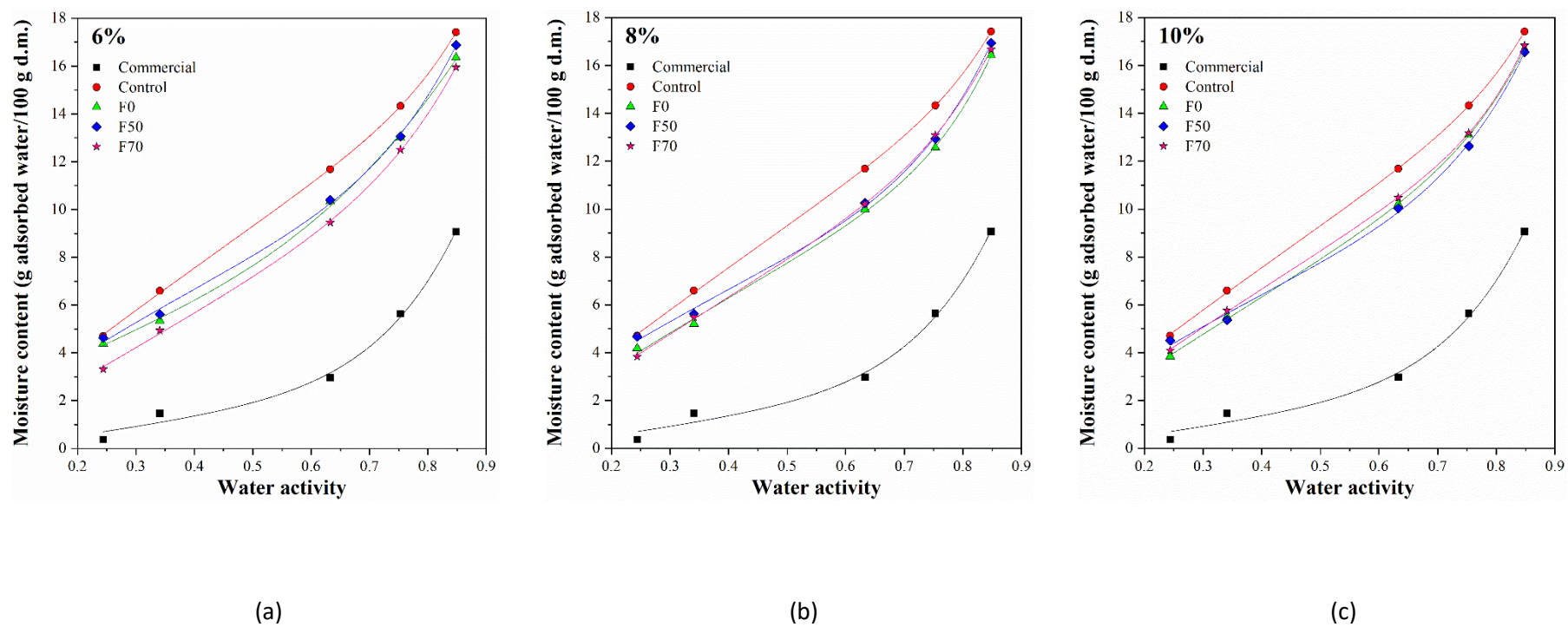| Formulation	Model	X_m (g H_2O/100g d.m.)	C	K	A	B	C	D	R^2	RMS (%)
NAS	GAB	2.08 ± 1.50	1.05 ± 1.32	0.96 ± 0.09	-	-	-	-	0.9921	7.7
	Halsey	-	-	-	1.35 ± 0.24	0.94 ± 0.09	-	-	0.9872	12.6
	Peleg	-	-	-	17.1 ± 6.64	6.78 ± 7.00	4.32 ± 7.79	1.29 ± 1.60	0.9936	6.2
	Oswin	-	-	-	2.00 ± 0.22	0.88 ± 0.07	-	-	0.9916	8.3
	Caurie	-	-	-	-1.83 ± 0.38	4.74 ± 0.48	-	-	0.9890	10.8
	Smith	-	-	-	-1.20 ± 0.66	5.12 ± 0.56	-	-	0.9649	34.4
Control	GAB	8.67 ± 0.96	4.45 ± 0.74	0.67 ± 0.04	-	-			0.9993	1.5
	Halsey	-	-	-	40.8 ± 25.0	1.90 ± 0.23			0.9682	71.1
	Peleg	-	-	-	10.7 ± 4.02	9.55 ± 3.26	17.7 ± 0.61	0.93 ± 0.03	0.9999	0.2
	Oswin	-	-	-	8.74 ± 0.39	0.42 ± 0.03	-	-	0.9867	29.8
	Caurie	-	-	-	1.16 ± 0.07	2.01 ± 0.09	-	-	0.9960	9.0
	Smith	-	-	-	3.13 ± 0.55	7.84 ± 0.47	-	-	0.9893	23.9
F0-6%	GAB	6.30 ± 0.60	5.24 ± 1.11	0.77 ± 0.03	-	-			0.9991	1.8
	Halsey	-	-	-	24.1 ± 10.3	1.76 ± 0.17			0.9809	39.3
	Peleg	-	-	-	13.3 ± 6.05	3.40 ± 2.16	9.59 ± 7.54	0.58 ± 0.53	0.9991	1.9
	Oswin	-	-	-	7.68 ± 0.26	0.45 ± 0.02	-	-	0.9939	12.6
	Caurie	-	-	-	0.94 ± 0.03	2.18 ± 0.05	-	-	0.9992	1.8
	Smith	-	-	-	2.36 ± 0.25	7.54 ± 0.21	-	-	0.9976	5.0

Table 5 (Continued). Predicted parameters obtained by the mathematical models used to fit the moisture sorption isotherm data of cornstarch

samples at 25 °C

Formulation	Model	X_m (g H_2O/100g d.m.)	C	K	A	B	C	D	R^2	RMS (%)
F0-8%	GAB	5.50 ± 0.49	6.08 ± 1.51	0.81 ± 0.03	-	-			0.9989	2.2
	Halsey	-	-	-	19.7 ± 6.66	1.69 ± 0.13			0.9872	26.7
	Peleg	-	-	-	16.2 ± 8.82	8.68 ± 5.18	14.6 ± 2.02	0.92 ± 0.13	0.9990	2.0
	Oswin	-	-	-	7.40 ± 0.18	0.47 ± 0.02	-	-	0.9971	6.0
	Caurie	-	-	-	0.86 ± 0.07	2.27 ± 0.09	-	-	0.9972	5.9
	Smith	-	-	-	2.08 ± 0.16	7.61 ± 0.14	-	-	0.9990	2.1
F0-10%	GAB	5.20 ± 0.42	7.04 ± 1.84	0.82 ± 0.02	-	-			0.9990	2.1
	Halsey	-	-	-	19.5 ± 5.85	1.70 ± 0.12			0.9899	20.6
	Peleg	-	-	-	16.7 ± 7.99	8.36 ± 4.74	14.0 ± 2.11	0.88 ± 0.14	0.9990	2.1
	Oswin	-	-	-	7.34 ± 0.14	0.47 ± 0.01	-	-	0.9982	3.7
	Caurie	-	-	-	0.86 ± 0.08	2.26 ± 0.10	-	-	0.9962	7.8
	Smith	-	-	-	2.11 ± 0.15	7.51 ± 0.13	-	-	0.9991	1.8
F50-6%	GAB	5.63 ± 0.41	7.52 ± 1.78	0.81 ± 0.02	-	-			0.9991	1.8
	Halsey	-	-	-	25.3 ± 8.30	1.77 ± 0.13			0.9889	23.3
	Peleg	-	-	-	14.2 ± 4.15	6.67 ± 4.08	13.8 ± 2.98	0.80 ± 0.18	0.9989	2.2
	Oswin	-	-	-	7.87 ± 0.15	0.45 ± 0.01	-	-	0.9979	4.4
	Caurie	-	-	-	0.97 ± 0.06	2.16 ± 0.08	-	-	0.9971	6.2
	Smith	-	-	-	2.51 ± 0.14	7.63 ± 0.12	-	-	0.9992	1.6

Table 5 (Continued). Predicted parameters obtained by the mathematical models used to fit the moisture sorption isotherm data of cornstarch samples at 25 °C

Formulation	Model	X_m (g H_2O/100g d.m.)	C	K	A	B	C	D	R^2	RMS (%)
F50-8%	GAB	5.27 ± 0.35	9.11 ± 2.34	0.83 ± 0.02	-	-			0.9992	1.8
	Halsey	-	-	-	24.5 ± 6.63	1.76 ± 0.11	-	-	0.9923	16.1
	Peleg	-	-	-	15.8 ± 4.58	6.89 ± 3.74	13.5 ± 2.71	0.78 ± 0.17	0.9990	2.2
	Oswin	-	-	-	7.82 ± 0.10	0.45 ± 0.01	-	-	0.9990	2.1
	Caurie	-	-	-	0.96 ± 0.08	2.17 ± 0.11	-	-	0.9952	10.0
	Smith	-	-	-	2.50 ± 0.13	7.62 ± 0.11	-	-	0.9993	1.4
F50-10%	GAB	5.20 ± 0.43	8.30 ± 2.5	0.83 ± 0.02	-	-			0.9987	2.5
	Halsey	-	-	-	22.3 ± 6.40	1.74 ± 0.11			0.9911	18.1
	Peleg	-	-	-	15.2 ± 5.36	6.83 ± 4.68	13.2 ± 3.39	0.80 ± 0.21	0.9984	3.2
	Oswin	-	-	-	7.59 ± 0.13	0.46 ± 0.01	-	-	0.9984	3.3
	Caurie	-	-	-	0.92 ± 0.08	2.20 ± 0.11	-	-	0.9956	9.0
	Smith	-	-	-	2.34 ± 0.16	7.51 ± 0.13	-	-	0.9990	1.9
F70-6%	GAB	6.25 ± 0.61	3.52 ± 0.61	0.78 ± 0.03	-	-			0.9994	1.2
	Halsey	-	-	-	14.7 ± 6.29	1.60 ± 0.17			0.9779	48.3
	Peleg	-	-	-	14.3 ± 1.94	1.01 ± 0.12	11.8 ± 2.33	6.79 ± 2.99	0.9997	0.7
	Oswin	-	-	-	6.91 ± 0.30	0.50 ± 0.03	-	-	0.9923	16.8
	Caurie	-	-	-	0.70 ± 0.06	2.44 ± 0.08	-	-	0.9980	4.4
	Smith	-	-	-	1.48 ± 0.25	7.79 ± 0.21	-	-	0.9978	4.9

Table 5. Predicted parameters obtained by the mathematical models used to fit the moisture sorption isotherm data of cornstarch samples at 25 °C

| Formulation	Model	X_m (g H_2O/100g d.m.)	C	K	A	B	C	D	R^2	RMS (%)
F70-8%	GAB	6.48 ± 0.55	4.30 ± 0.72	0.77 ± 0.03	-	-			0.9994	1.3
	Halsey	-	-	-	19.8 ± 8.64	1.68 ± 0.17			0.9793	46.6
	Peleg	-	-	-	13.2 ± 2.35	8.06 ± 1.90	15.5 ± 0.79	0.98 ± 0.05	0.9999	0.2
	Oswin	-	-	-	7.53 ± 0.28	0.47 ± 0.03	-	-	0.9933	15.1
	Caurie	-	-	-	0.86 ± 0.06	2.30 ± 0.08	-	-	0.9977	5.1
	Smith	-	-	-	1.99 ± 0.28	7.90 ± 0.24	-	-	0.9973	6.1
F70-10%	GAB	6.43 ± 0.66	5.02 ± 1.13	0.77 ± 0.03	-	-			0.9990	2.2
	Halsey	-	-	-	23.4 ± 10.1	1.74 ± 0.17			0.9807	42.3
	Peleg	-	-	-	16.9 ± 3.12	9.93 ± 1.62	16.0 ± 0.41	0.96 ± 0.03	1.0000	0.1
	Oswin	-	-	-	7.79 ± 0.26	0.46 ± 0.02	-	-	0.9941	13.0
	Caurie	-	-	-	0.94 ± 0.07	2.21 ± 0.09	-	-	0.9969	6.9
	Smith	-	-	-	2.30 ± 0.30	7.80 ± 0.26	-	-	0.9968	7.0

Reference: Own source

Cumulative size distribution curves depicted for the cornstarch samples are showed in Fig. 8.4. De Brouckere's, d_{10}, d_{50}, and d_{90} diameters, and span values are also presented in Table 8.4. As can be seen, the use of wet agglomeration promoted an increase in the diameters of cornstarch particles. The agglomeration of pure cornstarch with maltodextrin (control) increased in 23% the value of de Brouckere's volumetric mean diameter [$D_{4,3}$] compared to NAS sample. Moreover, the ternary blends exhibited even larger diameters of 82 up to 88% than NAS. In this context, maltodextrin has been widely applied as binder solution in food industry as it can improve functional properties of powders due to this increase in particle size (Jinapong et al., 2008). Also, although sucrose produces hard and brittle bridges during wet agglomeration, this disaccharide presents good bonding properties (Barbosa-Canovas & Juliano, 2005). An increase in size was also verified by Szulc & Lenart (2010) after mixing lecithins and sugars solutions during agglomeration. About d_{10} values, only NAS presented a fraction of fines with size smaller than 10 μm at this percentile, then classified as Geldart group C (Dacanal et al., 2016).

Regarding the d_{50} values, a decreasing trend was noticed with an increase in the number of dried vesicles in L50 and L70-based formulations. From Table 8.2, it can be seen that a slightly higher amount of maltodextrin was incorporated to cornstarch when liposome concentrations increased from 6 to 10% (Table 8.2). A similar decrease in size with the increase of binder concentration was also described in Jinapong et al. (2008) and Turchiuli et al. (2005). Span values ranged from 1.8 (from NAS sample) to 7.7 (from F0-10% sample). High span values could be due to the mixing of small particles derived from larger agglomerates to other over-sized particles during agglomeration (Lee et al. 2021). An increase in span was noted in L0 and L50-based formulations with an increase in the concentration of lyophilized vesicles from 6 to 10%. It is possible that the amount of binder solution used was not sufficient to form more homogeneous agglomerates and thus particles remained as the primary ones (Burggraeve et al., 2013). Overall, the presence of lyophilized liposomes increased the polydispersity of cornstarch as NAS and control samples presented the lowest values for this parameter (1.8 and 2.7, respectively).

Fig. 8.5 presents the SEM micrographs obtained for the cornstarch samples. Corroborating the values obtained for mean diameter, images show that agglomeration was achieved by the bonding of several smaller particles through liquid bridging into over-sized structures. The addition of the dried liposomes clearly contributed to the formation of larger

particles, as there is a tendency for the number of smaller particles to decrease with a higher addition of lyophilized vesicles. Agglomeration process did not cause a deformation in the native cornstarch microstructure as well-defined rounded particles are seen in the micrographs obtained for the blends. Agglomerated particles also presented a smooth and porous appearance. An increase in liposome concentration also led to a reduction in the number of finer powders with an increased number of relatively larger and more irregular particle shapes. No presence of crystalline compounds was perceived on the particles surface and no visible differences among samples were noted due to the addition of different concentrations of LS40-based liposomes. Overall, the morphology of powders can be affected by the type and concentration of the binder, and more compact particles were seen when binder concentration was higher. A similar behavior was also observed by the maltodextrin agglomerates produced by Martins & Kieckbusch (2008). Maltodextrin is a low-viscosity binder that can migrate to the surface of powders preventing roughness and keeping the roundness of agglomerated particles, which is also an indicative of increase in flowability (Kumar et al., 2017).

Figure 8.4. Cumulative size distribution of cornstarch samples. The ternary blends of cornstarch + maltodextrin + lyophilized liposomes were produced using different concentrations of dried vesicles (A) 6%, (B) 8 % and (C) 10% w/w at different phospholipid ratios of Phospholipon 90H and Lipoid S40 (P90H:LS40) - F0 (0:100), F50 (50:50), and F70 (30:70)

(a)

(b)

(c)
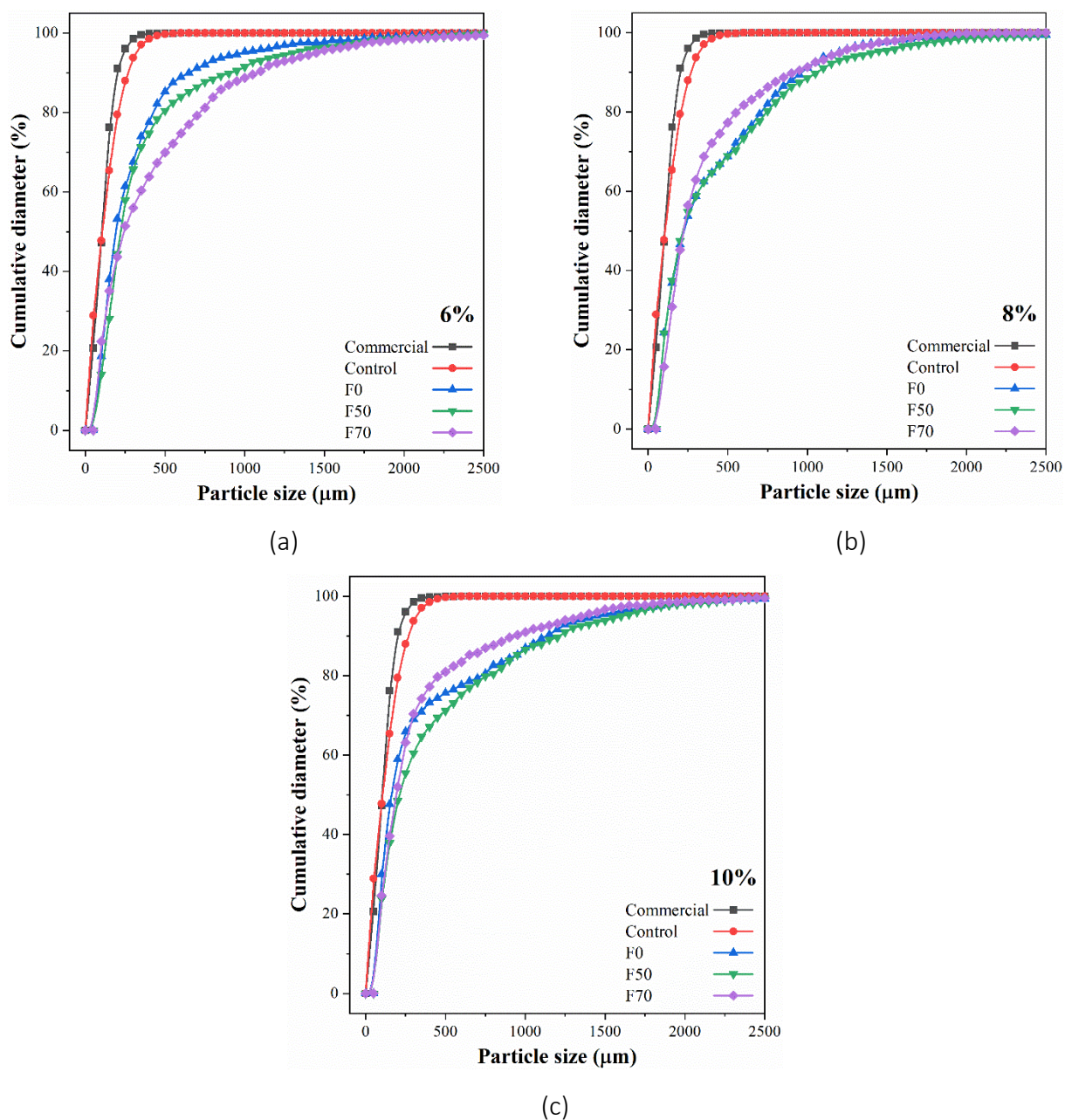
Figure 8.5. SEM micrographs obtained for cornstarch samples. Magnification: 100x.

Error bar: 1 mm
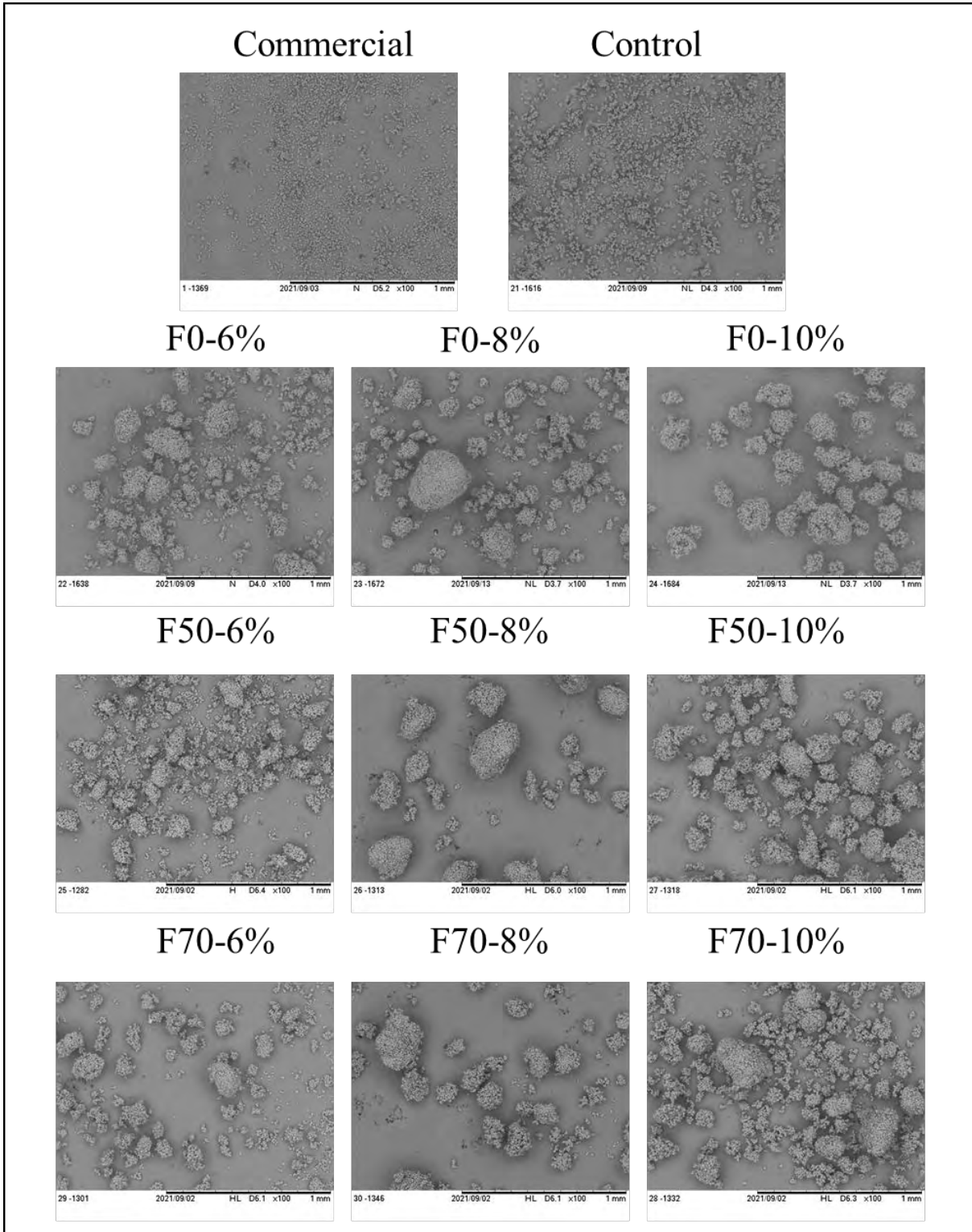
For density properties, NAS exhibited the lowest values for bulk and particle density as reported in Table 8.4. The loose bulk density was 510 ± 10 kg/m³, significantly (p <0.05) lower than values obtained for the remained samples. Particle density was 656 kg/m³ which was also significantly (p <0.05) lower than others. For this reason, this sample also presented the lowest value for porosity ($\varepsilon = 0.22$). Conversely, the blending with lyophilized liposomes led to an increase in bulk density as values retrieved were higher than for control sample ($>540 \pm 15$ kg/m³). In general, the density of a non-agglomerated powder is higher than for an agglomerated powder because of the formation of a porous structure during the process, which involves occluded air or a vacuole (Barkout et al., 2012). Additionally, a decrease in bulk density was noted for L0-based samples with an increase in content of dried vesicles, whereas no significant differences were found among the LS40-based samples.

For tapped density, L0 and L50-based blends displayed a decreasing trend with increasing lyophilized content, whereas no trend was observed for L70-based samples. In general, bulk and tapped density are also influenced by agglomeration as the larger the particle size, the lower is the density (Börjesson et al., 2014). However, this was not observed for the cornstarch samples as blends exhibited the highest values for density when compared to NAS. This was probably due to the presence of sucrose ($\rho_B \approx 1800$ kg/m³), which has a higher density than cornstarch ($\rho_B \approx 1600$ kg/m³). Moreover, food powders can be classified as materials with good flowability due to similar values of tapped and bulk densities. In this sense, F0-10% sample presented the highest similarity between the densities ($\rho_B/\rho_T = 0.93$), whereas pure cornstarch presented the lowest ($\rho_B/\rho_T = 0.69$), suggesting that NAS presented the poorest flowability among samples.

With respect to particle density, L0-based samples showed a decreasing trend with increasing lyophilized content, whereas no trend was observed for LS40-based samples, which indicates similar intra-granular porosity (Park & Yoo, 2020). Curiously, control sample exhibited the highest value for bulk porosity ($\varepsilon = 0.50$), whereas blended samples did not exhibit significant differences (p >0.05) concerning this parameter. Higher values of bulk density and lower values of porosity showed by the blended samples in relation to control may suggest the formation of thicker coating layers with high compactness onto the particles due to the presence of phospholipids (Ji et al., 2017).

The Carr Index (CI) and Hausner ratio (HR) of cornstarch samples are shown in Table 8.4. F0-10% presented the lowest values for CI (7%) and HR (1.08), which indicate "Excellent"

flowability and low cohesiveness (CI: 0-10% and 1.0 < HR < 1.11). On the other hand, samples F0-6%, F0-8% and F50-10% showed "Good" flowability (CI: 10-15% and 1.12 < HR < 1.18), whereas control, F50-6%, F50-8%, F70-8%, and F70-10% samples exhibited "Fair" flowability (CI: 16-20% and 1.19 < HR < 1.25). Lastly, F70-6% presented a "Possible" flowability (CI: 21-25% and 1.26 < HR < 1.34), whereas pure NAS showed "Poor" flowability (CI: 26-31% and 1.25 < HR < 1.45). Thus, wet agglomeration actually promoted an improvement in the handling properties of cornstarch. Another indicative of flowability is FLODEX index. In this context, the decrease of FLODEX values from 26 mm (pure cornstarch) to 4-8 mm (blended samples) also corroborates that agglomeration was improved with the addition of lyophilized liposomes and cornstarch (Toniazzo et al., 2017). It is worth mentioning that an increase in liposome ratio from 6 to 10% w/w improved the flowability of powders produced with L0 (from "Good" to "Excellent"), L50 (from "Fair" to "Good"), and L70 (from "Possible" to "Fair"). Finally, it is well known that powders with finer particles have their flowability compromised (Jinapong et al., 2008). The higher values of mean diameter obtained by the blends than by NAS supports the increased flowability and decreased cohesiveness after agglomeration.

Although agglomeration increases the wettability of food powders, the opposite was observed for the Cur-VD3-enriched cornstarch samples. An increase in the wetting time was significantly ($p < 0.05$) higher for the blended samples than NAS and control samples. This might be due to the higher levels of phospholipids presented in liposomes or superficial curcumin (Ferreira et al., 2018). The poor wettability of cornstarch samples was verified by some particles floating on the surface that did not sink completely below the surface even after several minutes. This impermeable layer at powder/water interface may have resulted in some non-hydrated regions, thus hindering the access of water to penetrate into the particles (Ji et al., 2016).

8.3.2.2. Instrumental colorimetry

The visual aspect of cornstarch samples produced by wet agglomeration is illustrated in Fig. 8.6, whereas CIEL*a*b* colorimetric parameters are summarized in Table 8.6. L* defines luminosity on a scale form black (0) to white (100), a* varies from green (-) to red (+), and b* varies from blue (-) to yellow (+). As reported in Fig. 8.4, NAS and control samples are clearly white, which supports the highest L* values obtained for these samples. However, L* observed for control significantly ($p < 0.05$) decreased over storage time (from 100.01 to 98.11), which

suggests a slight increase in opacity after 30 days. With respect to the blended samples, L* values ranged from 96.02 to 97.93 on the first day of storage, and from 95.90 to 97.45 on the last day of storage. Also, L* from sample F70-8% was the only that did not decrease significantly (p <0.05) over storage time, indicating a slight increase in opacity of most of blended powders. However, L* >90 suggests a high brightness of the samples even after 30 days of storage.

Regarding the results for a* and b*, all samples displayed negative values of a* and positive values for b*, which places them in the second quadrant of the CIEL*a*b* space, where a range from green to yellow is perceived. NAS and control samples presented the lowest results for a* and b* as expected, but only control sample exhibited a decrease (p <0.05) in both parameters over storage time. Values of a* for Cur-VD3-cornstarch samples ranged from -4.22 (F0-6%) to -7.96 (F50-10%) on the first storage day, and from -3.98 (F0-6%) to -8.16 (F50-10%) on the 30th day. On the other hand, values of b* ranged from 30.21 (F0-6%) to 57.27 (F50-10%) on the first storage day, and from 33.68 (F0-6%) to 56.99 (F50-10%) on the 30th day. As intended, an increase in lyophilized liposomes content from 6 to 10% increased the values of a* and b* regardless of formulation. In this context, an increase in curcumin concentration led to an increase of the greenish yellow color of samples as it promoted an increase in both yellow (more negative a*) and green (more positive b*) values.

Chroma (C*) and Hue angle (h*) values were calculated for the cornstarch samples based on the values of L*, a*, and b*. Values of C* ranged from 7.4 (NAS) to 57.8 (F50-10%) on the first storage day, and from 6.7 (NAS) to 57.6 (F50-10%) on the 30th day. The highest values noted for F50-10% reflected the highest a* and b* values obtained by this sample; a characteristic easily perceptible from its clear and stronger yellow coloration (Fig. 8.6). Curiously, blended powders produced with the lowest content of dried samples (F0-6%, F50-6%, and F70-6%) were those in which a C* decrease (p <0.05) was observed, suggesting an improvement in retained color with an increase of liposome content. Moreover, h* values between 90° and 180° were obtained for all the samples, corroborating their greenish yellow color. Interestingly, control and NAS also displayed values of Hue angle in this quadrant, but a yellow color is not visible to the eye due to high values of L*. Therefore, it is reasonable to conclude that these samples presented a "very light-yellow color" that is visibly white. Finally, the total color difference (ΔE) of samples F0-6% and F50-6% were higher than 2.0, which indicated significant changes in color over storage time (Francis & Clydesdale, 1975). Overall,

the lower values obtained for this parameter by most samples reinforced the suitable food coloring property attributed to curcumin.

Figure 8.6. Visual aspect of cornstarch samples on the first day of storage at 25 °C
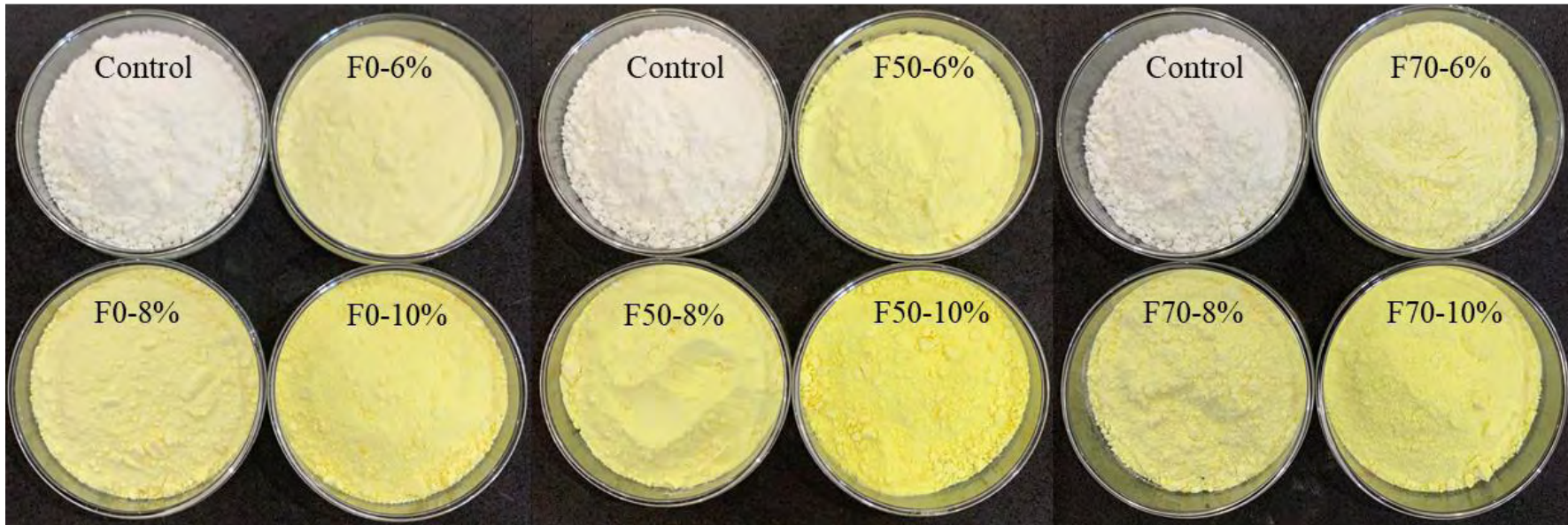
Table 8.6. Colorimetric parameters of the CIEL*a*b* system obtained for cornstarch samples

Parameter		Formulations										
		NAS	Control	F0-6%	F0-8%	F0-10%	F50-6%	F50-8%	F50-10%	F70-6%	F70-8%	F70-10%
a* (-)	1st day	$-0.74^{Ia} \pm 0.01$	$-0.72^{Ia} \pm 0.01$	$-4.22^{Ha} \pm 0.02$	$-4.67^{Ga} \pm 0.05$	$-6.24^{Ea} \pm 0.05$	$-7.44^{Ca} \pm 0.05$	$-7.46^{Ca} \pm 0.05$	$-7.96^{Aa} \pm 0.04$	$-5.61^{Fb} \pm 0.05$	$-6.74^{Da} \pm 0.07$	$-7.82^{Bb} \pm 0.07$
	30th day	$-0.75^{Ia} \pm 0.00$	$-0.65^{Ib} \pm 0.01$	$-3.98^{Hb} \pm 0.02$	$-4.41^{Gb} \pm 0.04$	$-5.30^{Fb} \pm 0.05$	$-7.25^{Cb} \pm 0.05$	$-7.17^{Cb} \pm 0.04$	$-8.16^{Aa} \pm 0.04$	$-6.20^{Ea} \pm 0.05$	$-6.54^{Db} \pm 0.05$	$-7.95^{Ba} \pm 0.04$
b* (-)	1st day	$9.28^{Ca} \pm 0.02$	$7.40^{Ca} \pm 0.03$	$30.21^{Bb} \pm 0.09$	$37.33^{Bb} \pm 0.13$	$44.18^{ABb} \pm 0.15$	$43.63^{ABa} \pm 0.34$	$43.46^{ABa} \pm 0.26$	$57.27^{Aa} \pm 0.36$	$35.82^{Bb} \pm 0.19$	$42.21^{ABa} \pm 0.27$	$49.26^{ABa} \pm 0.33$
	30th day	$9.25^{Ia} \pm 0.02$	$6.62^{Ib} \pm 0.01$	$33.68^{Ha} \pm 0.05$	$37.56^{Fa} \pm 0.10$	$45.14^{Ca} \pm 0.14$	$41.87^{Eb} \pm 0.21$	$43.46^{Da} \pm 0.18$	$56.99^{Ab} \pm 0.23$	$36.88^{Ga} \pm 0.15$	$41.67^{Eb} \pm 0.16$	$49.14^{Ba} \pm 0.15$
L* (-)	1st day	$100.00^{Aa} \pm 0.01$	$100.01^{Aa} \pm 0.01$	$97.28^{BCa} \pm 0.01$	$96.48^{CDa} \pm 0.01$	$95.16^{Ea} \pm 0.01$	$97.92^{Ba} \pm 0.01$	$97.53^{Ba} \pm 0.01$	$96.02^{DEa} \pm 0.02$	$97.93^{Ba} \pm 0.01$	$97.47^{BCa} \pm 0.02$	$96.84^{Ba} \pm 0.02$
	30th day	$100.00^{Aa} \pm 0.01$	$98.11^{Bb} \pm 0.00$	$96.14^{Gb} \pm 0.01$	$96.09^{Hb} \pm 0.01$	$95.88^{Ib} \pm 0.02$	$96.18^{Gb} \pm 0.02$	$97.08^{Eb} \pm 0.02$	$96.50^{Fb} \pm 0.02$	$97.15^{Db} \pm 0.02$	$97.45^{Ca} \pm 0.02$	$95.90^{Ib} \pm 0.02$
C* (-)	1st day	$7.4^{Ia} \pm 0.0$	$9.3^{Ha} \pm 0.0$	$30.5^{Ga} \pm 0.1$	$37.6^{Ea} \pm 0.1$	$44.6^{Ca} \pm 0.2$	$44.3^{Ca} \pm 0.3$	$44.1^{Ca} \pm 0.3$	$57.8^{Aa} \pm 0.4$	$36.3^{Fa} \pm 0.2$	$42.7^{Da} \pm 0.3$	$49.9^{Ba} \pm 0.3$
	30th day	$6.7^{Ib} \pm 0.0$	$9.3^{Ha} \pm 0.0$	$33.9^{Gb} \pm 0.0$	$37.8^{Fa} \pm 0.1$	$45.5^{Cb} \pm 0.1$	$42.5^{Eb} \pm 0.2$	$44.1^{Da} \pm 0.2$	$57.6^{Aa} \pm 0.2$	$37.4^{Fb} \pm 0.2$	$42.2^{Ea} \pm 0.2$	$49.8^{Ba} \pm 0.2$
h* (°)	1st day	$95.6^{Ha} \pm 0.1$	$94.6^{Ia} \pm 0.0$	$98.0^{Ea} \pm 0.0$	$97.1^{Ga} \pm 0.0$	$99.7^{Aa} \pm 0.0$	$99.7^{Aa} \pm 0.0$	$97.9^{Fa} \pm 0.0$	$98.9^{Da} \pm 0.0$	$98.9^{Da} \pm 0.0$	$99.1^{Ba} \pm 0.0$	$99.0^{Ca} \pm 0.0$
	30th day	$95.6^{Ha} \pm 0.0$	$94.6^{Ia} \pm 0.0$	$96.7^{Gb} \pm 0.0$	$96.7^{Gb} \pm 0.0$	$96.7^{Gb} \pm 0.0$	$99.8^{Ab} \pm 0.0$	$99.4^{Cb} \pm 0.0$	$98.1^{Fb} \pm 0.0$	$99.5^{Bb} \pm 0.0$	$98.9^{Eb} \pm 0.0$	$99.2^{Db} \pm 0.0$
ΔE (-)		$1.19^{E} \pm 0.01$	$1.90^{C} \pm 0.01$	$3.66^{A} \pm 0.04$	$0.53^{G} \pm 0.01$	$1.52^{D} \pm 0.01$	$2.48^{B} \pm 0.09$	$0.54^{G} \pm 0.01$	$0.60^{G} \pm 0.07$	$1.45^{D} \pm 0.03$	$0.58^{G} \pm 0.11$	$0.96^{F} \pm 0.03$

Means followed by the same uppercase letter in the same line and by the same lowercase letter in the same column for each parameter on different storage days were not significantly different ($p > 0.05$) by Tukey's test.

Reference: Own source

8.3.2.3. Pasting properties

Rapid Visco-Analyzer (RVA) pasting profiles obtained for the Cur-VD3-cornstarch samples are shown in Fig. 8.7. Parameters were assessed according to the temperature programming (heating, holding and cooling) and are listed in Table 8.7. Pasting temperature (T_p) was slightly reduced with the incorporation of lyophilized liposomes. This behavior suggests that agglomeration with phospholipid powders increased the hydration and the swelling of cornstarch granules (Luo et al., 2017). Curiously, lipids inhibit swelling, whereas sucrose delays gelatinization and enhances retrogradation (Gökşen & Ekiz, 2019). Therefore, the agglomeration and the blending with maltodextrin and liposomes may have contributed to this decrease in T_p. First, this reduction may be due to complexation of cornstarch with lipids by forming V-amylose structures (D'Silva, Taylor, & Emmambux, 2011). Second, the maltodextrin used in this study has low dextrose equivalent (DE = 10) and thus a high DP (polymerization degree), which confers it more swellable capacity than native starch (Juszczak et al., 2013). Also, the increase in size after agglomeration have led to an increase in the occupied volume by the granules, which also contributed to increase the swelling rate, and thus to reduce pasting temperature (Toniazzo et al., 2017). Furthermore, an increase in liposome (%) did not affect the T_p regardless of vesicle formulation used for blending (L0, L50 or L70). However, LS40-based samples showed lower values for this parameter at a fixed concentration when compared to samples produced with L0 solely. This result indicates higher interaction of unsaturated fatty acids from LS40 with amylose from cornstarch than the saturated from P90H, which contrasts the findings obtained for Yamada et al. (1998), where was verified an opposite effect.

Peak viscosity (P_v) was reached between 7 and 9 min at 95 °C. This phenomenon occurs when most of starch granules are fully swollen and other species remain molecularly non-aligned within the field of friction of the RVA (Ascheri et al., 2012). The agglomeration process and the blending with lyophilized liposomes also led to a decrease in the peak viscosity of cornstarch. On this basis, P_v values followed this specific trend: loaded agglomerated samples < unloaded agglomerated sample (control) < unloaded non-agglomerated sample (NAS). An increase in LS40 content promoted a decrease in viscosity at 6 and 8% w/w of dried vesicles. This increase in unsaturated phospholipids content promoted a smoother flow and restrained the abrasion of cornstarch during pasting. On the other hand, the starch matrix of NAS probably trapped higher amounts of water during pasting, which increased viscosity and hindered the slurry flow (Chen et al., 2020). An explanation for this reduction in viscosity in starches blended

with fatty acids was proposed by Raphaelides & Georgiadis (2006). Briefly, when starch is fully gelatinized and amylose is completely leached out, the polysaccharide interacts with the fatty acids and forms entangled helices-like structures. These structures are then destroyed during stirring, which decreases the overall viscosity of the system. In relation to peak time, control sample showed the highest value among all, followed by NAS, F0-10% and F70-10% samples. For most of the powders, peak viscosity time decreased after blending with lyophilized vesicles.

NAS also exhibited the highest values for breakdown (B_V) and final viscosity (F_V), whereas an addition of LS40-based lyophilized liposomes from 6 to 10% w/w resulted in higher values of F_V and lower values for B_V for cornstarch samples. The F_V indicated the re-association of the amylose molecules during the cooling period after gelatinization and a formation of a gel network (Rengsutthi & Charoenrein, 2011). On this basis, NAS showed the highest amylose content after pasting, which suggests that retrogradation phenomenon occurs more readily (Juszczak et al., 2013). In general, the produced powders exhibited higher values for F_V than P_V, which suggests that the agglomeration process and the presence of dried vesicles in blends did not promote a decrease in the stability of cornstarch pastes (Xie et al., 2021). The B_V is the difference between the P_V and the viscosity after holding for 30 min at 95 °C (Huang et al., 2010). The decrease in breakdown compared to NAS suggests that the agglomeration process and liposomes content helped to inhibit the disruption of starch granules, increasing the resistance against shear force during heating (Wang et al., 2018). D'Silva, Taylor, & Emmambux (2011) also observed a decrease in B_V of maize starch after addition of lipids (stearic acid).

Setback viscosity (S_v) suggests decreased tendencies of starch to retrograde and it is important in determining the quality of foods. A higher setback indicates that high rate of retrogradation will occur when amylose is free to associate into crystallites (Liang, King, & Shih, 2002). NAS presented S_v = 1557 cP, whereas control sample showed S_v = 1341 cP, suggesting that agglomeration tended to reduce retrogradation. However, F0-6%, F0-8%, F70-6%, and F70-8% samples exhibited higher Sv values than NAS, which implies an increase in amylose gelation and retrogradation. The S_v values found for F50-10% and F70-10% did not differ significantly (p <0.05) than NAS. Interestingly, the L0-based blends (F0-6%, F0-8%, and F0-10%) exhibited lower values of S_v than NAS regardless of vesicle content (%). In this sense, a reduction of setback in the presence of lipids suggest that the saturated phospholipids did not allow amylose chains to re-associate during cooling, increasing powder stability (D'Silva, Taylor, & Emmambux, 2011).

Figure 8.7. Rapid Visco-Analyzer (RVA) pasting profiles of cornstarch samples. Ternary blends of cornstarch + maltodextrin + lyophilized liposomes were produced using different concentrations of dried vesicles (A) 6%, (B) 8 % and (C) 10% w/w at different phospholipid ratios of Phospholipon 90H and Lipoid S40 (P90H:LS40) - F0 (0:100), F50 (50:50), and F70 (30:70)

(a)

(b)

(c)
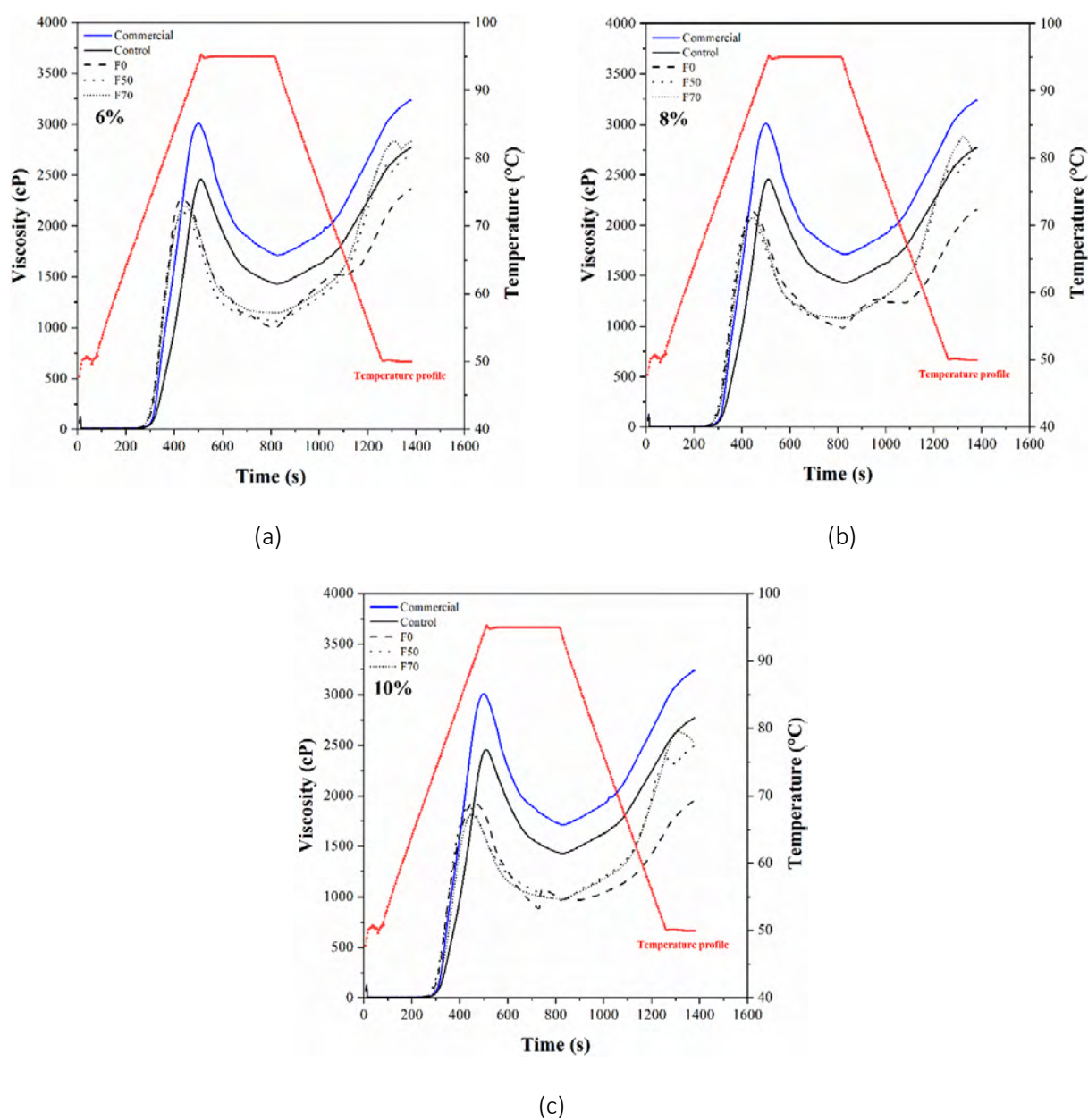
Table 8.7. Pasting properties obtained for cornstarch samples

Formulation	Pasting temperature (°C)	Peak viscosity (cP)	Time peak viscosity (min)	Breakdown viscosity (cP)	Final viscosity (cP)	Setback (cP)
NAS	$75^{AB} \pm 0$	$3012^{A} \pm 3$	$8^{B} \pm 0$	$1344^{A} \pm 65$	$3225^{A} \pm 18$	$1557^{C} \pm 44$
Control	$76^{A} \pm 0$	$2429^{B} \pm 43$	$9^{A} \pm 0$	$1028^{CD} \pm 6$	$2742^{BC} \pm 36$	$1341^{D} \pm 1$
F0-6%	$73^{CD} \pm 1$	$2284^{C} \pm 34$	$7^{C} \pm 0$	$1286^{A} \pm 47$	$2372^{E} \pm 13$	$1374^{D} \pm 25$
F0-8%	$73^{CD} \pm 0$	$2157^{D} \pm 18$	$7^{C} \pm 0$	$1164^{B} \pm 6$	$2159^{F} \pm 4$	$1167^{E} \pm 8$
F0-10%	$74^{BC} \pm 0$	$1935^{G} \pm 8$	$8^{B} \pm 0$	$938^{EF} \pm 37$	$1979^{G} \pm 40$	$983^{F} \pm 5$
F50-6%	$71^{E} \pm 0$	$2131^{DE} \pm 1$	$7^{C} \pm 0$	$1062^{C} \pm 10$	$2729^{C} \pm 47$	$1660^{A} \pm 36$
F50-8%	$72^{DE} \pm 1$	$2037^{F} \pm 22$	$7^{C} \pm 0$	$959^{DE} \pm 11$	$2716^{C} \pm 8$	$1638^{AB} \pm 20$
F50-10%	$72^{DE} \pm 0$	$1876^{G} \pm 22$	$7^{C} \pm 0$	$883^{EF} \pm 63$	$2488^{D} \pm 3$	$1495^{C} \pm 44$
F70-6%	$71^{E} \pm 0$	$2192^{D} \pm 4$	$7^{C} \pm 0$	$1055^{CD} \pm 9$	$2830^{B} \pm 1$	$1693^{A} \pm 13$
F70-8%	$71^{E} \pm 1$	$2060^{EF} \pm 23$	$7^{C} \pm 0$	$983^{CDE} \pm 23$	$2756^{BC} \pm 8$	$1679^{A} \pm 7$
F70-10%	$72^{DE} \pm 1$	$1869^{G} \pm 76$	$8^{B} \pm 0$	$855^{F} \pm 22$	$2582^{D} \pm 78$	$1568^{BC} \pm 25$

Means followed by the same uppercase letter in the same column were not significantly different ($p > 0.05$) by Tukey's test.

Reference: Own source

8.3.2.4. Fourier-transform infrared spectroscopy (FTIR)

FTIR spectra of pure ingredients, lyophilized liposomes and cornstarch samples are depicted in Fig. 8.8. Regarding the peaks observed for pure ingredients (Fig. 8.8A), maltodextrin exhibited a strong broad absorption centered at 3286 cm^{-1} and a weak band at 1643 cm^{-1} which arise from OH- stretching and OH-bending (in plane) modes, respectively, whereas a weak CH-stretching absorption band was found at 2912 cm^{-1} (Sritham & Gunasekaran, 2017). Carbohydrate fingerprint region of maltodextrin centered at 998 cm^{-1} was broader than the same region observed for sucrose. In this context, sucrose also presented an intense broad absorption peak related to OH- stretching at ~3315 cm^{-1} and the weak CH-stretching absorption band at 2927 cm^{-1}. Its fingerprint region from 1501 to 806 cm^{-1} comprised several overlapped absorption bands arose from C-O stretching, C-C stretching, and C-O-H bending vibrations (Sritham & Gunasekaran, 2017).

With respect to phospholipid patterns, the pair of peaks observed for LS40 (2923 and 2851 cm^{-1}) and P90H (2915 and 2851 cm^{-1}) are related to symmetric and asymmetric stretching

vibrations of C-H bonds in CH_2. The polar head groups of phospholipids (PO_2- groups) were found at 1051 and 1227 cm^{-1} for LS40 from symmetric/asymmetric stretching vibrations, whereas in P90H they were found at 1051 and 1253 cm^{-1}, respectively. Asymmetric stretching vibration due to choline (N^+-CH_3) was observed at 965 cm^{-1} for P90H and 968 cm^{-1} for LS40. As expected, a more pronounced peak was observed for P90H than for LS40 as the first is mainly composed of saturated PC, whereas the second contains several phospholipid species. The peak observed at 1738 cm^{-1} for both phospholipids is related to C=O vibration, and the fingerprint region from 1300 to 970 cm^{-1} comprised the PO_2 and P-O-C symmetrical vibration bands (Tai et al., 2020; Vergara & Shene, 2019).

Curcumin spectrum exhibited its characteristics peaks from 1475 to 1154 cm^{-1}. The peak at 1501 cm^{-1} corresponded to C=O stretching, C-C-C bending, and CC=O bending (Bourbon, Cerqueira & Vicente, 2016). On the other hand, Vitamin D_3 peaks were found at 3292 cm^{-1} (hydrogen bonds), 2934 cm^{-1} (=CH- stretching vibration), 1643 cm^{-1} (C=O stretching vibration), 1450 cm^{-1} (-CH_3 stretching vibration), 1051 cm^{-1} (C-O aromatic stretching vibration) and 890 cm^{-1} (stretching vibration of hydrogen on the substituent group of the ring) (Santos, Carvalho, & Garcia-Rojas, 2021).

The vibrational spectra observed for lyophilized liposomes are presented in Fig. 8.8B. Samples main peaks were found at (3289-3311) cm^{-1} related to OH- stretching of sucrose, (2915-2919) cm^{-1}, (2847-2851) cm^{-1} and (1738-1739) cm^{-1} related to the symmetric and asymmetric C-H stretching, and to C=O vibrations of P90H and LS40, and (1048-1051) cm^{-1}, and (983-987) cm^{-1} related to C-O and C-C stretching and C-OH bending vibrations of sucrose. Although VD3 also showed a pronounced peak at 1051 cm^{-1}, it is more plausible to consider that its contribution was little compared to sucrose and phospholipids that were added in much higher amounts (i.e. phospholipids = 33% wt sucrose = 66% wt, VD3 = 0.05% wt). Peaks found at 1410 and 1248 cm^{-1} in L0, 1463 and 1229 cm^{-1} in L50, and 1376 and 1225 cm^{-1} in L70 may be related to shifts in the 1475 and 1154 cm^{-1} peaks of curcumin, suggesting an interaction between this molecule and the other ingredients. Moreover, the absence of mostly peaks related to the crystalline structure of bioactives compounds in the spectra of lyophilized samples reflected their successful embedding into the lipid matrix (Chaves & Pinho, 2019; Chaves & Pinho, 2020). Interestingly, the C-H stretching vibrations observed in L0 spectra (2915 and 2847 cm^{-1}) tended to shift to higher wavenumbers as LS40 concentration increased (from 2915 to 2919 cm^{-1} and from 2847 to 2851 cm^{-1}), which is mainly attributed to the diverse

saturation of fatty acid chains in phospholipids. In this context, the lower wavenumbers observed for L0 may reflect a denser chain packing due to increased van der Waals attractions in this sample, besides a higher formation of H-bonds. Therefore, this combination of a denser lipid chain packing with the formation of more H-bonds usually make liposomes more stable (Tai et al., 2020).

FTIR spectrograms obtained for the cornstarch samples are depicted in Fig. 8.8C. As noted, the patterns of control and ternary blends were similar to the obtained for NAS. In fact, the spectra of pure cornstarch and maltodextrin were basically the same (Fig. 8.8A), which was expected since the latter is derived from the first after hydrolysis. Peaks found in cornstarch samples were as it follows: 3305 cm^{-1} for OH- stretching absorption, 2918 cm^{-1} for CH-stretching absorption, 1356 cm^{-1} for OH- bending and 997 cm^{-1} for C=C bending (center of carbohydrate region). No formation of new peaks was found in the blended spectra, suggesting that lyophilized liposomes were completely incorporated into the agglomerated cornstarch powders.

Figure 8.8. FTIR vibrational spectra of (A) pure ingredients, (B) Cur-VD3-co-loaded lyophilized liposomes and (C) Cur-VD3-enriched cornstarch samples

Reference: Own source
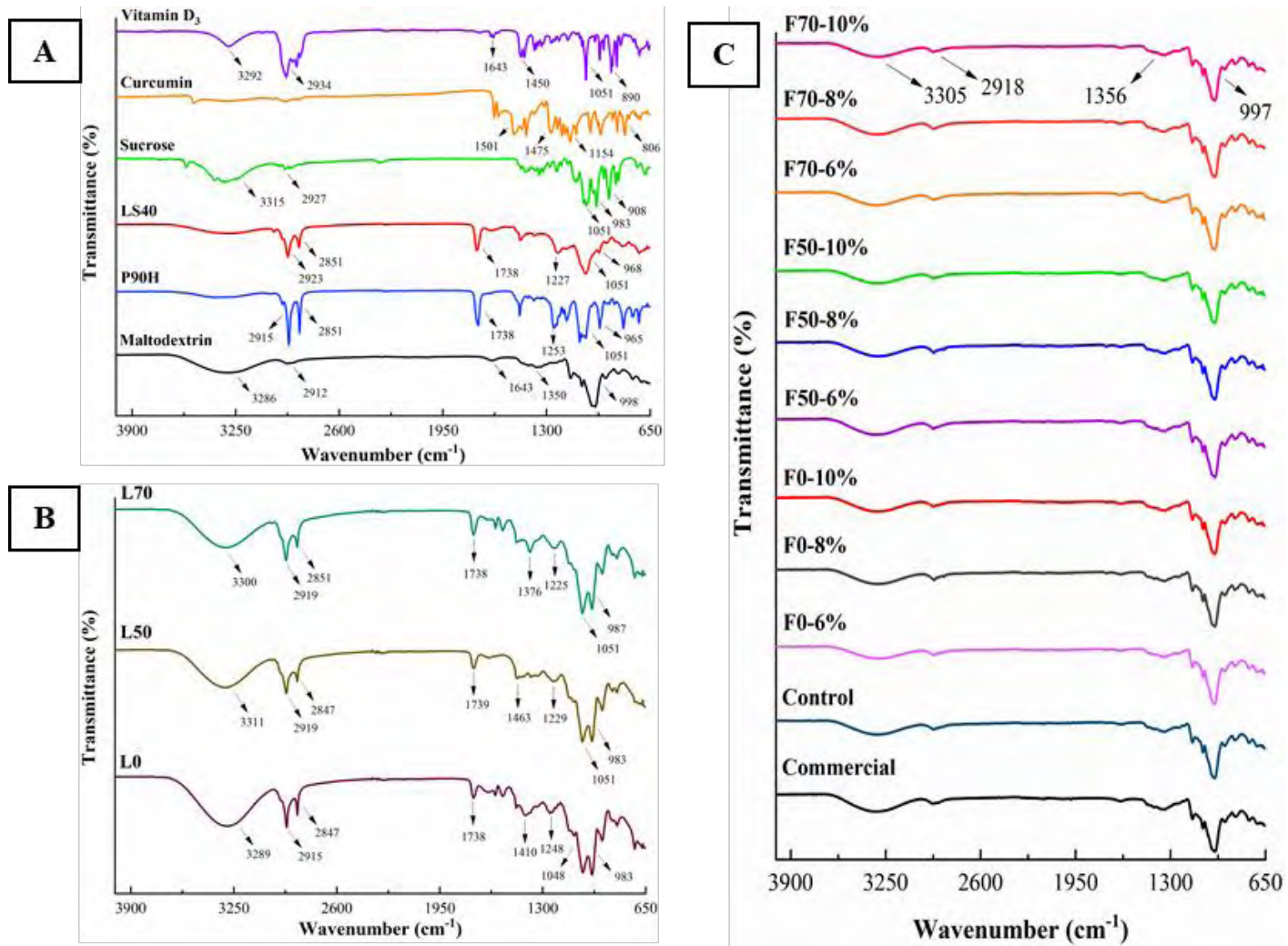
8.3.2.5. X-ray diffraction (XRD)

Diffractograms obtained by XRD of pure ingredients, lyophilized liposomes and cornstarch samples are depicted in Fig. 8.9. This analysis was performed to evaluate the remaining crystallinity of ingredients after lyophilization and agglomeration processes. From pure ingredients spectra (Fig. 8.9A), maltodextrin showed a single broad peak centered at 19.1°; P90H exhibited a broad band with a sharp and a broad peak at 20.2° and 21.4°, respectively; LS40 exhibited a single broad peak at 19.8°; sucrose main peaks were found at 11.7°, 19.7° and 24.9°; curcumin main peaks at 8.78°, 17.2°, 24.4° and 25.5°; and vitamin D_3 a single sharp peak at 17.8°. The broad bands observed for maltodextrin and LS40 suggested amorphous structures, whereas sucrose, curcumin and VD3 were all crystalline.

Fig. 8.9B presents the diffractograms shown for the dried vesicles. A semi-crystalline structure was observed for all the samples regardless of formulation due to the presence of several sharp peaks and a small but broader region. Sucrose characteristic peaks shifted slightly to lower degrees (around 11.6°, 19.6° and 24.7°). Peaks from LS40 and P90H have contributed to the appearance of a broad-like structure from 18° to 24°. Curcumin peak at 24.4° was probably overlapped to sucrose peak at 24.9° resulting in a shift to 24.7° in lyophilized patterns. The other peaks related to curcumin did not appear in liposomes patterns but some new peaks appeared at 8.2° and 16.6° suggesting interactions between curcumin and the other ingredients during lyophilization. On the other hand, VD3 peak at 17.8° shifted slightly to 18° which may also indicate some type of interaction. The sharp peak raised at 18.8° for all the samples may corroborate the strong intramolecular hydrogen bonding among OH groups of the ingredients. The meta-stable characteristic observed for liposomes is mainly due to the slow removal of water by lyophilization, which may have induced sucrose to a small re-crystallization (Costa Neto et al., 2019).

As observed by FTIR, diffractograms obtained by cornstarch blended samples (Fig. 8.9C) were also quite similar than NAS. The amorphous aspect of the powders may indicate that sucrose and liposomes may have infiltrated into the voids of over-sized particles produced by agglomeration.

Figure 8.9. X-ray diffractograms of (A) pure ingredients, (B) Cur-VD3-co-loaded lyophilized liposomes and (C) Cur-VD3-enriched cornstarch samples

Reference: Own source
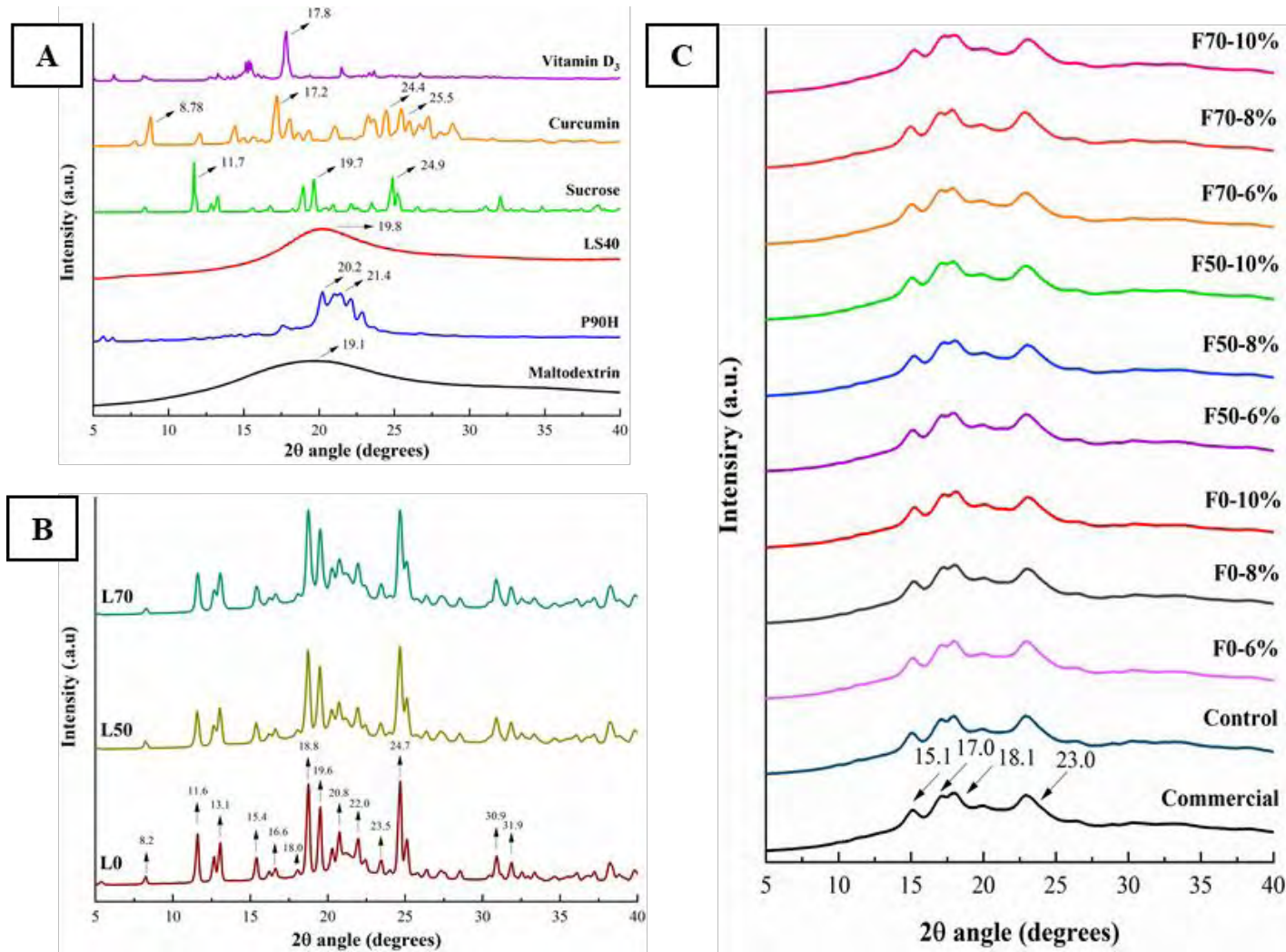
8.4. Conclusions

The results obtained by this work showed that it was possible to produce ternary blends of cornstarch, maltodextrin and lyophilized liposomes loaded with curcumin and vitamin D_3 using a wet agglomeration process. The concentration of unsaturated phospholipids in the liposome formulations had great effect in the physicochemical properties of dried vesicles as solubility and hygroscopicity were improved with increased nonpurified phospholipid concentration. The ratio between saturated and non-saturated phospholipids played also a major role regarding the encapsulation of bioactives, as curcumin was better encapsulated in saturated-based lipid bilayers, whereas vitamin D_3 was more retained in unsaturated-based bilayers. Furthermore, the agglomeration process promoted an increase in many physical properties of cornstarch such as solubility, hygroscopicity, mean diameter, density, and flowability, and also a decrease in water activity, relative humidity, and cohesiveness values, thus a remarkable improvement in handling characteristics. The nature of phospholipid used in liposome formulations have also influenced the retention of compounds presented in blended cornstarch, since an increase in the number of unsaturated phospholipids promoted an increase in the retention of both molecules. Also, the use of sucrose during lyophilization and maltodextrin during agglomeration have led to the production of more stable blends as observed from microstructural analyses. Overall, this work provides innovative potential to design new purposes for the wet agglomeration of food powders and to develop a new functional product with high-added value by using low-cost ingredients and a relatively simple process.

8.5. Acknowledgments

8.6. References

Adhikari, B. et al. (2004). Effect of addition of maltodextrin on drying kinetics and stickiness of sugar and acid-rich foods during convective drying: experiments and modelling. **Journal of Food Engineering**, 62(1), 53-68.

Al-Muhtaseb, A. H. et al. (2002). Moisture sorption isotherm characteristics of food products: A review. **Food and Bioproducts Processing**, 80(2), 118-128.

Ascheri, D. P. R. et al. (2012). Correlation between grain nutritional content and pasting properties of pre-gelatinized red rice flour. **Food Science & Technology**, 59(1), 16-24.

Balci-Torun, F., & Ozdemir, F. (2021). Encapsulation of strawberry flavour and physicochemical characterization of the encapsulated powders. **Powder Technology**, 380, 602-612.

Barbosa-Cánovas, G., & Juliano, P. (2005). Physical and chemical properties of food powders. In: **Encapsulated and Powdered Foods**. 1st ed. CRC Press: Boca Raton.

Barkout, A., Rondet, E., Delalonde, M., & Ruiz, T. (2012). Influence of physicochemical binder properties on agglomeration of wheat powder in couscous grain. **Journal of Food Engineering,** 111, 234-240.

Baysan, U. et al. (2021). The effect of coating material combination and encapsulation method on propolis powder properties. **Powder Technology**, 384, 332-341.

Beuchat, L. R. et al. (2013). Low-water activity foods: Increased concern as vehicles of foodborne pathogens. **Journal of Food Protection**, 76, 150–172.

Bhandari, B. (2013). 1 – Introduction to food powders. **Handbook of Food Powders - Processes and Properties**. Woodhead Publishing Series in Food Science, Technology and Nutrition. 1-25.

Bhandari, B. R. et al. (1993). Spray drying of concentrated fruit juices. **Drying Technology**, 11(5), 1081-1092.

Börjesson, E. et al. (2014). Evaluation of particle measures relevant for powder bed porosity—A study of spray dried dairy powders. **Powder Technology**, 253, 453-463.

Bourbon, A. I., Cerqueira, M. A., & Vicente, A. A. (2016). Encapsulation and controlled release of bioactive compounds in lactoferrin-glycomacropeptide nanohydrogels: Curcumin and caffeine as model compounds. **Journal of Food Engineering**, 180, 110-119.

Burggraeve, A. et al. (2013). Process analytical tools for monitoring, understanding, and control of pharmaceutical fluidized bed granulation: A review. **European Journal of Pharmaceutics and Biopharmaceutics**, 83(1), 2-15.

Cai, Y. Z., & Corke, H. (2000). Production and properties of spray-dried Amaranthus betacyanin pigments. **Journal of Food Science**, 65, 1248-1251.

Chaves, M. A., & Pinho, S. C. (2019). Curcumin-loaded proliposomes produced by the coating of micronized sucrose: Influence of the type of phospholipid on the physicochemical characteristics of powders and on the liposomes obtained by hydration. **Food Chemistry**, 291, 7-15.

Chaves, M. A., & Pinho, S. C. (2020). Unpurified soybean lecithins impact on the chemistry of proliposomes and liposome dispersions encapsulating vitamin D_3. **Food Bioscience**, 37, 100700.

Chaves, M. A. et al. (2018). Structural characterization of multilamellar liposomes coencapsulating curcumin and vitamin D_3. **Colloids and Surfaces A: Physicochemical and Engineering Aspects**, 549, 112-121.

Chen, Y., Dai, G., & Gao, Q. (2020). Preparation and properties of granular cold-water-soluble porous starch. **International Journal of Biological Macromolecules**, 144, 656-662.

Chezanoglou, E., & Goula, A. M. (2021). Co-crystallization in sucrose: A promising method for encapsulation of food bioactive components. **Trends in Food Science & Technology**, 114, 262-274.

Chin, S. F., Yazid, S. N. A. M., & Pang, S. C. (2014). Preparation and characterization of starch nanoparticles for controlled release of curcumin. **International Journal of Polymer Science**, 340121.

Chronakis, I. S. (1998). On the molecular characteristics, compositional properties, and structural-functional mechanisms of maltodextrins: A review. **Critical Reviews in Food Science and Nutrition**, 38(7), 599-637.

Costa Neto, J. J. G. et al. (2019). Microencapsulation of tiger nut milk by lyophilization: Morphological characteristics, shelf life and microbiological stability. **Food Chemistry**, 284, 133-139.

Cuq, B. et al. (2011). 7 - Agglomeration/granulation in food powder production. **Handbook of Food Powders – Processes and Properties**. Woodhead Publishing Series in Food Science, Technology and Nutrition, 150-177.

D'Silva, T. V., Taylor, J. R. N., & Emmambux, M. N. (2011). Enhancement of the pasting properties of teff and maize starches through wet–heat processing with added stearic acid. **Journal of Cereal Science**, 53(2), 192-197.

Dacanal, G. C., & Menegalli, F. C. (2010). Selection of operational parameters for the production of instant soy protein isolate by pulsed fluid bed agglomeration. **Powder Technology**, 203(3), 565-573.

Dacanal. G. C. et al. (2016). Effects of pulsating air flow in fluid bed agglomeration of starch particles. **Journal of Food Engineering**, 181, 67-83.

Dhakal, S. P., & He, J. (2020). Microencapsulation of vitamins in food applications to prevent losses in processing and storage: A review. **Food Research International**, 137, 109326.

Eastman, J. E.; & Moore, C. O. (1984). Cold water-soluble granular starch for gelled food composition. **U.S. Patent 4465702**.

Ferreira, L. S. et al. (2018). Wet agglomeration by high shear of binary mixtures of curcumin-loaded lyophilized liposomes and cornstarch: Powder characterization and incorporation in cakes. **Food Bioscience**, 25, 74-82.

Frabetti, A. C. C. et al. (2021). Strawberry-hydrocolloids dried by continuous cast-tape drying to produce leather and powder. **Food Hydrocolloids**, 121, 107041.

Francis, J. F., & Clydesdale, F. M. (1975). **Food Colorimetry, Theory and Application**, 1st ed, pp 477. Westport: AVI Publishing Company.

Göksen, G., & Ekiz, H. I. (2019). Pasting and gel texture properties of starch-molasses combinations. **Food Science and Technology**, 39(1), ISSN 1678-457X.

Huang, C-C. et al. (2010). Effects of mucilage on the thermal and pasting properties of yam, taro, and sweet potato starches. **LWT – Food Science and Technology**, 43(6), 849-855.

Iveson, S. M. et al. (2001). Nucleation, growth and breakage phenomena in agitated wet granulation processes: a review. **Powder Technology**, 117(1-2), 3-39.

Jaya, S., & Das, H. (2004). Effect of maltodextrin, glycerol monostearate and tricalcium phosphate on vacuum dried mango powder properties. **Journal of Food Engineering**, 63(2), 125-134.

Ji, J. et al. (2017). Enhanced wetting behaviours of whey protein isolate powder: The different effects of lecithin addition by fluidised bed agglomeration and coating processes. **Food Hydrocolloids**, 71, 94-101.

Ji, J. et al. (2016). Rehydration behaviours of high protein dairy powders: The influence of agglomeration on wettability, dispersibility and solubility. **Food Hydrocolloids**, 58, 194-203.

Jiang, T., Liao, W., & Charcosset, C. (2020). Recent advances in encapsulation of curcumin in nanoemulsions: A review of encapsulation technologies, bioaccessibility and applications. **Food Research International**, 132, 109035.

Jinapong, N., Suphantharika, M. & Jamnong, P. (2008). Production of instant soymilk powders by ultrafiltration, spray drying and fluidized bed agglomeration. **Journal of Food Engineering**, 84(2), 194-205.

Juszczak, L. et al. (2013). Effect of maltodextrins on the rheological properties of potato starch pastes and gels. International Journal of Food Science & Technology, 869362.

Kaushik, V., & Roos, Y. H. (2007). Limonene encapsulation in freeze-drying of gum Arabic–sucrose–gelatin systems. LWT – Food Science and Technology, 40(8), 1381-1391.

Kumar Lekshmi, R. G. et al. (2021). Binary blend of maltodextrin and whey protein outperforms gum Arabic as superior wall material for squalene encapsulation. Food Hydrocolloids, 121, 106976.

Kumar, S. Y. A., & Setty, C. M. (2017). Preparation and evaluation of maltodextrin based proniosomes containing capecitabine. International Journal of Research and Development in Pharmacy & Life Science, 6(7), 2856-2861.

Labuza, T. P. (1985). Moisture sorption: Practical aspects of isotherm measurement and use. 978-1-8911-2718-2, American Association of Cereal Chemists, St. Paul, MN, USA.

Lee, H., & Yoo, B. (2021). Agglomeration of galactomannan gum powders: Physical, rheological, and structural characterizations. Carbohydrate Polymers, 256, 117599.

Li, B.-Z. et al. (2009). Physical properties and loading capacity of starch-based microparticles crosslinked with trisodium trimetaphosphate. Journal of Food Engineering. 92, 255–260.

Liang, X., King, J. M., & Shih, F. F. (2002). Pasting property differences of commercial and isolated rice starch with added lipids and β-cyclodextrin. Cereal Chemistry, 79(6), 818-818.

Lopes, N. A. et al. (2021). Nisin induces lamellar to cubic liquid-crystalline transition in pectin and polygalacturonic acid liposomes. Food Hydrocolloids, 112, 106320.

Lopez-Polo, J. et al. (2020). Effect of lyophilization on the physicochemical and rheological properties of food grade liposomes that encapsulate rutin. Food Research International, 130, 108967.

Luo, S-j. et al. (2017). Investigation on the influence of pectin structures on the pasting properties of rice starch by multiple regression. Food Hydrocolloids, 63, 580-584.

Marefati, A. et al. (2015). Fabrication of encapsulated oil powders from starch granule stabilized W/O/W Pickering emulsions by freeze-drying. Food Hydrocolloids, 51, 261-271.

Martins, P. C., & Kieckbusch, T. G. (2008). Influence of a lipid phase on steam jet agglomeration of maltodextrin powders. Powder Technology, 185(3), 258-266.

Maurya, V. K., Bashir, K., & Aggarwal, M. (2020). Vitamin D microencapsulation and fortification: Trends and technologies. The Journal of Steroid Biochemistry and Molecular Biology, 196, 105489.

McClements, D. (2015). Encapsulation, protection, and release of hydrophilic active components: Potential and limitations of colloidal delivery systems. **Advances in Colloid and Interface Science**, 219, 27-53.

Mulrooney, S. L. et al. (2021). Vitamin D_3 bioaccessibility: Influence of fatty acid chain length, salt concentration and l-α-phosphatidylcholine concentration on mixed micelle formation and delivery of vitamin D_3. **Food Chemistry**, 344, 128722.

Mun, S., Kim, Y-R., & McClements, D. J. (2015). Control of β-carotene bioaccessibility using starch-based filled hydrogels. **Food Chemistry**, 173, 454-461.

Neves, M. I. L. et al. (2019). Encapsulation of curcumin in milk powders by spray-drying: Physicochemistry, rehydration properties, and stability during storage. **Powder Technology**, 345, 601-607.

Park, J., & Yoo, B. (2020). Particle agglomeration of gum mixture thickeners used for dysphagia diets. **Journal of Food Engineering**, 279, 109958.

Raphaelides, S. N., & Georgiadis, N. (2006). Effect of fatty acids on the rheological behaviour of maize starch dispersions during heating. **Carbohydrate Polymers**, 65(1), 81-92.

Rengsutthi, K., & Charoenrein, S. (2011). Physico-chemical properties of jackfruit seed starch (Artocarpus heterophyllus) and its application as a thickener and stabilizer in chilli sauce. **LWT – Food Science and Technology**, 44, 1309-1313.

Salvia-Trujillo, L. et al. (2013). Influence of particle size on lipid digestion and β-carotene bioaccessibility in emulsions and nanoemulsions. **Food Chemistry**, 141(2), 1472-1480.

Samborska, K., Langa, E., & Bakier, S. (2015). Changes in the physical properties of honey powder during storage. **International Journal of Food Science & Technology**, 50(6), 1359-1365.

Santos, M. B.; Carvalho, M. G.; & Garcia-Rojas, E. E. (2021). Carboxymethyl tara gum-lactoferrin complex coacervates as carriers for vitamin D_3: Encapsulation and controlled release. **Food Hydrocolloids**, 112, 106347.

Sepúlveda, C. T. et al. (2021). Characterization and storage stability of spray dried soy-rapeseed lecithin/trehalose liposomes loaded with a tilapia viscera hydrolysate. **Innovative Food Science & Emerging Technologies**, 71, 102708.

Soazo, M., Rubiolo, A. C., & Verdini, R. A. (2011). Effect of drying temperature and beeswax content on moisture isotherms of whey protein emulsion film. **Procedia Food Science. 11th International Congress on Engineering and Food (ICEF11)**, 210-215.

Spada, J. C. et al. (2013). Water adsorption isotherms of microcapsules with hydrolyzed pinhão (Araucaria angustifolia seeds) starch as wall material. **Journal of Food Engineering**, 114, 64-69.

Sritham, E., & Gunasekaran, S. (2017). FTIR spectroscopic evaluation of sucrose-maltodextrin-sodium citrate bioglass. **Food Hydrocolloids**, 70, 371-382.

Szulc, K., & Lenart, A. (2010). Effect of agglomeration on flowability of baby food powders. **Journal of Food Science**, 75(5), E276-E284.

Tai, K. et al. (2020). Stability and release performance of curcumin-loaded liposomes with varying content of hydrogenated phospholipids. **Food Chemistry**, 326, 126973.

Tan, S. P. et al. (2015). Effects of the spray-drying temperatures on the physiochemical properties of an encapsulated bitter melon aqueous extract powder. **Powder Technology**, 281, 65-75.

Taylor, T. M. et al. (2005). Liposomal nanocapsules in food science and agriculture. **Critical Reviews in Food Science and Nutrition**, 45(7-8), 587-605.

Toniazzo, T. et al. (2017). Production of cornstarch granules enriched with quercetin liposomes by aggregation of particulate binary mixtures using high shear process. **Journal of Food Science**, 82(11), 2626-2633.

Tonon, R. V. et al. (2009). Physicochemical and morphological characterisation of açai (Euterpe oleraceae Mart.) powder produced with different carrier agents. **International Journal of Food Science & Technology**, 44(10), 1950-1958.

Turchiuli, C. et al. (2005). Oil encapsulation by spray drying and fluidised bed agglomeration. **Innovative Food Science & Emerging Technologies**, 6(1), 29-35.

Valenzuela, C., & Aguilera, J. M. (2015). Effects of maltodextrin on hygroscopicity and crispness of apple leathers. **Journal of Food Engineering**, 144, 1-9.

Van Hoogevest, P. (2017). Review – An update on the use of oral phospholipid excipients. **European Journal of Pharmaceutical Sciences**, 108, 1-12.

Vélez, M. A. et al.(2019). Effect of lyophilization on food grade liposomes loaded with conjugated linoleic acid. **Journal of Food Engineering**, 240, 199-206.

Vergara, D., & Shene, C. (2019). Encapsulation of lactoferrin into rapeseed phospholipids based liposomes: Optimization and physicochemical characterization. **Journal of Food Engineering**, 262, 29-38.

Wang, F. et al. (2022). Fabrication and characterization of walnut peptides-loaded proliposomes with three lyoprotectants: Environmental stabilities and antioxidant/antibacterial activities. **Food Chemistry**, 366, 130643.

Wang, R. et al. (2019). Pasting, thermal, and rheological properties of rice starch partially replaced by inulin with different degrees of polymerization. **Food Hydrocolloids**, 92, 228-232.

Xie, F. et al. (2021). High methoxyl pectin enhances the expansion characteristics of the cornstarch relative to the low methoxyl pectin. **Food Hydrocolloids**, 110, 106131.

Xing, Y. et al. (2014). Effect of porous starch concentrations on the microbiological characteristics of microencapsulated Lactobacillus acidophilus. **Food & Function**, 5, 972-983.

Yamada, T. et al. (1998). Introduction of fatty acids to starch granules by ultra-high-pressure treatment. **Starch – Stärke**, 50(11-12), 484-486.

Yokota, D., Moraes, M., & Pinho, S. C. (2012). Characterization of lyophilized liposomes produced with non-purified soy lecithin: a case study of casein hydrolysate microencapsulation. **Brazilian Journal of Chemical Engineering**, 29(2). 325-335.

Zhu, J. et al. (2017). Structural features and thermal property of propionylated starches with different amylose/amylopectin ratio. **International Journal of Biological Macromolecules**, 97, 123-130.

Chapter 9. OVERALL CONCLUSION

Chapter 9. Overall conclusion

From the results obtained in this study, it was possible to verify that wet agglomeration was successfully used for the production of new enriched-cornstarch formulations containing curcumin and vitamin D_3 coencapsulated in lyophilized liposomes. The main conclusions are presented as it follows:

1) Proliposomes produced by the coating of micronized sucrose method proved to be suitable carriers for the entrapment of both curcumin and vitamin D_3 over storage time. The presence of sucrose increased their solubility, facilitating the further hydration. Higher amounts of saturated phospholipids led to improvements in bioactive retention;

2) Higher amounts of unsaturated phospholipids promoted an early destabilization of liposome vesicles produced by hydration of proliposomes, supporting the idea of lyophilization. However, liposome dispersions were efficiently incorporated into the well-accepted pineapple yoghurt formulations, showing their high potential as coloring substitutes for tartrazine yellow;

3) Supercritical technology was also successful to produce nanoliposomes co-loading curcumin and vitamin D_3. The SuperLip process allowed the formation of highly stable vesicles with high content of bioactives. A sustained release of curcumin was verified and much of its antioxidant potential was preserved after processing;

4) Lyophilization increased vesicles stability and bioactives encapsulation over storage time. The phospholipid ratio affected differently the retention of compounds: higher amounts of saturated species led to increased curcumin concentration, whereas higher amounts of unsaturated species led to increased vitamin D_3 concentration. Sucrose was efficiently used as cryoprotectant in a 2:1 w/w disaccharide: total phospholipids ratio.

5) Cornstarch particles were successfully blended to lyophilized liposomes using the wet agglomeration process and maltodextrin as binder solution. Enriched-agglomerated particles produced with higher amounts of unsaturated phospholipids retained higher amounts of both bioactives over storage time.

This work offered innovative potential and highlighted the versatility of agglomeration process by promoting the development of a new enriched product. The fortified food powders were produced using low-cost plentiful raw materials as sucrose, cornstarch, and maltodextrin. Unsaturated/nonpurified phospholipids were effectively used in the substitution of saturated species, emphasizing their potential use for food purposes.

ATTACHMENTS

ATTACHMENT A – PAPER PUBLISHED IN FOOD CHEMISTRY

CCC Marketplace™

Order Date	29-Sep-2021	Type of Use	Republish in a thesis/dissertation
Order License ID	1151040-1		
ISSN	1873-7072	Publisher	Elsevier Science
		Portion	Chapter/article

LICENSED CONTENT

Publication Title	Food chemistry	Publication Type	e-Journal
Article Title	Curcumin-loaded proliposomes produced by the coating of micronized sucrose: Influence of the type of phospholipid on the physicochemical characteristics of powders and on the liposomes obtained by hydration.	Start Page	7
		End Page	15
		Volume	291
		URL	http://www.sciencedirect.com/science/journal/03088146
Date	01/01/1976		
Language	English		
Country	Netherlands		
Rightsholder	Elsevier Science & Technology Journals		

REQUEST DETAILS

Portion Type	Chapter/article	Rights Requested	Main product
Page range(s)	1-9	Distribution	Worldwide
Total number of pages	9	Translation	Original language of publication
Format (select all that apply)	Print, Electronic	Copies for the disabled?	No
Who will republish the content?	Author of requested content	Minor editing privileges?	No
Duration of Use	Life of current edition	Incidental promotional use?	No
Lifetime Unit Quantity	Up to 499	Currency	USD

NEW WORK DETAILS

Title	ENRICHMENT OF CORNSTARCH WITH CURCUMIN AND VITAMIN D3 COENCAPSULATED IN LYOPHILIZED LIPOSOMES USING HIGH SHEAR WET AGGLOMERATION	Institution name	University of São Paulo
		Expected presentation date	2021-09-29
Instructor name	Matheus Andrade Chaves		

ADDITIONAL DETAILS

| Order reference number | N/A | The requesting person / organization to appear on the license | Matheus Andrade Chaves |

REUSE CONTENT DETAILS

Title, description or numeric reference of the portion(s)	2	Title of the article/chapter the portion is from	Curcumin-loaded proliposomes produced by the coating of micronized sucrose:
Editor of portion(s)	Chaves, Matheus A.; Pinho, Samantha C.		Influence of the type of phospholipid on the physicochemical characteristics of powders and on the liposomes obtained by hydration.
Volume of serial or monograph	291		
Page or page range of portion	7-15		
		Author of portion(s)	Chaves, Matheus A.; Pinho, Samantha C.
		Issue, if republishing an article from a serial	N/A
		Publication date of portion	2019-09-01

RIGHTSHOLDER TERMS AND CONDITIONS

Elsevier publishes Open Access articles in both its Open Access journals and via its Open Access articles option in subscription journals, for which an author selects a user license permitting certain types of reuse without permission. Before proceeding please check if the article is Open Access on http://www.sciencedirect.com and refer to the user license for the individual article. Any reuse not included in the user license terms will require permission. You must always fully and appropriately credit the author and source. If any part of the material to be used (for example, figures) has appeared in the Elsevier publication for which you are seeking permission, with credit or acknowledgement to another source it is the responsibility of the user to ensure their reuse complies with the terms and conditions determined by the rights holder. Please contact permissions@elsevier.com with any queries.

CCC Terms and Conditions

1. Description of Service; Defined Terms. This Republication License enables the User to obtain licenses for republication of one or more copyrighted works as described in detail on the relevant Order Confirmation (the "Work(s)"). Copyright Clearance Center, Inc. ("CCC") grants licenses through the Service on behalf of the rightsholder identified on the Order Confirmation (the "Rightsholder"). "Republication", as used herein, generally means the inclusion of a Work, in whole or in part, in a new work or works, also as described on the Order Confirmation. "User", as used herein, means the person or entity making such republication.

2. The terms set forth in the relevant Order Confirmation, and any terms set by the Rightsholder with respect to a particular Work, govern the terms of use of Works in connection with the Service. By using the Service, the person transacting for a republication license on behalf of the User represents and warrants that he/she/it (a) has been duly authorized by the User to accept, and hereby does accept, all such terms and conditions on behalf of User, and (b) shall inform User of all such terms and conditions. In the event such person is a "freelancer" or other third party independent of User and CCC, such party shall be deemed jointly a "User" for purposes of these terms and conditions. In any event, User shall be deemed to have accepted and agreed to all such terms and conditions if User republishes the Work in any fashion.

3. Scope of License; Limitations and Obligations.

   3.1. All Works and all rights therein, including copyright rights, remain the sole and exclusive property of the Rightsholder. The license created by the exchange of an Order Confirmation (and/or any invoice) and payment by User of the full amount set forth on that document includes only those rights expressly set forth in the Order Confirmation and in these terms and conditions, and conveys no other rights in the Work(s) to User. All rights not expressly granted are hereby reserved.

   3.2.
      General Payment Terms: You may pay by credit card or through an account with us payable at the end of the month. If you and we agree that you may establish a standing account with CCC, then the following

terms apply: Remit Payment to: Copyright Clearance Center, 29118 Network Place, Chicago, IL 60673-1291. Payments Due: Invoices are payable upon their delivery to you (or upon our notice to you that they are available to you for downloading). After 30 days, outstanding amounts will be subject to a service charge of 1-1/2% per month or, if less, the maximum rate allowed by applicable law. Unless otherwise specifically set forth in the Order Confirmation or in a separate written agreement signed by CCC, invoices are due and payable on "net 30" terms. While User may exercise the rights licensed immediately upon issuance of the Order Confirmation, the license is automatically revoked and is null and void, as if it had never been issued, if complete payment for the license is not received on a timely basis either from User directly or through a payment agent, such as a credit card company.

3.3. Unless otherwise provided in the Order Confirmation, any grant of rights to User (i) is "one-time" (including the editions and product family specified in the license), (ii) is non-exclusive and non-transferable and (iii) is subject to any and all limitations and restrictions (such as, but not limited to, limitations on duration of use or circulation) included in the Order Confirmation or invoice and/or in these terms and conditions. Upon completion of the licensed use, User shall either secure a new permission for further use of the Work(s) or immediately cease any new use of the Work(s) and shall render inaccessible (such as by deleting or by removing or severing links or other locators) any further copies of the Work (except for copies printed on paper in accordance with this license and still in User's stock at the end of such period).

3.4. In the event that the material for which a republication license is sought includes third party materials (such as photographs, illustrations, graphs, inserts and similar materials) which are identified in such material as having been used by permission, User is responsible for identifying, and seeking separate licenses (under this Service or otherwise) for, any of such third party materials; without a separate license, such third party materials may not be used.

3.5. Use of proper copyright notice for a Work is required as a condition of any license granted under the Service. Unless otherwise provided in the Order Confirmation, a proper copyright notice will read substantially as follows: "Republished with permission of [Rightsholder's name], from [Work's title, author, volume, edition number and year of copyright]; permission conveyed through Copyright Clearance Center, Inc. " Such notice must be provided in a reasonably legible font size and must be placed either immediately adjacent to the Work as used (for example, as part of a by-line or footnote but not as a separate electronic link) or in the place where substantially all other credits or notices for the new work containing the republished Work are located. Failure to include the required notice results in loss to the Rightsholder and CCC, and the User shall be liable to pay liquidated damages for each such failure equal to twice the use fee specified in the Order Confirmation, in addition to the use fee itself and any other fees and charges specified.

3.6. User may only make alterations to the Work if and as expressly set forth in the Order Confirmation. No Work may be used in any way that is defamatory, violates the rights of third parties (including such third parties' rights of copyright, privacy, publicity, or other tangible or intangible property), or is otherwise illegal, sexually explicit or obscene. In addition, User may not conjoin a Work with any other material that may result in damage to the reputation of the Rightsholder. User agrees to inform CCC if it becomes aware of any infringement of any rights in a Work and to cooperate with any reasonable request of CCC or the Rightsholder in connection therewith.

4. Indemnity. User hereby indemnifies and agrees to defend the Rightsholder and CCC, and their respective employees and directors, against all claims, liability, damages, costs and expenses, including legal fees and expenses, arising out of any use of a Work beyond the scope of the rights granted herein, or any use of a Work which has been altered in any unauthorized way by User, including claims of defamation or infringement of rights of copyright, publicity, privacy or other tangible or intangible property.

5. Limitation of Liability. UNDER NO CIRCUMSTANCES WILL CCC OR THE RIGHTSHOLDER BE LIABLE FOR ANY DIRECT, INDIRECT, CONSEQUENTIAL OR INCIDENTAL DAMAGES (INCLUDING WITHOUT LIMITATION DAMAGES FOR LOSS OF BUSINESS PROFITS OR INFORMATION, OR FOR BUSINESS INTERRUPTION) ARISING OUT OF THE USE OR INABILITY TO USE A WORK, EVEN IF ONE OF THEM HAS BEEN ADVISED OF THE POSSIBILITY OF SUCH DAMAGES. In any event, the total liability of the Rightsholder and CCC (including their respective employees and directors) shall not exceed the total amount actually paid by User for this license. User assumes full liability for the actions and omissions of its principals, employees, agents, affiliates, successors and assigns.

6.
Limited Warranties. THE WORK(S) AND RIGHT(S) ARE PROVIDED "AS IS". CCC HAS THE RIGHT TO GRANT TO USER THE RIGHTS GRANTED IN THE ORDER CONFIRMATION DOCUMENT. CCC AND THE RIGHTSHOLDER DISCLAIM ALL

OTHER WARRANTIES RELATING TO THE WORK(S) AND RIGHT(S), EITHER EXPRESS OR IMPLIED, INCLUDING WITHOUT LIMITATION IMPLIED WARRANTIES OF MERCHANTABILITY OR FITNESS FOR A PARTICULAR PURPOSE. ADDITIONAL RIGHTS MAY BE REQUIRED TO USE ILLUSTRATIONS, GRAPHS, PHOTOGRAPHS, ABSTRACTS, INSERTS OR OTHER PORTIONS OF THE WORK (AS OPPOSED TO THE ENTIRE WORK) IN A MANNER CONTEMPLATED BY USER; USER UNDERSTANDS AND AGREES THAT NEITHER CCC NOR THE RIGHTSHOLDER MAY HAVE SUCH ADDITIONAL RIGHTS TO GRANT.

7. Effect of Breach. Any failure by User to pay any amount when due, or any use by User of a Work beyond the scope of the license set forth in the Order Confirmation and/or these terms and conditions, shall be a material breach of the license created by the Order Confirmation and these terms and conditions. Any breach not cured within 30 days of written notice thereof shall result in immediate termination of such license without further notice. Any unauthorized (but licensable) use of a Work that is terminated immediately upon notice thereof may be liquidated by payment of the Rightsholder's ordinary license price therefor; any unauthorized (and unlicensable) use that is not terminated immediately for any reason (including, for example, because materials containing the Work cannot reasonably be recalled) will be subject to all remedies available at law or in equity, but in no event to a payment of less than three times the Rightsholder's ordinary license price for the most closely analogous licensable use plus Rightsholder's and/or CCC's costs and expenses incurred in collecting such payment.

8. Miscellaneous.

   8.1. User acknowledges that CCC may, from time to time, make changes or additions to the Service or to these terms and conditions, and CCC reserves the right to send notice to the User by electronic mail or otherwise for the purposes of notifying User of such changes or additions; provided that any such changes or additions shall not apply to permissions already secured and paid for.

   8.2. Use of User-related information collected through the Service is governed by CCC's privacy policy, available online here:https://marketplace.copyright.com/rs-ui-web/mp/privacy-policy

   8.3. The licensing transaction described in the Order Confirmation is personal to User. Therefore, User may not assign or transfer to any other person (whether a natural person or an organization of any kind) the license created by the Order Confirmation and these terms and conditions or any rights granted hereunder; provided, however, that User may assign such license in its entirety on written notice to CCC in the event of a transfer of all or substantially all of User's rights in the new material which includes the Work(s) licensed under this Service.

   8.4. No amendment or waiver of any terms is binding unless set forth in writing and signed by the parties. The Rightsholder and CCC hereby object to any terms contained in any writing prepared by the User or its principals, employees, agents or affiliates and purporting to govern or otherwise relate to the licensing transaction described in the Order Confirmation, which terms are in any way inconsistent with any terms set forth in the Order Confirmation and/or in these terms and conditions or CCC's standard operating procedures, whether such writing is prepared prior to, simultaneously with or subsequent to the Order Confirmation, and whether such writing appears on a copy of the Order Confirmation or in a separate instrument.

   8.5. The licensing transaction described in the Order Confirmation document shall be governed by and construed under the law of the State of New York, USA, without regard to the principles thereof of conflicts of law. Any case, controversy, suit, action, or proceeding arising out of, in connection with, or related to such licensing transaction shall be brought, at CCC's sole discretion, in any federal or state court located in the County of New York, State of New York, USA, or in any federal or state court whose geographical jurisdiction covers the location of the Rightsholder set forth in the Order Confirmation. The parties expressly submit to the personal jurisdiction and venue of each such federal or state court.If you have any comments or questions about the Service or Copyright Clearance Center, please contact us at 978-750-8400 or send an e-mail to support@copyright.com

Contents lists available at ScienceDirect

Food Chemistry

Curcumin-loaded proliposomes produced by the coating of micronized sucrose: Influence of the type of phospholipid on the physicochemical characteristics of powders and on the liposomes obtained by hydration

Matheus A. Chaves, Samantha C. Pinho*

Laboratory of Encapsulation and Functional Foods (LEnAlis), Department of Food Engineering, School of Animal Science and Food Engineering, University of São Paulo, Av. Duque de Caxias Norte 225, Pirassununga, SP, Brazil

ARTICLE INFO

ABSTRACT

The feasibility of producing proliposomes containing curcumin, as well as liposome dispersions, using different mixtures of purified and nonpurified soybean phospholipids was studied. Proliposomes were produced through coating of micronized sucrose and physicochemically characterized over 30 days of storage. In addition, the possible interactions among the components were investigated using X-ray powder diffraction (XRD) and Fourier transform infrared spectroscopy (FT-IR). The proliposomes demonstrated a low propensity of water adsorption and low hygroscopicity. In addition, the curcumin content retained in the powders ranged from 67 to 92%. The liposomes were produced following proliposome hydration. Atomic force microscopy indicated the vesicles presented spherical shapes and photon correlation spectroscopy detected that their hydrodynamic diameters ranged from 207 to 222 nm. Finally, the curcumin-loaded liposomes preserved up to 63% of the bioactive compound but remained stable for only 15 days of storage.

1. Introduction

Color is considered to be one of the most important attributes in the judgment of food quality and the acceptance of food products by consumers along with flavor, texture and aroma. In this context, synthetic colorants have been applied in food industries for several purposes, including maintaining the color lost during the processing and standardizing the color among different food product batches. However, studies have linked the intake of synthetic yellow dyes, such as tartrazine (E102), to adverse health effects in children, including allergies, attention deficit, irritability, restlessness and sleep disturbance. In this context, the natural yellow colorant curcumin (E100) appears to be a suitable natural alternative to tartrazine (Arango-Ruiz, Martin, Cosero, Jiménez, & Londoño, 2018).

Curcumin (diferulomethane) is the primary natural polyphenol found in the rhizome of the herbaceous plant *Curcuma longa* L., also known as turmeric. Curcumin is currently used in the food industry as a coloring, flavoring and preservative agent in several products, including cheeses, margarine, curry, soups, mustard and ice cream (Borrin, Georges, Moraes, & Pinho, 2016). In addition, curcumin exhibits several medicinal properties, including antioxidant, anti-

inflammatory, anticancer, and antimicrobial activities, all suggested to be related to its chemical structure, which includes hydroxyl groups linked to benzene rings, double bonds in the alkene portion, and a central β-diketone moiety (Liu, Ying, Cai, & Le, 2017). However, the direct incorporation of curcumin into aqueous-based food formulations is hampered due to its low solubility in water (11 ng.mL^{-1} at 25 °C), high photosensitivity and instability in the presence of chemical oxidants (Aditya et al., 2013). To overcome these disadvantages, the encapsulation of curcumin in lipid carriers as liposomes appears to be an alternative to increase its aqueous solubility, in addition to increasing its oral bioavailability (Chaves et al., 2018).

Liposomes are colloidal spherical vesicles with an internal aqueous core formed by the self-assembly of amphiphilic phospholipids in aqueous media (Lasic, 1998). These systems have been applied to improve the bioavailability of hydrophobic bioactive compounds and to promote their controlled release in food formulations (Taylor, Davidson, Bruce, & Weiss, 2005). Phosphatidylcholines are the most abundant phospholipids in nature and are also used the most frequently in liposome productions. In addition, other phospholipids, such as lysophosphatidylcholine, phosphatidylinositol, and phosphatidylethanolamine, can also be utilized to produce liposomes. These lecithins can

ATTACHMENT B – PAPER PUBLISHED IN FOOD BIOSCIENCE

CCC Marketplace™

This is a License Agreement between Matheus Andrade Chaves ("User") and Copyright Clearance Center, Inc. ("CCC") on behalf of the Rightsholder identified in the order details below. The license consists of the order details, the CCC Terms and Conditions below, and any Rightsholder Terms and Conditions which are included below.

All payments must be made in full to CCC in accordance with the CCC Terms and Conditions below.

Order Date	29-Sep-2021	Type of Use	Republish in a thesis/dissertation
Order License ID	1151037-1		
ISSN	2212-4292	Publisher	Elsevier Ltd
		Portion	Chapter/article

LICENSED CONTENT

Publication Title	FOOD BIOSCIENCE	Rightsholder	Elsevier Science & Technology Journals
Article Title	Unpurified soybean lecithins impact on the chemistry of proliposomes and liposome dispersions encapsulating vitamin D3	Publication Type	Journal
		Start Page	100700
		Volume	37
Date	01/01/2013		
Language	English		
Country	United Kingdom of Great Britain and Northern Ireland		

REQUEST DETAILS

Portion Type	Chapter/article	Rights Requested	Main product
Page range(s)	1-9	Distribution	Worldwide
Total number of pages	9	Translation	Original language of publication
Format (select all that apply)	Print, Electronic	Copies for the disabled?	No
Who will republish the content?	Author of requested content	Minor editing privileges?	No
Duration of Use	Life of current edition	Incidental promotional use?	No
Lifetime Unit Quantity	Up to 499	Currency	USD

NEW WORK DETAILS

Title	ENRICHMENT OF CORNSTARCH WITH CURCUMIN AND VITAMIN D3 COENCAPSULATED IN LYOPHILIZED LIPOSOMES USING HIGH SHEAR WET AGGLOMERATION	Institution name	University of São Paulo
		Expected presentation date	2021-09-29
Instructor name	Matheus Andrade Chaves		

ADDITIONAL DETAILS

Order reference number	N/A	The requesting person / organization to appear on the license	Matheus Andrade Chaves

REUSE CONTENT DETAILS

Title, description or numeric reference of the portion(s)	1	Title of the article/chapter the portion is from	Unpurified soybean lecithins impact on the chemistry of proliposomes and liposome dispersions encapsulating vitamin D3
Editor of portion(s)	Pinho, Samantha C.; Chaves, Matheus A.		
Volume of serial or monograph	37	Author of portion(s)	Pinho, Samantha C.; Chaves, Matheus A.
Page or page range of portion	100700	Issue, if republishing an article from a serial	N/A
		Publication date of portion	2020-10-01

RIGHTSHOLDER TERMS AND CONDITIONS

Elsevier publishes Open Access articles in both its Open Access journals and via its Open Access articles option in subscription journals, for which an author selects a user license permitting certain types of reuse without permission. Before proceeding please check if the article is Open Access on http://www.sciencedirect.com and refer to the user license for the individual article. Any reuse not included in the user license terms will require permission. You must always fully and appropriately credit the author and source. If any part of the material to be used (for example, figures) has appeared in the Elsevier publication for which you are seeking permission, with credit or acknowledgement to another source it is the responsibility of the user to ensure their reuse complies with the terms and conditions determined by the rights holder. Please contact permissions@elsevier.com with any queries.

CCC Terms and Conditions

1. Description of Service; Defined Terms. This Republication License enables the User to obtain licenses for republication of one or more copyrighted works as described in detail on the relevant Order Confirmation (the "Work(s)"). Copyright Clearance Center, Inc. ("CCC") grants licenses through the Service on behalf of the rightsholder identified on the Order Confirmation (the "Rightsholder"). "Republication", as used herein, generally means the inclusion of a Work, in whole or in part, in a new work or works, also as described on the Order Confirmation. "User", as used herein, means the person or entity making such republication.

2. The terms set forth in the relevant Order Confirmation, and any terms set by the Rightsholder with respect to a particular Work, govern the terms of use of Works in connection with the Service. By using the Service, the person transacting for a republication license on behalf of the User represents and warrants that he/she/it (a) has been duly authorized by the User to accept, and hereby does accept, all such terms and conditions on behalf of User, and (b) shall inform User of all such terms and conditions. In the event such person is a "freelancer" or other third party independent of User and CCC, such party shall be deemed jointly a "User" for purposes of these terms and conditions. In any event, User shall be deemed to have accepted and agreed to all such terms and conditions if User republishes the Work in any fashion.

3. Scope of License; Limitations and Obligations.

   3.1. All Works and all rights therein, including copyright rights, remain the sole and exclusive property of the Rightsholder. The license created by the exchange of an Order Confirmation (and/or any invoice) and payment by User of the full amount set forth on that document includes only those rights expressly set forth in the Order Confirmation and in these terms and conditions, and conveys no other rights in the Work(s) to User. All rights not expressly granted are hereby reserved.

   3.2. General Payment Terms: You may pay by credit card or through an account with us payable at the end of the month. If you and we agree that you may establish a standing account with CCC, then the following terms apply: Remit Payment to: Copyright Clearance Center, 29118 Network Place, Chicago, IL 60673-1291. Payments Due: Invoices are payable upon their delivery to you (or upon our notice to you that they are available to you for downloading). After 30 days, outstanding amounts will be subject to a service charge of 1-1/2% per month or, if less, the maximum rate allowed by applicable law. Unless otherwise specifically set forth in the Order Confirmation or in a separate written agreement signed by CCC, invoices are due and payable on "net 30" terms. While User may exercise the rights licensed immediately upon issuance of the Order Confirmation, the license is automatically revoked and is null and void, as if it had never been issued, if complete payment for the license is not received on a timely basis either from User directly or through a payment agent, such as a credit card company.

   3.3.
   Unless otherwise provided in the Order Confirmation, any grant of rights to User (i) is "one-time" (including

the editions and product family specified in the license), (ii) is non-exclusive and non-transferable and (iii) is subject to any and all limitations and restrictions (such as, but not limited to, limitations on duration of use or circulation) included in the Order Confirmation or invoice and/or in these terms and conditions. Upon completion of the licensed use, User shall either secure a new permission for further use of the Work(s) or immediately cease any new use of the Work(s) and shall render inaccessible (such as by deleting or by removing or severing links or other locators) any further copies of the Work (except for copies printed on paper in accordance with this license and still in User's stock at the end of such period).

3.4. In the event that the material for which a republication license is sought includes third party materials (such as photographs, illustrations, graphs, inserts and similar materials) which are identified in such material as having been used by permission, User is responsible for identifying, and seeking separate licenses (under this Service or otherwise) for, any of such third party materials; without a separate license, such third party materials may not be used.

3.5. Use of proper copyright notice for a Work is required as a condition of any license granted under the Service. Unless otherwise provided in the Order Confirmation, a proper copyright notice will read substantially as follows: "Republished with permission of [Rightsholder's name], from [Work's title, author, volume, edition number and year of copyright]; permission conveyed through Copyright Clearance Center, Inc. " Such notice must be provided in a reasonably legible font size and must be placed either immediately adjacent to the Work as used (for example, as part of a by-line or footnote but not as a separate electronic link) or in the place where substantially all other credits or notices for the new work containing the republished Work are located. Failure to include the required notice results in loss to the Rightsholder and CCC, and the User shall be liable to pay liquidated damages for each such failure equal to twice the use fee specified in the Order Confirmation, in addition to the use fee itself and any other fees and charges specified.

3.6. User may only make alterations to the Work if and as expressly set forth in the Order Confirmation. No Work may be used in any way that is defamatory, violates the rights of third parties (including such third parties' rights of copyright, privacy, publicity, or other tangible or intangible property), or is otherwise illegal, sexually explicit or obscene. In addition, User may not conjoin a Work with any other material that may result in damage to the reputation of the Rightsholder. User agrees to inform CCC if it becomes aware of any infringement of any rights in a Work and to cooperate with any reasonable request of CCC or the Rightsholder in connection therewith.

4. Indemnity. User hereby indemnifies and agrees to defend the Rightsholder and CCC, and their respective employees and directors, against all claims, liability, damages, costs and expenses, including legal fees and expenses, arising out of any use of a Work beyond the scope of the rights granted herein, or any use of a Work which has been altered in any unauthorized way by User, including claims of defamation or infringement of rights of copyright, publicity, privacy or other tangible or intangible property.

5. Limitation of Liability. UNDER NO CIRCUMSTANCES WILL CCC OR THE RIGHTSHOLDER BE LIABLE FOR ANY DIRECT, INDIRECT, CONSEQUENTIAL OR INCIDENTAL DAMAGES (INCLUDING WITHOUT LIMITATION DAMAGES FOR LOSS OF BUSINESS PROFITS OR INFORMATION, OR FOR BUSINESS INTERRUPTION) ARISING OUT OF THE USE OR INABILITY TO USE A WORK, EVEN IF ONE OF THEM HAS BEEN ADVISED OF THE POSSIBILITY OF SUCH DAMAGES. In any event, the total liability of the Rightsholder and CCC (including their respective employees and directors) shall not exceed the total amount actually paid by User for this license. User assumes full liability for the actions and omissions of its principals, employees, agents, affiliates, successors and assigns.

6. Limited Warranties. THE WORK(S) AND RIGHT(S) ARE PROVIDED "AS IS". CCC HAS THE RIGHT TO GRANT TO USER THE RIGHTS GRANTED IN THE ORDER CONFIRMATION DOCUMENT. CCC AND THE RIGHTSHOLDER DISCLAIM ALL OTHER WARRANTIES RELATING TO THE WORK(S) AND RIGHT(S), EITHER EXPRESS OR IMPLIED, INCLUDING WITHOUT LIMITATION IMPLIED WARRANTIES OF MERCHANTABILITY OR FITNESS FOR A PARTICULAR PURPOSE. ADDITIONAL RIGHTS MAY BE REQUIRED TO USE ILLUSTRATIONS, GRAPHS, PHOTOGRAPHS, ABSTRACTS, INSERTS OR OTHER PORTIONS OF THE WORK (AS OPPOSED TO THE ENTIRE WORK) IN A MANNER CONTEMPLATED BY USER; USER UNDERSTANDS AND AGREES THAT NEITHER CCC NOR THE RIGHTSHOLDER MAY HAVE SUCH ADDITIONAL RIGHTS TO GRANT.

7.

Effect of Breach. Any failure by User to pay any amount when due, or any use by User of a Work beyond the scope of the license set forth in the Order Confirmation and/or these terms and conditions, shall be a material breach of the license created by the Order Confirmation and these terms and conditions. Any breach not cured within 30 days of written notice thereof shall result in immediate termination of such license without further notice. Any

unauthorized (but licensable) use of a Work that is terminated immediately upon notice thereof may be liquidated by payment of the Rightsholder's ordinary license price therefor; any unauthorized (and unlicensable) use that is not terminated immediately for any reason (including, for example, because materials containing the Work cannot reasonably be recalled) will be subject to all remedies available at law or in equity, but in no event to a payment of less than three times the Rightsholder's ordinary license price for the most closely analogous licensable use plus Rightsholder's and/or CCC's costs and expenses incurred in collecting such payment.

8. Miscellaneous.

8.1. User acknowledges that CCC may, from time to time, make changes or additions to the Service or to these terms and conditions, and CCC reserves the right to send notice to the User by electronic mail or otherwise for the purposes of notifying User of such changes or additions; provided that any such changes or additions shall not apply to permissions already secured and paid for.

8.2. Use of User-related information collected through the Service is governed by CCC's privacy policy, available online here:https://marketplace.copyright.com/rs-ui-web/mp/privacy-policy

8.3. The licensing transaction described in the Order Confirmation is personal to User. Therefore, User may not assign or transfer to any other person (whether a natural person or an organization of any kind) the license created by the Order Confirmation and these terms and conditions or any rights granted hereunder; provided, however, that User may assign such license in its entirety on written notice to CCC in the event of a transfer of all or substantially all of User's rights in the new material which includes the Work(s) licensed under this Service.

8.4. No amendment or waiver of any terms is binding unless set forth in writing and signed by the parties. The Rightsholder and CCC hereby object to any terms contained in any writing prepared by the User or its principals, employees, agents or affiliates and purporting to govern or otherwise relate to the licensing transaction described in the Order Confirmation, which terms are in any way inconsistent with any terms set forth in the Order Confirmation and/or in these terms and conditions or CCC's standard operating procedures, whether such writing is prepared prior to, simultaneously with or subsequent to the Order Confirmation, and whether such writing appears on a copy of the Order Confirmation or in a separate instrument.

8.5. The licensing transaction described in the Order Confirmation document shall be governed by and construed under the law of the State of New York, USA, without regard to the principles thereof of conflicts of law. Any case, controversy, suit, action, or proceeding arising out of, in connection with, or related to such licensing transaction shall be brought, at CCC's sole discretion, in any federal or state court located in the County of New York, State of New York, USA, or in any federal or state court whose geographical jurisdiction covers the location of the Rightsholder set forth in the Order Confirmation. The parties expressly submit to the personal jurisdiction and venue of each such federal or state court.If you have any comments or questions about the Service or Copyright Clearance Center, please contact us at 978-750-8400 or send an e-mail to:support@copyright.com

v 1.1

Unpurified soybean lecithins impact on the chemistry of proliposomes and liposome dispersions encapsulating vitamin D3

Matheus A. Chaves, Samantha C. Pinho[*]

Laboratory of Encapsulation and Functional Foods (LEnAliz), Department of Food Engineering, School of Animal Science and Food Engineering, University of São Paulo, Pirassununga, São Paulo, Brasil

ARTICLE INFO

ABSTRACT

Vitamin D_3 (VD3)-loaded proliposomes using the micronized sucrose coating (MSC) technique and mixtures of soybean lecithins with variable degrees of purity were prepared. The phospholipid powders were characterized in terms of water activity, moisture content, solubility, hygroscopicity, moisture adsorption isotherms and the retained amount of VD3. X-ray diffraction and Fourier transform infrared spectroscopy were the techniques applied to investigate molecular interactions among the ingredients during the coating process, as well as the crystalline structure of the phospholipid powders. Liposome dispersions were produced by hydration of the proliposomes. The liposomal systems were analyzed in terms of hydrodynamic diameter, size distribution, zeta potential and the amount of encapsulated VD3. The morphologies of proliposomes and liposomes were observed using scanning electron microscopy and atomic force microscopy, respectively. The VD3-proliposomes showed low values for water activity, moisture content and solubility as well as high values for hygroscopicity. Liposome dispersions were in the nanometer range and showed high values for zeta potential, but remained stable for only 15 days, probably due to the high concentrations of unpurified lecithin used throughout the process (>50% w/w). However, the content of VD3 in proliposomes and in loaded-liposome dispersions reached 81.4 and 90.2%, respectively. The results suggested that it was feasible to prepare VD3-entrapped proliposomes using the MSC method, but storage conditions must be better controlled to maintain their stability.

1. Introduction

Vitamins have several fundamental roles, including the promotion of normal body growth, and the prevention and treatment of several disorders. Vitamin D (VD), which comprises vitamin D_2 (VD2, ergocalciferol) and vitamin D_3 (VD3, cholecalciferol), is a prohormone with different biological effects, including the control of calcium and phosphorus metabolism (Wiseman, 1993). VD3 is the most active form of VD, and it can be synthesized after the exposure to light of 7-dehydrocholesterol molecules present in the human epidermis (Lee et al., 2008). Nevertheless, VD3 deficiency is now recognized as a pandemic (Holick, 2017). The main cause for such deficiency is the lack of sunlight exposure due to several reasons, such as (a) staying indoors for long periods of time, (b) some geographic conditions at higher latitudes, and (c) the loss of 7-dehydrocholesterol reserves in the epidermis throughout the years (Holick, 2017).

Unfortunately, only a few foods naturally contain VD3. Examples include fresh salmon, cod liver oil, and egg yolk (Holick, 2007). The fortification of food products with VD3 appears to be a possible solution to overcome this drawback (Gomes et al., 2015). However, to optimize the fortification process, tighter control of processing conditions is necessary, as this vitamin is susceptible to degradation, especially when exposed to light, oxygen, elevated temperatures and humidity (Jakobsen & Knuthsen, 2014). Several colloidal systems are already being studied for the delivery of VD3, such as micelles (Desmarchelier et al., 2017), nanoemulsions (Ozturk et al., 2015), polymeric nanospheres (Ramezanli et al., 2017), water-in-oil-in-water double emulsions (Dima & Dima, 2020) and liposomes (Chaves et al., 2018). The incorporation of VD3 into lipid carrier systems as liposomes may create a barrier against prooxidant agents, in addition to increasing its bioavailability (Chaves et al., 2018).

Liposomes are amphipathic spherical-shaped vesicles that contain an internal aqueous phase surrounded by one or more concentric phospholipid bilayers. These systems are applied for encapsulation because

ATTACHMENT C – PAPER PUBLISHED IN JOURNAL OF FOOD PROCESSING AND PRESERVATION

**JOHN WILEY AND SONS LICENSE
TERMS AND CONDITIONS**

Jan 25, 2022

This Agreement between Mr. Matheus Andrade Chaves ("You") and John Wiley and Sons ("John Wiley and Sons") consists of your license details and the terms and conditions provided by John Wiley and Sons and Copyright Clearance Center.

License Number	5235940177005
License date	Jan 25, 2022
Licensed Content Publisher	John Wiley and Sons
Licensed Content Publication	Journal of Food Processing and Preservation
Licensed Content Title	Influence of phospholipid saturation on the physicochemical characteristics of curcumin/vitamin D3 co-loaded proliposomes obtained by the micronized sucrose coating process
Licensed Content Author	Matheus Andrade Chaves, Samantha Cristina Pinho
Licensed Content Date	Oct 11, 2021
Licensed Content Volume	45
Licensed Content Issue	12

292

Licensed Content Pages	10
Type of use	Dissertation/Thesis
Requestor type	Author of this Wiley article
Format	Print and electronic
Portion	Full article
Will you be translating?	No
Title	ENRICHMENT OF CORNSTARCH WITH CURCUMIN AND VITAMIN D3 COENCAPSULATED IN LYOPHILIZED LIPOSOMES USING HIGH SHEAR WET AGGLOMERATION
Institution name	University of São Paulo
Expected presentation date	Nov 2022
Order reference number	1
Requestor Location	Mr. Matheus Andrade Chaves Rua Jovelino do Amaral Camargo 350 JAÚ, São Paulo 17211-400 Brazil Attn: Mr. Matheus Andrade Chaves
Publisher Tax ID	EU826007151
Total	0.00 USD

Terms and Conditions

TERMS AND CONDITIONS

This copyrighted material is owned by or exclusively licensed to John Wiley & Sons, Inc. or one of its group companies (each a"Wiley Company") or handled on behalf of a society with which a Wiley Company has exclusive publishing rights in relation to a particular work (collectively "WILEY"). By clicking "accept" in connection with completing this licensing transaction, you agree that the following terms and conditions apply to this transaction (along with the billing and payment terms and conditions established by the Copyright Clearance Center Inc., ("CCC's Billing and Payment terms and conditions"), at the time that you opened your RightsLink account (these are available at any time at http://myaccount.copyright.com).

Terms and Conditions

- The materials you have requested permission to reproduce or reuse (the "Wiley Materials") are protected by copyright.

- You are hereby granted a personal, non-exclusive, non-sub licensable (on a stand-alone basis), non-transferable, worldwide, limited license to reproduce the Wiley Materials for the purpose specified in the licensing process. This license, and any CONTENT (PDF or image file) purchased as part of your order, is for a one-time use only and limited to any maximum distribution number specified in the license. The first instance of republication or reuse granted by this license must be completed within two years of the date of the grant of this license (although copies prepared before the end date may be distributed thereafter). The Wiley Materials shall not be used in any other manner or for any other purpose, beyond what is granted in the license. Permission is granted subject to an appropriate acknowledgement given to the author, title of the material/book/journal and the publisher. You shall also duplicate the copyright notice that appears in the Wiley publication in your use of the Wiley Material. Permission is also granted on the understanding that nowhere in the text is a previously published source acknowledged for all or part of this Wiley Material. Any third party content is expressly excluded from this permission.

- With respect to the Wiley Materials, all rights are reserved. Except as expressly granted by the terms of the license, no part of the Wiley Materials may be copied, modified, adapted (except for minor reformatting required by the new Publication), translated, reproduced, transferred or distributed, in any form or by any means, and no derivative works may be made based on the Wiley Materials without the prior permission of the respective copyright owner.**For STM Signatory Publishers clearing permission under the terms of the STM Permissions Guidelines only, the terms of the license are extended to include subsequent editions and for editions in other languages, provided such editions are for the work as a whole in situ and does not involve the separate exploitation of the permitted figures or extracts,** You may not alter, remove or suppress in any manner any copyright, trademark or other notices displayed by the Wiley Materials. You may not license, rent, sell, loan, lease, pledge, offer as security, transfer or assign the Wiley Materials on a stand-alone basis, or any of the rights granted to you hereunder to any other person.

- The Wiley Materials and all of the intellectual property rights therein shall at all times remain the exclusive property of John Wiley & Sons Inc, the Wiley Companies, or their respective licensors, and your interest therein is only that of having possession of and the right to reproduce the Wiley Materials pursuant to Section 2 herein during the continuance of this Agreement. You agree that you own no right, title or interest in or to the Wiley Materials or any of the intellectual property rights therein. You shall have no rights hereunder other than the license as provided for above in Section 2. No right,

294

license or interest to any trademark, trade name, service mark or other branding
("Marks") of WILEY or its licensors is granted hereunder, and you agree that you
shall not assert any such right, license or interest with respect thereto

- NEITHER WILEY NOR ITS LICENSORS MAKES ANY WARRANTY OR
  REPRESENTATION OF ANY KIND TO YOU OR ANY THIRD PARTY,
  EXPRESS, IMPLIED OR STATUTORY, WITH RESPECT TO THE MATERIALS
  OR THE ACCURACY OF ANY INFORMATION CONTAINED IN THE
  MATERIALS, INCLUDING, WITHOUT LIMITATION, ANY IMPLIED
  WARRANTY OF MERCHANTABILITY, ACCURACY, SATISFACTORY
  QUALITY, FITNESS FOR A PARTICULAR PURPOSE, USABILITY,
  INTEGRATION OR NON-INFRINGEMENT AND ALL SUCH WARRANTIES
  ARE HEREBY EXCLUDED BY WILEY AND ITS LICENSORS AND WAIVED
  BY YOU.

- WILEY shall have the right to terminate this Agreement immediately upon breach of
  this Agreement by you.

- You shall indemnify, defend and hold harmless WILEY, its Licensors and their
  respective directors, officers, agents and employees, from and against any actual or
  threatened claims, demands, causes of action or proceedings arising from any breach
  of this Agreement by you.

- IN NO EVENT SHALL WILEY OR ITS LICENSORS BE LIABLE TO YOU OR
  ANY OTHER PARTY OR ANY OTHER PERSON OR ENTITY FOR ANY
  SPECIAL, CONSEQUENTIAL, INCIDENTAL, INDIRECT, EXEMPLARY OR
  PUNITIVE DAMAGES, HOWEVER CAUSED, ARISING OUT OF OR IN
  CONNECTION WITH THE DOWNLOADING, PROVISIONING, VIEWING OR
  USE OF THE MATERIALS REGARDLESS OF THE FORM OF ACTION,
  WHETHER FOR BREACH OF CONTRACT, BREACH OF WARRANTY, TORT,
  NEGLIGENCE, INFRINGEMENT OR OTHERWISE (INCLUDING, WITHOUT
  LIMITATION, DAMAGES BASED ON LOSS OF PROFITS, DATA, FILES, USE,
  BUSINESS OPPORTUNITY OR CLAIMS OF THIRD PARTIES), AND WHETHER
  OR NOT THE PARTY HAS BEEN ADVISED OF THE POSSIBILITY OF SUCH
  DAMAGES. THIS LIMITATION SHALL APPLY NOTWITHSTANDING ANY
  FAILURE OF ESSENTIAL PURPOSE OF ANY LIMITED REMEDY PROVIDED
  HEREIN.

- Should any provision of this Agreement be held by a court of competent jurisdiction
  to be illegal, invalid, or unenforceable, that provision shall be deemed amended to
  achieve as nearly as possible the same economic effect as the original provision, and
  the legality, validity and enforceability of the remaining provisions of this Agreement
  shall not be affected or impaired thereby.

- The failure of either party to enforce any term or condition of this Agreement shall not
  constitute a waiver of either party's right to enforce each and every term and condition
  of this Agreement. No breach under this agreement shall be deemed waived or
  excused by either party unless such waiver or consent is in writing signed by the party
  granting such waiver or consent. The waiver by or consent of a party to a breach of
  any provision of this Agreement shall not operate or be construed as a waiver of or
  consent to any other or subsequent breach by such other party.

- This Agreement may not be assigned (including by operation of law or otherwise) by
  you without WILEY's prior written consent.

- Any fee required for this permission shall be non-refundable after thirty (30) days
  from receipt by the CCC.

- These terms and conditions together with CCC's Billing and Payment terms and conditions (which are incorporated herein) form the entire agreement between you and WILEY concerning this licensing transaction and (in the absence of fraud) supersedes all prior agreements and representations of the parties, oral or written. This Agreement may not be amended except in writing signed by both parties. This Agreement shall be binding upon and inure to the benefit of the parties' successors, legal representatives, and authorized assigns.

- In the event of any conflict between your obligations established by these terms and conditions and those established by CCC's Billing and Payment terms and conditions, these terms and conditions shall prevail.

- WILEY expressly reserves all rights not specifically granted in the combination of (i) the license details provided by you and accepted in the course of this licensing transaction, (ii) these terms and conditions and (iii) CCC's Billing and Payment terms and conditions.

- This Agreement will be void if the Type of Use, Format, Circulation, or Requestor Type was misrepresented during the licensing process.

- This Agreement shall be governed by and construed in accordance with the laws of the State of New York, USA, without regards to such state's conflict of law rules. Any legal action, suit or proceeding arising out of or relating to these Terms and Conditions or the breach thereof shall be instituted in a court of competent jurisdiction in New York County in the State of New York in the United States of America and each party hereby consents and submits to the personal jurisdiction of such court, waives any objection to venue in such court and consents to service of process by registered or certified mail, return receipt requested, at the last known address of such party.

WILEY OPEN ACCESS TERMS AND CONDITIONS

Wiley Publishes Open Access Articles in fully Open Access Journals and in Subscription journals offering Online Open. Although most of the fully Open Access journals publish open access articles under the terms of the Creative Commons Attribution (CC BY) License only, the subscription journals and a few of the Open Access Journals offer a choice of Creative Commons Licenses. The license type is clearly identified on the article.

The Creative Commons Attribution License

The Creative Commons Attribution License (CC-BY) allows users to copy, distribute and transmit an article, adapt the article and make commercial use of the article. The CC-BY license permits commercial and non-

Creative Commons Attribution Non-Commercial License

The Creative Commons Attribution Non-Commercial (CC-BY-NC)License permits use, distribution and reproduction in any medium, provided the original work is properly cited and is not used for commercial purposes.(see below)

Creative Commons Attribution-Non-Commercial-NoDerivs License

The Creative Commons Attribution Non-Commercial-NoDerivs License (CC-BY-NC-ND) permits use, distribution and reproduction in any medium, provided the original work is properly cited, is not used for commercial purposes and no modifications or adaptations are made. (see below)

Use by commercial "for-profit" organizations

296

Use of Wiley Open Access articles for commercial, promotional, or marketing purposes requires further explicit permission from Wiley and will be subject to a fee.

Further details can be found on Wiley Online Library
http://olabout.wiley.com/WileyCDA/Section/id-410895.html

Other Terms and Conditions:

v1.10 Last updated September 2015

Questions? customercare@copyright.com or +1-855-239-3415 (toll free in the US) or +1-978-646-2777.
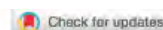
ORIGINAL ARTICLE

Influence of phospholipid saturation on the physicochemical characteristics of curcumin/vitamin D_3 co-loaded proliposomes obtained by the micronized sucrose coating process

Matheus Andrade Chaves [iD] | Samantha Cristina de Pinho [iD]

Laboratory of Encapsulation and Functional Foods (LEnAlis), Department of Food Engineering, School of Animal Science and Food Engineering, University of São Paulo, Pirassununga, Brazil

Correspondence
Samantha Cristina de Pinho, Department of Food Engineering, School of Animal Science and Food Engineering, University of São Paulo, Av. Duque de Caxias Norte, 225, Pirassununga, SP, Brazil.
Email: samantha@usp.br

Abstract

The effects of different ratios of food-grade saturated and unsaturated soy phospholipids on the production of proliposomes with curcumin and vitamin D_3 were studied. A micronized sucrose-coating process was employed to obtain the proliposomes. The phospholipid ratio had a minor influence on their physicochemical parameters, as low values for water activity ($A_w \leq 0.26$), moisture content ($X_w \leq 2.97\%$), hygroscopicity (≤ 8.62 g adsorbed water/100 g dry matter), and intermediate values for solubility ($\leq 44.8\%$ of solubilized powder) were obtained. Also, Fourier transform infrared and X-ray powder diffraction results revealed an improvement in their amorphous structure due to sucrose. The entrapment efficiency values for curcumin and vitamin D_3 were up to 100% and 98.7%, respectively, after 60 days. Additionally, the nanoliposomes resulting from the hydration of proliposomes exhibited sizes lower than 400 nm. The results shown herein are relevant to the production of lower-cost synergistic carriers with high bioactive retention using an abundant raw material such as sucrose.

Novelty impact statement: Purified phospholipids are commonly used in the production of liposomes, but their high cost may be a limiting factor for their large-scale production. Non-purified phospholipids can be up to 20% cheaper. The production of proliposomes containing different ratios of phospholipids with different degrees of saturation has never been explored for the coencapsulation of curcumin and vitamin D_3, two hydrophobic molecules with well-known biological activities. The micronized sucrose coating process allows the production of a cheaper and easily reproducible food-grade carrier with high bioactive retentions.

1 | INTRODUCTION

Curcumin (CUR, 1,7-diphenyl-1,6-heptadiene-3,5-dione) is a natural crystalline polyphenol extracted from the rhizome of turmeric plants. It is often used in supplements or as a preservative and food colorant due to its strong yellow color. Its multiple biological properties include anticarcinogenic, antioxidant, anti-inflammatory, and antimicrobial activities; these are mostly due to the presence of β-dione and keto-enol interconversion structures able to scavenge oxygen free radicals (Tai et al., 2020). Despite its biological activities,

extremely poor solubility in aqueous solutions, very low oral bioavailability and easy degradability hinder its direct incorporation in several food products. In addition, curcumin presents a high metabolic rate and rapid excretion, which decreases its absorption in the human body (Wang et al., 2021).

Vitamin D_3 (VD3, cholecalciferol) is a fat-soluble bioactive substance synthesized in human skin after sunlight exposure. It presents steroid hormone function and plays important roles in calcium and phosphorus homeostasis and bone health and in the inhibition of cardiovascular diseases, different types of cancer and diabetes

ATTACHMENT D – PAPER PUBLISHED IN INTERNATIONAL JOURNAL OF DAIRY TECHNOLOGY

License Number	5158840708007
License date	Sep 30, 2021
Licensed Content Publisher	John Wiley and Sons
Licensed Content Publication	International Journal of Dairy Technology
Licensed Content Title	Nanoliposomes coencapsulating curcumin and vitamin D3 produced by hydration of proliposomes: Effects of the phospholipid composition in the physicochemical characteristics of vesicles and after incorporation in yoghurts
Licensed Content Author	Samantha C. Pinho, Rita Sinigaglia-Coimbra, Vinicius Franckin, et al
Licensed Content Date	Aug 20, 2020
Licensed Content Volume	74
Licensed Content Issue	1

Licensed Content Pages	11
Type of use	Dissertation/Thesis
Requestor type	Author of this Wiley article
Format	Print and electronic
Portion	Full article
Will you be translating?	No
Title	ENRICHMENT OF CORNSTARCH WITH CURCUMIN AND VITAMIN D3 COENCAPSULATED IN LYOPHILIZED LIPOSOMES USING HIGH SHEAR WET AGGLOMERATION
Institution name	University of São Paulo
Expected presentation date	Nov 2021
Order reference number	3
Requestor Location	Mr. Matheus Andrade Chaves Rua Jovelino do Amaral Camargo 350 JAÚ, São Paulo 17211-400 Brazil Attn: Mr. Matheus Andrade Chaves
Publisher Tax ID	EU826007151
Total	0.00 USD

Terms and Conditions

- These terms and conditions together with CCC's Billing and Payment terms and conditions (which are incorporated herein) form the entire agreement between you and WILEY concerning this licensing transaction and (in the absence of fraud) supersedes all prior agreements and representations of the parties, oral or written. This Agreement may not be amended except in writing signed by both parties. This Agreement shall be binding upon and inure to the benefit of the parties' successors, legal representatives, and authorized assigns.

- In the event of any conflict between your obligations established by these terms and conditions and those established by CCC's Billing and Payment terms and conditions, these terms and conditions shall prevail.

- WILEY expressly reserves all rights not specifically granted in the combination of (i) the license details provided by you and accepted in the course of this licensing transaction, (ii) these terms and conditions and (iii) CCC's Billing and Payment terms and conditions.

- This Agreement will be void if the Type of Use, Format, Circulation, or Requestor Type was misrepresented during the licensing process.

- This Agreement shall be governed by and construed in accordance with the laws of the State of New York, USA, without regards to such state's conflict of law rules. Any legal action, suit or proceeding arising out of or relating to these Terms and Conditions or the breach thereof shall be instituted in a court of competent jurisdiction in New York County in the State of New York in the United States of America and each party hereby consents and submits to the personal jurisdiction of such court, waives any objection to venue in such court and consents to service of process by registered or certified mail, return receipt requested, at the last known address of such party.

WILEY OPEN ACCESS TERMS AND CONDITIONS

Wiley Publishes Open Access Articles in fully Open Access Journals and in Subscription journals offering Online Open. Although most of the fully Open Access journals publish open access articles under the terms of the Creative Commons Attribution (CC BY) License only, the subscription journals and a few of the Open Access Journals offer a choice of Creative Commons Licenses. The license type is clearly identified on the article.

The Creative Commons Attribution License

The Creative Commons Attribution License (CC-BY) allows users to copy, distribute and transmit an article, adapt the article and make commercial use of the article. The CC-BY license permits commercial and non-

Creative Commons Attribution Non-Commercial License

The Creative Commons Attribution Non-Commercial (CC-BY-NC)License permits use, distribution and reproduction in any medium, provided the original work is properly cited and is not used for commercial purposes.(see below)

Creative Commons Attribution-Non-Commercial-NoDerivs License

The Creative Commons Attribution Non-Commercial-NoDerivs License (CC-BY-NC-ND) permits use, distribution and reproduction in any medium, provided the original work is properly cited, is not used for commercial purposes and no modifications or adaptations are made. (see below)

Use by commercial "for-profit" organizations

304

ORIGINAL
RESEARCH

Nanoliposomes coencapsulating curcumin and vitamin D₃ produced by hydration of proliposomes: Effects of the phospholipid composition in the physicochemical characteristics of vesicles and after incorporation in yoghurts

MATHEUS A. CHAVES,[1] VINICIUS FRANCKIN,[1] RITA
SINIGAGLIA-COIMBRA[2] and SAMANTHA C. PINHO*[1]

[1]*Department of Food Engineering, Laboratory of Encapsulation and Functional Foods (LEnAlis), School of Animal Science and Food Engineering, University of São Paulo, Av. Duque de Caxias Norte 225, Pirassununga, SP 13635-000, and* [2]*Electron Microscopy Center, Federal University of São Paulo, Rua Botucatu 862, São Paulo, SP 04023-062, Brazil*

Nanoliposomes coencapsulating curcumin and vitamin D₃ (VD3) using different compositions of purified and unpurified lecithins were produced by hydration of proliposomes and characterised over 15 days of storage. The dispersions were incorporated to pineapple yoghurts produced in laboratory-scale, which were also characterised. Results showed that curcumin and vitamin D₃ were retained in the nanovesicles up to 86.1% and 94.1%, respectively. Most of the parameters assessed for the yoghurt samples were within the limits required by the Brazilian legislation and the Codex Alimentarius. Finally, the enriched product was well accepted by the panellists with the purchase intention ranging from 53 to 75%.

Keywords Dairy technology, Rheology, Fortification, Microencapsulation, Nutraceutical foods, Physicochemical properties.

INTRODUCTION

Currently, the search for new functional food products has been steadily growing as people are increasingly concerned about their eating habits and pursuing healthier lifestyles. Yoghurt is one of the most biologically active foods consumed by humans as probiotic carriers, and its ingestion is currently linked to health benefits, including a reduction in cholesterol levels, the stimulation of the immune system and the supply of proteins, lipids and micronutrients (Campo *et al.* 2019; Abdesslem *et al.* 2020; Hadjimbei *et al.* 2020; Khaledabad *et al.* 2020). On the other hand, even though yoghurts are not considered rich sources of bioactive compounds, their enrichment can be simple and effective due to their structural characteristics. In this context, nanoencapsulation has been widely reported as a successful method to improve the

application and bioavailability of bioactives in water-formulated foods by preserving and protecting against harmful conditions during processing (Rostamabadi *et al.* 2019).

Nanoliposomes are the nanometric version of liposomes and consist in spherical vesicles containing one or more phospholipid bilayer membranes surrounding an aqueous core formed after an input of energy (Khorasani *et al.* 2018). Among the lipid components used in nanoliposome production, phosphatidylcholine, phosphatidylethanolamine, phosphatidylserine and phosphatidylinositol are the most known and all can be found in lecithins extracted from both soybean or egg yolk. In this sense, unpurified soy lecithins can cost at least 20% less than hydrogenated phospholipids (Chaves and Pinho 2019).

Curcumin is a low-molecular-weight natural polyphenolic compound found in the rhizome of the *Curcuma longa L.* Due to its intense yellow

*Author for
correspondence. E-mail:
samantha@usp.br

ATTACHMENT E – PAPER PUBLISHED IN JOURNAL OF THE TAIWAN INSTITUTE OF CHEMICAL ENGINEERS

CCC Marketplace™

This is a License Agreement between Matheus Andrade Chaves ("User") and Copyright Clearance Center, Inc. ("CCC") on behalf of the Rightsholder identified in the order details below. The license consists of the order details, the CCC Terms and Conditions below, and any Rightsholder Terms and Conditions which are included below.

All payments must be made in full to CCC in accordance with the CCC Terms and Conditions below.

Order Date	27-Jan-2022	Type of Use	Republish in a thesis/dissertation
Order License ID	1182830-1	Publisher	Elsevier; c/o Department of Chemical Engineering, National Taiwan University
ISSN	1876-1070		
		Portion	Chapter/article

LICENSED CONTENT

Publication Title	Journal of the Taiwan Institute of Chemical Engineers	Language	English
		Country	Netherlands
Article Title	Co-encapsulation of curcumin and vitamin D3 in mixed phospholipid nanoliposomes using a continuous supercritical CO2 assisted process	Rightsholder	Elsevier Science & Technology Journals
		Publication Type	Journal
Author/Editor	Zhongguo hua xue gong cheng xue hui.		
Date	01/01/2009		

REQUEST DETAILS

Portion Type	Chapter/article	Rights Requested	Main product
Page range(s)	104120	Distribution	Worldwide
Total number of pages	10	Translation	Original language of publication
Format (select all that apply)	Print, Electronic	Copies for the disabled?	No
Who will republish the content?	Author of requested content	Minor editing privileges?	No
		Incidental promotional use?	No
Duration of Use	Life of current edition		
Lifetime Unit Quantity	Up to 499	Currency	USD

NEW WORK DETAILS

Title	Enrichment of cornstarch with curcumin and vitamin D3 coencapsulated in lyophilized liposomes using high shear wet agglomeration	Institution name	University of São Paulo
		Expected presentation date	2022-01-26
Instructor name	Matheus Andrade Chaves		

ADDITIONAL DETAILS

Order reference number	N/A	The requesting person / organization to appear on the license	Matheus Andrade Chaves

REUSE CONTENT DETAILS

Title, description or numeric reference of the portion(s)	Enrichment of cornstarch with curcumin and vitamin D3 coencapsulated in lyophilized liposomes using high shear wet agglomeration	**Title of the article/chapter the portion is from**	Co-encapsulation of curcumin and vitamin D3 in mixed phospholipid nanoliposomes using a continuous supercritical CO2 assisted process
Editor of portion(s)	Chaves, Matheus A.; Baldino, Lucia; Pinho, Samantha C.; Reverchon, Ernesto	**Author of portion(s)**	Chaves, Matheus A.; Baldino, Lucia; Pinho, Samantha C.; Reverchon, Ernesto
Volume of serial or monograph	N/A	**Issue, if republishing an article from a serial**	N/A
Page or page range of portion	1-10	**Publication date of portion**	2021-10-01

RIGHTSHOLDER TERMS AND CONDITIONS

Elsevier publishes Open Access articles in both its Open Access journals and via its Open Access articles option in subscription journals, for which an author selects a user license permitting certain types of reuse without permission. Before proceeding please check if the article is Open Access on http://www.sciencedirect.com and refer to the user license for the individual article. Any reuse not included in the user license terms will require permission. You must always fully and appropriately credit the author and source. If any part of the material to be used (for example, figures) has appeared in the Elsevier publication for which you are seeking permission, with credit or acknowledgement to another source it is the responsibility of the user to ensure their reuse complies with the terms and conditions determined by the rights holder. Please contact permissions@elsevier.com with any queries.

CCC Terms and Conditions

1. Description of Service; Defined Terms. This Republication License enables the User to obtain licenses for republication of one or more copyrighted works as described in detail on the relevant Order Confirmation (the "Work(s)"). Copyright Clearance Center, Inc. ("CCC") grants licenses through the Service on behalf of the rightsholder identified on the Order Confirmation (the "Rightsholder"). "Republication", as used herein, generally means the inclusion of a Work, in whole or in part, in a new work or works, also as described on the Order Confirmation. "User", as used herein, means the person or entity making such republication.

2. The terms set forth in the relevant Order Confirmation, and any terms set by the Rightsholder with respect to a particular Work, govern the terms of use of Works in connection with the Service. By using the Service, the person transacting for a republication license on behalf of the User represents and warrants that he/she/it (a) has been duly authorized by the User to accept, and hereby does accept, all such terms and conditions on behalf of User, and (b) shall inform User of all such terms and conditions. In the event such person is a "freelancer" or other third party independent of User and CCC, such party shall be deemed jointly a "User" for purposes of these terms and conditions. In any event, User shall be deemed to have accepted and agreed to all such terms and conditions if User republishes the Work in any fashion.

3. Scope of License; Limitations and Obligations.

   3.1. All Works and all rights therein, including copyright rights, remain the sole and exclusive property of the Rightsholder. The license created by the exchange of an Order Confirmation (and/or any invoice) and payment by User of the full amount set forth on that document includes only those rights expressly set forth in the Order Confirmation and in these terms and conditions, and conveys no other rights in the Work(s) to User. All rights not expressly granted are hereby reserved.

   3.2.
   General Payment Terms: You may pay by credit card or through an account with us payable at the end of the month. If you and we agree that you may establish a standing account with CCC, then the following terms apply: Remit Payment to: Copyright Clearance Center, 29118 Network Place, Chicago, IL 60673-1291. Payments Due: Invoices are payable upon their delivery to you (or upon our notice to you that they are available to you for downloading). After 30 days, outstanding amounts will be subject to a service charge of 1-1/2% per month or, if less, the maximum rate allowed by applicable law. Unless otherwise specifically set forth in the Order Confirmation or in a separate written agreement signed by CCC, invoices are due and payable on "net 30" terms. While User may exercise the rights licensed immediately upon issuance of the

Order Confirmation, the license is automatically revoked and is null and void, as if it had never been issued, if complete payment for the license is not received on a timely basis either from User directly or through a payment agent, such as a credit card company.

3.3. Unless otherwise provided in the Order Confirmation, any grant of rights to User (i) is "one-time" (including the editions and product family specified in the license), (ii) is non-exclusive and non-transferable and (iii) is subject to any and all limitations and restrictions (such as, but not limited to, limitations on duration of use or circulation) included in the Order Confirmation or invoice and/or in these terms and conditions. Upon completion of the licensed use, User shall either secure a new permission for further use of the Work(s) or immediately cease any new use of the Work(s) and shall render inaccessible (such as by deleting or by removing or severing links or other locators) any further copies of the Work (except for copies printed on paper in accordance with this license and still in User's stock at the end of such period).

3.4. In the event that the material for which a republication license is sought includes third party materials (such as photographs, illustrations, graphs, inserts and similar materials) which are identified in such material as having been used by permission, User is responsible for identifying, and seeking separate licenses (under this Service or otherwise) for, any of such third party materials; without a separate license, such third party materials may not be used.

3.5. Use of proper copyright notice for a Work is required as a condition of any license granted under the Service. Unless otherwise provided in the Order Confirmation, a proper copyright notice will read substantially as follows: "Republished with permission of [Rightsholder's name], from [Work's title, author, volume, edition number and year of copyright]; permission conveyed through Copyright Clearance Center, Inc. " Such notice must be provided in a reasonably legible font size and must be placed either immediately adjacent to the Work as used (for example, as part of a by-line or footnote but not as a separate electronic link) or in the place where substantially all other credits or notices for the new work containing the republished Work are located. Failure to include the required notice results in loss to the Rightsholder and CCC, and the User shall be liable to pay liquidated damages for each such failure equal to twice the use fee specified in the Order Confirmation, in addition to the use fee itself and any other fees and charges specified.

3.6. User may only make alterations to the Work if and as expressly set forth in the Order Confirmation. No Work may be used in any way that is defamatory, violates the rights of third parties (including such third parties' rights of copyright, privacy, publicity, or other tangible or intangible property), or is otherwise illegal, sexually explicit or obscene. In addition, User may not conjoin a Work with any other material that may result in damage to the reputation of the Rightsholder. User agrees to inform CCC if it becomes aware of any infringement of any rights in a Work and to cooperate with any reasonable request of CCC or the Rightsholder in connection therewith.

4. Indemnity. User hereby indemnifies and agrees to defend the Rightsholder and CCC, and their respective employees and directors, against all claims, liability, damages, costs and expenses, including legal fees and expenses, arising out of any use of a Work beyond the scope of the rights granted herein, or any use of a Work which has been altered in any unauthorized way by User, including claims of defamation or infringement of rights of copyright, publicity, privacy or other tangible or intangible property.

5. Limitation of Liability. UNDER NO CIRCUMSTANCES WILL CCC OR THE RIGHTSHOLDER BE LIABLE FOR ANY DIRECT, INDIRECT, CONSEQUENTIAL OR INCIDENTAL DAMAGES (INCLUDING WITHOUT LIMITATION DAMAGES FOR LOSS OF BUSINESS PROFITS OR INFORMATION, OR FOR BUSINESS INTERRUPTION) ARISING OUT OF THE USE OR INABILITY TO USE A WORK, EVEN IF ONE OF THEM HAS BEEN ADVISED OF THE POSSIBILITY OF SUCH DAMAGES. In any event, the total liability of the Rightsholder and CCC (including their respective employees and directors) shall not exceed the total amount actually paid by User for this license. User assumes full liability for the actions and omissions of its principals, employees, agents, affiliates, successors and assigns.

6.

Limited Warranties. THE WORK(S) AND RIGHT(S) ARE PROVIDED "AS IS". CCC HAS THE RIGHT TO GRANT TO USER THE RIGHTS GRANTED IN THE ORDER CONFIRMATION DOCUMENT. CCC AND THE RIGHTSHOLDER DISCLAIM ALL OTHER WARRANTIES RELATING TO THE WORK(S) AND RIGHT(S), EITHER EXPRESS OR IMPLIED, INCLUDING WITHOUT LIMITATION IMPLIED WARRANTIES OF MERCHANTABILITY OR FITNESS FOR A PARTICULAR PURPOSE. ADDITIONAL RIGHTS MAY BE REQUIRED TO USE ILLUSTRATIONS, GRAPHS, PHOTOGRAPHS, ABSTRACTS, INSERTS OR OTHER PORTIONS OF THE WORK (AS OPPOSED TO THE ENTIRE WORK) IN A MANNER CONTEMPLATED BY USER; USER UNDERSTANDS AND AGREES THAT NEITHER CCC NOR THE RIGHTSHOLDER MAY HAVE SUCH ADDITIONAL RIGHTS TO GRANT.

7. Effect of Breach. Any failure by User to pay any amount when due, or any use by User of a Work beyond the scope of the license set forth in the Order Confirmation and/or these terms and conditions, shall be a material breach of the license created by the Order Confirmation and these terms and conditions. Any breach not cured within 30 days of written notice thereof shall result in immediate termination of such license without further notice. Any unauthorized (but licensable) use of a Work that is terminated immediately upon notice thereof may be liquidated by payment of the Rightsholder's ordinary license price therefor; any unauthorized (and unlicensable) use that is not terminated immediately for any reason (including, for example, because materials containing the Work cannot reasonably be recalled) will be subject to all remedies available at law or in equity, but in no event to a payment of less than three times the Rightsholder's ordinary license price for the most closely analogous licensable use plus Rightsholder's and/or CCC's costs and expenses incurred in collecting such payment.

8. Miscellaneous.

   8.1. User acknowledges that CCC may, from time to time, make changes or additions to the Service or to these terms and conditions, and CCC reserves the right to send notice to the User by electronic mail or otherwise for the purposes of notifying User of such changes or additions; provided that any such changes or additions shall not apply to permissions already secured and paid for.

   8.2. Use of User-related information collected through the Service is governed by CCC's privacy policy, available online here:https://marketplace.copyright.com/rs-ui-web/mp/privacy-policy

   8.3. The licensing transaction described in the Order Confirmation is personal to User. Therefore, User may not assign or transfer to any other person (whether a natural person or an organization of any kind) the license created by the Order Confirmation and these terms and conditions or any rights granted hereunder; provided, however, that User may assign such license in its entirety on written notice to CCC in the event of a transfer of all or substantially all of User's rights in the new material which includes the Work(s) licensed under this Service.

   8.4. No amendment or waiver of any terms is binding unless set forth in writing and signed by the parties. The Rightsholder and CCC hereby object to any terms contained in any writing prepared by the User or its principals, employees, agents or affiliates and purporting to govern or otherwise relate to the licensing transaction described in the Order Confirmation, which terms are in any way inconsistent with any terms set forth in the Order Confirmation and/or in these terms and conditions or CCC's standard operating procedures, whether such writing is prepared prior to, simultaneously with or subsequent to the Order Confirmation, and whether such writing appears on a copy of the Order Confirmation or in a separate instrument.

   8.5. The licensing transaction described in the Order Confirmation document shall be governed by and construed under the law of the State of New York, USA, without regard to the principles thereof of conflicts of law. Any case, controversy, suit, action, or proceeding arising out of, in connection with, or related to such licensing transaction shall be brought, at CCC's sole discretion, in any federal or state court located in the County of New York, State of New York, USA, or in any federal or state court whose geographical jurisdiction covers the location of the Rightsholder set forth in the Order Confirmation. The parties expressly submit to the personal jurisdiction and venue of each such federal or state court.If you have any comments or questions about the Service or Copyright Clearance Center, please contact us at 978-750-8400 or send an e-mail to support@copyright.com.

v 1.1

Co-encapsulation of curcumin and vitamin D$_3$ in mixed phospholipid nanoliposomes using a continuous supercritical CO$_2$ assisted process

Matheus A. Chaves[a,b], Lucia Baldino[b,*], Samantha C. Pinho[a], Ernesto Reverchon[b]

[a] Laboratory of Encapsulation and Functional Foods (LEnAlis), Department of Food Engineering, School of Animal Science and Food Engineering, University of São Paulo, Av. Duque de Caxias Norte, 225, Pirassununga, SP, Brazil
[b] Department of Industrial Engineering, University of Salerno, Via Giovanni Paolo II, 132, Fisciano, SA 84084, Italy

ABSTRACT

Background: Curcumin and vitamin D$_3$ (VD3) are nutraceutical compounds that exert important roles in the human health. Nanoencapsulation in liposomes appears as a suitable target delivery system that can also enhance the bioavailability of these biomolecules.
Methods: Vesicles were prepared using different ratios of hydrogenated and non-hydrogenated phospholipids, obtained from soy and egg-yolk. A supercritical CO$_2$ assisted process was used to produce the nanoliposomes. The operative parameters were 40 °C and 100 bar, using a water flow rate of 10 mL/min. Nanoliposomes were characterized by scanning electron microscopy and dynamic light scattering to determine their morphology and stability; whereas biomolecules encapsulation efficiency and release kinetics were measured by a UV/Vis spectrophotometer. Antioxidant activity and the effect of stress-induced conditions on the nanoliposomes were also investigated.
Significant findings: Nanoliposomes mean diameters ranged from 128 to 228 nm, with encapsulation efficiencies up to 95% for curcumin and 74% for VD3. The addition of 30% w/w of saturated phospholipids to the starting formulation promoted an increase in size of vesicles and a consequent increase in the encapsulation efficiency of both biomolecules. The antioxidant activity of curcumin was preserved after processing and the co-loaded nanovesicles demonstrated a good stability under different stress conditions.

© 2021 Taiwan Institute of Chemical Engineers. Published by Elsevier B.V. All rights reserved.

1. Introduction

The attention towards a healthier lifestyle is demanding new efforts to the food industry, mostly to offer clear-label products with lower levels of artificial preservatives. In this context, nutraceuticals/functional foods emerge as health-promoting products that can contribute to the prevention of some diseases due to the action of the bioactive molecules present in their composition.

Nanoencapsulation technologies are extensively used to protect sensitive food nutraceuticals and to enhance their bioavailability and stability in the gastrointestinal tract [1]. These techniques consist of trapping the bioactive molecules within nanocarriers, such as nanoemulsions, nanoliposomes, solid-lipid nanoparticles and nanostructured lipid carriers, ensuring a higher efficiency of the materials and improving the optimal dosage over time [2].

Specifically, nanoliposomes are spherical vesicles consisting of one or more phospholipid bilayers, concentrically arranged and containing an aqueous core [3]. They are considered as the most promising lipid-based nanocarriers, due to the ability of encapsulating both hydrophilic and/or hydrophobic compounds, protecting them from the gastric fluid (pH 5) and favoring their proper absorption in the intestine (pH 7) [4]. Moreover, nanoliposomes are produced from natural phospholipids, known as nontoxic, biocompatible, biodegradable and non-immunogenic food-grade ingredients [5], and show a higher stability against creaming, sedimentation and aggregation than liposomes, thanks to their smaller size [6]. It is worth to note that nano-sized liposomes can also improve the performance of bioactive molecules, in terms of dissolution rate and bioavailability [7]. Nevertheless, despite the above-mentioned advantages, nanoliposomes are susceptible to hydrolysis and oxidation that can disrupt their phospholipid membrane and induce an early bioactive leakage [8].

Conventional methods for liposome production include thin-film hydration, solvent injection, and reverse phase evaporation. They are multi-step methods that need additional downstream processing, as sonication or extrusion, to obtain vesicles with homogeneous size distributions. Also, the use of toxic organic solvents can be considered a relevant concern regarding the applicability of liposomes in food and pharmaceutical formulations.

Supercritical CO$_2$ (SC—CO$_2$) assisted technologies can be suitable alternatives to the conventional methods and have been successfully

ATTACHMENT F – PAPER PUBLISHED IN JOURNAL OF FOOD ENGINEERING

CCC Marketplace™

This is a License Agreement between Matheus Andrade Chaves ("User") and Copyright Clearance Center, Inc. ("CCC") on behalf of the Rightsholder identified in the order details below. The license consists of the order details, the CCC Terms and Conditions below, and any Rightsholder Terms and Conditions which are included below.

All payments must be made in full to CCC in accordance with the CCC Terms and Conditions below.

Order Date	25-Jan-2022	Type of Use	Republish in a thesis/dissertation
Order License ID	1181962-1		
ISSN	0260-8774	Publisher	ELSEVIER LTD,
		Portion	Chapter/article

LICENSED CONTENT

Publication Title	Journal of food engineering	Country	United Kingdom of Great Britain and Northern Ireland
Article Title	Supercritical CO2 assisted process for the production of mixed phospholipid nanoliposomes: Unloaded and vitamin D3-loaded vesicles	Rightsholder	Elsevier Science & Technology Journals
		Publication Type	Journal
		Start Page	110851
Author/Editor	International Society of Food Engineering,	Volume	316
Date	01/01/1982		
Language	English		

REQUEST DETAILS

Portion Type	Chapter/article	Rights Requested	Main product
Page range(s)	1-9	Distribution	Worldwide
Total number of pages	9	Translation	Original language of publication
Format (select all that apply)	Print, Electronic	Copies for the disabled?	No
Who will republish the content?	Author of requested content	Minor editing privileges?	No
		Incidental promotional use?	No
Duration of Use	Life of current edition		
Lifetime Unit Quantity	Up to 499	Currency	USD

NEW WORK DETAILS

Title	Enrichment of cornstarch with curcumin and vitamin D3 coencapsulated in lyophilized liposomes using high shear wet agglomeration	Institution name	University of São Paulo
		Expected presentation date	2022-01-25
Instructor name	Matheus Andrade Chaves		

ADDITIONAL DETAILS

Order reference number	N/A	The requesting person / organization to appear on the license	Matheus Andrade Chaves

REUSE CONTENT DETAILS

Title, description or numeric reference of the portion(s)	Enrichment of cornstarch with curcumin and vitamin D3 coencapsulated in lyophilized liposomes using high shear wet agglomeration	Title of the article/chapter the portion is from	Supercritical CO2 assisted process for the production of mixed phospholipid nanoliposomes: Unloaded and vitamin D3-loaded vesicles
Editor of portion(s)	Chaves, Matheus A.; Baldino, Lucia; Pinho, Samantha C.; Reverchon, Ernesto	Author of portion(s)	Chaves, Matheus A.; Baldino, Lucia; Pinho, Samantha C.; Reverchon, Ernesto
Volume of serial or monograph	316	Issue, if republishing an article from a serial	N/A
Page or page range of portion	110851	Publication date of portion	2022-03-01

RIGHTSHOLDER TERMS AND CONDITIONS

Elsevier publishes Open Access articles in both its Open Access journals and via its Open Access articles option in subscription journals, for which an author selects a user license permitting certain types of reuse without permission. Before proceeding please check if the article is Open Access on http://www.sciencedirect.com and refer to the user license for the individual article. Any reuse not included in the user license terms will require permission. You must always fully and appropriately credit the author and source. If any part of the material to be used (for example, figures) has appeared in the Elsevier publication for which you are seeking permission, with credit or acknowledgement to another source it is the responsibility of the user to ensure their reuse complies with the terms and conditions determined by the rights holder. Please contact permissions@elsevier.com with any queries.

CCC Terms and Conditions

1. Description of Service; Defined Terms. This Republication License enables the User to obtain licenses for republication of one or more copyrighted works as described in detail on the relevant Order Confirmation (the "Work(s)"). Copyright Clearance Center, Inc. ("CCC") grants licenses through the Service on behalf of the rightsholder identified on the Order Confirmation (the "Rightsholder"). "Republication", as used herein, generally means the inclusion of a Work, in whole or in part, in a new work or works, also as described on the Order Confirmation. "User", as used herein, means the person or entity making such republication.

2. The terms set forth in the relevant Order Confirmation, and any terms set by the Rightsholder with respect to a particular Work, govern the terms of use of Works in connection with the Service. By using the Service, the person transacting for a republication license on behalf of the User represents and warrants that he/she/it (a) has been duly authorized by the User to accept, and hereby does accept, all such terms and conditions on behalf of User, and (b) shall inform User of all such terms and conditions. In the event such person is a "freelancer" or other third party independent of User and CCC, such party shall be deemed jointly a "User" for purposes of these terms and conditions. In any event, User shall be deemed to have accepted and agreed to all such terms and conditions if User republishes the Work in any fashion.

3. Scope of License; Limitations and Obligations.

    3.1. All Works and all rights therein, including copyright rights, remain the sole and exclusive property of the Rightsholder. The license created by the exchange of an Order Confirmation (and/or any invoice) and payment by User of the full amount set forth on that document includes only those rights expressly set forth in the Order Confirmation and in these terms and conditions, and conveys no other rights in the Work(s) to User. All rights not expressly granted are hereby reserved.

    3.2.
    General Payment Terms: You may pay by credit card or through an account with us payable at the end of the month. If you and we agree that you may establish a standing account with CCC, then the following terms apply: Remit Payment to: Copyright Clearance Center, 29118 Network Place, Chicago, IL 60673-1291. Payments Due: Invoices are payable upon their delivery to you (or upon our notice to you that they are available to you for downloading). After 30 days, outstanding amounts will be subject to a service charge of 1-1/2% per month or, if less, the maximum rate allowed by applicable law. Unless otherwise specifically set forth in the Order Confirmation or in a separate written agreement signed by CCC, invoices are due and payable on "net 30" terms. While User may exercise the rights licensed immediately upon issuance of the Order Confirmation, the license is automatically revoked and is null and void, as if it had never been

312

issued, if complete payment for the license is not received on a timely basis either from User directly or through a payment agent, such as a credit card company.

3.3. Unless otherwise provided in the Order Confirmation, any grant of rights to User (i) is "one-time" (including the editions and product family specified in the license), (ii) is non-exclusive and non-transferable and (iii) is subject to any and all limitations and restrictions (such as, but not limited to, limitations on duration of use or circulation) included in the Order Confirmation or invoice and/or in these terms and conditions. Upon completion of the licensed use, User shall either secure a new permission for further use of the Work(s) or immediately cease any new use of the Work(s) and shall render inaccessible (such as by deleting or by removing or severing links or other locators) any further copies of the Work (except for copies printed on paper in accordance with this license and still in User's stock at the end of such period).

3.4. In the event that the material for which a republication license is sought includes third party materials (such as photographs, illustrations, graphs, inserts and similar materials) which are identified in such material as having been used by permission, User is responsible for identifying, and seeking separate licenses (under this Service or otherwise) for, any of such third party materials; without a separate license, such third party materials may not be used.

3.5. Use of proper copyright notice for a Work is required as a condition of any license granted under the Service. Unless otherwise provided in the Order Confirmation, a proper copyright notice will read substantially as follows: "Republished with permission of [Rightsholder's name], from [Work's title, author, volume, edition number and year of copyright]; permission conveyed through Copyright Clearance Center, Inc. " Such notice must be provided in a reasonably legible font size and must be placed either immediately adjacent to the Work as used (for example, as part of a by-line or footnote but not as a separate electronic link) or in the place where substantially all other credits or notices for the new work containing the republished Work are located. Failure to include the required notice results in loss to the Rightsholder and CCC, and the User shall be liable to pay liquidated damages for each such failure equal to twice the use fee specified in the Order Confirmation, in addition to the use fee itself and any other fees and charges specified.

3.6. User may only make alterations to the Work if and as expressly set forth in the Order Confirmation. No Work may be used in any way that is defamatory, violates the rights of third parties (including such third parties' rights of copyright, privacy, publicity, or other tangible or intangible property), or is otherwise illegal, sexually explicit or obscene. In addition, User may not conjoin a Work with any other material that may result in damage to the reputation of the Rightsholder. User agrees to inform CCC if it becomes aware of any infringement of any rights in a Work and to cooperate with any reasonable request of CCC or the Rightsholder in connection therewith.

4. Indemnity. User hereby indemnifies and agrees to defend the Rightsholder and CCC, and their respective employees and directors, against all claims, liability, damages, costs and expenses, including legal fees and expenses, arising out of any use of a Work beyond the scope of the rights granted herein, or any use of a Work which has been altered in any unauthorized way by User, including claims of defamation or infringement of rights of copyright, publicity, privacy or other tangible or intangible property.

5. Limitation of Liability. UNDER NO CIRCUMSTANCES WILL CCC OR THE RIGHTSHOLDER BE LIABLE FOR ANY DIRECT, INDIRECT, CONSEQUENTIAL OR INCIDENTAL DAMAGES (INCLUDING WITHOUT LIMITATION DAMAGES FOR LOSS OF BUSINESS PROFITS OR INFORMATION, OR FOR BUSINESS INTERRUPTION) ARISING OUT OF THE USE OR INABILITY TO USE A WORK, EVEN IF ONE OF THEM HAS BEEN ADVISED OF THE POSSIBILITY OF SUCH DAMAGES. In any event, the total liability of the Rightsholder and CCC (including their respective employees and directors) shall not exceed the total amount actually paid by User for this license. User assumes full liability for the actions and omissions of its principals, employees, agents, affiliates, successors and assigns.

6. Limited Warranties. THE WORK(S) AND RIGHT(S) ARE PROVIDED "AS IS". CCC HAS THE RIGHT TO GRANT TO USER THE RIGHTS GRANTED IN THE ORDER CONFIRMATION DOCUMENT. CCC AND THE RIGHTSHOLDER DISCLAIM ALL OTHER WARRANTIES RELATING TO THE WORK(S) AND RIGHT(S), EITHER EXPRESS OR IMPLIED, INCLUDING WITHOUT LIMITATION IMPLIED WARRANTIES OF MERCHANTABILITY OR FITNESS FOR A PARTICULAR PURPOSE. ADDITIONAL RIGHTS MAY BE REQUIRED TO USE ILLUSTRATIONS, GRAPHS, PHOTOGRAPHS, ABSTRACTS, INSERTS OR OTHER PORTIONS OF THE WORK (AS OPPOSED TO THE ENTIRE WORK) IN A MANNER CONTEMPLATED BY USER; USER UNDERSTANDS AND AGREES THAT NEITHER CCC NOR THE RIGHTSHOLDER MAY HAVE SUCH ADDITIONAL RIGHTS TO GRANT.

7. Effect of Breach. Any failure by User to pay any amount when due, or any use by User of a Work beyond the scope of the license set forth in the Order Confirmation and/or these terms and conditions, shall be a material breach of the license created by the Order Confirmation and these terms and conditions. Any breach not cured within 30 days of written notice thereof shall result in immediate termination of such license without further notice. Any unauthorized (but licensable) use of a Work that is terminated immediately upon notice thereof may be liquidated by payment of the Rightsholder's ordinary license price therefor; any unauthorized (and unlicensable) use that is not terminated immediately for any reason (including, for example, because materials containing the Work cannot reasonably be recalled) will be subject to all remedies available at law or in equity, but in no event to a payment of less than three times the Rightsholder's ordinary license price for the most closely analogous licensable use plus Rightsholder's and/or CCC's costs and expenses incurred in collecting such payment.

8. Miscellaneous.

   8.1. User acknowledges that CCC may, from time to time, make changes or additions to the Service or to these terms and conditions, and CCC reserves the right to send notice to the User by electronic mail or otherwise for the purposes of notifying User of such changes or additions; provided that any such changes or additions shall not apply to permissions already secured and paid for.

   8.2. Use of User-related information collected through the Service is governed by CCC's privacy policy, available online here:https://marketplace.copyright.com/rs-ui-web/mp/privacy-policy

   8.3. The licensing transaction described in the Order Confirmation is personal to User. Therefore, User may not assign or transfer to any other person (whether a natural person or an organization of any kind) the license created by the Order Confirmation and these terms and conditions or any rights granted hereunder; provided, however, that User may assign such license in its entirety on written notice to CCC in the event of a transfer of all or substantially all of User's rights in the new material which includes the Work(s) licensed under this Service.

   8.4. No amendment or waiver of any terms is binding unless set forth in writing and signed by the parties. The Rightsholder and CCC hereby object to any terms contained in any writing prepared by the User or its principals, employees, agents or affiliates and purporting to govern or otherwise relate to the licensing transaction described in the Order Confirmation, which terms are in any way inconsistent with any terms set forth in the Order Confirmation and/or in these terms and conditions or CCC's standard operating procedures, whether such writing is prepared prior to, simultaneously with or subsequent to the Order Confirmation, and whether such writing appears on a copy of the Order Confirmation or in a separate instrument.

   8.5. The licensing transaction described in the Order Confirmation document shall be governed by and construed under the law of the State of New York, USA, without regard to the principles thereof of conflicts of law. Any case, controversy, suit, action, or proceeding arising out of, in connection with, or related to such licensing transaction shall be brought, at CCC's sole discretion, in any federal or state court located in the County of New York, State of New York, USA, or in any federal or state court whose geographical jurisdiction covers the location of the Rightsholder set forth in the Order Confirmation. The parties expressly submit to the personal jurisdiction and venue of each such federal or state court.If you have any comments or questions about the Service or Copyright Clearance Center, please contact us at 978-750-8400 or send an e-mail to support@copyright.com.

v 1.1

Supercritical CO$_2$ assisted process for the production of mixed phospholipid nanoliposomes: Unloaded and vitamin D$_3$-loaded vesicles

Matheus A. Chaves [a,b], Lucia Baldino [b,*], Samantha C. Pinho [a], Ernesto Reverchon [b]

[a] Laboratory of Encapsulation and Functional Foods (LEnAlis), Department of Food Engineering, School of Animal Science and Food Engineering, University of Sao Paulo, Av. Duque de Caxias Norte, 225, Pirassununga, SP, Brazil
[b] Department of Industrial Engineering, University of Salerno, Via Giovanni Paolo II, 132, 84084, Fisciano, SA, Italy

ARTICLE INFO

ABSTRACT

In this study, SuperLip, an innovative technology assisted by supercritical carbon dioxide (SC–CO$_2$), was used to produce unloaded and vitamin D$_3$ (VD3)-loaded nanoliposomes. Vesicles were produced using hydrogenated and nonhydrogenated phosphatidylcholine from food-grade lecithins at ratios of 30:70, 20:80 and 0:100. SuperLip was operated at 100 bar and 40 °C using water flow rates ranging from 2.5 to 10 mL/min. The results showed that unloaded liposomes produced by SuperLip presented a unimodal size distribution at a water flow rate of 10 mL/min, regardless of the phospholipid ratio, and mean diameters ranging from 125 to 141 nm. VD3-loaded liposomes also presented a unimodal size distribution at this water flow rate, but slightly higher diameters that ranged from 144 to 252 nm. Furthermore, the addition of 20% purified phospholipids to liposomes led to an increase in the mean size of VD3-loaded vesicles from 144 to 218 nm and an increase in the encapsulation efficiency from 66.7 to 88.9%.

1. Introduction

Supercritical fluid technologies are receiving attention for the production of liposomes due to their advantages over conventional methods. They are green/er technologies due to the significant decrease or complete elimination of the use of organic solvents and do not require multiple steps or postprocessing downstream methods, such as sonication or extrusion, to produce nanosized vesicles (Penoy et al., 2021). Moreover, the considerable increases in reproducibility and encapsulation efficiency related to supercritical methods are advantages regarding processing time and costs (Bigazzi et al., 2020; Penoy et al., 2021), in addition to the ease of scaling up from the laboratory to industrial scale (Maqbool et al., 2019). Finally, better control of the physicochemical properties of liposomes can also be achieved using supercritical fluids (Penoy et al., 2021).

Supercritical carbon dioxide (SC–CO$_2$), an inexpensive, inert, nontoxic, nonflammable and environmentally friendly alternative to organic solvents, has been used in various fields (Baldino et al., 2019a, 2019b, 2020a; Sarno et al., 2017), including liposome production, due to its unique properties, such as high diffusivity, zero surface tension, low viscosity and high density (Zhao et al., 2017; Sharifi et al., 2019; Trucillo et al., 2020). In addition, SC–CO$_2$ exhibits mild critical

parameters (T$_c$ = 31.1 °C and P$_c$ = 7.39 MPa), which are less likely to cause the degradation of thermosensitive molecules and can be easily achieved and controlled during industrial processes (Baldino et al., 2020b; Tanaka et al., 2020).

Briefly, liposomes are spherical vesicles composed of an aqueous compartment enclosed by one or more lipid bilayers formed by self-aggregated phospholipids. These carriers are recognized as efficient target delivery vesicles for both water-soluble and/or lipid-soluble molecules and have been extensively studied in the food area due to their nontoxicity, biodegradability and versatility (Lopes et al., 2021). Presently, several phospholipids, such as phosphatidylcholine (PC), phosphatidylethanolamine (PE) and phosphatidylinositol (PI), have been used to produce liposomes, all of which can be obtained from natural sources, such as soybean and egg yolk (Chaves and Pinho, 2020). In particular, the composition of the bilayer can regulate the intermolecular interactions and the stability of the vesicles. These interactions include hydrophilic interactions (polar head groups and water molecules), hydrogen bonding (water molecules and head groups/phosphates/carbonyl) and van der Waals interactions (hydrocarbon chains), all of which lead to the formation of closed bilayers after the supply of energy in an aqueous environment (Muñoz-Shugulí et al., 2021). Moreover, the method applied for liposome production also